CHALCOCARBONYL CHEMISTRY: APPLICATION IN HORMONAL RECEPTOR DETERMINATION, METALLOPORPHYRINS AND METAL-ARENE BOND ACTIVATION

by

Ashraf A. Ismail

A Thesis Submitted to the Faculty of Graduate Studies and Research in Partial Fulfillment of the Requirements for the Degree of Doctor of Philosophy

McGill University
Montreal, Quebec

July, 1985.

CHALCOCARBONYL CHEMISTRY: APPLICATION IN HORMONAL RECEPTOR DETERMINATION, METALLOPORPHYRINS AND METAL-ARENE BOND ACTIVATION

Ph.D. Department of Chemistry

Ashraf A. Ismail

Abstract

The reaction of $(\eta\text{-Arene})Cr(CO)_2(CX)$ (X = S, Se) complexes with excess $(RO)_3P$ (R = Me, Et, n-Bu, Ph) yields $Cr(CO)_2(CX)[(RO)_3P]_3$, predominantly as the mer I isomer, in which a phosphite ligand is trans to CX. Arene displacement from $(\eta\text{-}C_6H_6)Cr(CO)_2(CX)$ by tridentate phosphine ligands L-L-L [L-L-L = $(Me)C(CH_2P(Ph)_2)_3$, $(Ph_2PCH_2CH_2)_2PhP$] gives fac-$(L\text{-}L\text{-}L)Cr(CO)_2(CX)$ products. The molecular structures of $Cr(CO)_2(CX)[(MeO)_3P]_3$ have been determined by single crystal X-ray diffraction. Intramolecular isomerization of these complexes as well as their tricarbonyl analogue has been demonstrated and activation parameters have been calculated for the rearrangement processes. Two-dimensional ^{31}P NMR spectroscopy has provided evidence that isomerization occurs via trigonal prismatic intermediates. Kinetic investigations of the reaction of $(\eta\text{-}C_6H_6)Cr(CO)_2(CX)$ with $(MeO)_3P$ have established a first-order rate dependence on both the complex and the entering ligand. The faster reaction rate of the selenocarbonyl derivative relative to its thiocarbonyl analogue originates in a lower entropy of activation in the former case. The effect on the reaction rate of variation in the nature of the arene and of the entering ligand has been investigated.

An approach to hormonal receptor assay involving the detection by FT-IR spectroscopy of $Cr(CO)_3$-labelled modified estradiol bound to estrogen receptors in target tissue is reported.

The FT-IR spectra of FeTPP(CX) [FeTPP = (5,10,15,20-tetraphenylporphinato)Fe(II); X = S, Se] and FeTPP(CX)L (X = S, Se; L = pyridine, ethanol) have been obtained. Some changes in the porphyrin spectrum were observed with variation or removal of L, but not with variation of X.

CHALCOCARBONYL CHEMISTRY: APPLICATION IN HORMONAL RECEPTOR DETERMINATION, METALLOPORPHYRINS AND METAL-ARENE BOND ACTIVATION

Ph.D. Département de chimie

Ashraf A. Ismail

Résumé

La réaction des complexes (η-arène)$Cr(CO)_2(CX)$ (X = S, Se) en présence d'excès de $(RO)_3P$ (R = Me, Et, n-Bu, Ph) produit $Cr(CO)_2(CX)[(RO)_3P]_3$, avec la prédominance de l'isomère mer I, chez lequel le ligand phosphite est en position trans du groupe CX. Le déplacement du groupe arène des complexes (η-C_6H_6)$Cr(CO)_2(CX)$ par les ligands phosphines tridentates L-L-L [L-L-L = $(Me)C(CH_2P(Ph)_2)_3$, $(Ph_2PCH_2CH_2)_2PhP$] conduit aux dérivés fac-(L-L-L)-$Cr(CO)_2(CX)$. Les structures moléculaires des complexes $Cr(CO)_2(CX)[(MeO)_3P]_3$ ont été déterminées par diffraction des rayons-X des cristaux uniques. L'isomérisation intramoléculaire de ces complexes et de leurs analogues tricarbonylés a été démontré, et les paramètres d'activation ont été calculés pour les processus de réarrangement. La spectroscopie RMN ^{31}P bidimensionelle a procuré des évidences montrant que l'isomérisation survient via des intermédiaires "prismatiques trigonales". Les études cinétiques de la réaction des complexes (η-C_6H_6)$Cr(CO)_2(CX)$ avec $(MeO)_3P$ ont établi la dépendance de la vitesse de premier-order pour chacun, le complexe et le ligand. Le dérivé sélénocarbonylé possède une vitesse de réaction la plus rapide relativement au dérivé thiocarbonylé, laquelle provient d'une entropie d'activation plus faible. L'effet sur la vitesse de la réaction de la variation de la nature du groupe arène et du ligand substituant a été étudié.

Une approche sur l'analyse des récepteurs hormonaux par détection des récepteurs estrogènes liés a des estradiols marqués de $Cr(CO)_3$ par spectroscopie IR-TF dans des tissus cibles est rapportée.

Les spectres IR-TF des complexes FeTPP(CX) [FeTPP = (5,10,15,20-tetraphenylporphinato)Fe(II); X = S, Se] et FeTPP(CX)L (X = S, Se; L = pyridine, éthanol) ont été obtenus. Quelques changements dans le spectre du groupe porphyrinique ont été observés avec la variation ou l'absence du ligand, et non pas avec la variation du groupe X.

To my parents

TABLE OF CONTENTS

Acknowledgements

I would like to thank Dr. Ian S. Butler for his guidance, support and encouragement. I would also like to express my deepest appreciation to Jacqueline Sedman for the many helpful discussions during the course of this work and for her valuable comments and suggestions in reading this thesis.

I also wish to express my gratitude to:

- Dr. Gérard Jaouen and Dr. Anne Vessières of l'Ecole Nationale Supérieure de Chimie de Paris for providing all the samples for the investigations reported in Chapter 6 of this thesis, and for their hospitality during my visit to Paris;

- Dr. Françoise Sauriol for obtaining the 2-D NMR spectra, for introducing me to 2-D NMR techniques and for her contributions to the elucidation of the mechanism of stereochemical nonrigidity;

- Paul Fitzpatrick for providing some samples of (η-Arene)$Cr(CO)_2(CS)$ complexes;

- Drs. D. Mansuy and J.P. Battioni of Laboratoire de Chimie de l'Ecole Normale Supérieure, Paris, for providing iron tetraphenylporphyrin complexes;

- Dr. Peter Bird of Concordia University for introducing me to crystallographic techniques and for the determination of the crystal structure of $Cr(CO)_2(CS)[(MeO)_3P]_3$;

- Drs. Jean-Jacques Bonnet and Salomon Askenazy of the CNRS Laboratoire de Chimie de Coordination, Toulouse, France, and Dr. Ian Butler for the crystal structure of $Cr(CO)_2(CSe)[(MeO)_3P]_3$;

- Dr. Barbara Gour for her advice on kinetic measurements;

- Dr. Bernard Belleau for permission to use the Cary 210 UV-vis spectrometer;

- Mr. Fred Kluck for his contribution to the design of specialized apparatus required during the course of this work;

- Ms. Carla Durston for her care in the final correction of the thesis;

- Pierre Harvey for his skillful drawing of figures;

- Dr. Rita Werbowyj for proofreading the final draft of the thesis.

The financial support of McGill University, in the form of the Coll McFee Memorial Scholarship and the McConnell Memorial Fellowship, of NSERC and of le Gouvernement du Québec is gratefully acknowledged.

List of Abbreviations

acac	acetylacetonate anion (-1)
(bz)	(η^6-benzene)
(cht)	(η^6-cycloheptatriene)
dpm	disintegrations per minute
(est)	(η^6-estradiol)
fmol	fantamole (10^{-15} mole)
Im	imidazole
(mbz)	(η^6-methyl benzoate)
MeIm	methyl imidazole
NOE	nuclear Overhauser effect
OEP	octaethylporphyrin
OLRC	organometallic-labelled receptor complex
py	pyridine
THF	tetrahydrofuran
TMS	tetramethylsilane
TPP	tetraphenylporphyrin
triphos	bis-(2-diphenylphosphinoethyl)phenylphosphine
triphos-U	1,1,1-tris(diphenylphosphinomethyl)ethane
(o-xyl)	(η^6-o-xylene)

NOTE ON UNITS

The parameters used in the text in units other than SI are shown below:

Parameter	Symbol	Unit	SI equivalent
energy-factored CO force constant	k_{CO}	mdyn $Å^{-1}$	(100) N m^{-1}
enthalpy of activation	$\Delta H^{\#}$	kcal mol^{-1}	(4.184) kJ mol^{-1}
entropy of activation	$\Delta S^{\#}$	cal mol^{-1} deg^{-1}	(4.184) J mol^{-1}
pressure	P	atm	(101,325) N m^{-2}
wavenumber	$\tilde{\nu}$	cm^{-1}	(10^{-2}) m^{-1}

LIST OF FIGURES

Chapter 3

Chapter 4

Chapter 5

Chapter 6

Chapter 7

LIST OF TABLES

Chapter 3

Chapter 4

Chapter 6

Chapter 7

Appendix A

Appendix B

Introduction

Since the first synthesis of an (η-Arene)$Cr(CO)_3$ complex in 1957 [1], the chemical reactivities of this class of complexes have been extensively investigated. Among the major and, from a practical point of view, most important findings of such studies is the utility of (η-Arene)$Cr(CO)_3$ complexes as catalysts in a variety of systems, particularly in the hydrogenation of dienes. The catalytically active species in the latter case has been established to involve partial or total loss of the arene [2,3].

The first syntheses of (η-Arene)$Cr(CO)_2(CS)$ and (η-Arene)$Cr(CO)_2(CSe)$ complexes were reported in 1974 [4] and 1975 [5], respectively. Although the physical properties of these thio- and selenocarbonyl derivatives have been examined extensively, studies of their chemical behaviour have been limited. A striking aspect of their reactivity is a markedly enhanced arene lability relative to their tricarbonyl analogues, as evidenced by their reaction with CO under mild conditions to yield the corresponding pentacarbonyl complexes, $Cr(CO)_5(CS)$ and $Cr(CO)_5(CSe)$ [6]. In view of the nature of the catalytically active species formed from (η-Arene)$Cr(CO)_3$ in the hydrogenation of dienes it could reasonably be anticipated that (η-Arene)$Cr(CO)_2(CX)$ (X = S, Se) complexes would be excellent catalysts for such processes. However, investigation of such complexes as

catalysts has revealed that they completely lack activity [7].

Part I of this thesis concerns the study of arene lability in arene chromium chalcocarbonyl complexes. This research was undertaken to extend the known chemistry of thiocarbonyl and selenocarbonyl complexes, to obtain quantitative measurements of arene labilization in (η-Arene)-$Cr(CO)_2(CX)$ (X = S, Se) and to probe the reasons for their reported inactivity as catalysts. Chapter 1 presents a brief review of mechanistic studies of (η-Arene)$Cr(CO)_3$-catalyzed hydrogenation of dienes to monoolefins. In Chapter 2, the reactions of (η-Arene)$Cr(CO)_2(CX)$ (X = S, Se) with tertiary phosphite and tridentate phosphine ligands will be described. The spectroscopic properties of new thio- and selenocarbonyl complexes obtained, as well as the crystal structures of two typical products, will be presented, followed, in Chapter 3, by an investigation of stereochemical nonrigidity in these systems. The kinetics and mechanism of arene displacement from (η-Arene)$Cr(CO)_2$-(CX) (X = S, Se) by tertiary phosphites will be the subject of Chapter 4, which concludes Part I.

In Part II, the combined use of FT-IR spectroscopy and metal chalcocarbonyl chemistry in two different types of biological applications will be demonstrated. While infrared spectroscopy has been among the major techniques

employed in the study of organometallic complexes throughout the history of organometallic chemistry, its application in the study of biological systems has been fairly limited in the past. This situation has largely been due to the complexity of such systems and the presence of biomolecules of interest in low concentration, as well as the unsuitability of water as an IR solvent. The recent development of FT-IR spectroscopy has led to the alleviation of these problems, as described in Chapter 5. Chapter 6 concerns a novel application of FT-IR spectroscopy and arene chromium chalocarbonyl chemistry in a biological system: the incorporation of a $Cr(CO)_3$ moiety in a biological molecule as a label for detection by FT-IR spectroscopy. In a collaborative project with Drs. G. Jaouen and A. Vessières of l'Ecole Nationale Supérieure de Chimie de Paris, $Cr(CO)_3$-labelled hormonal steriods have been bound to receptors in their target tissue. The subsequent detection of the carbonyl label by FT-IR spectroscopy and the potential utility of this procedure as an alternative to radioisotopic methods in receptor assay will be described in Chapter 6. An FT-IR study of chalcocarbonyl ligands coordinated to metalloporphyrins will be presented in Chapter 7. This represents an example of the use of FT-IR spectroscopy in the study of biological model compounds.

Finally, a summary of the contributions to knowledge,

suggestions for future work, and a list of publications and papers presented at scientific conferences which pertain to this work are given.

References

1. E.O. Fischer and K. Ofele, Chem. Ber., 90, 2532 (1957).
2. E.N. Frankel, E. Selke and C.A. Glass, J. Am. Chem. Soc., 90, 2446 (1968).
3. M. Cais and A. Rejoan, Inorg. Chim. Acta, 14, 509 (1970).
4. G. Jaouen and R. Dabard, J. Organometal. Chem., 72, 377 (1974).
5. I.S. Butler, D. Cozak and S.R. Stobart, J. Chem. Soc., Chem. Commun., 103 (1975).
6. A.M. English, K.R. Plowman, I.S. Butler, G. Jaouen, P. Le Maux and J.-Y. Thépot, J. Organometal. Chem., 132, C1 (1977).
7. R. Dabard, G. Jaouen, G. Simonneaux, M. Cais, D.H. Cohn, L. Lapid and D. Tatarsky, J. Organometal. Chem., 91, 1841 (1980).

PART I

Metal-Arene Bond Activation in Arene Chromium Chalcocarbonyl Complexes

Chapter 1

Catalytic Activity of Arene Chromium Chalcocarbonyl Complexes

(η-Arene)$Cr(CO)_3$ complexes have found extensive use as catalysts in a variety of systems [1,2]. Among the most important catalytic applications of this class of compound is the hydrogenation of dienes to monoolefins [2-6]. As homogeneous catalysts (η-Arene)$Cr(CO)_3$ complexes effect stereospecific cis-addition of H_2 to one double bond of the diene with some regioselectivity [Eq. 1.1].

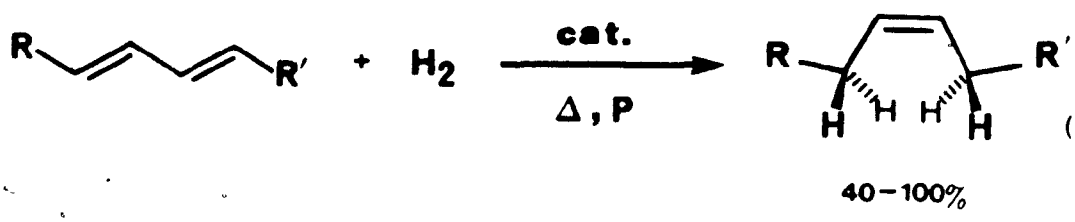

(1.1)

The conditions required for efficient catalysis depend critically on the nature of the arene. For monosubstituted arenes, high hydrogen pressure (30-50 atm) and high temperature (150-200°C) are needed (Table 1.1). The presence of electron-withdrawing substituents on the arene, which weaken the metal-arene bond, accelerates the rate of hydrogenation and shortens the induction period. However, polycyclic derivatives are even more favourable; for instance, with (η-anthracene)$Cr(CO)_3$ and (η-naphthalene)$Cr(CO)_3$ efficient

Table 1.1. Hydrogenation of Methyl Sorbate (0.2 M) to Methyl 3-Hexenoate (I) and Methyl 2-Hexenoate (II) Catalyzed by (η-Arene)$Cr(CO)_3$ in Cyclohexane[a]

Arene in (η-Arene)$Cr(CO)_3$ catalyst[b]	% Conversion	Product (% distribution)[c] I	II	Reaction conditions $P(H_2)$ atm	T °C	Time h
Benzene	100	94	4	48	165	8
Benzene	100	94	4	30	175	4
Toluene	100	94	5	48	150	7
Mesitylene	80	95	5	30	175	6
Ethylbenzene	95	95	5	48	150	7
Hexamethylbenzene	92	91	5	30	200	6
Anisole	12	100		48	150	6
Cycloheptatriene	100	98	1	30	120	1
Chlorobenzene	100	96	4	30	150	2
Methyl benzoate	100	99	1	48	150	2
Methyl benzoate	100	95	4	30	160	4
Phenanthrene	100	97	3	48	150	0.3

[a]Data from References 1 and 3.
[b]Catalyst concentration, 1×10^{-2} M.
[c]Balance of % distribution is methyl hexanoate.

hydrogenation is achieved under mild conditions (80°C, 1 atm H_2) [4]. This is particularly advantageous and leads to a much cleaner reaction since decomposition of the catalyst, which occurs at higher temperature, is eliminated and unwanted side reactions are minimized. Also, less H_2 pressure is needed, thereby reducing cost.

From the observations concerning the variation of catalytic behaviour with change in arene-metal bond strength, the catalytically active species has been postulated to result from partial or total arene loss [1,3,5]. Two mechanisms have been proposed: Frankel et al. [2] postulated a dissociative mechanism in which the (η-Arene)$Cr(CO)_3$ complex totally dissociates into arene + $Cr(CO)_3$. The catalytically active species is subsequently produced by reaction of the $Cr(CO)_3$ moiety with H_2 to give a dihydride which then reacts with a diene to afford 1,4-cis-addition of hydrogen, forming the monoene (Figure 1.1). Cais and Rejoan [3,5] later proposed an associative mechanism (Figure 1.2), involving a stepwise displacement of the arene, resulting in slippage of the arene to occupy ultimately a single coordination site of the metal (path a) or eventual total loss of arene (path b). The initial step involves the reversible dissociation of one double bond of the arene, followed by attack of the diene substrate. This is supported by the experimental observation that heating the substrate in the absence of H_2,

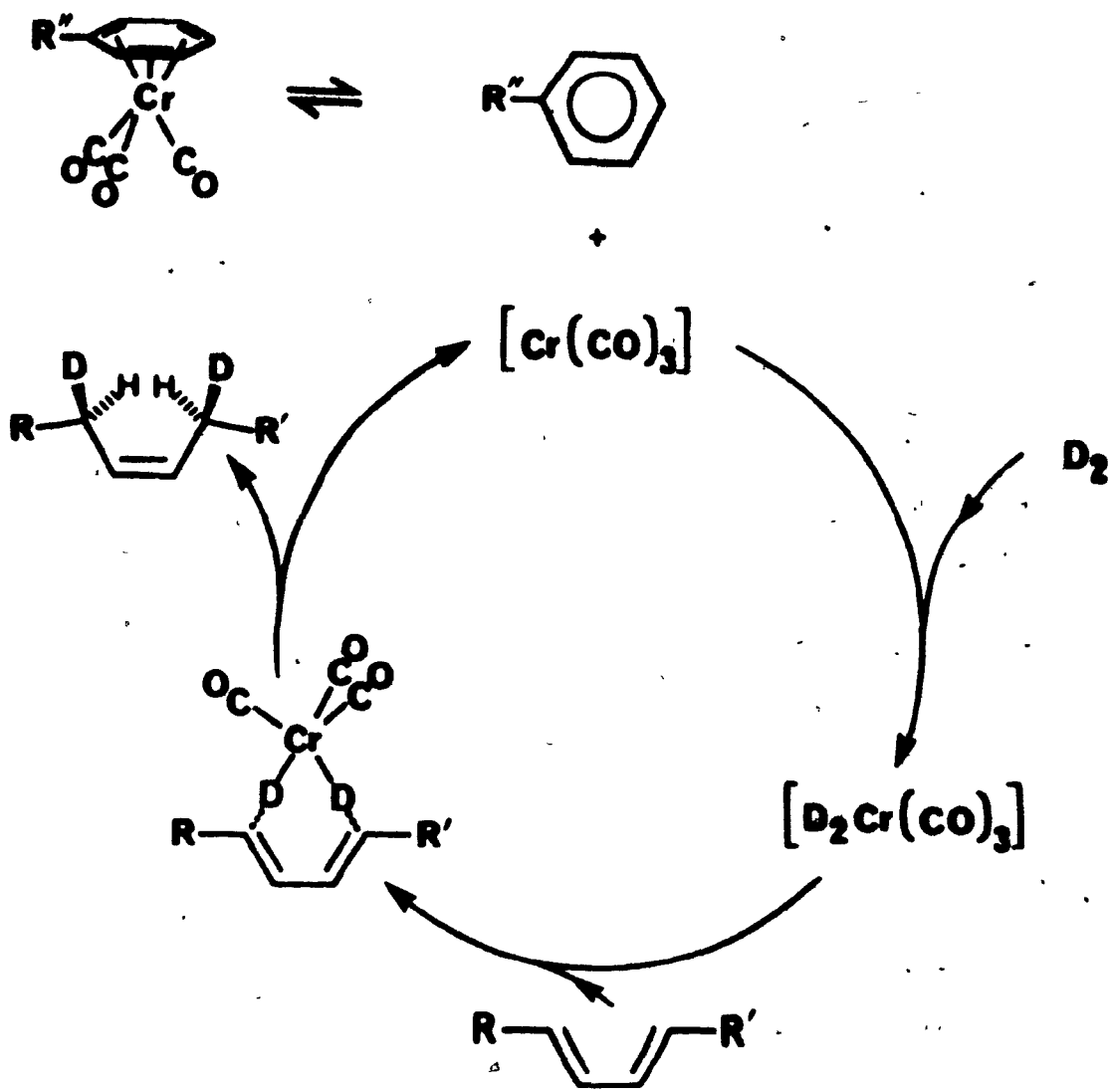

Figure 1.1. Mechanism proposed by Frankel *et al.* for the (η-Arene)$Cr(CO)_3$-catalyzed hydrogenation of dienes to monoenes. Adapted from Reference 2.

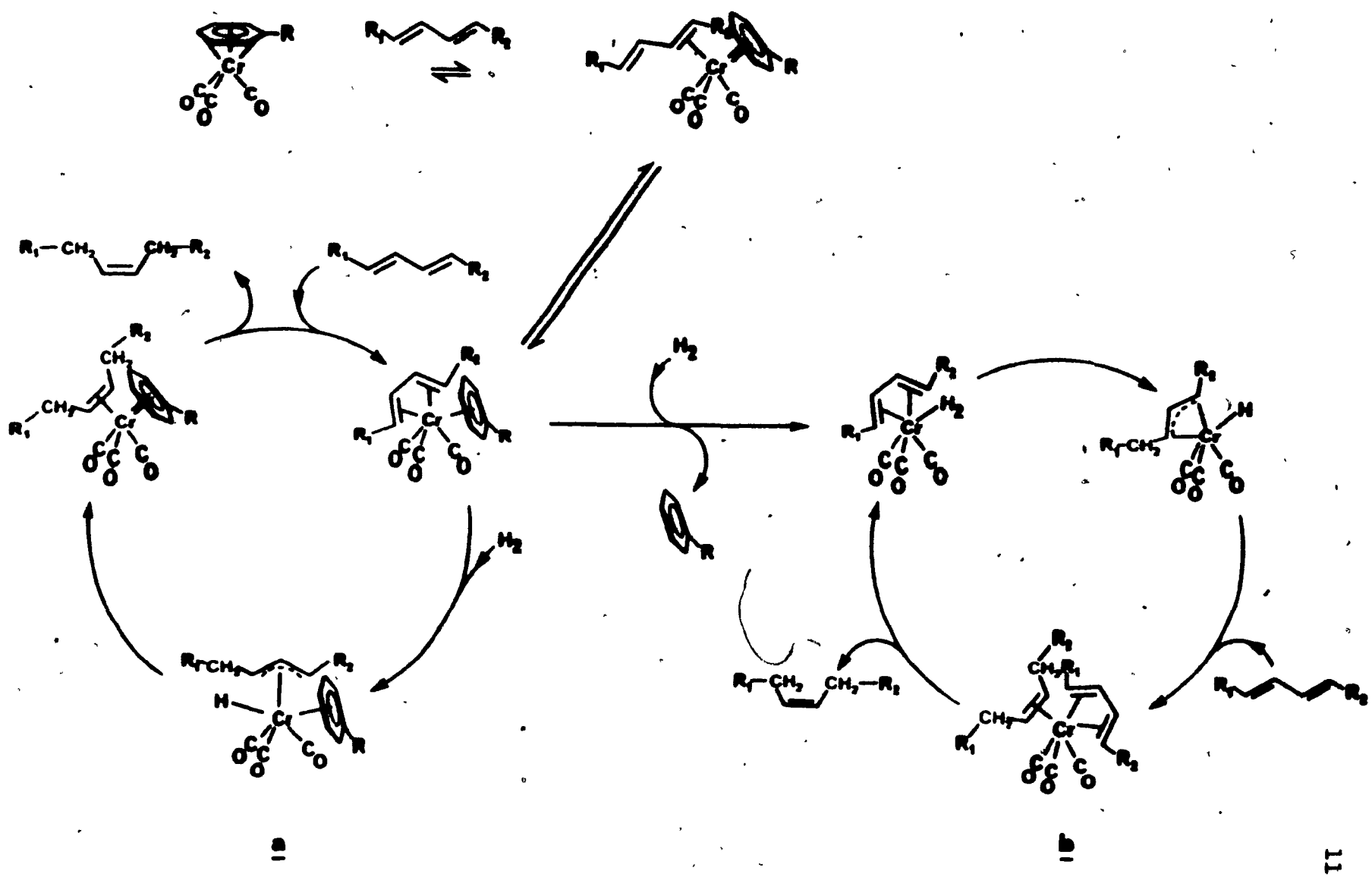

Figure 1.2. Mechanism proposed by Cais and Rejoan for the (η-Arene)$Cr(CO)_3$-catalyzed hydrogenation of dienes to monoenes. Adapted from Reference 5.

followed by the introduction of H_2, eliminated the induction period for the onset of hydrogenation. Conversely, heating the catalyst in the presence of H_2 did not alter the induction period significantly [3].

In order to investigate the true nature of the catalytic species, the $Cr(CO)_3(THF)_3$ species has been formed <u>in situ</u> by reaction of (η-Arene)$Cr(CO)_3$ with THF as solvent [7]. It was found that addition of substrate to a solution containing this species effects catalysis at maximum rate with the elimination of the induction period normally seen with (η-Arene)$Cr(CO)_3$. Also, addition of arene inhibited the reaction. Therefore, the catalytically active species in the hydrogenation of dienes appears to be formed by the total loss of arene in the presence of a coordinating solvent. In a separate kinetic investigation arene displacement has been found to occur via a stepwise displacement of the ring by the entering ligand [4], thus supporting path b of Cais and Rejoan's mechanism.

As indicated in Table 1.1, various attempts have been made to improve catalytic performance by experimenting with a variety of arenes [3-5,7]. However, the metal-arene bond strength in complexes of this type and consequently the ease of labilization of the arene which has proven necessary for effective catalysis is also a function of the electronic properties of the other ligands bonded to the metal. There-

fore, substituting a carbonyl group by another ligand will also modify the catalytic behaviour of the complex. This is of particular interest in the expectation that the use of a catalyst of the type (η-Arene)Cr(CO)(L)(L") would enhance the regioselectivity of the catalytic process [8-10].

The catalytic behaviour of complexes in which one of the carbonyl ligands has been replaced by a tertiary phosphine has been investigated [11,12]. The results for the hydrogenation of norbornadiene at 170°C under H_2 (48 atm) with these complexes are given in Table 1.2. It is apparent from these results that incorporation of a phosphine ligand into the catalyst brings about serious deterioration or total loss of catalytic activity. This has been attributed to two possible effects. First, the steric effect caused by the substituents on the phosphine may hinder the binding of the substrate. Secondly, the stronger σ-donor and weaker π-acceptor properties of the phosphine relative to CO lead to an increased electron density at the metal, resulting in strengthening of the metal-arene bond due to increased metal → arene π-back-donation [11,12]. One then concludes that ligands chosen to replace CO should be similar to CO in their electronic properties.

Another ligand type with analogous binding properties to those of CO is the isocyanide CNR (R = alkyl or aryl). Initial testing of these complexes for catalytic activity

Table 1.2. Hydrogenation of Norbornadiene (0.1 M) to Nortricyclene (I), Norbornene (II) and Norbornane (III) Catalyzed by (η-Arene)$Cr(CO)_2L$[a]

Catalyst[b]	% Conversion	Product (% distribution)[c]			Rxn. time
		I	II	III	h
(phen)$Cr(CO)_3$[d]	100	38	43	19	3
	100	80	20	0	2
(dmt)$Cr(CO)_3$	95	35	45	15	6
(phen)$Cr(CO)_2(Et_3P)$	0	–	–	–	15
(phen)$Cr(CO)_2[(EtO)_3P]$	0	–	–	–	15
(phen)$Cr(CO)_2(Ph_3P)$	10	5	2	2	8
	30	12	15	3	30
(mbz)$Cr(CO)_2[(PhO)_3P]$	15	3	10	2	30
(dmt)$Cr(CO)_2(CNCH_2Ph)$	20	8	10	2	15
(mbz)$Cr(CO)_2$[CNC(O)Ph]	53	15	30	7	7
(dmt)$Cr(CO)_2$[CNC(O)Me]	65	30	32	3	27
(mbz)$Cr(CO)_2$(CS)	2	<1	<1	<1	20

[a]Data from References 10 and 11.
[b]Catalyst concentration, 5×10^{-3} M.
[c]Reaction conditions: 48 atm H_2, 170°C, cyclohexane solution.
[d]phen = phenanthrene, dmt = dimethyl terephthalate, mbz = methyl benzoate.

proved disappointing (Table 1.2) [11], indicating that the isocyanide ligands used were similar in bonding properties to tertiary phosphines. Dabard et al. [11] postulated that with the proper modification of the R group through the introduction of an N-acyl moiety [CNC(O)R] the π-acceptor properties of the isocyanide could be enhanced sufficiently to effect ring lability under catalytic conditions. Preliminary testing of these complexes proved that they indeed possessed catalytic activity superior to that of (η-Arene)-$(CO)_2$(CNR) [11]. Hence an increase in the π-acceptor properties of the isocyanide ligand was found to enhance catalytic activity.

Among the coordinating ligands that exhibit similar binding properties to those of CO and are known to be stronger π-acceptors than CO are the thiocarbonyl and selenocarbonyl ligands [13]. They thus appear to be very suitable candidates for enhancing the accessibility of the catalytic species. However, an investigation of the catalytic activity of (mbz)$Cr(CO)_2$(CS) (Table 1.2) has shown the thiocarbonyl complex to be one of the worst catalysts for the hydrogenation of dienes tested [11]: Under mild conditions no reaction took place, while at higher temperatures total decomposition of the complex was observed [11].

In the next chapter, the reactivities of Group VIB metal thiocarbonyl and selenocarbonyl complexes will be

reviewed. Investigations of arene displacement reactions of (η-Arene)$Cr(CO)_2(CX)$ (X = S, Se) complexes will then be presented. Subsequently, the kinetic studies of such reactions will be described, and the results compared to those for analogous carbonyl complexes. This should provide some reasons for the lack of catalytic activity of (η-Arene)-$Cr(CO)_2(CS)$ complexes and give some indication as to the catalytic potential of the corresponding selenocarbonyl complexes in the hydrogenation of dienes to monoolefins.

References

1. M.F. Farona, in "Organometallic Reactions and Synthesis", Vol. 6, E.I. Becker and M. Tsutsui, eds., Plenum Press, New York, 1977, Chap. 3, and references therein.
2. E.N. Frankel, E. Selke and C.A. Glass, J. Am. Chem. Soc., 90, 2446 (1968).
3. M. Cais and A. Rejoan, Inorg. Chim. Acta, 14, 509 (1970).
4. G. Yagupsky and M. Cais, Inorg. Chim. Acta, 12, L27 (1975).
5. M. Cais, D. Fraenkel and K. Weidenbaum, Coord. Chem. Rev., 16, 27 (1975).
6. R.P.A. Sneeden, "Organochromium Compounds", Academic Press, New York, 1975, pp. 18-25, 114-123, 189-214 and references therein.
7. P. Le Maux, J.Y. Saillard, D. Grandjean and G. Jaouen, J. Org. Chem., 45, 4524 (1980).
8. G. Jaouen, Tetrahedron Lett., 52, 5159 (1973).
9. G. Jaouen, A. Meyer and G. Simonneaux, Tetrahedron Lett., 52, 5163 (1973).
10. G. Simonneaux, P. Le Maux, G. Jaouen and R. Dabard, Inorg. Chem., 18, 3167 (1979).

11. R. Dabard, G. Jaouen, G. Simonneaux, M. Cais, D.H. Kohn, L. Lapid and D. Tatarsky, J. Organometal. Chem., 184, 91 (1980).

12. M. Cais, M. Kaftory, D.H. Kohn and D. Tatarsky, J. Organometal. Chem., 184, 103 (1980).

13. I.S. Butler, Acc. Chem. Res., 10, 359 (1977) and references therein.

Chapter 2

Reactions of (η-Arene)$Cr(CO)_2$(CX) (X = S, Se) Complexes with Tertiary Phosphites and Tridentate Phosphine Ligands

2.1 Thermal Reactivity of Group VIB Metal(0) Thiocarbonyl and Selenocarbonyl Complexes

The bonding properties of the thiocarbonyl and selenocarbonyl ligands in Group VIB metal complexes have been investigated extensively by a variety of spectroscopic and other techniques [1,2]. The two spectroscopic methods which have been most widely used are vibrational [2-7] and ^{13}C NMR spectroscopy [5,8-10]. Other investigations have employed ^{17}O NMR [11], photoelectron [12,13], electronic [5,14], and mass spectroscopy [15], and ESCA [16]. The body of evidence thus obtained has revealed that both the thiocarbonyl and selenocarbonyl ligands are stronger σ-donors and π-acceptors than CO in complexes with low oxidation state metals. For instance, in the case of IR studies, comparison between the carbonyl stretching force constants of π-bonded arene metal tricarbonyl complexes and those of their corresponding thio- or selenocarbonyl derivatives where one of the CO ligands has been replaced by a CS or CSe ligand shows an increase in carbonyl bond order in the latter complexes [2,4,9]. This observation indicates that the carbonyl groups receive less electron density from the metal, illustrating that the CS

and CSe groups are capable of accepting more electron density from the metal than is CO. Good correlations between carbonyl stretching force constants and the carbonyl resonances in the ^{13}C NMR spectra of (η-Arene)$M(CO)_2(CX)$ (X = S, Se) complexes have been reported [5,8,9]. The incorporation of a CX ligand into a complex results in an upfield shift of the carbonyl resonances, indicative of a decrease in the donation of electron density from the metal to the CO groups.

In view of the differences between the CX and CO ligands, the chemical behaviour of thio- and selenocarbonyl complexes and their carbonyl analogues would also be expected to differ. The existing data on the thermal reactivity of Group VIB metal thio- and selenocarbonyl complexes are discussed below and are schematically reviewed in Figures 2.1 and 2.2.

Treatment of $Cr(CO)_5(CS)$ in refluxing toluene or of $W(CO)_5(CS)$ in refluxing xylene with Ph_3P [Eq. 2.1] yields both <u>cis</u> and <u>trans</u> isomers of $M(CO)_4(CS)(Ph_3P)$.

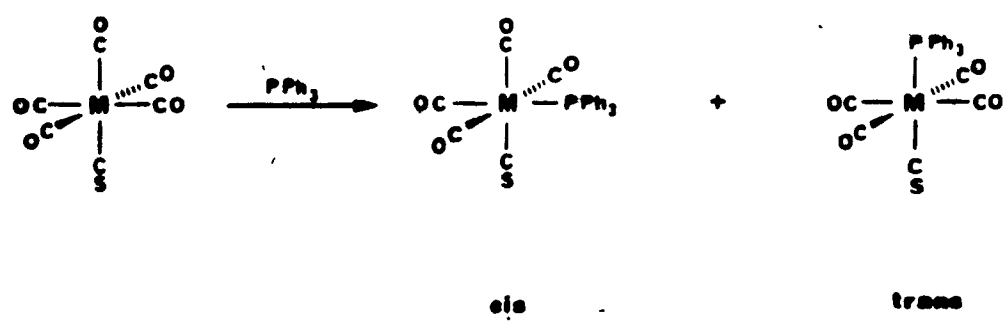

(2.1)

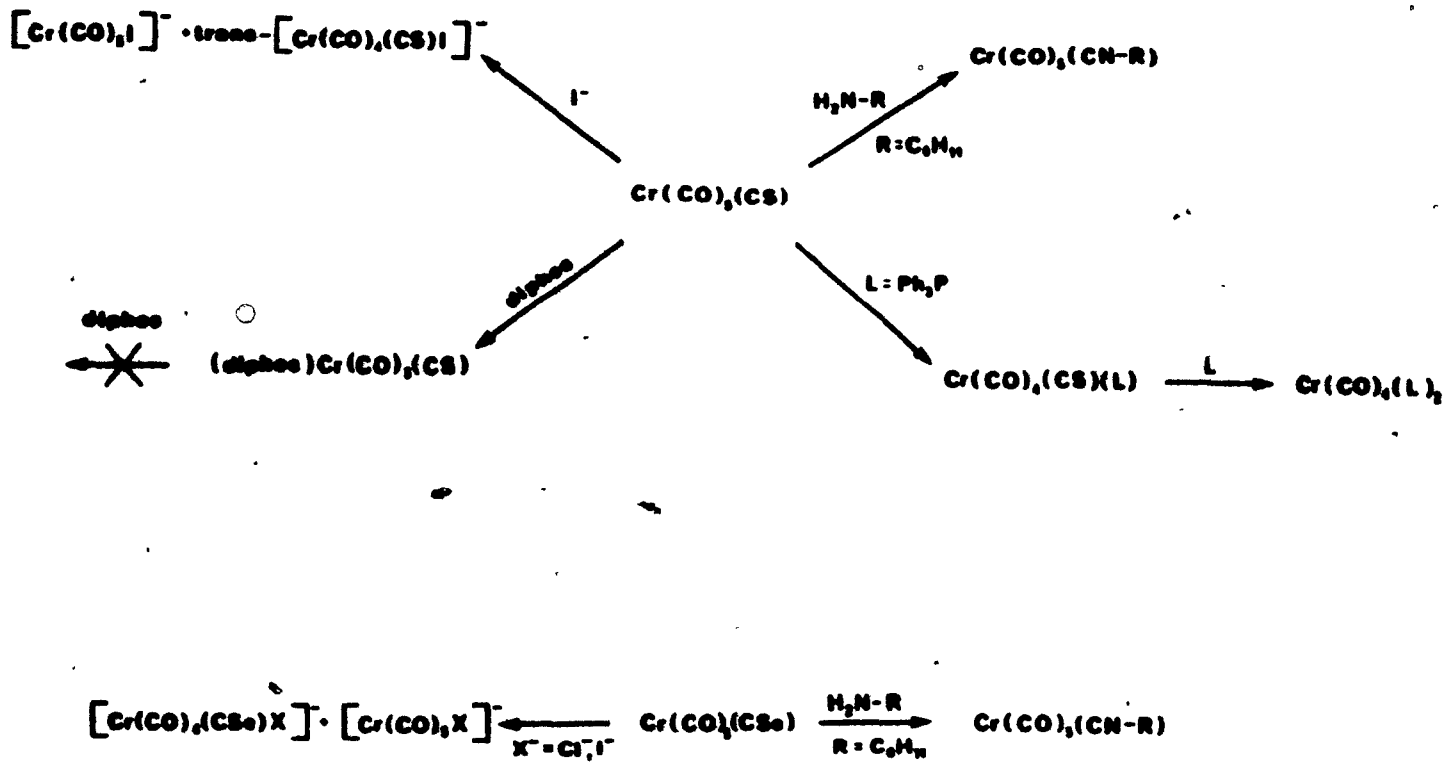

Figure 2.1. Thermal reactivities of $Cr(CO)_5(CS)$ and $Cr(CO)_5(CSe)$.

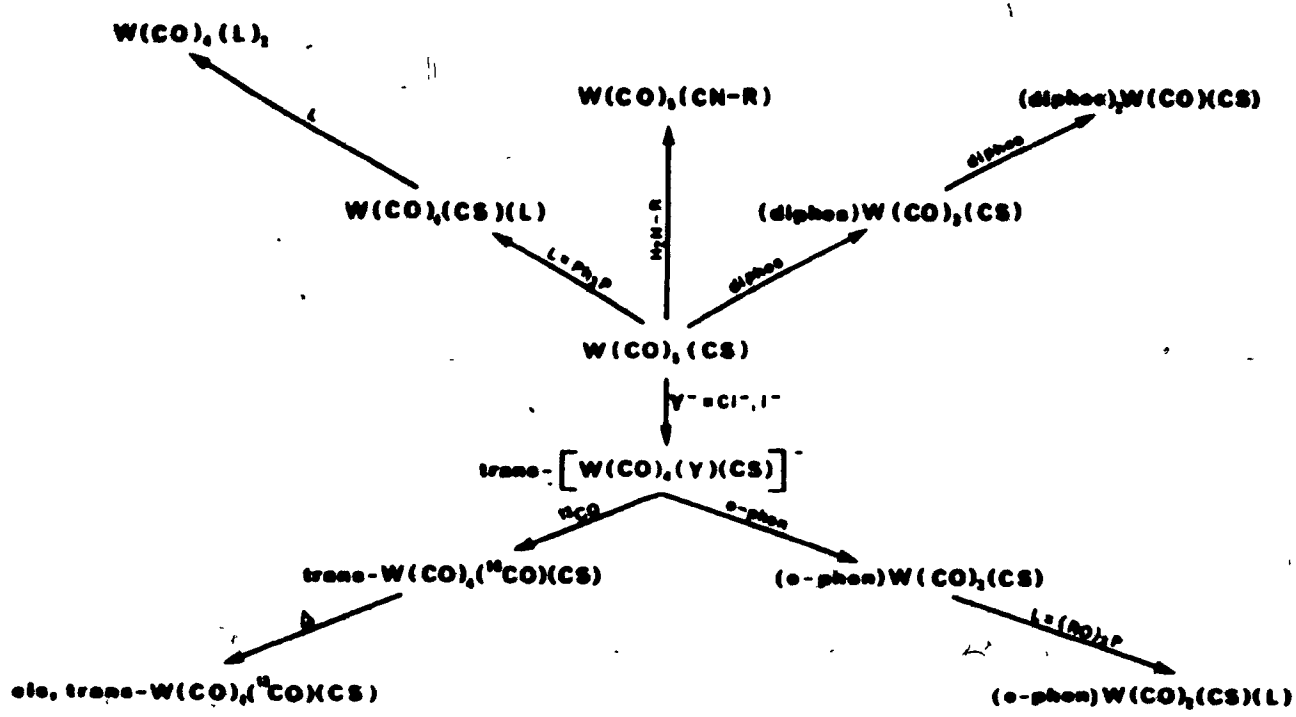

Figure 2.2. Thermal reactivities of $W(CO)_5(CS)$.

These isomers were inseparable by either column chromatography or fractional distillation [17]. Synthesis of pure trans-$W(CO)_4(CS)(Ph_3P)$ by a different route (vide infra; Eq. 2.2) and subsequent heating at 105°C results in its isomerization to an equilibrium mixture of cis and trans with a much higher proportion of trans (cis:trans ~ 0.7:1) isomer than predicted on the basis of a statistical distribution of the phosphine (cis:trans 4:1), demonstrating that the configuration in which the CS ligand is trans to a weak π-acceptor such as Ph_3P rather than trans to CO is favoured [18]. Investigations [19] using stereospecifically ^{13}CO-labelled trans-$W(CO)_4(^{13}CO)(CS)$ revealed that this complex undergoes intramolecular isomerization to form cis- and trans-$W(CO)_4(^{13}CO)(CS)$ isomers in both decalin solution and the gas phase.

Further attempts to displace a second CO with another phosphine yielded $M(CO)_4(Ph_3P)_2$ as the major product, as well as spectroscopic amounts of $M(CO)_3(CS)(Ph_3P)_2$, which was not isolated [17]. However, the bidentate ligand ethylenebis(diphenylphosphine) (diphos) was found to react with $M(CO)_5(CS)$ (M = Cr, W) to yield one product [17], $M(CO)_3(CS)$(diphos), which was assigned a mer geometry on the basis of its IR spectrum; two carbonyl stretching modes were observed - a weak band at higher energy, attributed to the a' stretching mode of the two trans carbonyls, and a strong

band at lower frequency assigned to the a" mode. The third band expected for this structure was presumed hidden under the strong lower-frequency band. Extended reaction of $W(CO)_5(CS)$ in excess diphos at very high temperatures yielded $W(CO)(CS)(diphos)_2$. However, no substitution beyond a single diphos ligand was observed for chromium [17]. Reactions of $W(CO)_5(CS)$ with other bidentate ligands containing nitrogen, such as 2,2'-bipyridine (bpy) or o-phenanthroline (o-phen), yielded no thiocarbonyl-containing products, giving only $W(CO)_4$(bpy) and $W(CO)_4$(o-phen), respectively [17]. Reaction with pyridine (py) produced large amounts of $W(CO)_5$(py) [17]. $Cr(CO)_5(CX)$ (X = S, Se) reacts with tetrabutylammonium halides to give a mixture of $[Cr(CO)_5(Y)]^-$ and trans-$[Cr(CO)_4(CX)(Y)]^-$ in a ratio of 2/3 for X = S and $Y^- = I^-$, Cl^- [5], while for X = Se a 5/4 mixture is obtained for $Y^- = Cl^-$ and a 3/1 mixture for $Y^- = I^-$ [5,20]. In order to establish if $[Cr(CO)_5(Y)]^-$ was produced by thermal decomposition of the trans-$[Cr(CO)_4(CX)(Y)]^-$ ion, thermal decomposition of a $[Cr(CO)_5(Y)]^-$/trans-$[Cr(CO)_4(CX)(Y)]^-$ mixture was monitored by IR spectroscopy; no increase in the intensities of the ν(CO) bands due to the $[Cr(CO)_5(Y)]^-$ ion was observed [20]. On the other hand, $W(CO)_5(CS)$ reacts with tetrabutylammonium halides in a coordinating solvent (e.g., acetone, THF) to produce only one product [17], trans-$[W(CO)_4(CS)(Y)]^-$ ($Y^- = Cl^-$, Br^-, I^-).

The iodide complex undergoes halide abstraction and ligand substitution forming exclusively the <u>trans</u> product according to Eq. 2.2 [17].

$$[\underline{trans}\text{-}W(CO)_4(CS)(I)]^- + Ag^+ + L \rightarrow \underline{trans}\text{-}W(CO)_4(CS)(L) + AgI \qquad (2.2)$$

Halide abstraction and subsequent coordination of bpy or <u>o</u>-phen in the presence of a coordinating solvent yields <u>mer</u>-$W(CO)_3(CS)(bpy)$ or <u>mer</u>-$W(CO)_3(CS)$(<u>o</u>-phen), respectively [21]. These products were inaccessible through direct reaction of the bidentate ligand with $W(CO)_5(CS)$.

It should be mentioned that $M(CO)_5(CX)$ (X = S, Se) complexes exhibit other types of thermal reactivity, in addition to ligand substitution. Both chromium and tungsten thiocarbonyls as well as the chromium selenocarbonyl derivative undergo reactions with primary amines to produce $M(CO)_5(CNR)$ (R = alkyl group) [20,22]. $W(CO)_5(CS)$ has also been found [22] to react with secondary amines forming thioformamide complexes, $W(CO)_5(S{=}C(H)NR_2)$. Kinetic investigations of the reaction of $W(CO)_5(CS)$ with primary amines revealed a second-order dependence on amine concentration and a first-order dependence on the concentration of the thiocarbonyl complex [22]. The mechanism proposed on the basis of these data involves attack of a hydrogen-bonded

amine molecule, $RHN\text{-}H...NH_2R$, at the carbon of the thiocarbonyl ligand. Thus a second amine molecule acts as a catalyst, presumably by increasing the nucleophilicity of the attacking amine [22]. The reaction of cis- and trans-$W(CO)_4(CS)(Ph_3P)$ with primary amines was found to be much slower than that of $W(CO)_5(CS)$, with the cis isomer reacting faster than the trans [22]. The low reactivity of trans-$W(CO)_4(CS)(Ph_3P)$ [approx. 20,000 times slower than $W(CO)_5(CS)$] has been attributed to increased electron density at the thiocarbonyl carbon due to the trans Ph_3P ligand, rendering attack by a nucleophile less favourable.

The kinetics of carbonyl substitution in $W(CO)_5(CS)$ by Ph_3P were studied [17] to gain quantitative information about the reactivity of this complex compared to that of $W(CO)_6$. The rate was found to have a ligand-independent term and a ligand-dependent term as shown in Eq. 2.3.

$$\text{rate} = k_1[W(CO)_5(CS)] + k_2[W(CO)_5(CS)][Ph_3P] \qquad (2.3)$$

This is analogous to the accepted mechanism for CO substitution in $W(CO)_6$ [23]. Comparison of k_1 and k_2 for the thiocarbonyl complex with values obtained for the reaction of $W(CO)_6$ with Ph_3P reveals that the dissociative mechanism is approximately 75 times faster in $W(CO)_5(CS)$

while the associative (k_2) route is 250 times faster [17]. Another kinetic study [17] involving the associative reaction of $W(CO)_5(CS)$ with I^- showed that $W(CO)_5(CS)$ reacts more than 1000 times faster with I^- than does $W(CO)_6$ under the same conditions.

The reaction of trans-$W(CO)_4(^{13}CO)(CS)$ with I^- revealed that the trans CO is lost with high specificity [19]. The mechanism was postulated to involve attack by I^- at the metal accompanied by dissociation of the trans CO. Alternatively, the I^- may attack the C atom of the trans CO; subsequent rearrangement and loss of the trans CO would give the observed product. These two possibilities could not be distinguished on the basis of the kinetic data available [19].

A kinetic study of carbonyl dissociation from $W(CO)_3$-(CS)(o-phen) has also been reported [Eq. 2.4] [21].

$$W(CO)_3(CS)(o\text{-phen}) + L \rightarrow W(CO)_2(CS)(o\text{-phen})(L) + CO$$
$$[L = (MeO)_3P,\ (EtO)_3P,\ Ph_3P] \qquad (2.4)$$

The rate of the reaction follows a general two-term rate expression [Eq. 2.5] in which $k_{obsd} = k_1 + k_2[L]$ under pseudo-first-order conditions.

$$\text{Rate} = k_1 [W(CO)_3(CS)(\underline{o}\text{-phen})] + k_2 [W(CO)_3(CS)(\underline{o}\text{-phen})][L] \quad (2.5)$$

At higher temperatures, the k_1 term predominates and k_{obsd} is independent of the concentration and the nature of the ligand [21]. At lower temperatures the rate shows a small but significant dependence on ligand concentration. A direct comparison of the rates of the dissociative pathway for the thiocarbonyl complex and $W(CO)_4(\underline{o}\text{-phen})$, made by extrapolating the rate constant for the thiocarbonyl reaction to the temperature at which the reaction of $W(CO)_4(\underline{o}\text{-phen})$ was studied [24], yields a k_1 value approximately 140 times faster for CO dissociation from the thiocarbonyl complex than from the carbonyl analogue.

The only kinetic data obtained for the reaction of Group VIB metal thiocarbonyl complexes have been those presented above for $W(CO)_5(CS)$ and its derivatives. These data have illustrated the difference between carbonyl and thiocarbonyl reactivity. The CS ligand, being a stronger π-acceptor than CO, limits the electron density available at the metal for π-backbonding to the carbonyl groups, especially the carbonyl <u>trans</u> to it. The CS ligand thus activates the complex to substitution by weakening the M-CO bonds (predominantly the <u>trans</u> M-CO bond), thereby reducing the activation energy and enhancing the rate of CO dissociation [17].

A striking example of labilization of ligands other than CO resulting from the presence of a thiocarbonyl or a selenocarbonyl ligand in a complex is the arene labilization observed for (η-Arene)$Cr(CO)_2(CX)$ (X = S, Se) [2,5,20]. $Cr(CO)_5(CS)$ can be prepared by heating (mbz)$Cr(CO)_2(CS)$ under CO pressure (10 atm) at 65°C for 5 h. These conditions are much milder than those required to produce $Cr(CO)_6$ from (mbz)$Cr(CO)_3$ (65°C, 20 atm CO, 6 days). In addition, the lability of the arene in (η-Arene)$Cr(CO)_2(CSe)$ complexes is even more pronounced; (mbz)$Cr(CO)_2(CSe)$ reacts with CO at 10 atm pressure in 1 h at 65°C to yield $Cr(CO)_5(CSe)$.

Apart from the reactions with CO mentioned above, the thermal reactivity of (η-Arene)$Cr(CO)_2(CX)$ (X = S, Se) has not been previously investigated. In the present chapter, reactions of these complexes involving arene displacement by trialkyl- and triarylphosphites and selected tridentate phosphine ligands will be described.

2.2 Experimental

All synthetic reactions were performed under an atmosphere of prepurified nitrogen. All solvents were freshly distilled over sodium strips under nitrogen prior to use with the exception of 1,2-dichloroethane and CS_2 which were distilled over calcium chloride and molecular sieves, respectively.

Trialkyl- and triarylphosphites were purchased from Aldrich Chemical Co., with the exception of $(C_6H_{11}O)_3P$ which was obtained from Strem Chemicals. Carbon diselenide, chromium hexacarbonyl and the tridentate ligands bis(2-diphenylphosphinoethyl)phenylphosphine (triphos), 1,1,1-tris(diphenylphosphinomethyl)ethane (triphos-U) and 1,1,1-tris(diphenylphosphino)methane (tripod) were purchased from Strem. $(cht)Cr(CO)_3$ was either prepared by the literature method [25], or purchased from Strem.

FT-IR spectra were recorded on a Nicolet 6000 spectrometer (32 scans, 1 cm^{-1} resolution). Proton, ^{13}C and ^{31}P NMR spectra were measured on a Varian XL-200 or XL-300 spectrometer equipped with a broad-band probe. The chemical shifts reported here are relative to TMS (^{1}H and ^{13}C) and 85% H_3PO_4 (^{31}P).

Chromatographic separation of the products was performed by column chromatography (silica gel 60-200 mesh) under N_2 atmosphere or on preparative TLC plates (1 mm) prepared from a slurry of 80 g silica gel G (Macherey, Nagel & Co., 516 Durn, West Germany) and 180 ml water. The plates were activated prior to use by heating them at 110°C for 1 h.

2.2.1 Synthesis of (η-Arene)$Cr(CO)_3$

All (η-Arene)$Cr(CO)_3$ complexes were prepared according to a literature method [26], outlined below for (o-xyl)Cr-$(CO)_3$. A 1-liter three-necked flask fitted with a reflux condenser and a cold finger was used. The addition of the cold finger is a new modification that has been found to eliminate the possibility of the condenser blocking with the easily sublimable starting material $Cr(CO)_6$.

Preparation of (o-xyl)$Cr(CO)_3$. $Cr(CO)_6$ (9.6 g), o-xylene (50 ml), THF (35 ml) and Bu_2O (230 ml) were added under a stream of N_2 to the 1-liter flask. The mixture was heated slowly (at the reflux temperature of THF) overnight with magnetic stirring, allowing the $Cr(CO)_6$ to dissolve. The temperature was then increased to the reflux temperature of Bu_2O for 2 days. An IR spectrum was measured to confirm the complete disappearance of $Cr(CO)_6$ [ν(CO) 1980 cm^{-1}]. The flask was then cooled and the reaction mixture filtered in air using a sintered glass funnel (medium porosity) to remove any decomposition products. The solvent was then evaporated on a rotary evaporator using a liquid nitrogen trap to collect the solvent. Bright yellow crystals were obtained (yield 9.4 g, 88%).

2.2.2 Synthesis of (η-Arene)$Cr(CO)_2(CS)$

The procedure for arene chromium thiocarbonyl synthesis was identical to that in the literature [27]. However since a large amount of $(bz)Cr(CO)_2(CS)$ was needed for kinetic studies, the procedure was modified to allow bulk synthesis of this complex.

$(bz)Cr(CO)_3$ (6 g) was dissolved in 1.8 liter of benzene and 300 ml of cis-cyclooctene under N_2 in a 3-liter flask. A stainless steel transfer needle (18 gauge) was then used to transfer 700 ml of the solution to a quartz reactor [27]. The solution was then irradiated with a 450-W quartz mercury vapour lamp for 60 min. The reaction was monitored by the increase in the IR carbonyl peaks of $(bz)Cr(CO)_2(C_8H_{14})$ [ν(CO) 1900, 1850 cm^{-1}]. The irradiated solution was then transferred to another 3-liter flask. After two additional cycles of this procedure, 500 ml of CS_2 were added to the irradiated solution. The workup at this point was identical to the established method [27].

2.2.3 Synthesis of (η-Arene)$Cr(CO)_2(CSe)$

(η-Arene)$Cr(CO)_2(CSe)$ complexes were synthesized according to the previously reported procedure [28]; attempts to scale up the reaction resulted in poor yields.

2.2.4 Synthesis of $Cr(CO)_2(CX)[(RO)_3P]_3$ (X = S, Se), (R = Me, Et, n-Bu, Ph)

All $Cr(CO)_2(CX)[(RO)_3P]_3$ complexes were prepared according to the method outlined below for $Cr(CO)_2$-$(CS)[(MeO)_3P]_3$ and $Cr(CO)_2(CSe)[(MeO)_3P]_3$.

Preparation of $Cr(CO)_2(CS)[(MeO)_3P]_3$. $(mbz)Cr(CO)_2(CS)$ (200 mg, 0.69 mmol) was dissolved in toluene (25 ml). $(MeO)_3P$ (1.5 ml, 12.7 mmol) was added and the reaction mixture was heated for 12 h at 65°C under N_2. After allowing the solution to cool to room temperature, all volatile material was removed under reduced pressure on a rotary evaporator. The yellow solid remaining was purified by preparative TLC on silica gel plates (eluent: 1,2-dichloroethane). Yield 275 mg (75%). Anal. (Guelph Chemical Laboratories, Guelph, Ontario, Canada) Calcd. for $C_{12}H_{27}O_{11}P_3SCr$: C, 27.6; H, 5.19; P, 17.7. Found: C, 27.2; H, 5.15; P, 17.0. FT-IR (methylcyclohexane): ν(CO) 1976(w), 1899(vs) cm^{-1}; ν(CS) 1199(m) cm^{-1}. ^1H NMR (CD_2Cl_2): 3.40 (d, J = 11 Hz, 1), 3.72 ppm (d, J = 11 Hz, 2). ^{13}C NMR (CD_2Cl_2): 224.2 (q, J = 22 Hz, 2CO), 336.5 ppm (td, J_t = 30 Hz, J_d = 6 Hz, CS). ^{31}P NMR ($C_6D_5CD_3$): 181.2 (t, J = 65 Hz, 1), 188.6 ppm (d, J = 65 Hz, 2). Crystals were grown in pentane at -20°C.

Preparation of $Cr(CO)_2(CSe)[(MeO)_3P]_3$. The same procedure as described above was utilized for the synthesis of $Cr(CO)_2(CSe)[(MeO)_3P]_3$ from $(bz)Cr(CO)_2(CSe)$ (250 mg, 0.90 mmol) and $(MeO)_3P$ (2.1 ml, 17.8 mmol). Purification by TLC as above gave a bright yellow solid. Yield 355 mg (69%). Anal. (Guelph Chemical Laboratories, Guelph, Ontario, Canada) Calcd. for $C_{12}H_{27}O_{11}P_3SeCr$: C, 25.26; H, 4.74. Found: C, 25.09; H, 4.90. FT-IR (CS_2): ν(CO) 1980.1(w), 1902.8(vs) cm^{-1}; ν(CSe) 1018(m) cm^{-1}. ^1H NMR (C_6D_6): 3.37 (d, J = 10 Hz, 1), 3.81 ppm (d, J = 10 Hz, 2). ^{13}C NMR (C_6D_6): 223.8 (q, J = 22 Hz, 2CO), 356.5 ppm (td, J_t = 29 Hz, J_d = 6 Hz, CSe). ^{31}P NMR ($C_6D_5CD_3$): 177.5 (t, J = 65 Hz, 1), 184.9 ppm (d, J = 64 Hz, 2). Yellow crystals of $Cr(CO)_2(CSe)[(MeO)_3P]_3$ were obtained upon cooling a saturated pentane solution of the complex to -20°C.

2.2.5 Preparation of $(triphos\text{-}U)Cr(CO)_2(CS)$

Triphos-U $[(Me)C(CH_2P(Ph)_2)_3]$ (985 mg, 1.58 mmol) and $(bz)Cr(CO)_2(CS)$ (197 mg, 0.855 mmol) were dissolved under N_2 in 25 ml of toluene. The reaction was heated at 90°C overnight. The resulting solution was evaporated under reduced pressure, affording a yellow solid. The product was purified by TLC on silica gel plates using CS_2 as the moving phase. The yellow fraction was extracted with methylene chloride and evaporated to dryness. The solid obtained was

dissolved in a minimal amount of benzene and hexane was added slowly to precipitate bright yellow crystals. Yield 617 mg (93%). Anal. (Guelph Chemical Laboratories, Guelph, Ontario, Canada) Calcd. for $C_{44}H_{39}O_2P_3SCr$: C, 68.04; H, 5.02. Found: C, 67.87; H, 5.25. FT-IR (CH_2Cl_2): ν(CO) 1927.7(s), 1866.1(s) cm^{-1}; ν(CS) 1190(m) cm^{-1}.

2.2.6 Preparation of (triphos)$Cr(CO)_2$(CS)

Triphos [$(Ph_2PCH_2CH_2)_2PhP$] (1.02 g, 1.91 mmol) and (bz)$Cr(CO)_2$(CS) (203 mg, 0.88 mmol) were dissolved in 25 ml of toluene and heated at 95°C overnight while stirring under nitrogen. The workup was identical to the procedure described above for (triphos-U)$Cr(CO)_2$(CS). Attempts to separate the isomers of (triphos)$Cr(CO)_2$(CS) by TLC using various eluents (1,2-dichloroethane:hexane 3:1, benzene:CS_2 2:1, ethyl acetate:petroleum ether 3:2) were unsuccessful. Yield 570 mg (94%). Anal. (Guelph Chemical Laboratories, Guelph, Ontario, Canada) Calcd. for $C_{37}H_{33}O_2P_3SCr$: C, 64.66; H, 4.85. Found: C, 64.24; H, 5.02. IR (CH_2Cl_2): ν(CO) 1924.0(s), 1860.9(s) cm^{-1}; ν(CS) 1191.4(m) cm^{-1}. ^{31}P NMR ($C_6D_5CD_3$): isomers **A** and **A*** 67.4 (dd, I = 1), 79.8 (dd, I = 1), 107.5 ppm (dd, I = 1); isomer **B** 100.9 (t, I = 1), 71.9 ppm (d, I = 2).

2.2.7 Synthesis of $(L\text{-}L\text{-}L)Cr(CO)_2(CSe)$ (L-L-L = triphos-U, triphos)

These complexes were prepared in quantitative yield according to the methods outlined above for the corresponding thiocarbonyl derivatives.

2.2.8 Reaction of Tripod $[HC(P(Ph)_2)_3]$ with $(bz)Cr(CO)_2(CX)$ (X = S, Se)

583 mg (1.01 mmol) of tripod and an equimolar amount of $(bz)Cr(CO)_2(CX)$ were dissolved in 25 ml of benzene. Decomposition occurred upon heating the reaction mixture with no new peaks appearing in the carbonyl region of the IR spectrum.

2.2.9 Synthesis of $Cr(CO)_3[(RO)_3P]_3$ (R = Me, Et, n-Bu, Ph) and $(L\text{-}L\text{-}L)Cr(CO)_3$ (L-L-L = triphos and triphos-U)

The above complexes were prepared from $(cht)Cr(CO)_3$ by the same procedures as described above for the corresponding thio- and selenocarbonyl derivatives.

2.2.10 Attempted Synthesis of $(cht)Cr(CO)_2(CS)$ by Photolysis of $(cht)Cr(CO)_3$

$(cht)Cr(CO)_3$ (200 mg) was irradiated in 150 ml of toluene in the presence of excess cis-cyclooctene (50% by volume) under N_2 for periods ranging from 1 to 4 h using a

450-W quartz mercury vapour lamp. No changes in the ν(CO) absorptions were observed in the FT-IR spectrum. Warming the solution during irradiation brought about decomposition.

2.2.11 Reaction of $Cr(CO)_5(CS)$ with Cycloheptatriene

$Cr(CO)_5(CS)$ (30 mg) (prepared according to Reference 20) was refluxed in neat cycloheptatriene (30 ml) under N_2. No product formation was detected by FT-IR spectroscopy. In the presence of THF or acetonitrile (10% by volume) decomposition occurred.

2.2.12 Attempted Synthesis of $(cht)Cr(CO)_2(CS)$ by Arene Exchange

$(mbz)Cr(CO)_2(CS)$ (30 mg) was dissolved in 10 ml of neat cycloheptatriene, or in cycloheptatriene containing 10% (by volume) THF or acetonitrile and heated at 65°C under N_2 for periods of 6-48 h. The progress of the reaction was monitored by difference FT-IR spectroscopy. In all cases, gradual decomposition was observed with no appearance of new ν(CO) peaks in the IR spectrum.

2.3 Results and Discussion

Since the synthesis of the first $(\eta\text{-Arene})Cr(CO)_2(CS)$ and $(\eta\text{-Arene})Cr(CO)_2(CSe)$ complexes a decade ago, few chemi-

cal reactions have been reported for them. However, a variety of spectroscopic techniques have provided a clear indication of the bonding properties of the CS and CSe ligands. The synthetic investigations described here have probed further the chemical behaviour of arene chromium thio- and selenocarbonyl complexes. The thermal reactivities of (η-Arene)$Cr(CO)_2(CX)$ (X = S, Se) complexes established in this study together with those reported in the literature are summarized in Figure 2.3.

The major reaction of (η-Arene)$Cr(CO)_2CX$ complexes identified in this work, the kinetics of which will be the subject of Chapter 4, is the displacement of the arene by three tertiary phosphite ligands under relatively mild conditions:

$$(\eta\text{-Arene})Cr(CO)_2(CX) + 3(RO)_3P \rightarrow Cr(CO)_2(CX)[(RO)_3P]_3 + \text{Arene} \qquad (2.6)$$

(R = alkyl or aryl)

The spectroscopic properties and the crystal and molecular structure of a typical product, $Cr(CO)_2(CS)$-$[(MeO)_3P]_3$, are presented in this and the next section. Following this, the crystal structure of the analogous selenocarbonyl derivative will be described.

The $Cr(CO)_2(CS)[(MeO)_3P]_3$ complex is the first example

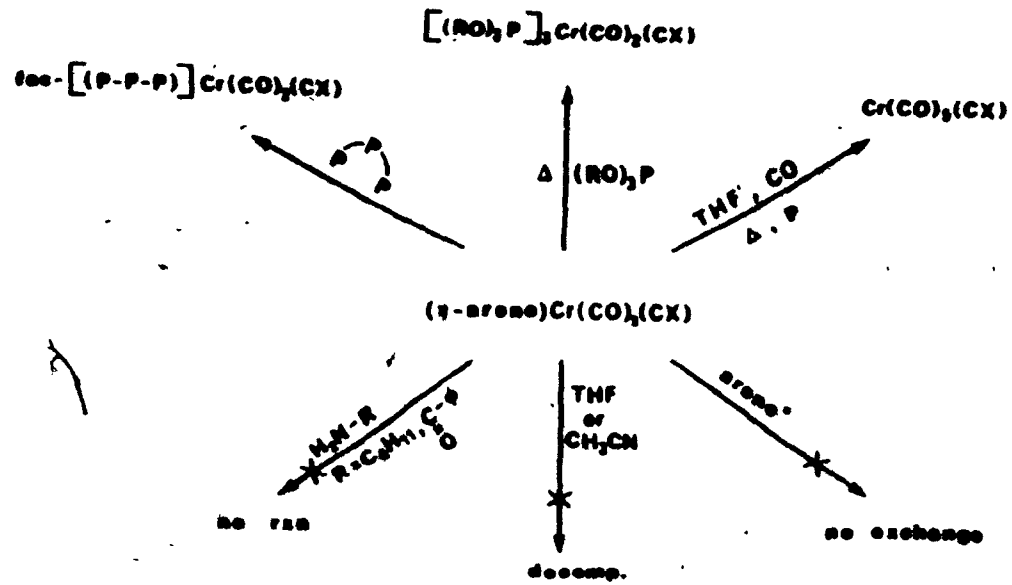

Figure 2.3. Thermal reactivities of $(\eta\text{-Arene})Cr(CO)_2(CX)$ (X = S, Se).

of a substituted Group VIB metal thiocarbonyl complex containing more than one monodentate ligand other than CO. Attempts to prepare such complexes from $Cr(CO)_5(CS)$ by thermal replacement of the CO groups have only resulted in the loss of the CS ligand following the first substitution step, i.e., yielding first $Cr(CO)_4(CS)L$ and then $Cr(CO)_4L_2$ [17]. Thus, arene substitution provides the first entry into multi-substituted complexes of the type $Cr(CO)_2(CS)L_3$.

Arene displacement in (η-Arene)$M(CO)_3$ complexes affords <u>fac</u>-$M(CO)_3L_3$ (M = Cr, L = CH_3CN [29]; M = Mo, L = $(MeO)_3P$, Cl_3P, Ph_2ClP, <u>n</u>-Bu_3P [30,31]; M = W, L = $(MeO)_3P$ [32]). <u>fac</u>-$M(CO)_3[(MeO)_3P]_3$ (M = Cr, Mo, W) has also been synthesized by the substitution of cycloheptatriene in (cht)$M(CO)_3$ by $(MeO)_3P$ [25]. The <u>fac</u> stereochemistry of the products was established by the appearance of two strong ν(CO) peaks in the IR spectra, in accord with the C_{3v} local symmetry of the $M(CO)_3$ moiety [Γ(CO) = a_1 + e]. In the present work, as well as in other studies [25], it has been observed that cycloheptatriene displacement from (cht)$Cr(CO)_3$ by $(MeO)_3P$ in refluxing methylcyclohexane yields a mixture of <u>fac</u>- and <u>mer</u>-$Cr(CO)_3[(MeO)_3P]_3$. Similar mixtures are obtained from the reactions of (η-Arene)$Cr(CO)_3$ complexes with monodentate ligands at high temperatures, as evidenced by the appearance of a third ν(CO) band in the IR spectra and the splitting patterns in the ^{31}P NMR spectra of the products [33].

While the reactions of the tricarbonyl complexes described above give predominantly the fac isomer under the conditions employed in this work, the ν(CO) region in the FT-IR spectrum of $Cr(CO)_2(CS)[(MeO)_3P]_3$ with one very strong and one very weak band being observed is clearly at variance with the intensity pattern expected for the fac isomer. The spectrum of the latter should most likely resemble that of fac-$Cr(CO)_3L_3$ with two strong peaks of comparable intensity. The FT-IR spectrum of the crude product of this reaction, prior to TLC purification, exhibits an additional peak in the CO stretching region at 1961 cm^{-1} of weak intensity (~10% of that of the 1899 cm^{-1} peak) (Figure 2.4). It will be shown below that this peak can be assigned to fac-$Cr(CO)_2(CS)[(MeO)_3P]_3$.

The very low intensity of the 1976 cm^{-1} peak of the major product is immediately suggestive of the mer geometry (mer I, Figure 2.5) in which the two CO groups are trans to each other. The mer stereochemistry is further indicated by the similarity of the ^{31}P NMR spectrum to that of mer-$Cr(CO)_3[(MeO)_3P]_3$ in $C_6D_5CD_3$ solution (Table 2.10), even down to the $^2J_{^{31}P\,^{31}P}$ couplings (64 Hz). The solitary ^{13}C resonance for the CO groups is evidence of the absence of mer II and its appearance as a quartet is in complete agreement with the splitting pattern expected for mer I provided that the two different tertiary phosphite environments are

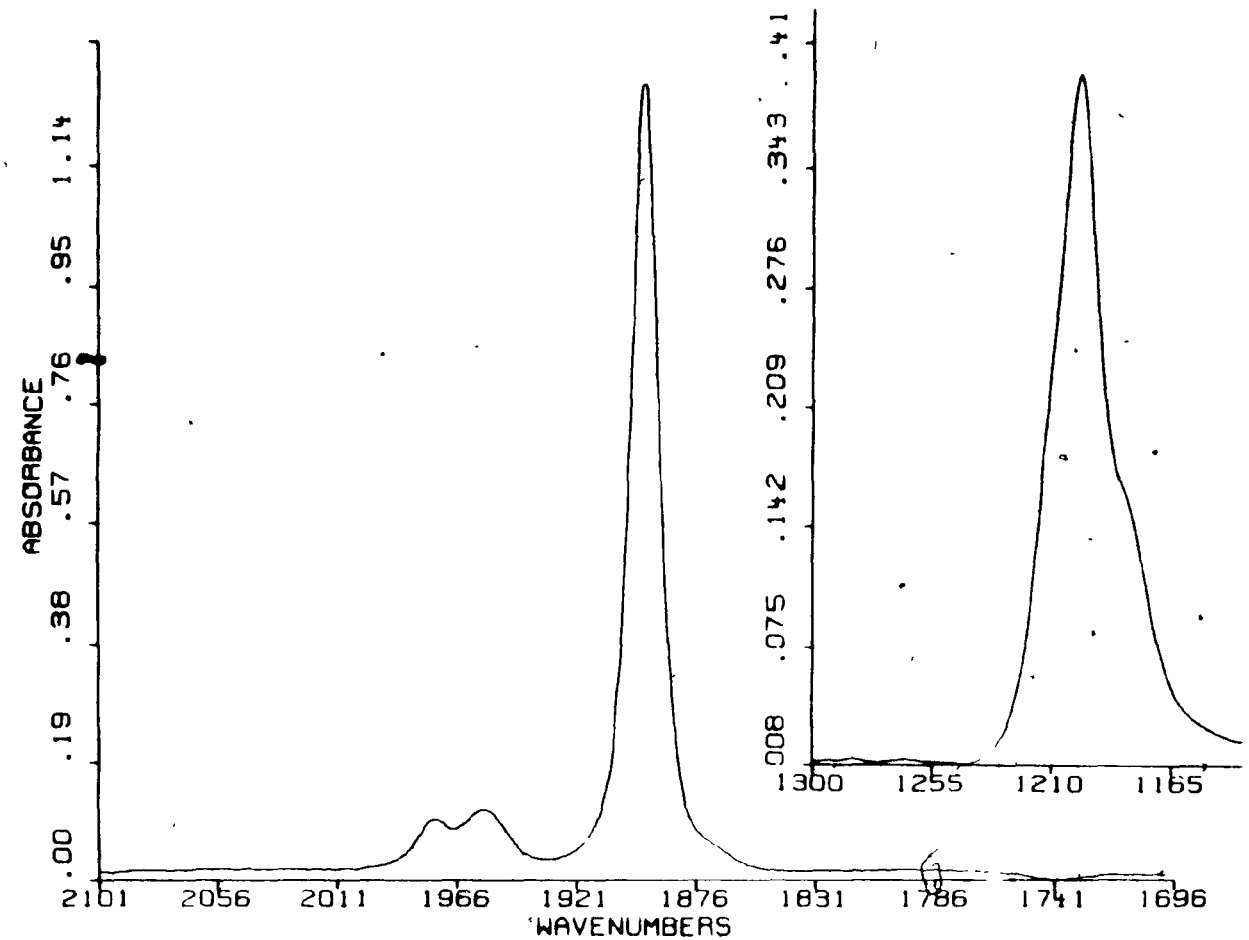

Figure 2.4. The ν(CO) region of the FT-IR spectrum (in methylcyclohexane) of the crude product of the reaction of (mbz)$Cr(CO)_2$(CS) with $(MeO)_3P$. Inset: ν(CS) region.

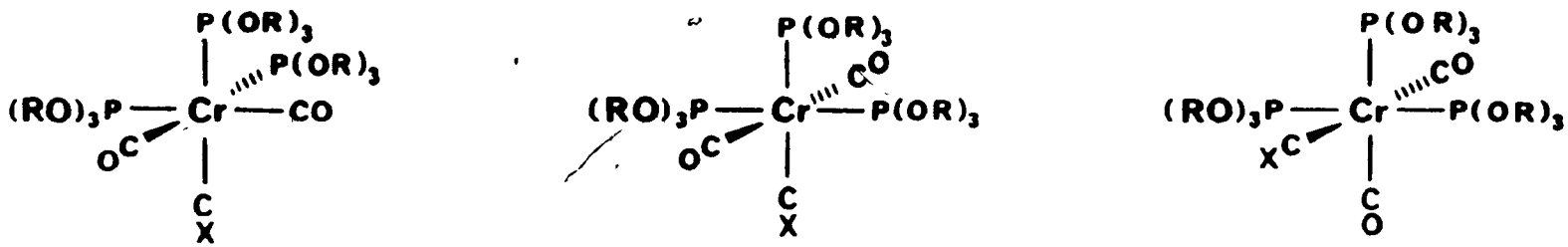

R = Me, Et, n-Bu, Ph
X = S, Se

Figure 2.5. The three possible isomers of $Cr(CO)_2(CX)[(MeO)_3P]_3$ (X = S, Se).

sufficiently similar to afford comparable $^{2}J^{cis}_{^{13}C\,^{31}P}$ values. The observed coupling constant (22 Hz) is very close to the $^{2}J^{cis}_{^{13}C\,^{31}P}$ value reported for $Cr(CO)_5[(MeO)_3P]$ and trans-$Cr(CO)_4[(MeO)_3P]_2$ (21 Hz) [34]. The ^{13}CS resonance appears as a doublet, due to coupling with the trans ^{31}P nucleus, split into a triplet by the other two equivalent ^{31}P nuclei, again in accord with the predictions for mer I.

As mentioned above, the CO stretching region of the IR spectrum of the crude product obtained in the synthesis of $Cr(CO)_2(CS)[(MeO)_3P]_3$ contains, in addition to the peaks of mer-$Cr(CO)_2(CS)[(MeO)_3P]_3$, a weak peak at 1961 cm^{-1}. Subtraction of the spectrum of the pure mer product from this spectrum reveals a second peak at 1899 cm^{-1} of comparable intensity to that at 1961 cm^{-1}, as well as a peak in the $\nu(CS)$ region at 1199 cm^{-1}. These data indicate that some quantity of either the fac or mer II isomer is present in the crude product. Further examination of the crude product using ^{13}C and ^{31}P NMR spectroscopy provided definitive evidence that the minor component present is fac-$Cr(CO)_2(CS)$-$[(MeO)_3P]_3$. In addition to the peaks attributable to the mer I isomer, the ^{13}C NMR spectrum exhibits a single ^{13}CO resonance (δ = 226.3 ppm) split into a doublet of triplets and a ^{13}CS resonance (δ = 335.3 ppm) also split into a doublet of triplets. It is well established [8,34] that chalcocarbonyl resonances exhibit a downfield shift when

they are trans to a stronger σ-donor or a weaker π-acceptor than CO. On this basis the mer II isomer would be expected to exhibit a thiocarbonyl resonance at higher field than observed for the mer I isomer and two distinct carbonyl resonances, one at higher field than that of the mer I for the CO trans to the CS ligand, and the other at lower field for the CO trans to the phosphite group. Therefore, the ^{13}C NMR data are inconsistent with the identification of the minor product as the mer II isomer. For the fac isomer a single carbonyl resonance situated at lower field than that of the mer I isomer is expected, while the thiocarbonyl resonance is anticipated to appear at higher field on the basis that the CO groups should remove a larger share of the electron density donated by the tertiary phosphites to the metal in the fac isomer (CO trans to phosphite) than in the mer I (CO cis to phosphite) isomer. These predictions are completely in accord with the observed ^{13}C NMR spectra. The peaks in the ^{31}P NMR spectrum attributed to the minor product are also consistent with its identification as fac-$Cr(CO)_2(CS)[(MeO)_3P]_3$ with the two equivalent phosphorus nuclei (trans to CO) being split into a doublet by the third phosphorus (trans to CS) which in turn is split into a triplet. The fact that this doublet is at higher field than the doublet of the mer I is in line with the ^{31}P NMR observations made by Poilblanc and his coworkers that two trans

phosphorus ligands appear at lower field than a phosphorus ligand trans to CO for $M(CO)_3[(MeO)_3P]_3$ (M = Cr, Mo, W) [33].

The IR, ^{13}C NMR and ^{31}P NMR spectra of the crude and the purified product from the reaction of (η-Arene)-$Cr(CO)_2(CSe)$ with $(MeO)_3P$ exhibit the same intensity patterns as observed for the thiocarbonyl product. Thus, the characterization of both the mer I and fac isomers was established in a similar manner to the spectroscopic analysis described for $Cr(CO)_2(CS)[(MeO)_3P]_3$. The FT-IR spectrum of the crude $Cr(CO)_2(CSe)[(MeO)_3P]_3$ product is shown in Figure 2.6, while that of the yellow crystals obtained by TLC purification is displayed in Figure 2.7. The difference spectrum generated by subtraction of Figure 2.7 from Figure 2.6 is displayed in Figure 2.8, revealing the hidden ν(CO) peak of the fac isomer. The ^{13}C NMR spectrum (Figure 2.9) clearly shows the patterns expected for the mer I and fac isomers. The spectroscopic properties of $Cr(CO)_2(CX)$-$[(RO)_3P]_3$ (X = O, S, Se; R = Me, Et, n-Bu, Ph) derivatives will be discussed more fully in Section 2.3.3.

2.3.1 Crystal and Molecular Structure of $Cr(CO)_2(CS)$-$[(MeO)_3P]_3$

The mer stereochemistry (mer I) of the chromium thiocarbonyl derivative was confirmed by single-crystal X-ray

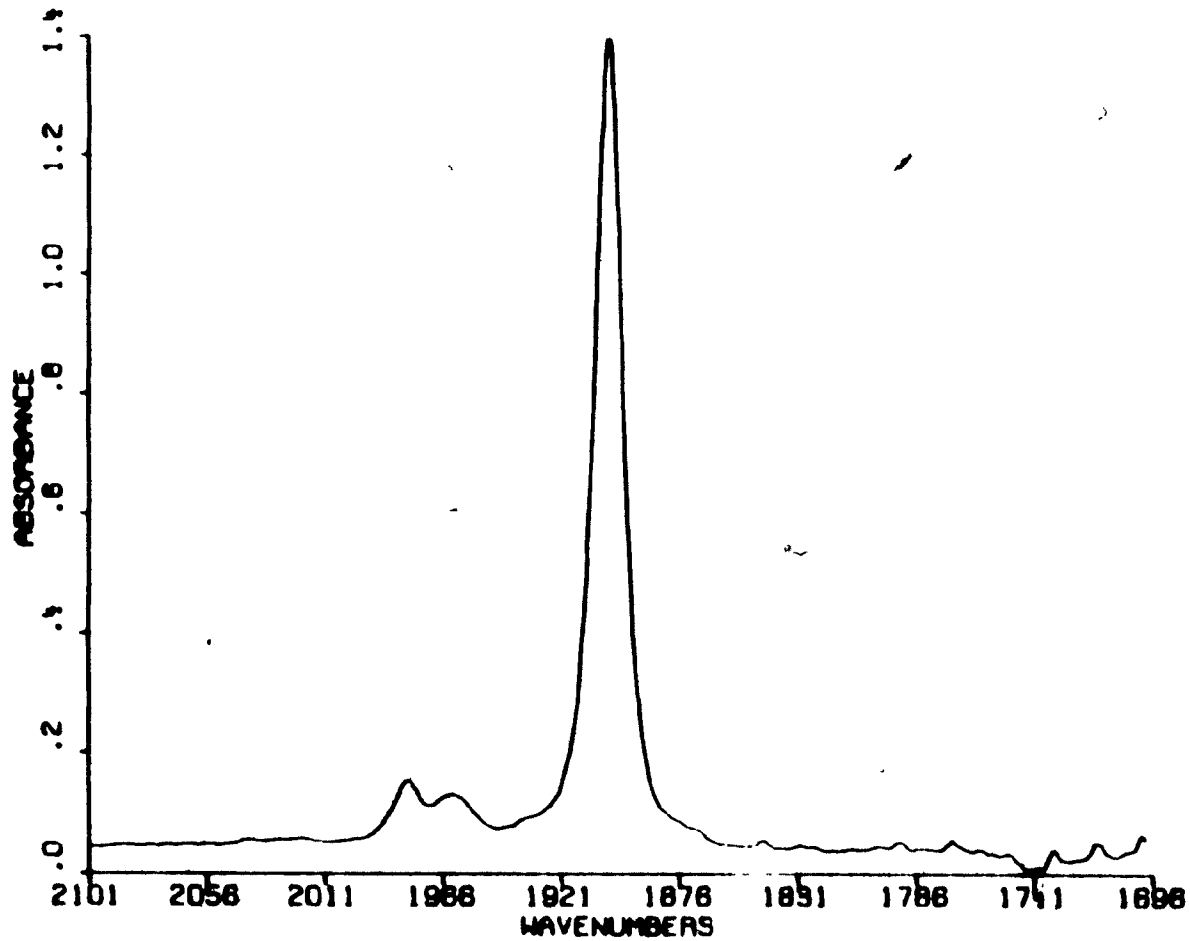

Figure 2.6. The ν(CO) region of the FT-IR spectrum (in CS_2) of the crude product of the reaction of (mbs)$Cr(CO)_2$(CSe) with $(MeO)_3P$.

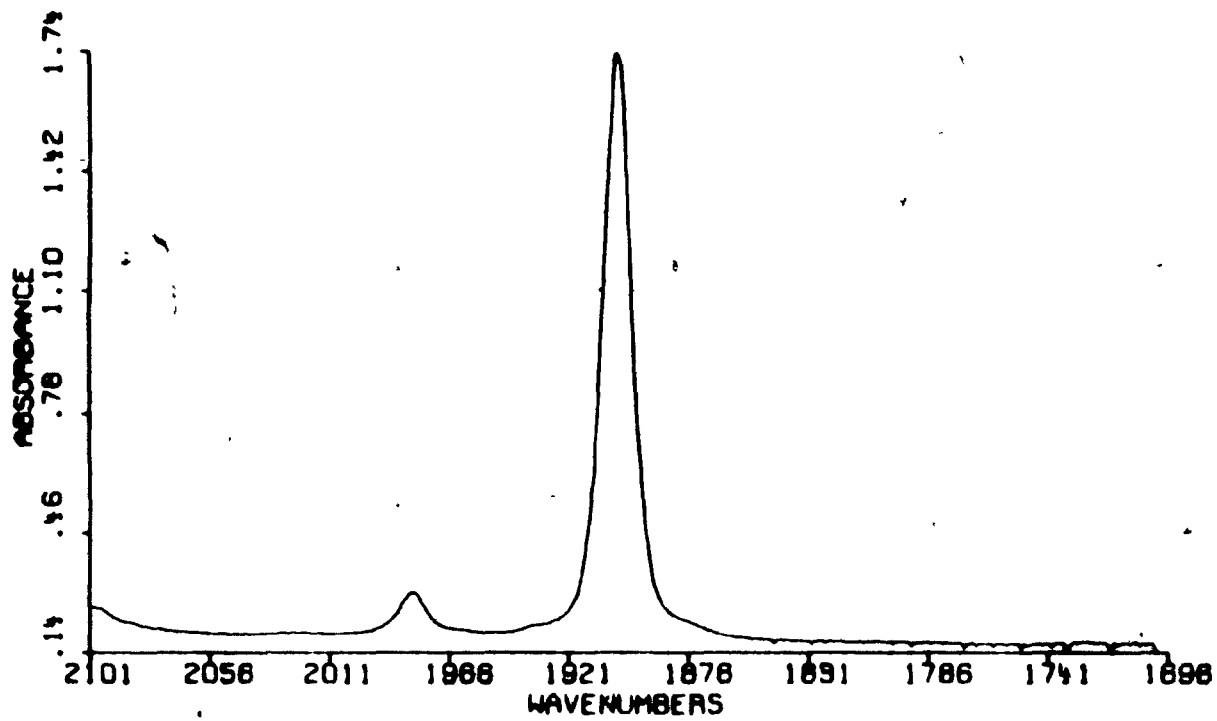

Figure 2.7. The ν(CO) region of the FT-IR spectrum of the <u>mer</u> I isomer of $Cr(CO)_2(CSe)[(MeO)_3P]_3$ in CS_2.

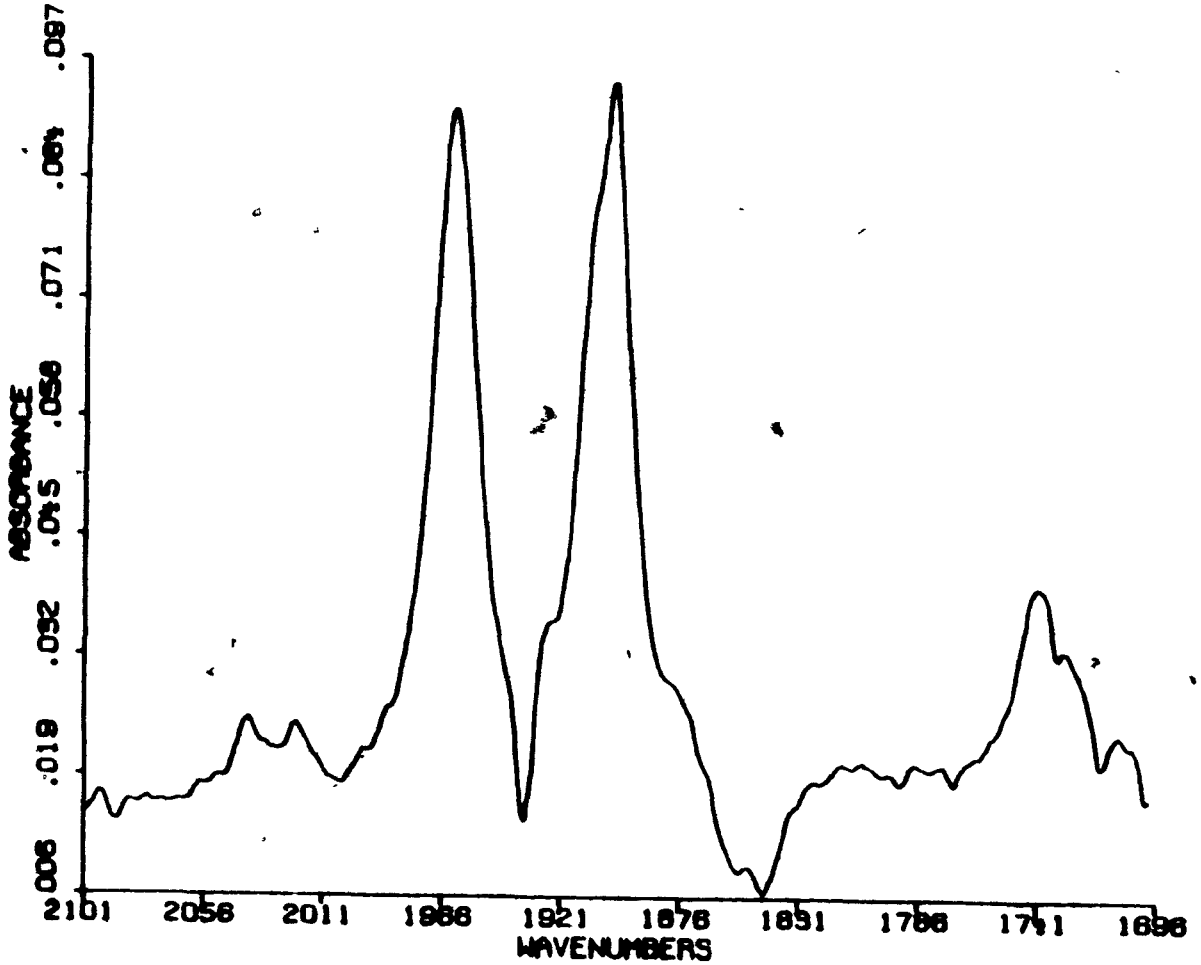

Figure 2.8. The ν(CO) region of the FT-IR spectrum of <u>fac</u>-$Cr(CO)_2(CSe)[(MeO)_3P]_3$ obtained by subtraction of the spectrum in Figure 2.7 from that in Figure 2.6.

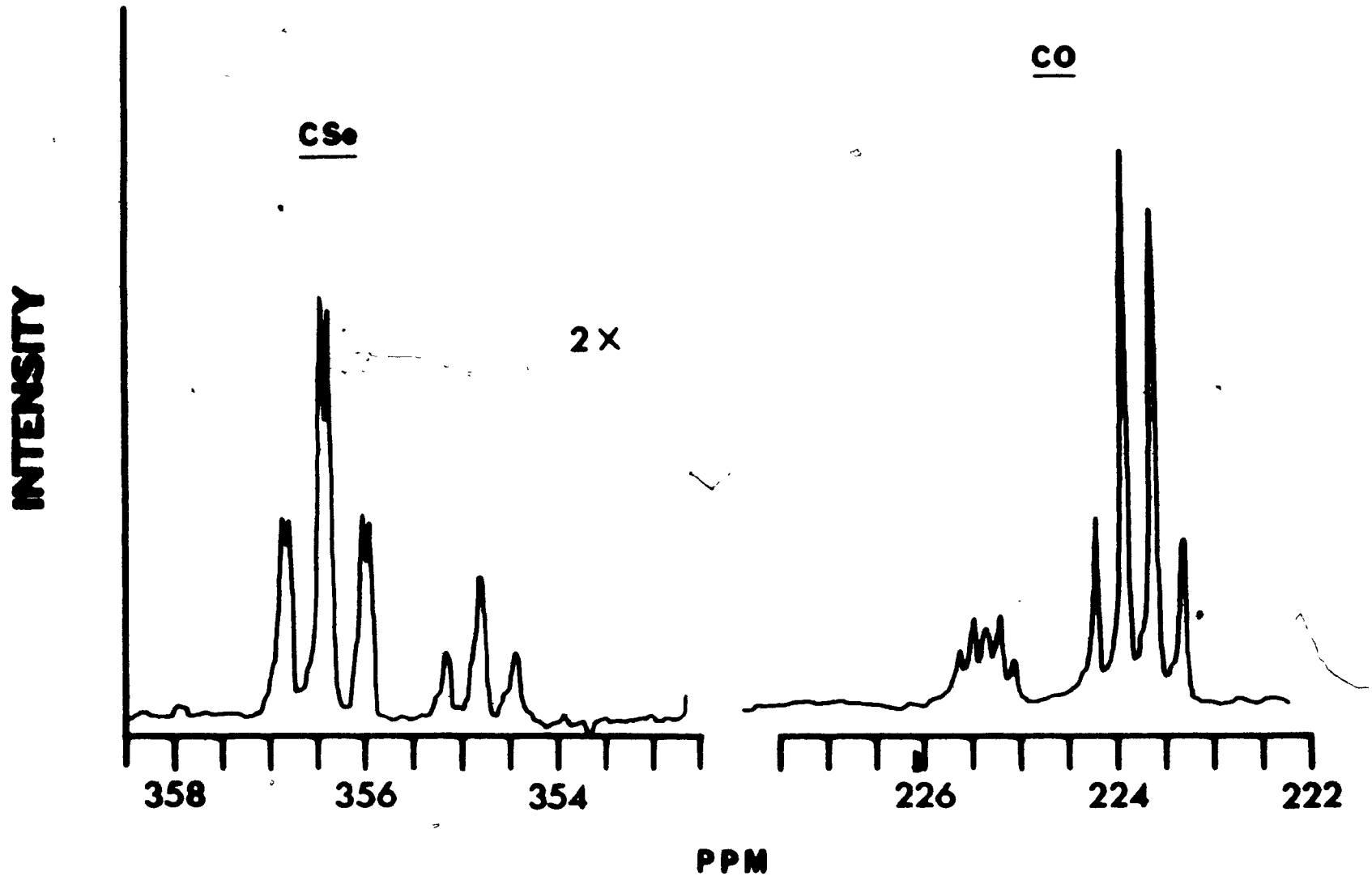

Figure 2.9. The chalcocarbonyl resonances in the ^{13}C NMR spectrum (in C_6D_6) of a mixture of the fac and mer I isomers of $Cr(CO)_2(CSe)[(MeO)_3P]_3$. Conditions: obtained on a Varian XL-300 FT spectrometer operating at 75.43 MHz; ^1H-decoupled; sweep width = 30,200 Hz; offset = 7,100 Hz; flip angle = 20°; repetition time = 0.6 s; number of scans = 2,624. Sample contained 0.1 M $Cr(acac)_3$.

diffraction (see Appendix A for crystal parameters, final positional parameters and structure factors). The resulting perspective diagram including the labelling scheme is shown in Figure 2.10. The arrangement of the ligands around the central Cr(0) atom is slightly distorted from idealized octahedral geometry (see Table 2.1 for the interatomic angles). The OC-Cr-CO angle is 175.2(4)°, while the trans phosphorus atoms are bent away from P(2) with P(1)-Cr-P(3) = 174.0(1)°, presumably to minimize steric interactions between the three $(MeO)_3P$ groups.

The interatomic distances are given in Table 2.2. The trans Cr-P bond lengths are equal within experimental error [mean value = 2.262(3) Å], while the Cr-P bond trans to CS is appreciably longer [2.346(3) Å], i.e., an increase of 0.084(3) Å. This is attributed to the strong electron-withdrawing capacity of the CS ligand, leading to less π-back-donation from the metal to the phosphite and thus to a weakening (and lengthening) of the trans Cr-P bond.

A comparison of the Cr-C(S) and C-S bond lengths reported here with those in related metal thiocarbonyl complexes containing terminal CS linkages [35] reveals that these distances are among the longest C-S and shortest Cr-C(S) distances known. This effect is also reflected in the low value of the CS stretching mode (1199 cm^{-1}). The Cr-C(S) bond distance is significantly shorter than the mean Cr-C(O)

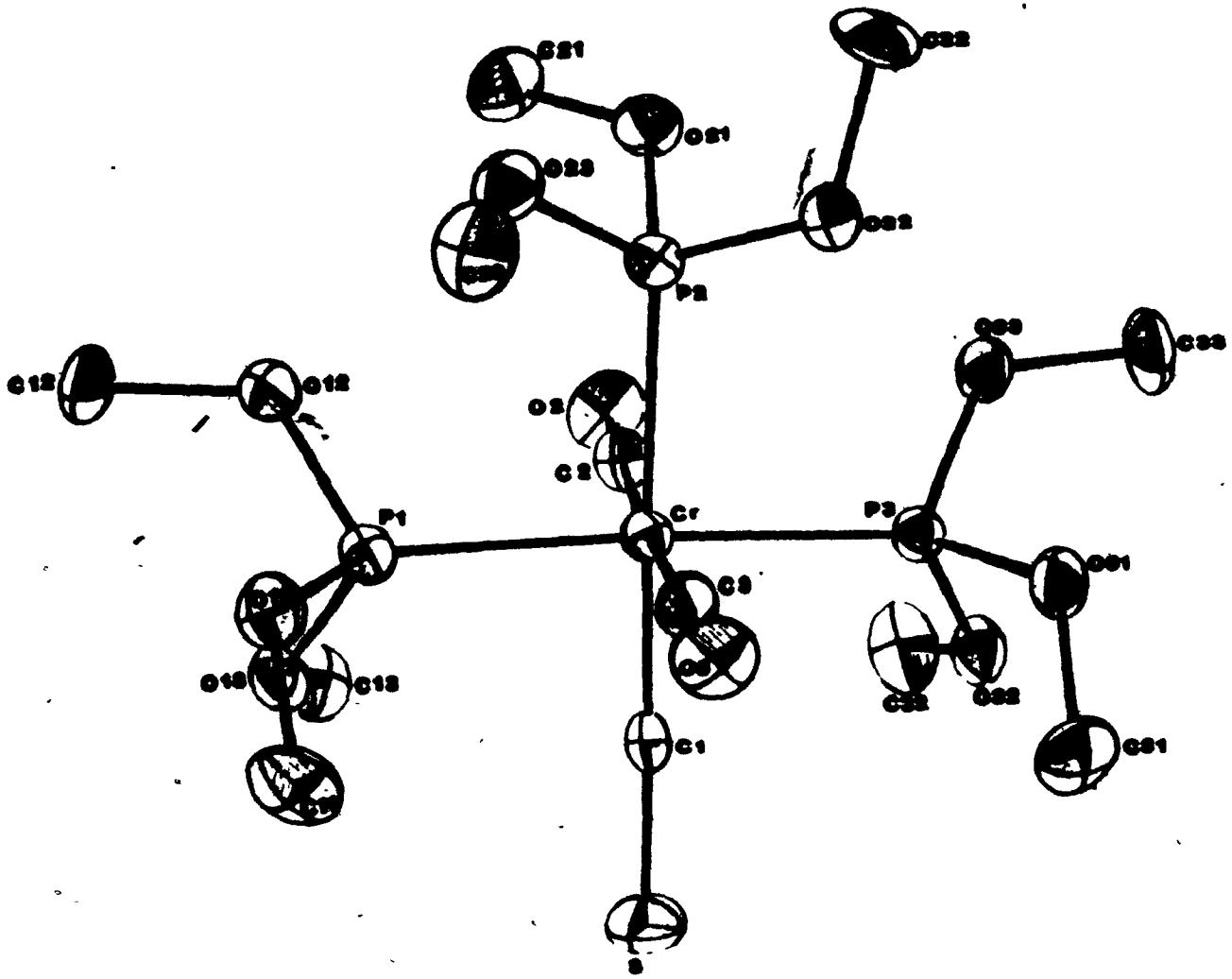

Figure 2.10. A perspective drawing of the mer I isomer of $Cr(CO)_2(CS)[(MeO)_3P]_3$, with hydrogen atoms omitted for clarity.

Table 2.1. Bond Angles (deg) in $Cr(CO)_2(CS)[(MeO)_3P]_3$[a]

Angles about chromium atom		Angles about phosphorus atoms	
Cis angles			
C1-Cr-C2	96.0(4)	Cr-P1-O11	120.3(2)
C1-Cr-C3	87.8(4)	Cr-P1-O12	114.9(2)
C1-Cr-P1	87.6(3)	Cr-P1-O13	118.8(2)
C1-Cr-P3	87.8(3)	Cr-P2-O21	119.4(2)
C2-Cr-P1	86.9(3)	Cr-P2-O22	111.4(2)
C2-Cr-P2	89.6(3)	Cr-P2-O23	120.2(2)
C2-Cr-P3	89.7(3)	Cr-P3-O31	119.6(2)
C3-Cr-P1	90.4(3)	Cr-P3-O32	119.4(2)
C3-Cr-P2	86.6(3)	Cr-P3-O33	116.0(2)
C3-Cr-P3	93.4(3)	O11-P1-O12	100.2(3)
P1-Cr-P2	91.6(1)	O11-P1-O13	96.5(4)
P2-Cr-P3	93.3(1)	O12-P1-O13	102.6(4)
		O21-P2-O22	101.3(3)
Trans angles		O21-P2-O23	97.9(3)
C1-Cr-P2	174.4(3)	O22-P2-O23	104.0(3)
C2-Cr-C3	175.2(4)	O31-P3-O32	96.2(3)
P1-Cr-P3	174.0(1)	O31-P3-O33	98.8(3)
		O32-P3-O33	103.0(3)

Table 2.1 (Cont'd)

Angles in Cr-C(X) linkages		Angles about oxygen atoms in phosphite ligands	
Cr-C1-S	176.4(6)		
Cr-C2-O2	177.2(8)	P1-O11-C11	119.8(6)
Cr-C3-O3	178.7(8)	P1-O12-C12	121.6(6)
		P1-O13-C13	120.3(6)
		P2-O21-C21	124.1(6)
		P2-O22-C22	121.6(6)
		P2-O23-C23	121.7(6)
		P3-O31-C31	119.5(6)
		P3-O32-C32	122.1(6)
		P3-O33-C33	122.0(6)

[a]Values in parentheses are estimated standard deviations in the last figure quoted.

Table 2.2. Bond Lengths (Å) in $Cr(CO)_2(CS)[(MeO)_3P]_3$

Cr-P1	2.265(3)	P2-O21	1.581(6)	O11-C11	1.434(12)
Cr-P2	2.346(3)	P2-O22	1.582(6)	O12-C12	1.488(11)
Cr-P3	2.260(3)	P2-O23	1.591(6)	O13-C13	1.440(13)
Cr-C1	1.782(9)	P3-O31	1.607(6)	O21-C21	1.433(11)
Cr-C2	1.844(9)	P3-O32	1.586(6)	O22-C22	1.465(11)
Cr-C3	1.834(9)	P3-O33	1.577(6)	O23-C23	1.424(12)
P1-O11	1.597(6)	C1-S	1.585(9)	O31-C31	1.430(12)
P1-O12	1.569(6)	C2-O2	1.148(11)	O32-C32	1.465(12)
P1-O13	1.594(7)	C3-O3	1.157(11)	O33-C33	1.474(11)

[a]Numbers in parentheses are estimated standard deviations in the last figure quoted.

value [1.839(9) Å]. These different observations are attributed to the relatively large amount of electron density available for π-backbonding at the metal centre resulting from the presence of the three strongly σ-donating tertiary phosphite ligands.

Woodard *et al.* have reported a linear relationship between the CS stretching frequency and the C-S bond length in a series of terminal thiocarbonyl complexes [35]. Least-squares analysis of the currently available data given in Table 2.3 [excluding Fe(OEP)(CS)] yields a correlation coefficient of 0.99. Inclusion of Fe(OEP)(CS) reduces the correlation significantly (r = 0.94). This difference may be attributed to appreciable mixing of ν(CS) with ν[M-C(S)], as observed in analogous porphinato thiocarbonyl complexes [36].

2.3.2 Crystal and Molecular Structure of $Cr(CO)_2(CSe)[(MeO)_3P]_3$

In this section, the crystal and molecular structure determined by a single-crystal X-ray diffraction study at 118 K of a typical selenocarbonyl product, $Cr(CO)_2(CSe)[(MeO)_3P]_3$, of the reaction of ($\eta$-Arene)$Cr(CO)_2$(CSe) with trialkylphosphite is presented. These data confirm the *mer* I configuration postulated on the basis of spectroscopic properties (FT-IR; ^{13}C, ^{31}P NMR) and the established struc-

Table 2.3. ν(CS) Frequencies and C-S Bond Distances in Selected Transition Metal Thiocarbonyl Complexes[a]

Complex	ν(CS) cm^{-1}	d(C-S) Å
$[(\eta-C_5H_5)Fe(CO)_2(CS)]PF_6$	1348	1.501
$[Ir(Ph_3P)_2(CO)_2(CS)]PF_6$	1321	1.511
$(\eta-C_5H_5)Mn(CS)(NO)(I)$	1291	1.513
<u>trans</u>-$RhCl(Ph_3P)_2(CS)$	1299	1.536
$Fe(OEP)(CS)$[b]	1292	1.559
<u>trans</u>-$W(CO)_4(CNC_6H_{11})(CS)$	1240	1.564
$(\eta-C_6H_5CO_2CH_3)Cr(CO)_2(CS)$	1225	1.570
$Cr(CO)_2(CS)[(MeO)_3P]_3$[c]	1205	1.585
$(\eta-C_{10}H_{10}O)Cr(CO)(CS)(Ph_3P)$[d]	-	1.59
<u>cis</u>-$[(\eta-C_5H_5)Fe(CO)(CS)]_2$ (bridging thiocarbonyl ligands)	1124	1.592 1.587

[a]Data from Reference 35 and references therein except [b]from Reference 42 (OEP = octaethylporphyrin), [c]from this thesis (in KBr pellet), and [d]from Reference 43.

ture of the thiocarbonyl analogue described in the previous section.

The final atomic coordinates are given in Appendix B (along with the crystal parameters and structure factors), while the bond angles and distances are listed in Tables 2.4 and 2.5, respectively. A perspective view of the structure indicating the atom labelling scheme used is shown in Figure 2.11. The coordination around the central Cr atom is essentially octahedral. The Cr-C-Se linkage is linear [176.9(2)°] with bond distances of Cr-C = 1.785(3) Å and C-Se = 1.750(3) Å. These values for the selenocarbonyl linkage are much more precise than those in the literature from the room temperature studies on $(mbz)Cr(CO)_2(CSe)$ (Cr-C-Se = 179.0(7)°, Cr-C = 1.79(1) Å, C-Se = 1.73(1) Å; [37]) and $RuCl_2(CO)(CSe)[(C_6H_5)_3P]_2$ (Ru-C-Se = 174(1)°, C-Se = 1.07(2) Å; [38]). The Cr-C(Se) distance in the present case is 0.108(1) Å shorter than the mean Cr-C(O) distance [1.893(3) Å] and the Cr-P distance for the $(MeO)_3P$ ligand <u>trans</u> to CSe is 0.091(1) Å longer than the mean Cr-P value [2.282(1) Å] for the other two $(MeO)_3P$ ligands. While these trends are identical to those observed for the thiocarbonyl analogue, the lengthening in the Cr-P bond <u>trans</u> to CSe is about 0.02 Å more than the corresponding lengthening for the thiocarbonyl complex suggesting that CSe is slightly better than CS in terms of electron-withdrawing capacity. A

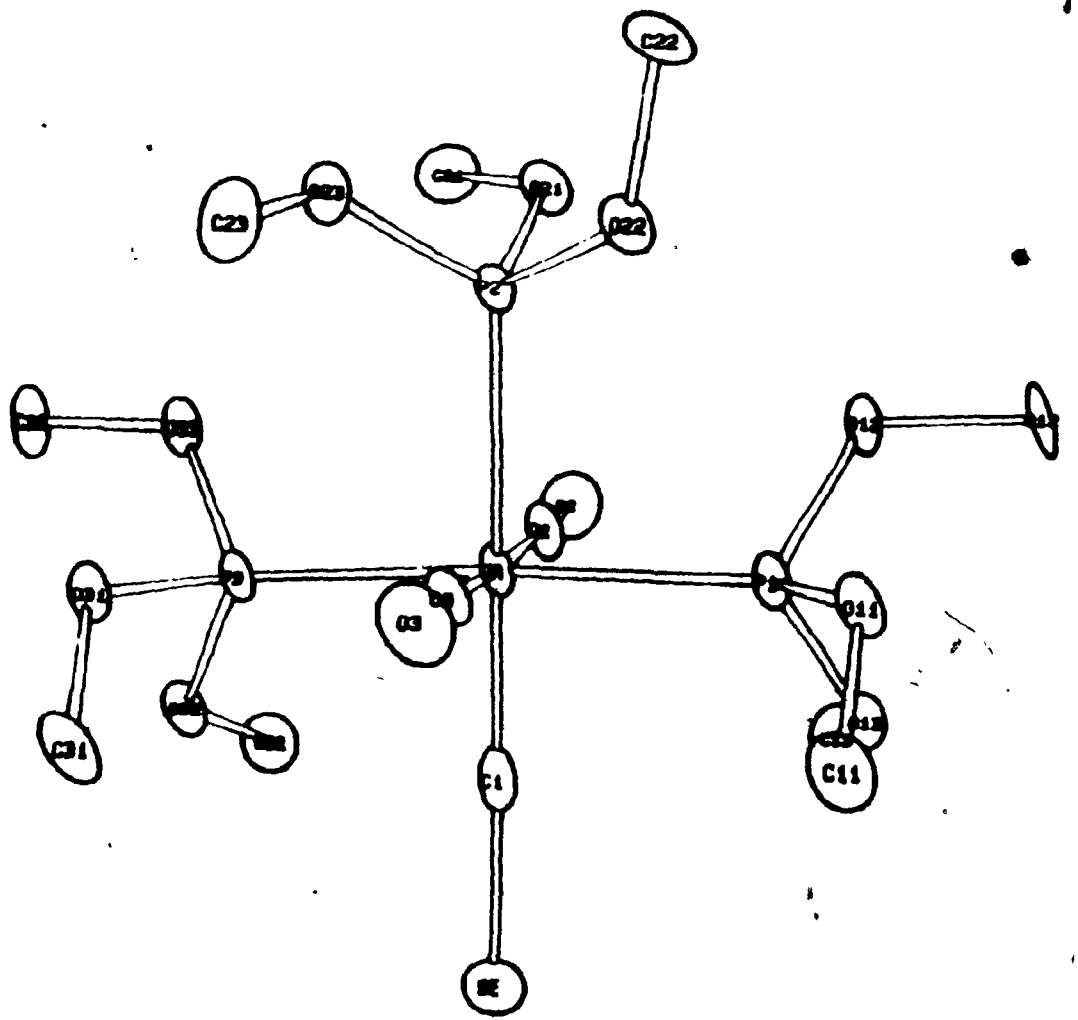

Figure 2.11. A perspective drawing of the <u>mer</u> I isomer of $Cr(CO)_2(CSe)[(MeO)_3P]_3$, with hydrogen atoms omitted for clarity.

Table 2.4. Bond Angles (deg) in $Cr(CO)_2(CSe)[(MeO)_3P]_3$[a]

Angles about chromium atom		Angles about phosphorus atoms	
Cis angles			
C1-Cr-C2	96.4(1)	Cr-P1-O11	120.44(9)
C1-Cr-C3	88.1(1)	Cr-P1-O12	114.48(9)
C1-Cr-P1	88.4(1)	Cr-P1-O13	118.24(9)
C1-Cr-P3	87.8(1)	Cr-P2-O21	119.30(9)
C2-Cr-P1	87.4(1)	Cr-P2-O22	111.34(9)
C2-Cr-P2	89.0(1)	Cr-P2-O23	120.91(9)
C2-Cr-P3	89.4(1)	Cr-P3-O31	119.26(9)
C3-Cr-P1	91.3(1)	Cr-P3-O32	118.88(9)
C3-Cr-P2	86.5(1)	Cr-P3-O33	115.45(9)
C3-Cr-P3	92.3(1)	O11-P1-O12	100.2(1)
P1-Cr-P2	90.92(3)	O11-P1-O13	96.4(1)
P2-Cr-P3	93.18(1)	O12-P1-O13	103.8(1)
		O21-P2-O22	101.2(1)
Trans angles		O21-P2-O23	97.8(1)
C1-Cr-P2	174.5(1)	O22-P2-O23	103.3(1)
C2-Cr-C3	175.3(1)	O31-P3-O32	96.8(1)
P1-Cr-P2	174.75(4)	O31-P3-O33	99.8(1)
		O32-P3-O33	103.1(1)

Table 2.4 (Cont'd)

Angles in Cr-C(X) linkages		Angles about oxygen atoms in phosphite ligands	
Cr-C1-Se	176.9(2)		
Cr-C2-O2	178.3(3)	P1-O11-C11	119.2(2)
Cr-C3-O3	176.7(3)	P1-O12-C12	121.1(2)
		P1-O13-C13	120.1(2)
		P2-O21-C21	121.9(2)
		P2-O22-C22	120.6(2)
		P2-O23-C23	119.8(2)
		P3-O31-C31	119.8(2)
		P3-O32-C32	122.0(2)
		P3-O33-C33	121.1(2)

[a]Values in parentheses are estimated standard deviations in the last figure quoted.

Table 2.5. Bond Lengths (Å) in $Cr(CO)_2(CSe)[(MeO)_3P]_3$[a]

Cr-P1	2.285(1)	P2-021	1.600(2)	011-C11	1.457(4)
Cr-P2	2.373(1)	P2-022	1.590(2)	012-C12	1.456(4)
Cr-P3	2.279(1)	P2-023	1.613(2)	013-C13	1.442(4)
Cr-C1	1.785(3)	P3-031	1.612(2)	021-C21	1.440(4)
Cr-C2	1.891(3)	P3-032	1.614(2)	022-C22	1.461(4)
Cr-C3	1.895(3)	P3-033	1.600(2)	023-C23	1.430(4)
P1-011	1.608(2)	C1-Se	1.750(3)	031-C31	1.431(4)
P1-012	1.597(2)	C2-02	1.153(4)	032-C32	1.444(4)
P1-013	1.612(2)	C3-03	1.142(4)	033-C33	1.451(4)

[a]Values in parentheses are estimated standard deviations in the last figure quoted.

similar very strong electron-withdrawing effect was found for CSe in $RuCl_2(CO)(CSe)[(C_6H_5)_3P]_2$ since the Ru-Cl distance trans to CSe is 2.480(5) Å, while the one trans to CO is 2.427(5) Å [38].

2.3.3 FT-IR and ^{31}P NMR Spectra of $Cr(CO)_2(CX)[(RO)_3P]_3$ (X = O, S, Se)

Arene displacement from (η-Arene)$Cr(CO)_2(CX)$ (X = S, Se) by tertiary phosphite ligands affords a variety of novel complexes of spectroscopic interest. The IR data for these complexes give added support as to the effectiveness of the thiocarbonyl group in decreasing the net electron density at a metal centre compared to CO in the analogous parent carbonyl complexes. This can be clearly seen from the increase in the mean IR wavenumber for the carbonyl groups in the thiocarbonyl complexes in Tables 2.6 and 2.7 resulting from the decreased back-donation of electron density from the metal to the π^* orbitals of the CO groups [1].

The number of known Group VIB metal selenocarbonyl complexes is quite limited and restricted to chromium for reasons discussed elsewhere [5]. The compounds listed in Tables 2.6-2.8 are the first examples of Group VIB metal complexes containing both phosphorus and selenocarbonyl ligands. These complexes triple the number of selenocarbonyls known for Group VIB metals and provide further sup-

Table 2.6. ν(CX) Frequencies (cm^{-1}) in the FT-IR Spectra of *fac*-$Cr(CO)_2(CX)[(RO)_3P]_3$ (X = O, S, Se)[a]

Complex	ν(CO)[b]	Average ν(CO)	ν(CS)/ ν(CSe)
$Cr(CO)_3[(MeO)_3P]_3$	1962(s), 1875(s)	1919	
$Cr(CO)_2(CS)[(MeO)_3P]_3$	1957(s), 1895(s)	1926	1199(m)
$Cr(CO)_2(CSe)[(MeO)_3P]_3$	1962(s), 1903(s)	1933	1018(m)
$Cr(CO)_3[(EtO)_3P]_3$	1957(s), 1867(s)	1912	
$Cr(CO)_2(CS)[(EtO)_3P]_3$	1950(s), 1889(s)	1920	1193(m)
$Cr(CO)_2(CSe)[(EtO)_3P]_3$	1957(s), 1898(s)	1928	1016(m)
$Cr(CO)_3[(n\text{-}BuO)_3P]_3$	1956(s), 1867(s)	1912	
$Cr(CO)_2(CS)[(n\text{-}BuO)_3P]_3$	1950(s), 1889(s)	1920	1192(m)
$Cr(CO)_2(CSe)[(n\text{-}BuO)_3P]_3$	1956(s), 1897(s)	1927	1016(m)
$Cr(CO)_3[(PhO)_3P]_3$	1982(s), 1910(s)	1946	
$Cr(CO)_2(CS)[(PhO)_3P]_3$	1973(s), 1929(s)	1951	1220(s)
$Cr(CO)_2(CSe)[(PhO)_3P]_3$	1974(s), 1940(s)	1957	1023(m)

[a] In CS_2 solution; s = strong, m = medium.
[b] For *fac*-$Cr(CO)_3L_3$, $\Gamma_{CO} = a_1 + e$, with the a_1 mode assigned to the higher-frequency peak; for *fac*-$Cr(CO)_2(CX)L_3$ (X = S, Se), $\Gamma_{CO} = a' + a''$, with the a′ mode assigned to the higher-frequency peak. These symmetry assignments are based on the assumption of C_{3v} and C_s local symmetry of the $Cr(CO)_3$ and $Cr(CO)_2(CS)/Cr(CO)_2$-(CSe) moieties, respectively; the validity of this assumption is indicated by the appearance of only two (CO) modes in the spectra of the tricarbonyl species.

Table 2.7. ν(CX) Frequencies (cm^{-1}) in the FT-IR Spectra of *mer*-$Cr(CO)_2(CX)[(RO)_3P]_3$ (X = O, S, Se)[a,b]

Complex	ν(CO)[c]	Average ν(CO)	ν(CS)/ ν(CSe)
$Cr(CO)_3[(MeO)_3P]_3$	1979(w), 1875(vs)	1927	
$Cr(CO)_2(CS)[(MeO)_3P]_3$	1974(w), 1895(vs)	1935	1199(m)
$Cr(CO)_2(CSe)[(MeO)_3P]_3$	1980(w), 1903(vs)	1942	1018(m)
$Cr(CO)_3[(EtO)_3P]_3$	1973(w), 1867(vs)	1920	
$Cr(CO)_2(CS)[(EtO)_3P]_3$	1970(w), 1889(vs)	1930	1193(m)
$Cr(CO)_2(CSe)[(EtO)_3P]_3$	1975(w), 1898(vs)	1937	1016(m)
$Cr(CO)_3[(n\text{-}BuO)_3P]_3$	1973(w), 1867(vs)	1920	
$Cr(CO)_2(CS)[(n\text{-}BuO)_3P]_3$	1971(w), 1889(vs)	1930	1192(m)
$Cr(CO)_2(CSe)[(n\text{-}BuO)_3P]_3$	1974(w), 1897(vs)	1936	1016(m)
$Cr(CO)_3[(PhO)_3P]_3$	2004(w), 1910(vs)	1957	
$Cr(CO)_2(CS)[(PhO)_3P]_3$	1987(w), 1929(vs)	1958	1220(s)
$Cr(CO)_2(CSe)[(PhO)_3P]_3$	1996(w), 1940(s)	1968	1023(m)

[a] In CS_2 solution; vs = very strong, s = strong, m = medium, w = weak.
[b] In the case of X = S or Se, *mer* = *mer* I.
[c] For *mer*-$Cr(CO)_3L_3$, $\Gamma_{CO} = 2a_1 + b_1$, with one of the a_1 modes assigned to the higher-frequency peak; the a_1 and b_1 components of the lower-frequency peak were not resolved. For the *mer* I isomer of $Cr(CO)_2(CX)L_3$ (X = S, Se), $\Gamma_{CO} = a_1 + b_1$, with the a_1 mode assigned to the higher-frequency peak. These symmetry assignments are based on the assumption of C_{2v} local symmetry for all species.

Table 2.8. ν(CX) Frequencies (cm^{-1}) in the FT-IR Spectra of (triphos-U)$Cr(CO)_2$(CX) and (triphos)$Cr(CO)_2$(CX) (X = O, S, Se)[a]

Complex	ν(CO)	ν(CS)/ ν(CSe)
(triphos-U)$Cr(CO)_3$	1931(s), 1830(s)	
(triphos-U)$Cr(CO)_2$(CS)	1929(s), 1871(s)	1190(m)
(triphos-U)$Cr(CO)_2$(CSe)	1937(s), 1881(s)	1031(s)
(triphos)$Cr(CO)_3$	1934(s), 1844(s)	
(triphos)$Cr(CO)_2$(CS)[b]	1924(s), 1861(s)	1191(m)
(triphos)$Cr(CO)_2$(CSe)[b]	1940(s), 1885(s)	1037(s)

[a]In CS_2 solution; s = strong, m = medium.
[b]The peaks due to isomers **A** and **B** were not resolved.

port of the superiority of CSe to either CS or CO in depleting electron density from metals and other coordinated ligands, as indicated by the further increase in the stretching frequencies of the carbonyl ligands.

The poor correlation between the CX (X = S, Se) wavenumber and the σ-donor/π-acceptor properties of the other bound ligands in chalcocarbonyl complexes has been reported by English et al. and attributed to appreciable mixing of the ν(CX) and ν[M-C(X)] modes [3,4]. However, a qualitative trend can be seen for the ν(CX) modes as the σ-donor/π-acceptor properties of the ligands are varied. This trend appears to be sensitive to the net electron density at the metal rather than the stereochemistry of the ligands relative to each other. This is illustrated by comparison of the data for the fac and mer isomers in Tables 2.6 and 2.7. A similar result has also been noted by Woodard et al. for cis- and trans-$W(CO)_4(CS)(L)$ derivatives [18].

To date, no ^{31}P NMR data have been obtained for phosphorus-containing thio- or selenocarbonyl complexes of Group VIB metals. The ^{31}P NMR spectra of $M(CO)_{6-n}[(MeO)_3P]_n$ (M = Cr, Mo, W) complexes have been examined by Mathieu and co-workers (Table 2.9) [33]. From their investigation, they concluded that the nature of the central atom appears to be the major factor influencing the chemical shifts, and that the resonance of the phosphorus atom trans to a carbonyl

Table 2.9. ^{31}P NMR Chemical Shifts and IR $\nu(CO)$ Frequencies of Selected Group VIB $M(CO)_{6-n}[(MeO)_3P]_n$ Complexes[a]

Complex	$\delta(^{31}P)$[b] ppm	$\nu(CO)$[c] cm^{-1}
$Cr(CO)_5(MeO)_3P$	179.6	2073, 1985, 1963, 1948
cis-$Cr(CO)_4[(MeO)_3P]_2$	180.2	2026, 1947, 1939, 1913
trans-$Cr(CO)_4[(MeO)_3P]_2$	193.1	1914
fac-$Cr(CO)_3[(MeO)_3P]_3$	186[d]	1966, 1888 sh, 1879
mer-$Cr(CO)_3[(MeO)_3P]_3$	189.1(I = 1)[d] 197.4(I = 2)	1981, 1891 sh, 1878.1
cis-$Cr(CO)_2[(MeO)_3P]_4$	187(I = 1) 198(I = 2)	1901, 1847
$Mo(CO)_5(MeO)_3P$	162	2080, 1993, 1965, 1952
cis-$Mo(CO)_4[(MeO)_3P]_2$	164	2037, 1945, 1926, 1921
trans-$Mo(CO)_4[(MeO)_3P]_2$	174	1972, 1921
fac-$Mo(CO)_3[(MeO)_3P]_3$	168.5[d]	1976, 1893 sh, 1883
mer-$Mo(CO)_3[(MeO)_3P]_3$	164.5(I = 1)[d,e] 174.2(I = 2)	1993, 1919, 1890
cis-$Mo(CO)_2[(MeO)_3P]_4$	166.9(I = 1)	1909, 1856

Table 2.9 (Cont'd)

$W(CO)_5(MeO)_3P$	137.3	2081, 1988, 1951, 1936
cis-$W(CO)_4[(MeO)_3P]_2$	141.1	2035, 1947, 1939, 1915
trans-$W(CO)_4[(MeO)_3P]_2$	147	1915
fac-$W(CO)_3[(MeO)_3P]_3$	146.6[d]	1973, 1894 sh, 1880
mer-$W(CO)_3[(MeO)_3P]_3$	144.4(I = 1)[d]	1989, 1890 sh, 1871
cis-$W(CO)_2[(MeO)_3P]_4$	148.6	1905, 1845

[a]Data from Reference 33.
[b]Most compounds were examined in benzene; chemical shifts are in ppm downfield from 85% H_3PO_4.
[c]In hexadecane solution.
[d]Remeasured in this study on a Varian XL-200 spectrometer.
[e]Assigned to the *fac* isomer in Reference 33.

group occurs at higher field than that for a phosphorus atom trans to another phosphorus. The latter trend was rationalized using Eq. 2.7 derived by Van Wazer and Letcher [39] where the ^{31}P chemical shift is treated as the summation of the σ-bond and π-bond contributions:

$$\delta - \delta_o = \delta_\sigma + \delta_\pi \qquad (2.7)$$

where δ_o is a constant associated with the particular reference standard employed. Both the δ_σ and δ_π terms are negative and so an increase in the amount of metal $d\pi$ electron density transferred to the $d\pi$ orbitals or a decrease in the σ-donation from the phosphorus atom to the metal results in a shift of the ^{31}P resonance towards lower fields [33].

Table 2.10 summarizes the ^{31}P NMR data obtained for the $Cr(CO)_2(CX)[(RO)_3P]_3$ (X = O, S, Se; R = Me, Et, n-Bu, Ph) complexes. A comparison of the ^{31}P resonance for the two phosphorus atoms trans to each other in the chalcocarbonyl triad reveals an upfield shift of about 7 ppm for the thiocarbonyl derivative and about 11.5 ppm for the selenocarbonyl derivative when compared to the tricarbonyl complex. These upfield shifts are indicative of a net decrease in electron density at the metal centre available for donation to the $d\pi$ orbitals of the phosphorus atoms and are consistent with the established order of π-acidity for chalcocar-

Table 2.10. ^{31}P NMR Data[a] for *mer*-$Cr(CO)_2(CX)[(RO)_3P]_3$ (X = O, S, Se)[b] and *fac*-$Cr(CO)_2(CX)[(RO)_3P]_3$ (X = S, Se)

Complex	$^2J_{PP}$ Hz	$\delta(^{31}P)$ (d, I=2) ppm	$\delta(^{31}P)$ (t, I=1) ppm
mer isomers			
$Cr(CO)_3[(MeO)_3P]_3$	64	197.4	189.1
$Cr(CO)_2(CS)[(MeO)_3P]_3$	65	188.6	181.2
$Cr(CO)_2(CSe)[(MeO)_3P]_3$	64	184.9	177.5
$Cr(CO)_3[(EtO)_3P]_3$	60	193.3	184.9
$Cr(CO)_2(CS)[(EtO)_3P]_3$	65	186.3	177.4
$Cr(CO)_2(CSe)[(EtO)_3P]_3$	64	181.6	172.5
$Cr(CO)_3[(n\text{-}BuO)_3P]_3$	59	193.0	184.6
$Cr(CO)_2(CS)[(n\text{-}BuO)_3P]_3$	64	186.2	177.2
$Cr(CO)_2(CSe)[(n\text{-}BuO)_3P]_3$	64	181.5	172.8
$Cr(CO)_3[(PhO)_3P]_3$	65	177.7	168.6
$Cr(CO)_2(CS)[(PhO)_3P]_3$	62	170.5	162.6
$Cr(CO)_2(CSe)[(PhO)_3P]_3$	62	166.0	159.9
fac isomers			
$Cr(CO)_2(CS)[(MeO)_3P]_3$	72	180.7	178.2
$Cr(CO)_2(CSe)[(MeO)_3P]_3$	72	178.4	174.7
$Cr(CO)_2(CSe)[(PhO)_3P]_3$	68	160.1	157.0

[a]In $C_6D_5CD_3$ solution; chemical shifts are in ppm (±0.1 ppm) downfield from 85% H_3PO_4.
[b]In the case of X = S or Se, *mer* = *mer* I.

bonyl ligands (CSe > CS > CO). An increase in electron density donation from the phosphorus atoms to the relatively electron-deficient metal in the thio- and selenocarbonyl complexes may also contribute to the observed effect.

The signal for the phosphorus atom trans to the CX ligand is shifted upfield from that for the two trans phosphorus atoms. This resonance also is observed to shift to higher fields with increasing π-acidity of the CX ligand. The magnitudes of the shifts with variation in the CX ligand are comparable to those for the resonances of the two trans phosphorus atoms.

2.3.4 Reaction of (η-Arene)$Cr(CO)_2$(CX) with Tridentate Phosphine Ligands

Reaction of triphos-U with (η-Arene)$Cr(CO)_2$(CX) (X = S, Se) yields novel complexes characterized as fac-(triphos-U)$Cr(CO)_2$(CX) (Figure 2.12). The IR and ^{31}P NMR data are presented in Tables 2.8 and 2.11, respectively, together with data for the corresponding tricarbonyl complex. As expected, the mean IR ν(CO) frequency shifts to higher wavenumber on descending the chalcocarbonyl triad. The ^{31}P NMR spectrum of the (triphos-U)$Cr(CO)_3$ complex exhibits only one signal since the three phosphorus atoms are equivalent. In the case of (triphos-U)$Cr(CO)_2$(CX) (X = S, Se), one phosphorus atom is trans to CX while two phosphorus atoms are

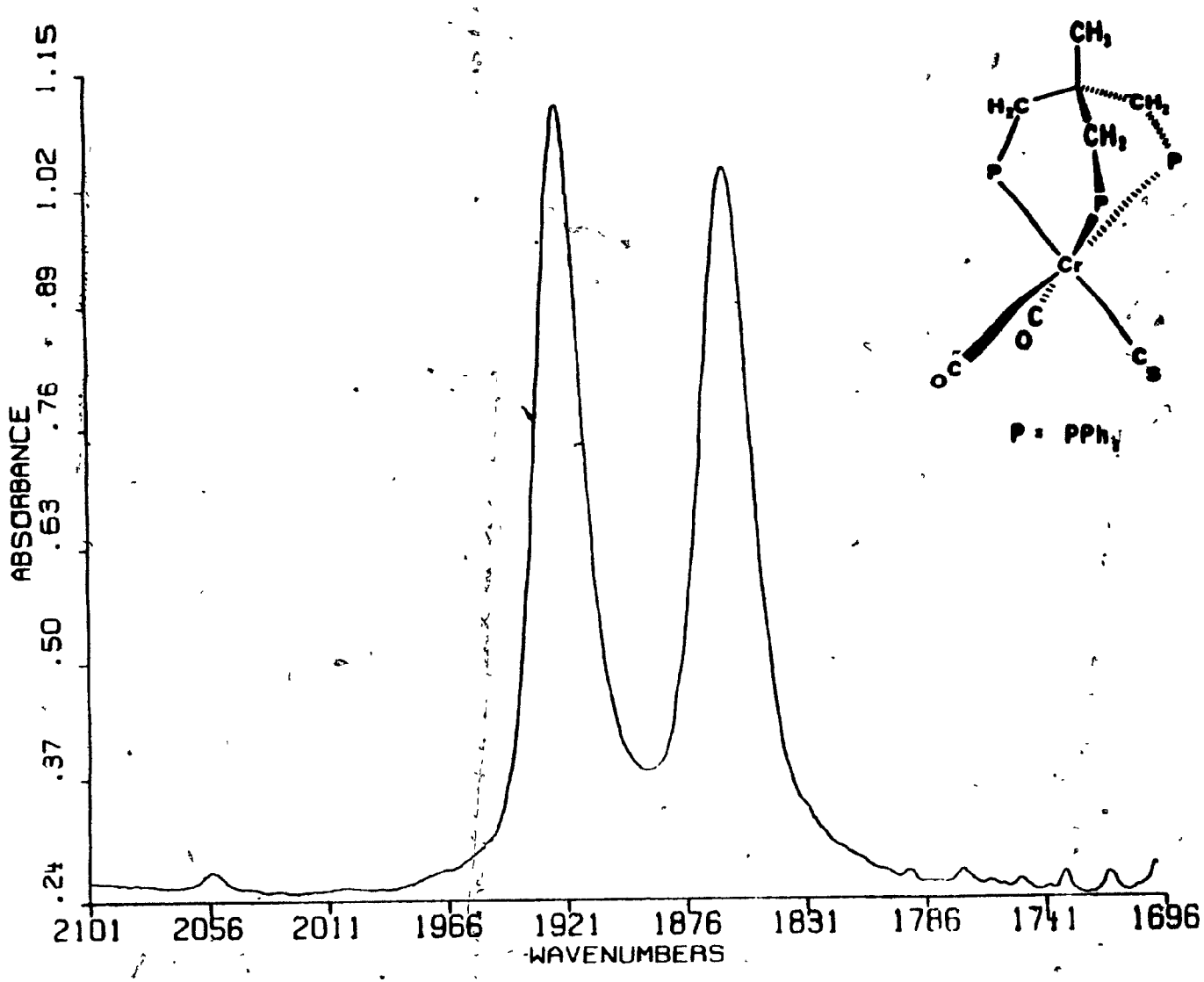

Figure 2.12. The ν(CO) region of the FT-IR spectrum of (triphos-U)Cr(CO)$_2$(CS) in CH_2Cl_2.

Table 2.11. ^{31}P NMR Data for (triphos-U)$Cr(CO)_2(CX)$ and (triphos)$Cr(CO)_2(CX)$ (X = O, S, Se)[a]

Complex	J_{PP} Hz	$\delta(^{31}P)$ ppm
(triphos-U)		-24.8
(triphos-U)$Cr(CO)_3$		39.6
(triphos-U)$Cr(CO)_2(CSe)$	31	31.5(d, I = 2) 26.9(t, I = 1)
triphos	28	-11.7(d, I = 2) -15.6(t, I = 1)
(triphos)$Cr(CO)_3$	12	84.0(d, I = 2) 115.2(t, I = 1)
(triphos)$Cr(CO)_2(CS)$ (A)	10,24	67.4(dd, I = 1) 79.8(dd, I = 1) 107.5(dd, I = 1)
(triphos)$Cr(CO)_2(CS)$ (B)	9	71.9(d, I = 2) 100.9(t, I = 1)
(triphos)$Cr(CO)_2(CSe)$ (A)	10,24	64.4(dd, I = 1) 76.9(dd, I = 1) 104.0(dd, I = 1)
(triphos)$Cr(CO)_2(CSe)$ (B)	10	68.6(d, I = 2) 96.7(t, I = 1)

[a]In CD_2Cl_2 solution; chemical shifts (±0.1 ppm) are given with positive values downfield from 85% H_3PO_4.

trans to CO. The different environments result in a doublet and a triplet splitting pattern for these complexes where the ^{31}P signal trans to CX (triplet) is further upfield than the ^{31}P resonance (doublet) of the two phosphorus atoms trans to CO. Comparison of the ^{31}P resonance for (triphos-U)$Cr(CO)_3$ with that of the corresponding resonance of the phosphorus atoms trans to CO in (triphos-U)$Cr(CO)_2$-(CSe) indicates an upfield shift of 8 ppm in the selenocarbonyl complex. The phosphorus trans to CSe is approximately 5 ppm upfield from the other two phosphorus atoms trans to CO in the same complex.

Arene displacement by triphos from (η-Arene)$Cr(CO)_2$-(CX) (X = S, Se) affords three new interesting types of fac isomer (A, A* and B, where A* is an enantiomer of A) (Figure 2.13) that are not available to the parent tricarbonyl complex. The IR spectra (Figure 2.14) of the complexes in the carbonyl stretching region display only two strong absorptions with mean values at higher energies than those for the corresponding tricarbonyl complexes [40]. Moreover, the mean ν(CO) value in the case of the selenocarbonyl derivative is higher than that for the thiocarbonyl derivative. The ν(CX) (X = S, Se) modes for the A and B isomers appear as one unresolved peak. As will be shown below, the ^{31}P NMR data for the complexes proved crucial in verifying the presence of the two isomers and in establishing their rela-

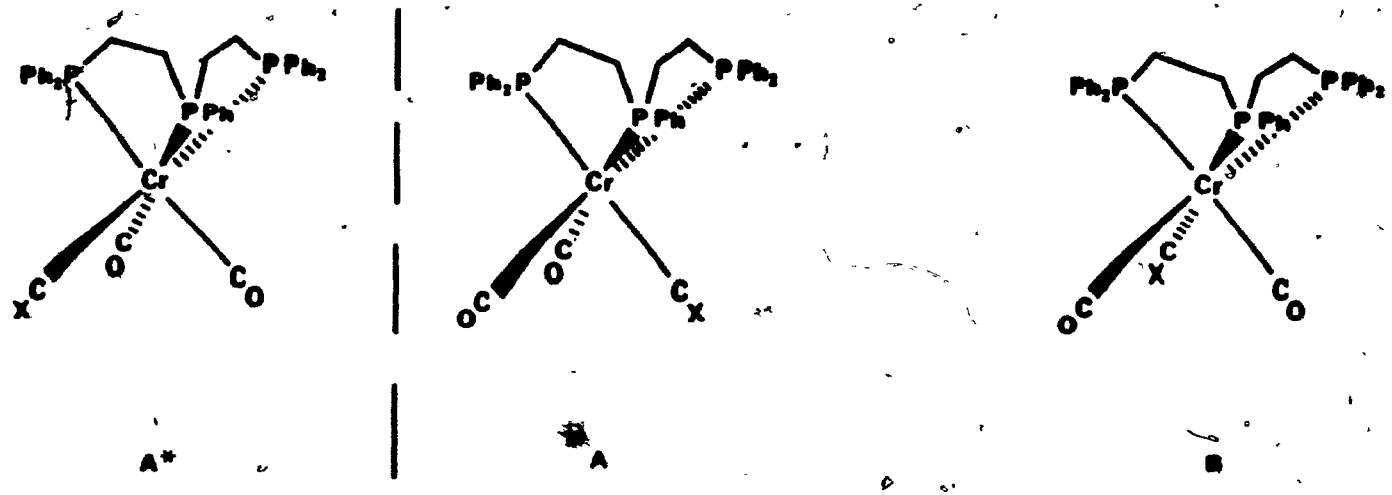

Figure 2.13. The two possible isomers of (triphos)$Cr(CO)_2(CX)$ (X = S, Se). Isomer A exists in two enantiomeric forms.

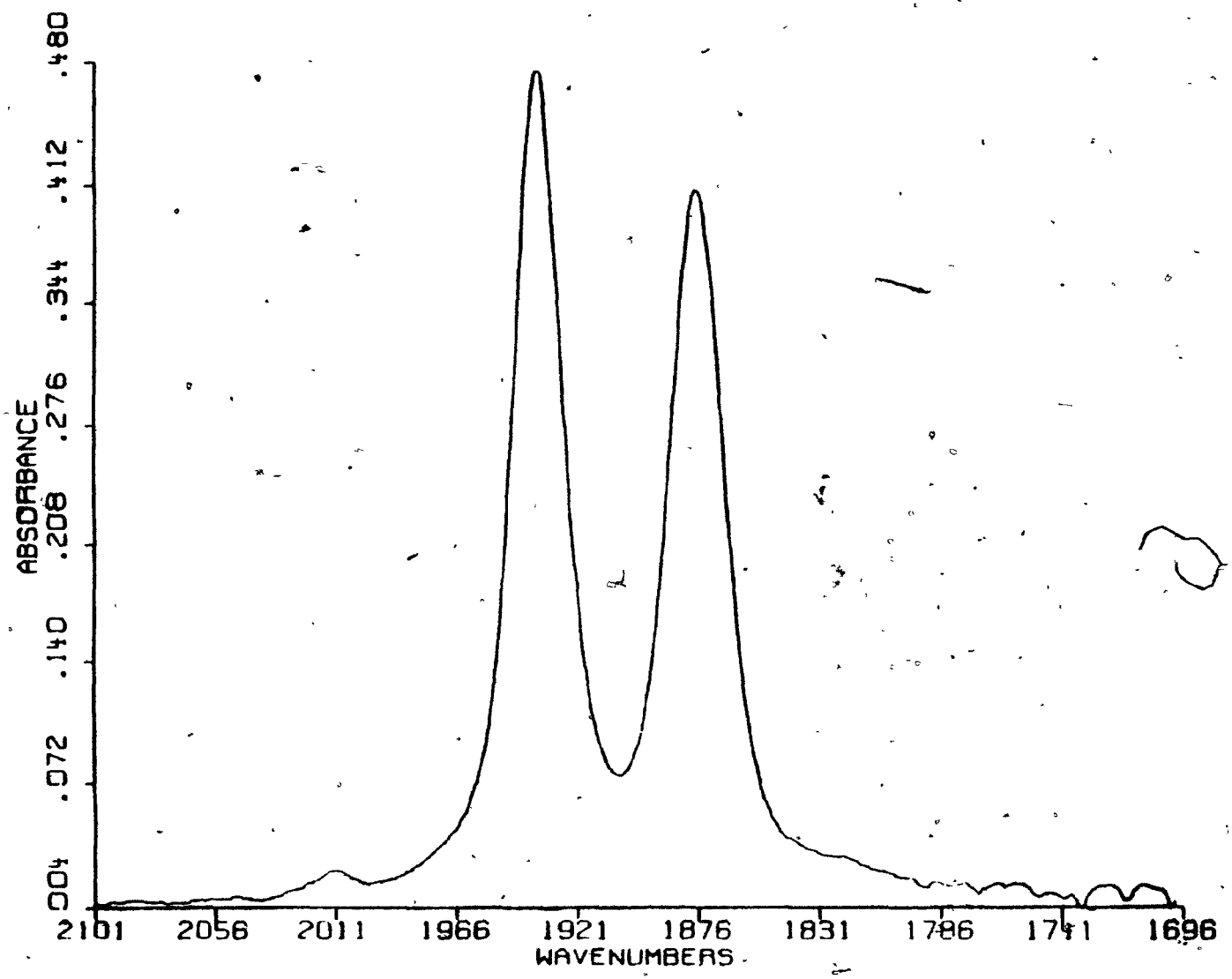

Figure 2.14. The ν(CO) region of the FT-IR spectrum of (triphos)$Cr(CO)_2$(CSe) in CH_2Cl_2.

tive concentrations.

Isomer **A** (and **A***) of (triphos)$Cr(CO)_2(CX)$ (X = S, Se) is expected to exhibit three ^{31}P NMR signals since the two terminal phosphorus atoms of the triphos ligand are trans to different ligands and the bridging phosphorus atom is in a different environment from the other two phosphorus atoms in the pure ligand. Isomer **B** with the bridging phosphine trans to the CX ligand is expected to have two signals since the terminal phosphorus nuclei experience identical environments. The isomers were detected in the ^{31}P NMR spectrum (Figure 2.15) in a 4:1 ratio (**A**:**B**). The assignment of the resonances for isomer **A** was facilitated by comparison with the spectrum of the parent tricarbonyl which enabled the resonance due to the bridging phosphorus atom to be easily identified. The resonances due to the terminal phosporus atoms were assigned on the basis of the trend observed for ^{31}P resonances in the chalcocarbonyl complexes presented in this chapter. Thus, the resonance at higher field was assigned to the phosphorus atom trans to CX (X = S, Se). The ^{31}P NMR spectrum of isomer **B** was directly assigned by comparison with the spectrum of (triphos)$Cr(CO)_3$ [41].

2.3.5. Attempted Synthesis of (cht)$Cr(CO)_2(CS)$

In Chapter 4 of this thesis, a kinetic investigation of

Figure 2.15. ^{31}P NMR spectrum of (triphos)$Cr(CO)_2(CSe)$ in $C_6D_5CD_3$. Conditions: obtained on a Varian XL-300 FT spectrometer operating at 121.42 MHz; ^1H-decoupled; sweep width = 6,300 Hz; offset = 10,200 Hz; flip angle = 66°; repetition time = 20 s; number of scans = 200.

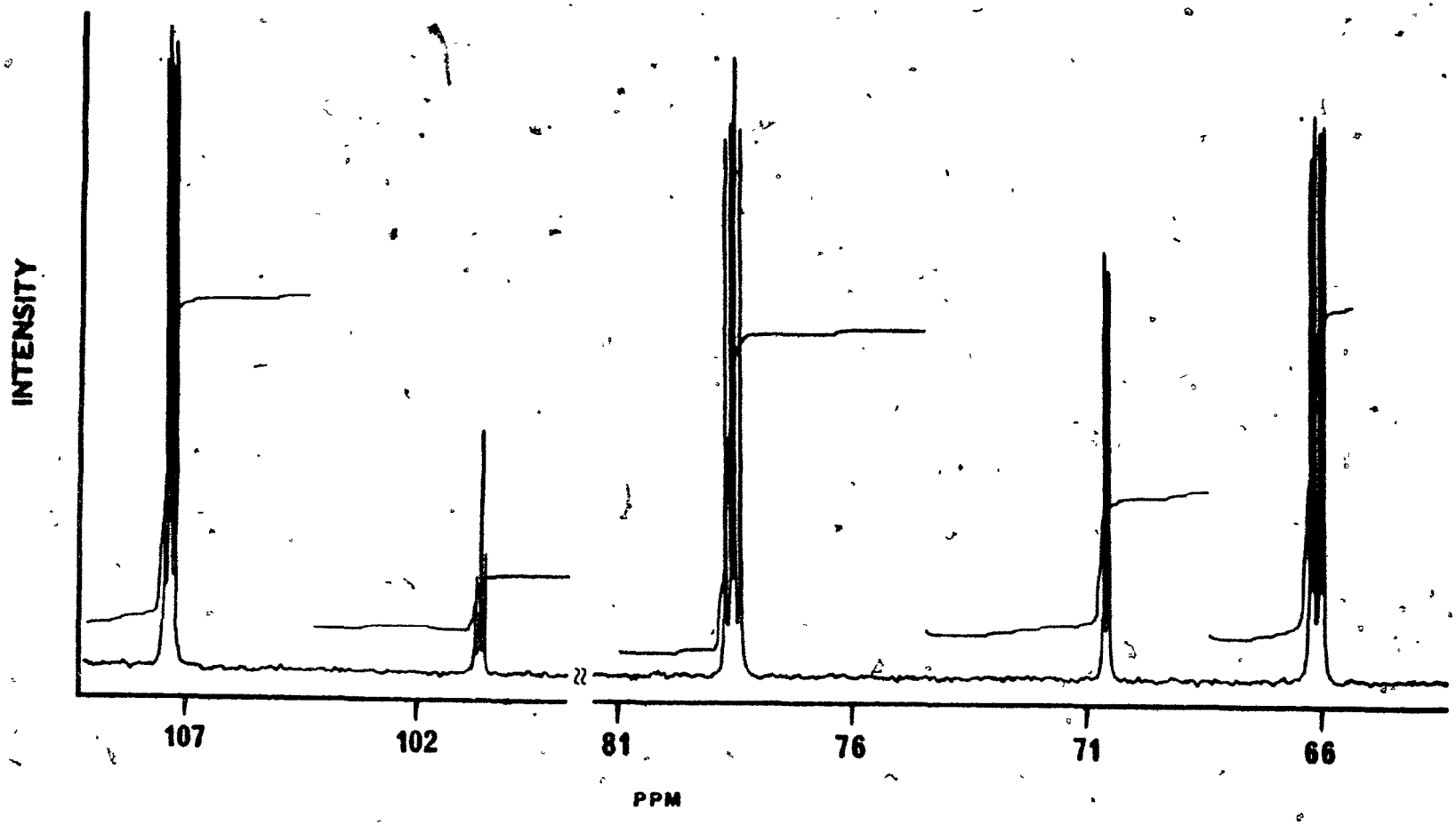
INTENSITY
107
102
81
76
71
66
PPM

arene displacement reactions of (η-Arene)$Cr(CO)_2(CX)$ (X = S, Se) complexes with $(RO)_3P$ ligands will be presented. Similar kinetic studies have been reported in the literature for (cht)$M(CO)_3$ (M = Cr, Mo, W) and (η-Arene)$M(CO)_3$ (M = Mo, W) but not for (η-Arene)$Cr(CO)_3$ complexes because the reactions are too slow. It would be of interest to compare kinetic data for tricarbonyl, thiocarbonyl and selenocarbonyl complexes. However, it appears that molybdenum and tungsten arene thiocarbonyls are not accessible [5] due to the inability to photochemically or thermally generate the (η-Arene)$M(CO)_2(L)$ (L = C_8H_{14}, THF) precursor necessary to afford (η-Arene)$M(CO)_2(CS)$ [1]. Therefore, synthesis of (cht)$Cr(CO)_2(CS)$ was attempted in an effort to obtain a basis for direct comparison of the effects of CS and CO ligands on the lability of the metal-arene bond in analogous complexes. The conventional synthetic route to thiocarbonyls through photolysis of the parent tricarbonyl complex in <u>cis</u>-cyclooctene and subsequent addition of CS_2 to yield the thiocarbonyl complex [1] proved unfeasible because (cht)$Cr(CO)_3$ was photochemically inactive under the conditions employed. Only one research group has obtained spectroscopic evidence for photochemical formation of (cht)-$Cr(CO)_2(L)$ [L = py, $(PhO)_3P$], this after irradiation for 40 h at -40°C [42]. For L = C_8H_{14}, no product formation was detected. Consequently, they postulated initial forma-

tion of $(\eta^4\text{-cht})Cr(CO)_3(L)$ prior to CO dissociation for the reactions where L = py and $(PhO)_3P$. The poor nucleophilicity and the size of the cyclooctene ligand may hinder its binding to the metal at such a low temperature [42]. In the present work UV photolysis of $(cht)Cr(CO)_3$ in 1:1 toluene/cyclooctene at 0°C and at room temperature produced no detectable concentration of the cyclooctene complex. Heating the sample in conjunction with photolysis resulted in decomposition. The ring exchange procedure, which was reported for the synthesis of $(cht)M(CO)_3$ (M = Mo, W) from $(\eta\text{-Arene})M(CO)_3$ in excess cht [25], resulted in decomposition in the case of $(mbz)Cr(CO)_2(CS)$. Another synthetic route to $(cht)Cr(CO)_3$ involves refluxing a mixture of cht and $Cr(CO)_6$ either in neat ligand or in a high-boiling solvent such as heptane [25]. Therefore, $Cr(CO)_5(CS)$ was synthesized following the established procedure [20], and its reaction with cht was investigated. After refluxing for 24 h, no product was obtained. Finally, attempted synthesis of $Cr(CO)_2(CS)(CH_3CN)_3$ from either $(\eta\text{-Arene})Cr(CO)_2(CS)$ or $Cr(CO)_5(CS)$ resulted in decomposition. This complex would have provided another route to the coordination of cht to the chromium thiocarbonyl moiety, as demonstrated by the synthesis of $(cht)W(CO)_3$ from $W(CO)_3(RCN)_3$ (R = alkyl) [43].

References

1. I.S. Butler, Acc. Chem. Res., 10, 359 (1977) and references therein.
2. A.M. English, Ph.D. thesis, McGill University, Montreal, Quebec, Canada, 1980.
3. A.M. English, K.R. Plowman and I.S. Butler, Inorg. Chem., 21, 338 (1982).
4. A.M. English, K.R. Plowman and I.S. Butler, Inorg. Chem., 20, 2553 (1981).
5. I.M. Baibich, Ph.D. thesis, McGill University, Montreal, Quebec, Canada, 1981.
6. I.M. Baibich, A.M. English and I.S. Butler, Organometallics, 3, 1786 (1984).
7. J.-Y. Saillard, G. LeBorgne and D. Grandjean, J. Organometal. Chem. 94, 409 (1975).
8. D. Cozak, I.M. Baibich and I.S. Butler, J. Organometal. Chem., 169, 381 (1979).
9. D. Cozak, Ph.D. thesis, McGill University, Montreal, Quebec, Canada 1977.
10. D. Cozak, I.S. Butler, J.P. Hickey and L.J. Todd, J. Magn. Reson., 33, 149 (1979).
11. J.P. Hickey, I.M. Baibich, I.S. Butler and L.J. Todd, Spectrosc. Lett., 11, 671 (1978).

12. D.L. Lichtenberger and R.F. Fenske, Inorg. Chem., 15, 2015 (1976).

13. A.M. English, K.R. Plowman, I.S. Butler, E. Diemann and A. Muller, Inorg. Chim. Acta, 32, 113 (1979).

14. I.M. Baibich and I.S. Butler, Inorg. Chim. Acta, 89, 73 (1984).

15. D. Cozak and I.S. Butler, Can. J. Spectrosc., 27, 141 (1982).

16. H.W. Chen, W.L. Jolly, S.F. Xiang, I.S. Butler and J. Sedman, J. Electron Spectrosc. Relat. Phenom., 24, 121 (1981).

17. B.D. Dombek and R.J. Angelici, Inorg. Chem. 15, 1089 (1976).

18. E.S. Woodard, R.J. Angelici and B.D. Dombek, Inorg. Chem., 17, 1634 (1978).

19. B.D. Dombek and R.J. Angelici, J. Am. Chem. Soc., 98, 4110 (1976).

20. A.M. English, K.R. Plowman, I.M. Baibich, J.P. Hickey, I.S. Butler, G. Jaouen and P. Le Maux, J. Organometal. Chem., 205, 177 (1981).

21. R.A. Pickering and R.J. Angelici, Inorg. Chem., 17, 2035 (1978).

22. B.D. Dombek and R.J. Angelici, Inorg. Chem., 15, 2403 (1976).

23. J.R. Graham and R.J. Angelici, Inorg. Chem., 6, 2082 (1967).

24. J.R. Graham and R.J. Angelici, Inorg. Chem., 6, 992 (1967).

25. A. Pidcock and B.W. Taylor, J. Chem. Soc. (A), 877 (1967).

26. C.A.L. Mahaffy and P.L. Pauson, Inorg. Synth., 19, 154 (1979).

27. G. Jaouen and G. Simonneaux, Inorg. Synth., 19, 197 (1979).

28. I.S. Butler, A.M. English and K.R. Plowman, Inorg. Synth., 21, 1 (1982).

29. G. Yaguspsky and M. Cais, Inorg. Chim. Acta, 12, L27 (1975)

30. A. Pidcock, J.D. Smith and B.W. Taylor, J. Chem. Soc. (A), 872 (1967).

31. F. Zingales, A. Chiesa and F. Basolo, J. Am. Chem. Soc., 88, 2707 (1966).

32. A. Pidcock, J.D. Smith and B.W. Taylor, J. Chem. Soc. (A), 1604 (1969).

33. R. Mathieu, M. Lenzi and R. Poilblanc, Inorg. Chem., 9, 2030 (1970).

34. G.M. Bodner, Inorg. Chem., 14, 2694 (1975).

35. S.S. Woodard, R.A. Jacobson and R.J. Angelici, J. Organometal. Chem., 117, C75 (1976).

36. P.D. Smith, D. Dolphin and B.R. James, J. Organometal. Chem., 208, 239 (1981).

37. J.-Y.Saillard and D. Grandjean, Acta Cryst., B34, 3772 (1978).

38. G.R. Clark, K.R. Grundy, R.O. Harris, S.M. James, and W.R. Roper, J. Organometal. Chem. 90, C37 (1975).

39. J.R. Van Wazer and J.H. Letcher, Topics in Phosphorus Chemistry, 5, 169 (1967).

40. R.B. King, P.N. Kapoor and R.N. Kapoor, Inorg. Chem., 10, 1841 (1971).

41. R.B. King and J.C. Cloyd Jr., Inorg. Chem., 14, 1550 (1974).

42. W.P. Anderson, W.G. Blenderman and K.A. Drews, J. Organometal. Chem., 42, 139 (1972).

43. G.J. Kubas, Inorg. Chem., 22, 692 (1983).

44. R. Scheidt and D.K. Geiger, Inorg. Chem., 21, 1208 (1982).

45. D. Korp and I. Bernal, Cryst. Struct. Commun., 9, 821 (1980).

Chapter 3

Intramolecular Isomerization of $Cr(CO)_2(CX)[(MeO)_3P]_3$ (X = O, S, Se) Complexes

3.1 Introduction

An unexpected feature of the arene displacement reactions of (η-Arene)$Cr(CO)_2(CX)$ (X = S, Se) complexes investigated in Chapter 2 is the involvement of an isomerization process. The major product isolated from these reactions has been characterized as the *mer* I isomer and not the *fac* isomer observed as the major product in triene displacement reactions of Group VIB (cht)$M(CO)_3$ and arene displacement reactions of (η-Arene)$M(CO)_3$ (M = Mo, W). The formation of the *mer* I isomer may be postulated to result from the isomerization of an intermediate in the reaction pathway. However, in recent years several reports have appeared in the literature [1-10] of intramolecular isomerization of Group VIB metal carbonyl complexes. Accordingly, the possibility that *mer*-$Cr(CO)_2(CX)[(MeO)_3P]_3$ complexes are formed as a result of the intramolecular isomerization of the corresponding *fac* isomers was investigated.

Intramolecular rearrangement of octahedral complexes is thought to proceed through either a trigonal prismatic [11] or bicapped-tetrahedral [12] intermediate or transition

state. The schematic representation of these processes is shown in Figure 3.1. One of the first examples reported of intramolecular rearrangement in Group VIB metal carbonyl complexes was the isomerization of $Cr(CO)_4[C(OMe)Me](R_3P)$ (R = Et, Cy) [1,2]. Shortly after, the thiocarbonyl-containing complex trans-$W(CO)_4(^{13}CO)(CS)$ was investigated by Angelici and his co-workers and was also shown to undergo isomerization through a non-dissociative mechanism [3]. Since then, Darensbourg and his research group have found that other complexes such as $M(CO)_{6-n}(R_3P)_n$ (M = Cr, Mo, W; n = 1,2; R = Me, Et, i-Pr, n-Bu, OMe, OEt) undergo isomerization by a non-dissociative pathway [4-7], with the rate of rearrangement decreasing in the order Cr > W > Mo [6,7]. Similarly intramolecular isomerization of $M(CO)_4(PF_3)_2$ (M = Cr, Mo, W) has been reported [8]. Activation parameters were determined for some of the above complexes (Table 3.1). In the case of the chromium and tungsten complexes trans-$Cr(CO)_4(^{13}CO)(Et_3P)$ [7] and trans-$W(CO)_4(^{13}CO)(CS)$ [3], large positive enthalpies of activation and positive entropies of activation were obtained for the isomerization to the cis isomers. On the basis of the large enthalpies of activation, significant bond lengthening in the activated states was postulated to occur. For trans-$W(CO)_4(^{13}CO)(Et_3P)$ [7], isomerization exhibited a small enthalpy and a large negative entropy, supportive of a trigonal prismatic twist.

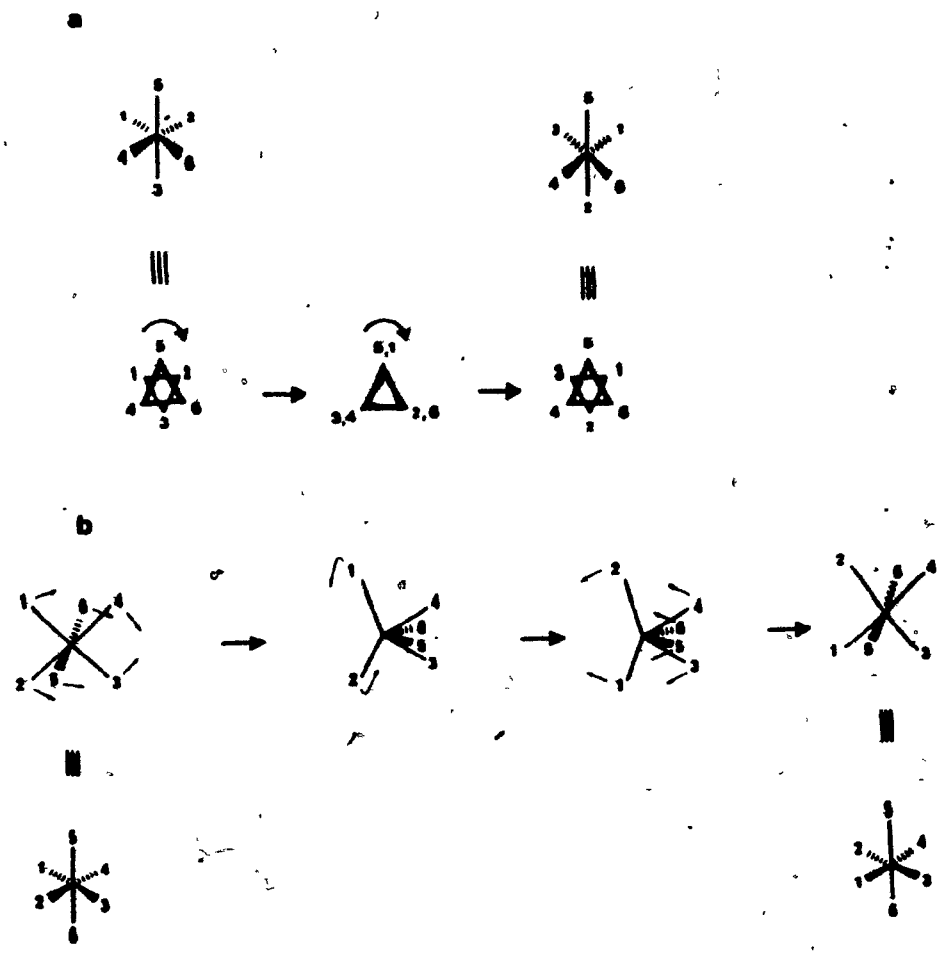

Figure 3.1. Proposed rearrangement pathways available to octahedral complexes: (a) through a trigonal prismatic intermediate; (b) through a bicapped-tetrahedral intermediate.

Table 3.1. Activation Parameters Reported for Intramolecular Isomerizations of Group VIB Metal Carbonyl Complexes

Complex	Process	$\Delta H^{\#}$ kcal mol^{-1}	$\Delta S^{\#}$ cal mol^{-1} deg^{-1}	Reference
$Cr(CO)_4[C(OMe)Me](Et_3P)$	cis ---> trans	21.2±0.5	-6.5±1.5	1,2
	trans ---> cis	22.5±0.5	-3.5±1.5	
$Cr(CO)_4(^{13}CO)(Et_3P)$	cis ---> trans	26.6±4.3	1.8±13.1	7
$Mo(CO)_4(n\text{-}Bu_3P)_2$	cis ---> trans	24.5±1.6	-5.6±4.8	4
	trans ---> cis	24.2±1.3	-9.8±4.0	
$W(CO)_4(^{13}CO)(Et_3P)$	cis ---> trans	9.2±3.7	-54.9±11.4	7
$W(CO)_4(^{13}CO)(CS)$	trans ---> cis	31.5±1.9	9.1±5	3

3.2 Experimental

3.2.1 Synthesis of $Cr(CO)_2(^{13}CO)_3(CS)$

(mbz)$Cr(CO)_2(CS)$ (10 mg) was dissolved in 10 ml of THF and transferred under N_2 to a specially constructed high-pressure stainless steel reaction vessel, lined with a Teflon jacket and connected to a second stainless steel chamber containing a measured amount of ^{13}CO (transferred on a vacuum line through a manometer and adsorbed on charcoal at 77 K). The solution was degassed by three freeze-thaw cycles and frozen in liquid nitrogen. The ^{13}CO was transferred to the solution chamber to give 20 atm pressure. The valve to the ^{13}CO storage chamber was then closed. The solution was heated at 65°C for periods of 6-24 h. Unreacted ^{13}CO was then readsorbed on the charcoal in the storage chamber by opening the valve between the chambers while both were submerged in liquid N_2. The product was isolated by evaporation of the solvent under reduced pressure with the temperature maintained at -15°C due to the volatility of $Cr(CO)_5(CS)$ [13]. ^{13}C NMR (10 scans) (relative to TMS): 212.1 (d, J = 5 Hz, cis CO) and 209.2 ppm (t, J = 5 Hz, trans CO). FT-IR (CS_2): ν(CO) 2066(m), 2056(w), 2008(m), 1988(m), 1978(s), 1958(vs), 1956(vs), 1945(m) cm^{-1}. The high-resolution mass spectrum of the product was obtained with a DuPont 21-492B spectrometer interfaced to a Hewlett Packard computer. Mol. wt: calculated for $^{13}C_3{}^{12}C_3O_5SCr$, 238.897; found, 238.894.

When the above reaction was carried out with less than 1 atm ^{13}CO pressure, partial decomposition of the starting material was observed. With the use of octane in place of THF as solvent under identical conditions to those described in the above procedure, no reaction occurred and the starting material was recovered with no observed decomposition.

3.2.2 Kinetic Investigation of Isomerization of $Cr(CO)_2(CX)[(MeO)_3P]_3$ (X = O, S, Se)

The *fac* ⟷ *mer* I isomerization reactions of $Cr(CO)_2(CX)[(MeO)_3P]_3$ (X = O, S, Se) were monitored by FT-IR spectroscopy. Solutions of complex in DCE were prepared and transferred under nitrogen to a thermostatted IR cell (0.1 mm pathlength, NaCl windows) (constructed in-house in accordance with a design published in Reference 14). The thermostatted cell assembly was placed in the IR beam, and IR spectra were acquired at recorded time intervals. The rate of *fac* → *mer* isomerization for the tricarbonyl complex was followed by monitoring the decrease of the a_1 ν(CO) peak of the *fac* isomer, while the rate of *mer* I → *fac* isomerization for the thio- and selenocarbonyl derivatives was monitored by the growth of the a' ν(CO) peak of the *fac* isomer. Rate constants (k_1 + k_{-1}) were calculated from the first-order rate plot of $\ln[A_e/(A_e-A_t)]$ vs. time, where A_t is the absorbance at time t and A_e is the absorbance at equili-

brium, using a linear least-squares program (Plotrax 2 from Engineering-Science Inc., Atlanta, Georgia, U.S.A.). The rate constants for the forward and reverse reactions were obtained by solving the equations:

$$k_c = k_1 + k_{-1}$$

$$K_{eq} = k_1/k_{-1}$$

where k_c is the calculated rate constant and K_{eq} was determined from the integrated areas of the resonances of the isomers in the ^{31}P NMR spectrum recorded on a Varian XL-300 NMR spectrometer. The activation parameters were calculated from the rate constants at three different temperatures.

3.2.3 Monitoring of Stereochemically Nonrigid Behaviour of $Cr(CO)_2(CX)[(MeO)_3P]_3$ (X = O, S, Se) Complexes

Two-dimensional (2-D) NOE ^{31}P NMR experiments were performed on a Varian XL-300 spectrometer, equipped with a 5-mm broad-band probe. $Cr(CO)_2(CX)[(MeO)_3P]_3$ (X = O, S, Se) was dissolved under N_2 in deuterotoluene and heated in the probe at temperatures ranging from 30-80°C. Usually 4-32 transients were co-added to achieve a good signal-to-noise ratio. A total of 128 or 256 FIDs were acquired and zero filling was performed in the evolution domain. The 2-D NOE Accordian pulse sequence used was: ($\pi/2$, t_1, $\pi/2$, mix, π, t_2) with a repetition delay of 2 s and incrementing the

mixing time according to the equation $t_{mix} = \kappa \times t_1$ with κ = 30. ^{31}P nuclei were proton-decoupled during the evolution and detection periods. The FIDs were collected in either a [512 X 512] or [1024 X 1024] matrix. The data matrix was Fourier transformed in two dimensions and plotted by a contour plot program. The digital resolution in the evolution domain is sw_2/NI, where sw_2 is the spectral width in the evolution domain and NI is the number of increments or FIDs, while the digital resolution in the detection domain is equal to 1/AT (AT = acquisition time) and is approximately 8 Hz.

3.3 Results and Discussion

The isomerization of mer-$Cr(CO)_2(CX)[(MeO)_3P]_3$ (X = S, Se) in solution at room temperature was established by monitoring the changes with time in the carbonyl region of the IR spectrum of the pure mer I isomer, obtained by TLC purification as described in Chapter 2. The mer I to fac interconversion is illustrated in Figure 3.2 for the case of the selenocarbonyl derivative, displaying the growth of the peak at 1962 cm^{-1} characteristic of the fac isomer (Figure 2.8).

The study was also extended to the analogous fac-$Cr(CO)_3[(MeO)_3P]_3$ complex. The higher-frequency $\nu(CO)$ mode in the FT-IR spectrum of this complex in solution at room

temperature was observed to decrease with time, accompanied by the growth of a new peak at 1977 cm^{-1} (Figure 3.3) attributable to mer-$Cr(CO)_3[(MeO)_3P]_3$ (see Table 2.7). The intensity of the second $\nu(CO)$ mode of the fac isomer increased with time due to its coincidence with the intense lower-frequency $\nu(CO)$ mode of the mer isomer (Figure 3.4). Thus fac-$Cr(CO)_3[(MeO)_3P]_3$ has been shown to also undergo rearrangement in solution at room temperature. In a recent publication [9], electrochemical oxidation has been reported to induce intramolecular isomerization of fac-$M(CO)_3[(MeO)_3P]_3$ (M = Cr, Mo). This process occurs through the generation of the fac-$\{M(CO)_3[(MeO)_3P]_3\}^+$ cationic complex which undergoes rapid conversion to mer-$\{M(CO)_3[(MeO)_3P]_3\}^+$. Addition of one electron to the cationic mer isomer generates mer-$M(CO)_3[(MeO)_3P]_3$. The authors mention that the neutral chromium complex also exhibits intramolecular isomerization, but at a much slower rate than the cation.

In order to establish that the isomerization of $Cr(CO)_2(CX)[(MeO)_3P]_3$ (X = S, Se) proceeds through a non-dissociative mechanism, the isomerization of mer-$Cr(CO)_2$-$(CX)[(MeO)_3P]_3$ was followed in solution in the presence of excess $(PhO)_3P$ at 60°C using FT-IR spectroscopy. No incorporation of $(PhO)_3P$ into the complex was observed, as evidenced by the lack of any peaks in the FT-IR difference spectrum of the equilibrium mixtures obtained in the

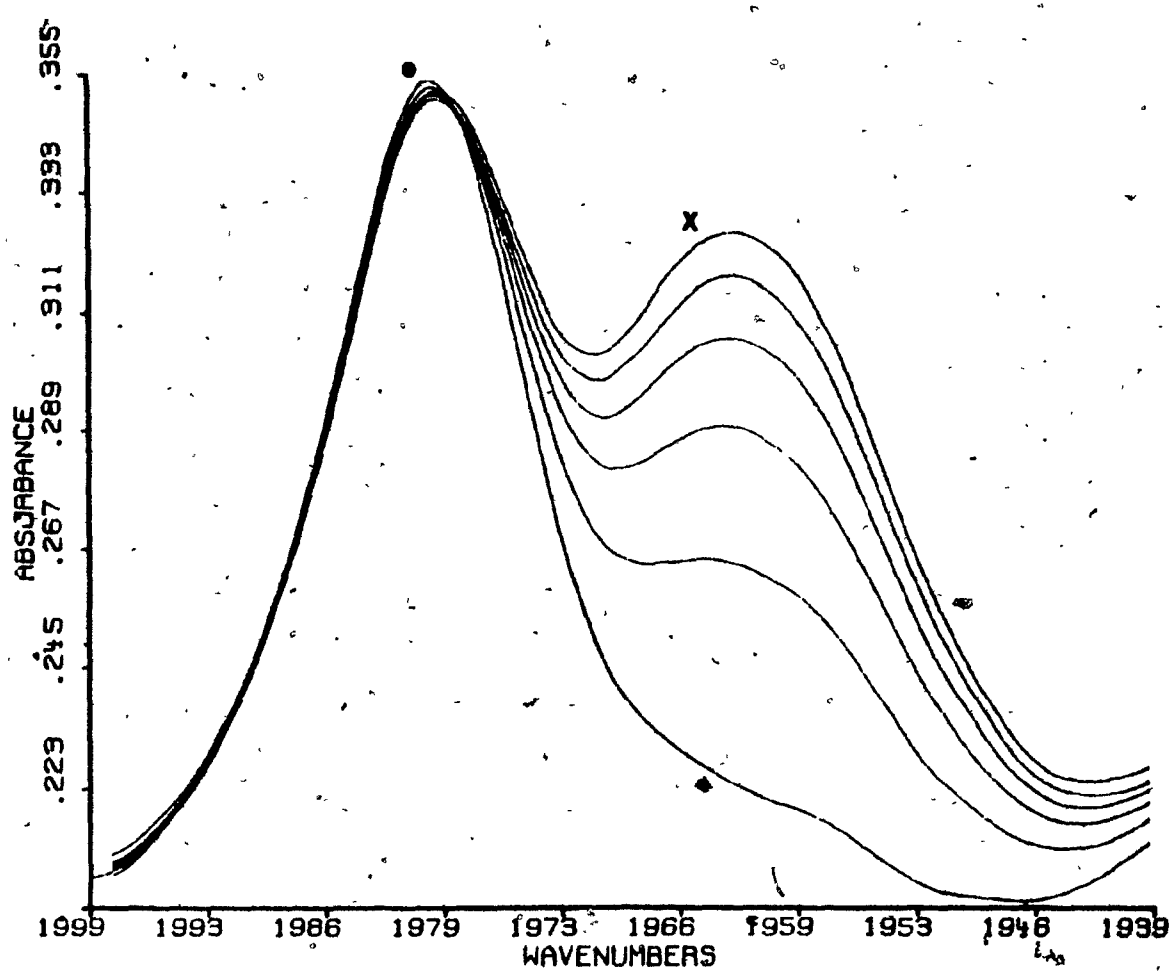

Figure 3.2. Isomerization of mer-$Cr(CO)_2(CSe)[(MeO)_3P]_3$ (•) in dichloroethane solution at 38.0 °C as monitored by FT-IR spectroscopy, showing the formation of fac-$Cr(CO)_2(CSe)[(MeO)_3P]_3$ (X).

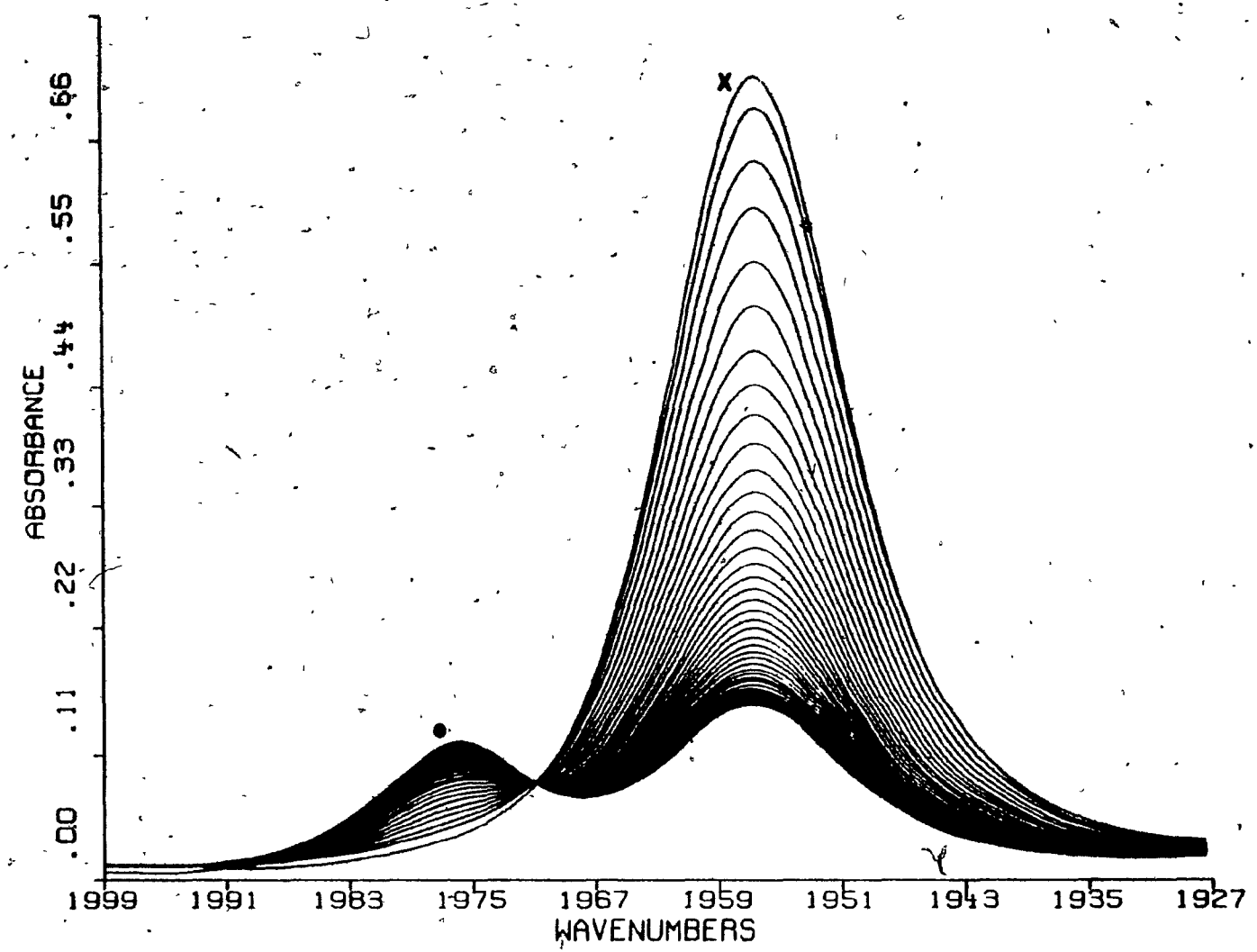

Figure 3.3. Isomerization of <u>fac</u>-$Cr(CO)_3[(MeO)_3P]_3$ (X) in dichloroethane solution at 49.2°C as monitored by FT-IR spectroscopy, showing the formation of <u>mer</u>-$Cr(CO)_3[(MeO)_3P]_3$ (●).

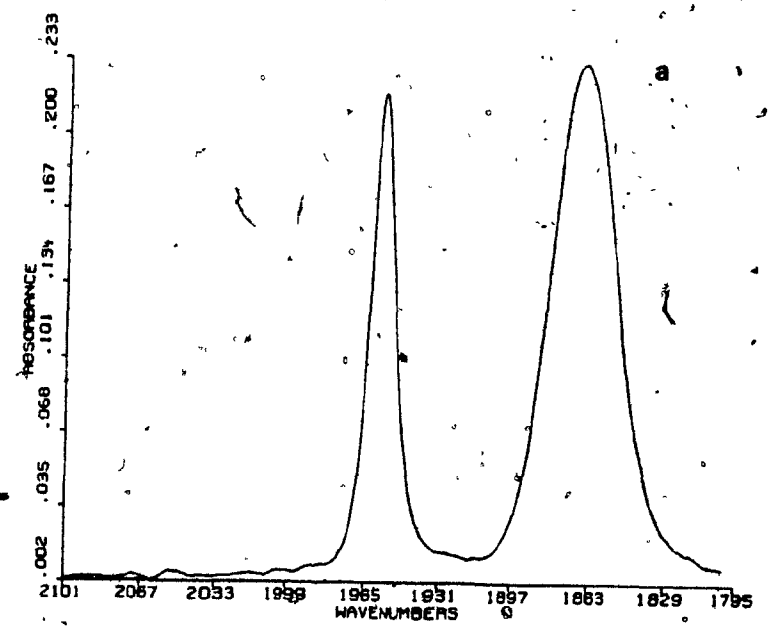

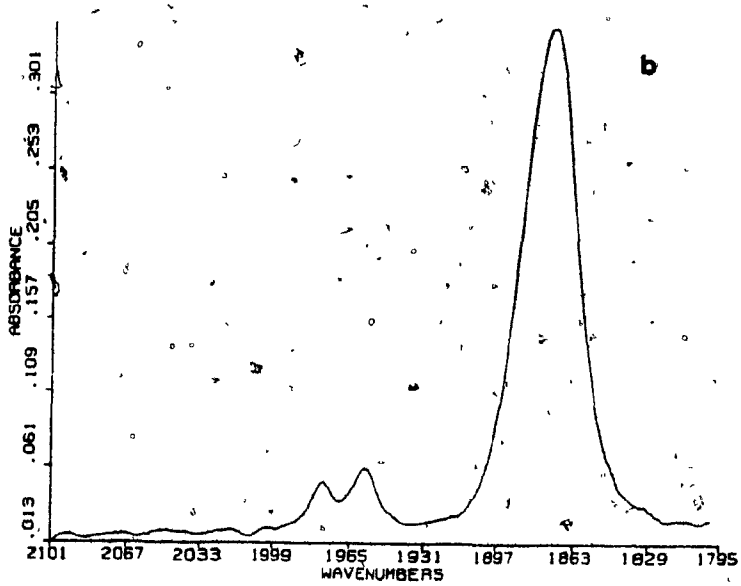

Figure 3.4. FT-IR spectra (in dichloroethane) in the carbonyl stretching region of (a) <u>fac</u>-$Cr(CO)_3[(MeO)_3P]_3$ and (b) an equilibrium mixture of this complex and its <u>mer</u> isomer.

presence and absence of $(PhO)_3P$. Furthermore, there was no shift in the position of the isosbestic point obtained for the isomerization process. The above evidence indicates that the isomerization occurs through a non-dissociative pathway.

In a second experiment, arene displacement from $(mbz)Cr(CO)_2(CS)$ was effected in the presence of ^{13}CO at 60°C for 6 h in THF to yield $Cr(CO)_2(^{13}CO)_3(CS)$. The splitting pattern in the ^{13}C NMR spectrum of this product (Figure 3.5) reveals that only three labelled carbonyl groups are present, while a fourth ^{13}CO ligand would have been incorporated if isomerization occurred by a dissociative mechanism subsequent to product formation. The two ^{13}CO resonances observed were identified on the basis of the previous assignment of the ^{13}C NMR spectrum of $Cr(CO)_5(CS)$ [13]. The higher-field resonance (209.2 ppm) is attributed to ^{13}CO <u>trans</u> to the CS ligand and is split into a triplet, while the lower-field resonance (212.1 ppm) due to ^{13}CO in the equatorial plane is split into a doublet. This splitting pattern is consistent with both the <u>fac</u> and <u>mer</u> I configurations of $Cr(CO)_2(CS)L_3$ (L = ^{13}CO), whereas the <u>mer</u> II isomer, having three ^{13}CO ligands in the equatorial plane, would give rise to a singlet which may be hidden under the doublet. While the number of isomers of $Cr(CO)_2(^{13}CO)(CS)$ in the sample thus cannot be established from the ^{13}C NMR

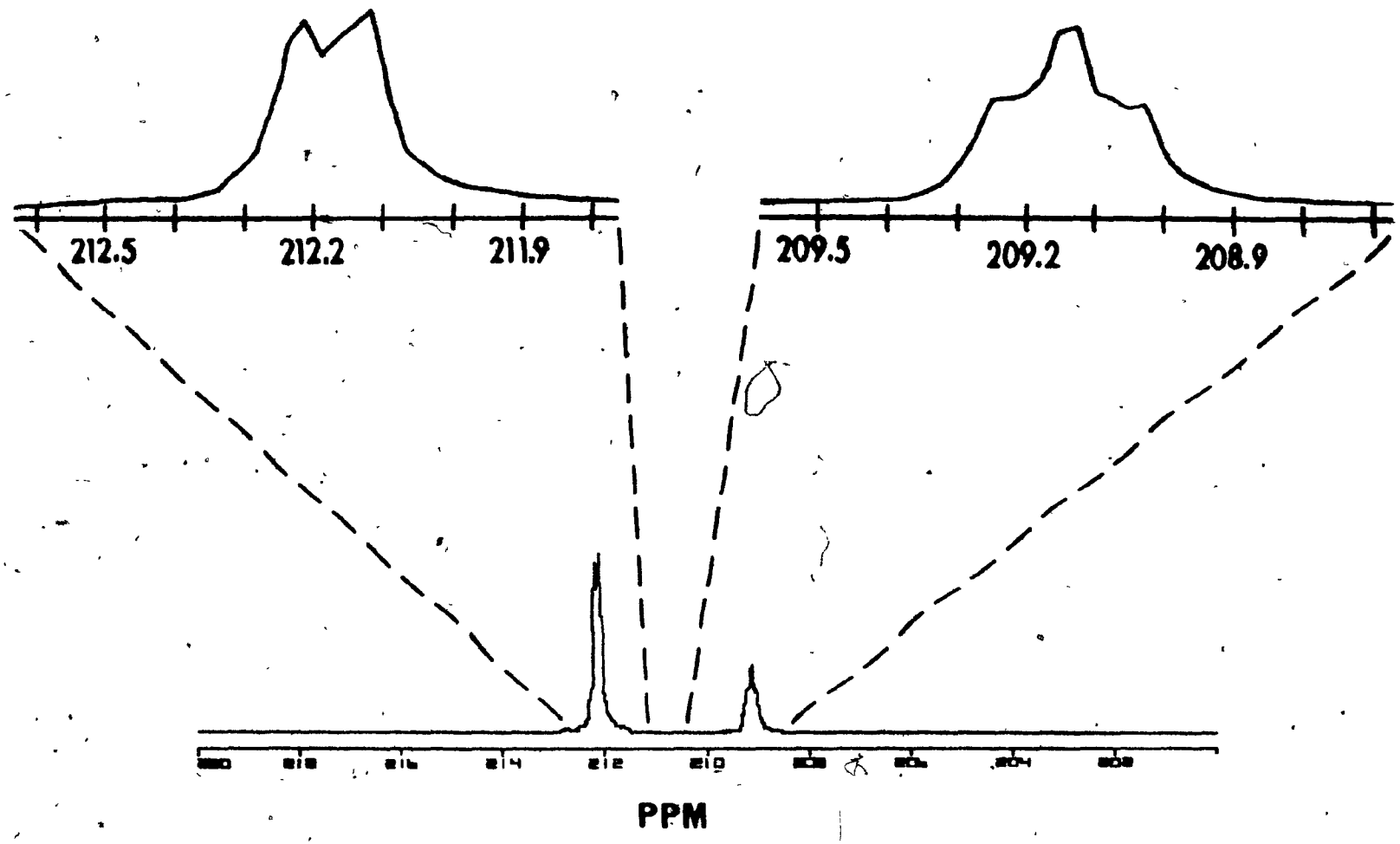

Figure 3.5. ^{13}C NMR spectrum of $Cr(CO)_2(^{13}CO)_3(CS)$ in CD_2Cl_2. Conditions: obtained on a Varian XL-200 FT spectrometer operating at 50.31 MHz; sweep width = 20,000 Hz; offset = 5,000 Hz; flip angle = 30°; repetition time = 0.6 s; number of scans = 10.

spectrum, the abundance of peaks in the carbonyl region of the IR spectrum (Figure 3.6) establishes that more than a single isomer is present. The observed frequencies are tabulated in Table 3.2, together with the frequencies calculated in the energy-factored force field approximation on the basis of force constants reported for $Cr(CO)_5(CS)$ [15]. The comparison of the observed and calculated frequencies reveals that fac-$Cr(CO)_2(^{13}CO)_3(CS)$ is present togther with some amount of either the mer I or the mer II isomer or both. These results do not demonstrate definitively that $Cr(CO)_2(^{13}CO)_3(CS)$ also undergoes intramolecular isomerization, since the observation of at least two isomers of this complex may be the result of a rearrangement process during the course of the arene displacement reaction. However, they do establish that if $Cr(CO)_2(^{13}CO)_3(CS)$ does isomerize, it does so by a non-dissociative mechanism, as does $W(CO)_4(^{13}CO)(CS)$ [3].

The rate constants for fac → mer and mer → fac isomerization of $Cr(CO)_2(CX)[(MeO)_3P]_3$ (X = S, Se; mer = mer I) and $Cr(CO)_3[(MeO)_3P]_3$ were calculated from the opposing first-order reactions

$$\text{fac-}Cr(CO)_2(CX)[(MeO)_3P]_3 \underset{k_{-1}}{\overset{k_1}{\rightleftharpoons}} \text{mer-}Cr(CO)_2(CX)[(MeO)_3P]_3$$

(X = O, S, Se)

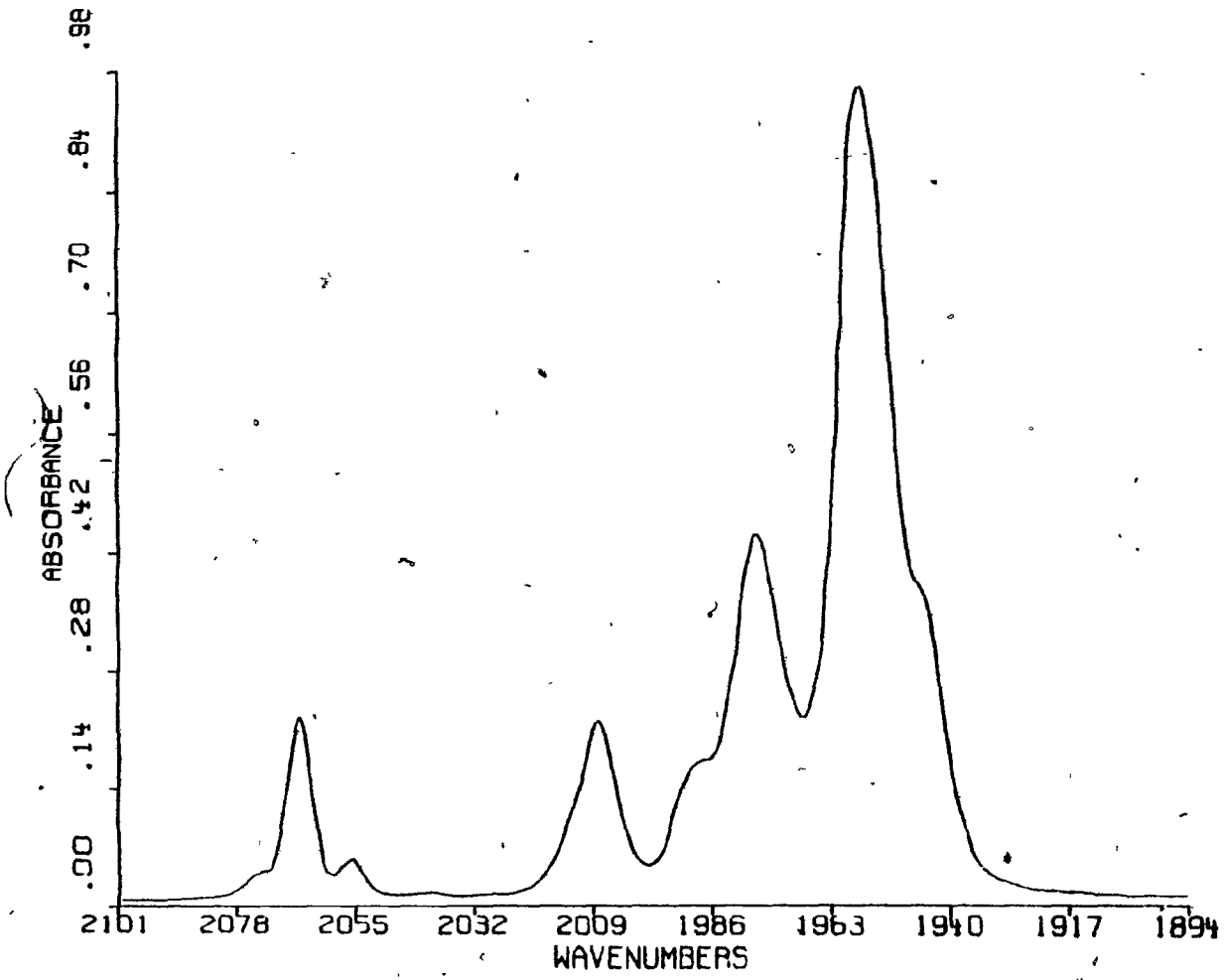

Figure 3.6. FT-IR spectrum in the carbonyl stretching region of $Cr(CO)_2(^{13}CO)_3(CS)$ in CS_2.

Table 3.2. Observed and Calculated Frequencies (cm^{-1}) for ν(CO) Modes of $Cr(CO)_2(^{13}CO)_3(CS)$ in CS_2

Observed	Calculated[a]		
	fac	mer I	mer II
2066	2067	2069	2066
2056	-	-	-
2008	2007		2014
1988		1991 1989	1986
1978	1978		
		1972	
1958	1959		
1956	1955		1957
1945		1945	1945

[a]Calculated from energy-factored anharmonic force constants reported in Reference 15 for $Cr(CO)_5(CS)$ in CS_2 solution: $k_{CO}(ax) = 16.63$; $k_{CO}(eq) = 16.46$; $k_{CO,CO}(ax,eq) = 0.22$; $k_{CO,CO(\underline{cis})}(eq,eq) = 0.24$; $k_{CO,CO(\underline{trans})}(eq,eq) = 0.47$ mdyn $Å^{-1}$.

using the equations:

$$K_{eq} = k_1/k_{-1} = \frac{[\underline{mer}\text{-}Cr(CO)_2(CX)[(MeO)_3P]_3]}{[\underline{fac}\text{-}Cr(CO)_2(CX)[(MeO)_3P]_3]}$$

and

$$k_1 + k_{-1} = t^{-1} \ln A_e/(A_e - A_t)$$

where A_t is the absorbance at time t and A_e is the absorbance at equilibrium of a ν(CO) mode in the FT-IR spectrum.

In order to determine the rates of the forward and reverse reactions, it was necessary to measure the distribution of the isomers at equilibrium. ^{31}P NMR spectroscopy was the technique chosen. The relative intensities of the peaks in a ^{31}P FT-NMR spectrum are a reliable measure of relative concentration providing the nuclei are given sufficient time to relax between pulses. Consequently, the spin-lattice relaxation times, T_1, were determined for the isomers under investigation and the values obtained are shown in Table 3.3. It is of interest to note that the relaxation times decrease in the order P <u>trans</u> to P > P <u>trans</u> to CX (X = O, S, Se). This trend has been observed for other $M(CO)_n[R_3P]_{6-n}$ complexes and is attributed mainly to dipole-dipole relaxation [16]. Using gated decoupling, with an interval between pulses approximately ten times longer than

Table 3.3. Spin-Lattice Relaxtion Times (T_1) for Phosphorus Nuclei in $Cr(CO)_2(CX)[(MeO)_3P]_3$ (X = O, S, Se)

Complex	T_1 (s)		
	P *trans* to P	P *trans* to CS/CSe	P *trans* to CO
fac-$Cr(CO)_3[(MeO)_3P]_3$			2.35±0.03
mer-$Cr(CO)_3[(MeO)_3P]_3$	1.84±0.03		2.37±0.06
fac-$Cr(CO)_2(CS)[(MeO)_3P]_3$		2.40±0.04	2.28±0.03
mer I $Cr(CO)_2(CS)[(MeO)_3P]_3$	1.76±0.05	2.45±0.02	
mer II $Cr(CO)_2(CS)[(MeO)_3P]_3$	1.86±0.05		2.41±0.10
fac-$Cr(CO)_2(CSe)[(MeO)_3P]_3$		3.17±0.24	2.84±0.22
mer I $Cr(CO)_2(CSe)[(MeO)_3P]_3$	2.40±0.14	3.18±0.23	

T_1, thus allowing the nuclei sufficient time to relax, the relative ratios of the isomers present were obtained (Figures 3.7-3.9). The equilibrium constants were not found to be temperature dependent in the range of 20°C to 80°C. For all three complexes, the mer isomer (mer I in the case of the CS and CSe complexes) is predominant and the equilibrium mer/fac ratio is approximately the same (K_{eq} = 5.0).

Although the mer II isomer has not been observed spectroscopically by FT-IR or ^{13}C NMR, the ^{31}P NMR spectra of both the thiocarbonyl and selenocarbonyl complexes provided some empirical evidence of a minor component (~ 5% of the mer I isomer) with a splitting pattern and chemical shift values consistent with the mer II configuration (Figures 3.8 and 3.9). The appearance of a doublet and a triplet with a coupling constant similar to that of the mer I isomer indicates a structure in which two $(MeO)_3P$ ligands are trans to each other and cis to a third $(MeO)_3P$. The location of the triplet resonance downfield from the triplet of both fac and mer I isomers is indicative of a phosphorus trans to a CO rather than a CX, while the upfield shift of the doublet resonance relative to that of mer-$Cr(CO)_3[(MeO)_3P]_3$ (see Table 2.10), indicating a lower electron density at the metal centre, confirms the presence of a CX ligand. The low concentration of the mer II isomer relative to the fac or mer I isomer can be interpreted in terms of a site

Figure 3.7. ^{31}P NMR spectrum (in deuterotoluene) of an equilibrium mixture of the isomers of $Cr(CO)_3[(MeO)_3P]_3$. K_{eq} = mer /fac = 5.0. Conditions: obtained on a Varian XL-300 FT spectrometer operating at 121.42 MHz; ^1H-decoupled; sweep width = 2,700 Hz; offset = 22,900 Hz; flip angle = 66°; repetition time = 20 s; number of scans = 4.

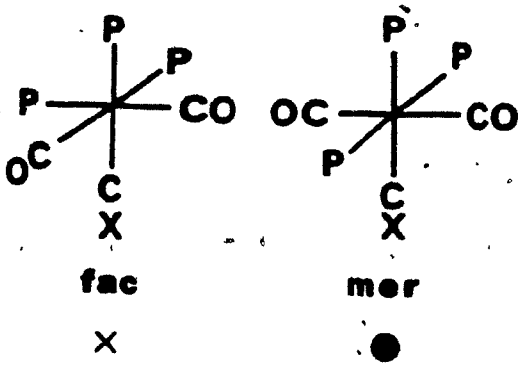
P
P
P
CO
OC
C
X
fac
P
P
OC
CO
P
C
X
mer

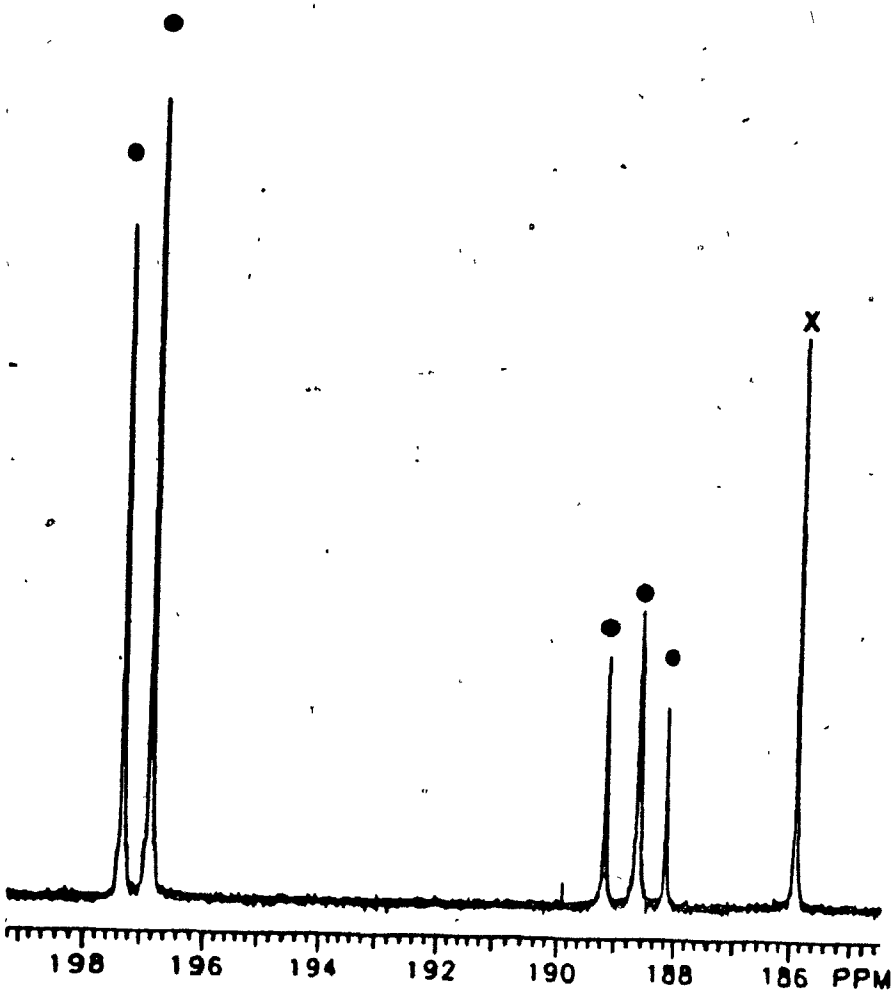
X
198
196
194
192
190
188
186
PPM

Figure 3.8. ^{31}P NMR spectrum (in deuterotoluene) of an equilibrium mixture of the isomers of $Cr(CO)_2(CS)[(MeO)_3P]_3$. K_{eq} = mer I/fac = 5.0, mer I/mer II = 20.3. Conditions: obtained on a Varian XL-300 FT spectrometer operating at 121.42 MHz; ^1H-decoupled; sweep width = 2,600 Hz; offset = 22,100 Hz; flip angle = 90°; repetition time = 40 s; number of scans = 400.

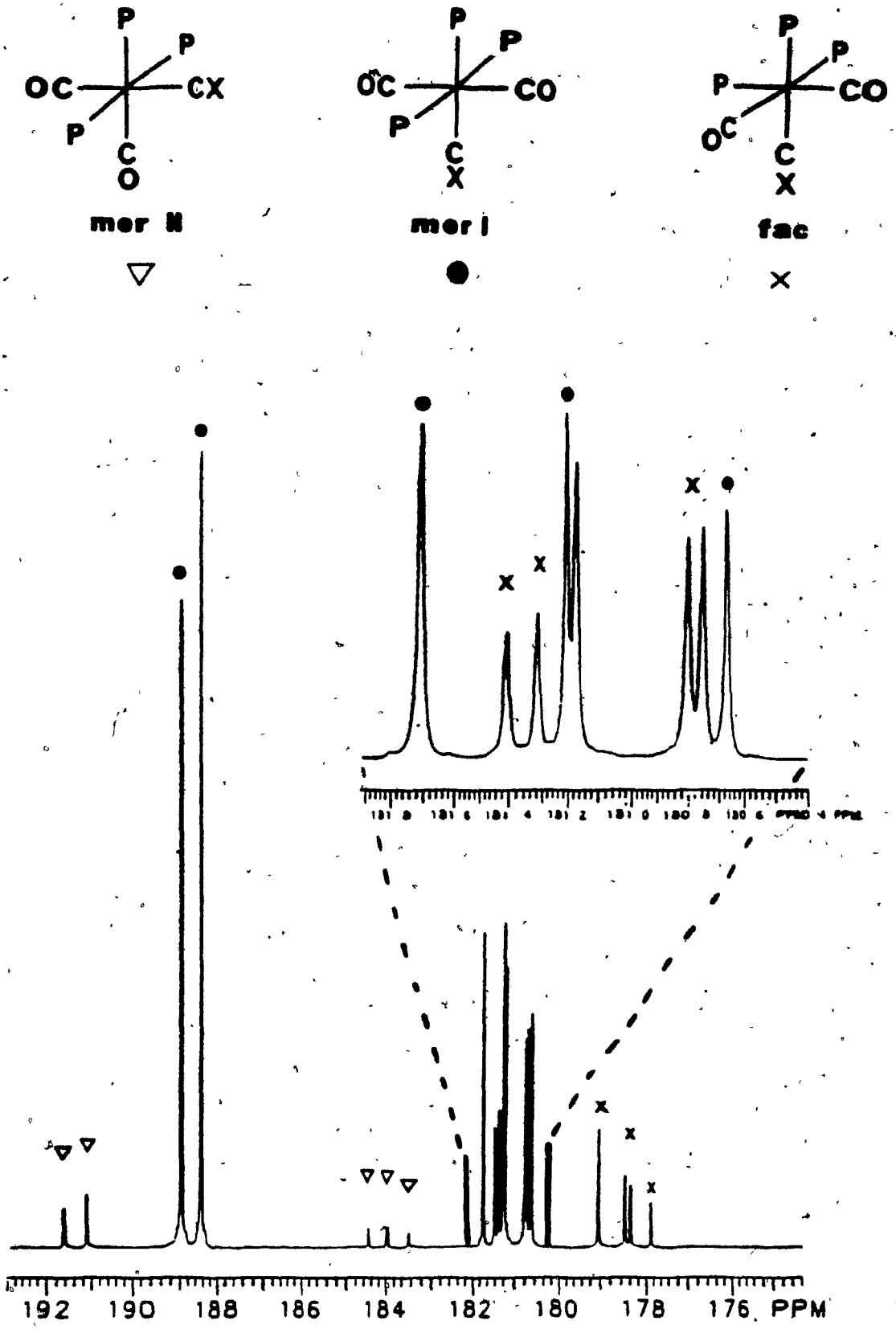
P
P
OC
CX
P
C
O
mer II
▽
P
P
OC
CO
P
C
X
mer I
●
P
P
P
CO
OC
C
X
fac
×
192
190
188
186
184
182
180
178
176
PPM

Figure 3.9. ^{31}P NMR spectrum (in deuterotoluene) of an equilibrium mixture of the isomers of $Cr(CO)_2(CSe)[(MeO)_3P]_3$. K_{eq} = mer I/fac = 5.0, mer I/mer II = 20.3. Conditions: obtained on a Varian XL-300 FT spectrometer operating at 121.42 MHz; ^1H-decoupled; sweep width = 3,400 Hz; offset = 20,900 Hz; flip angle = 90°; repetition time = 40 s; number of scans = 400.

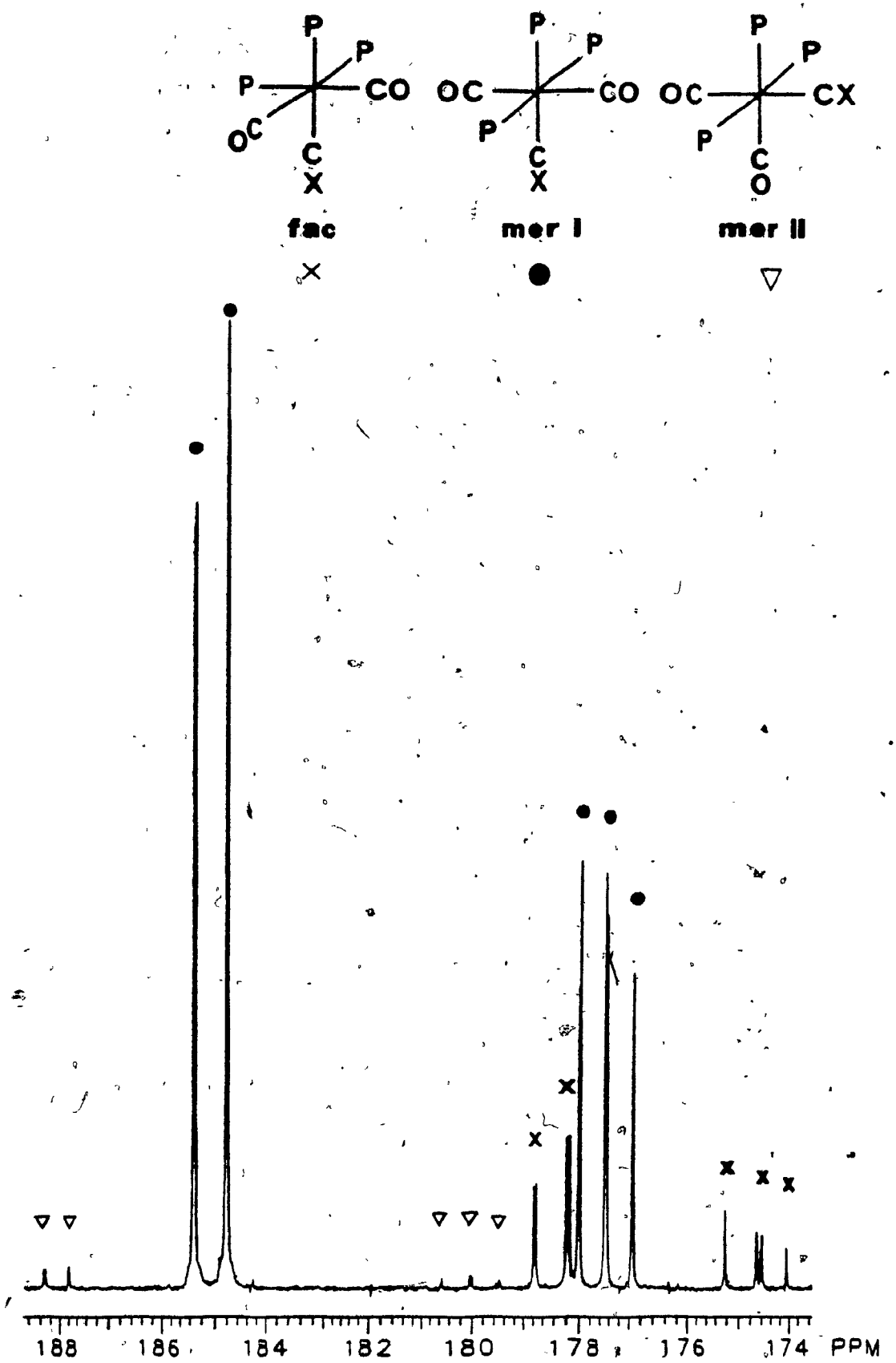
P
P
P
CO
OC
C
X
fac
P
P
OC
CO
P
C
X
mer I
P
P
OC
CX
P
C
O
mer II
188
186
184
182
180
178
176
174
PPM

preference of the CX ligand. In studies of the trans → cis isomerization of a series of $W(CO)_4(CS)(L)$ complexes [17], it was found that K_{eq} = [cis]/[trans] decreased with an increase in the ratio of σ-donor/π-acceptor strength of the ligand L. Therefore, the thiocarbonyl ligand appears to exhibit a preference for a site trans to a strong σ-donor/ weak π-acceptor. Consequently, the fac and mer I isomers of $Cr(CO)_2(CS)[(MeO)_3P]_3$, in which the CS ligand is trans to $(MeO)_3P$, would be predicted to be favoured with respect to the mer II isomer, in which CS is trans to CO. While the site preference of the CSe ligand has not been investigated, it is expected to be the same as that of CS, due to the similarity in the bonding properties of these ligands.

The rate constants for the fac ⟷ mer isomerization of $Cr(CO)_2(CX)[(MeO)_3P]_3$ (mer I for X = S, Se) revealed that $k_1 > k_{-1}$ (Table 3.4) and that k_1 decreases in the order X = Se > S > O. The ln k_1 vs 1/T plots are shown in Figure 3.10. The activation parameters for the forward and reverse processes are given in Table 3.5. The activation enthalpies are large and positive while the entropies are negative. Moreover, for the three chalcocarbonyl complexes examined, the forward and reverse reactions differ mainly in the entropy value, indicating steric factors determine the equilibrium ratio. The greater stability of the mer or mer I isomers may thus be postulated to result from the

Table 3.4. First-Order Rate Constants for the Isomerization Processes of $Cr(CO)_2(CX)[(MeO)_3P]_3$ (X = O, S, Se) in Dichloroethane

CX	Observed process	T °C	Rate constants X 10^4 (s^{-1}) $k_1 + k_{-1}$	k_1	k_{-1}
CSe	mer I ---> fac	50.4	8.82	7.35	1.47
		38.0	3.28	2.73	0.55
		32.6	2.14	1.78	0.36
CS	fac ---> mer I	61.8	15.28	12.73	2.55
		45.3	3.88	3.23	0.65
		23.4	5.96	0.50	0.10
CO	fac ---> mer	59.0	3.58	2.98	0.60
		49.2	1.64	1.37	0.27
		22.0	0.12	0.10	0.02

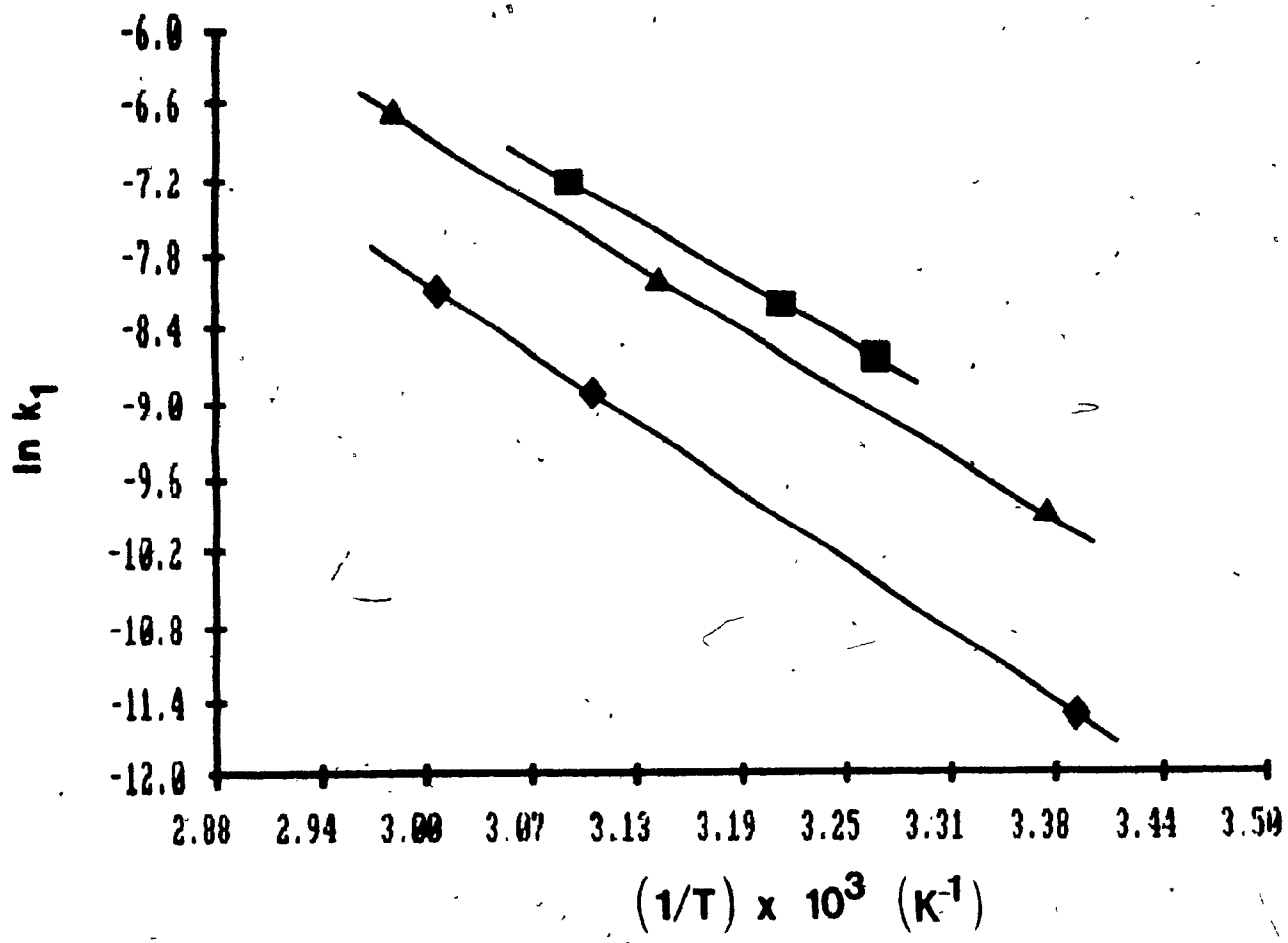

Figure 3.10. Plots of ln k_1 vs. 1/T for the fac ⟷ mer isomerization of $Cr(CO)_3[(MeO)_3P]_3$ (♦) and the fac ⟷ mer I isomerization of $Cr(CO)_2(CS)[(MeO)_3P]_3$ (▲) and $Cr(CO)_2(CSe)[(MeO)_3P]_3$ (■).

Table 3.5. Activation Parameters for Isomerization Processes of $Cr(CO)_2(CX)[(MeO)_3P]_3$ (X = O, S, Se)

Complex	Process	$\Delta H^{\#}$ kcal mol^{-1}	$\Delta S^{\#}$ cal mol^{-1} deg^{-1}
$Cr(CO)_2(CSe)[(MeO)_3P]_3$	fac ---> mer I	15.6±0.3	-25±1
$Cr(CO)_2(CSe)[(MeO)_3P]_3$	mer I ---> fac	15.5±0.3	-28±1
$Cr(CO)_2(CS)[(MeO)_3P]_3$	fac ---> mer I	16.6±0.4	-22±1
$Cr(CO)_2(CS)[(MeO)_3P]_3$	mer I ---> fac	16.6±0.4	-25±1
$Cr(CO)_3[(MeO)_3P]_3$	fac ---> mer	18.0±0.3	-20±1
$Cr(CO)_3[(MeO)_3P]_3$	mer ---> fac	18.0±0.3	-24±1

decreased steric interaction between phosphite ligands in these isomers relative to the fac isomers.

Large enthalpies of activation have been measured for the intramolecular isomerization of other Group VIB metal carbonyl complexes (Table 3.1) and have been accounted for in terms of bond lengthening in the activated complex prior to or during the course of rearrangement [7]. In comparing the activation parameters of the selenocarbonyl and thiocarbonyl complexes to those of their tricarbonyl analogue, it is of interest to note that the enthalpy of activation is smaller for the former complexes. This is in line with the observed trans labilizing effect of CS and CSe ligands in dissociative processes. The increasing negative entropy of activation in the order O < S < Se can be related to the relative sizes of these atoms (Se > S > O).

Two-dimensional NMR spectroscopy [18] has recently been employed in the study of chemical exchange processes of organometallic complexes [19,20]. In the present work, a 2-D NOE ^{31}P NMR investigation demonstrated dynamic intramolecular interconversion between the mer I and mer II isomers of $Cr(CO)_2(CX)[(MeO)_3P]_3$ (X = S, Se) taking place on the time scale of the NMR experiment at temperatures above 50°C (Figures 3.11-3.13). The intramolecular nature of the process was demonstrated by the lack of correlation in 2-D NMR between resonances of the complexes and those of excess ligand present in solution. However, the fac to mer I or

Figure 3.11. 2-D ^{31}P contour map for $Cr(CO)_2(CS)[(MeO)_3P]_3$ in deuterotoluene at 61°C on a Varian XL-300 spectrometer; an NOE accordian pulse sequence was employed with κ = 30. All three isomers exhibit an AB_2 coupling pattern (chemical shifts are relative to H_3PO_4 as external standard): ▽ = <u>mer</u> II P_2,P_3(d) 191.4 ppm, P_1(t) 184.0 ppm (J = 64 Hz); ● = <u>mer</u> I P_2,P_3(d) 188.6 ppm, P_1(t) 181.2 ppm (J = 64 Hz); X = <u>fac</u> P_2,P_3(d) 181.1 ppm, P_1(t) 178.5 ppm (J = 72 Hz).

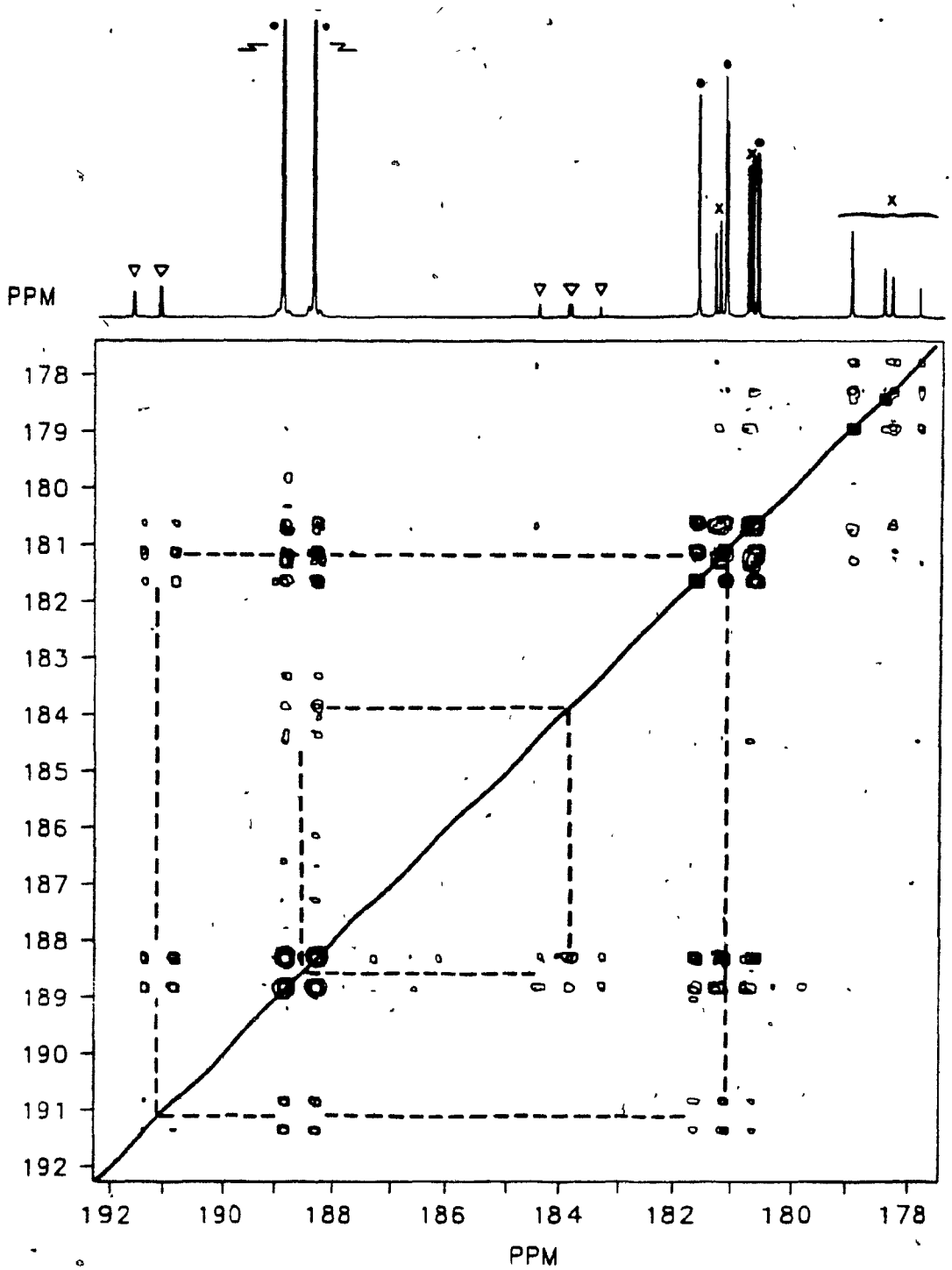
PPM
178
179
180
181
182
183
184
185
186
187
188
189
190
191
192
192
190
188
186
184
182
180
178
PPM

Figure 3.12. 2-D ^{31}P contour map for $Cr(CO)_2(CSe)[(MeO)_3P]_3$ in deuterotoluene at 61°C on a Varian XL-300 spectrometer; an NOE accordian pulse sequence was employed with κ = 30. All three isomers exhibit an AB_2 coupling pattern (chemical shifts are relative to H_3PO_4 as external standard): ▽ = <u>mer</u> II P_2,P_3(d) 187.2 ppm, P_1(t) 180.3 ppm (J = 63 Hz); ● = <u>mer</u> I P_2,P_3(d) 184.9 ppm, P_1(t) 177.5 ppm (J = 63 Hz); X = <u>fac</u> P_2,P_3(d) 178.6 ppm, P_1(t) 174.7 ppm (J = 72 Hz).

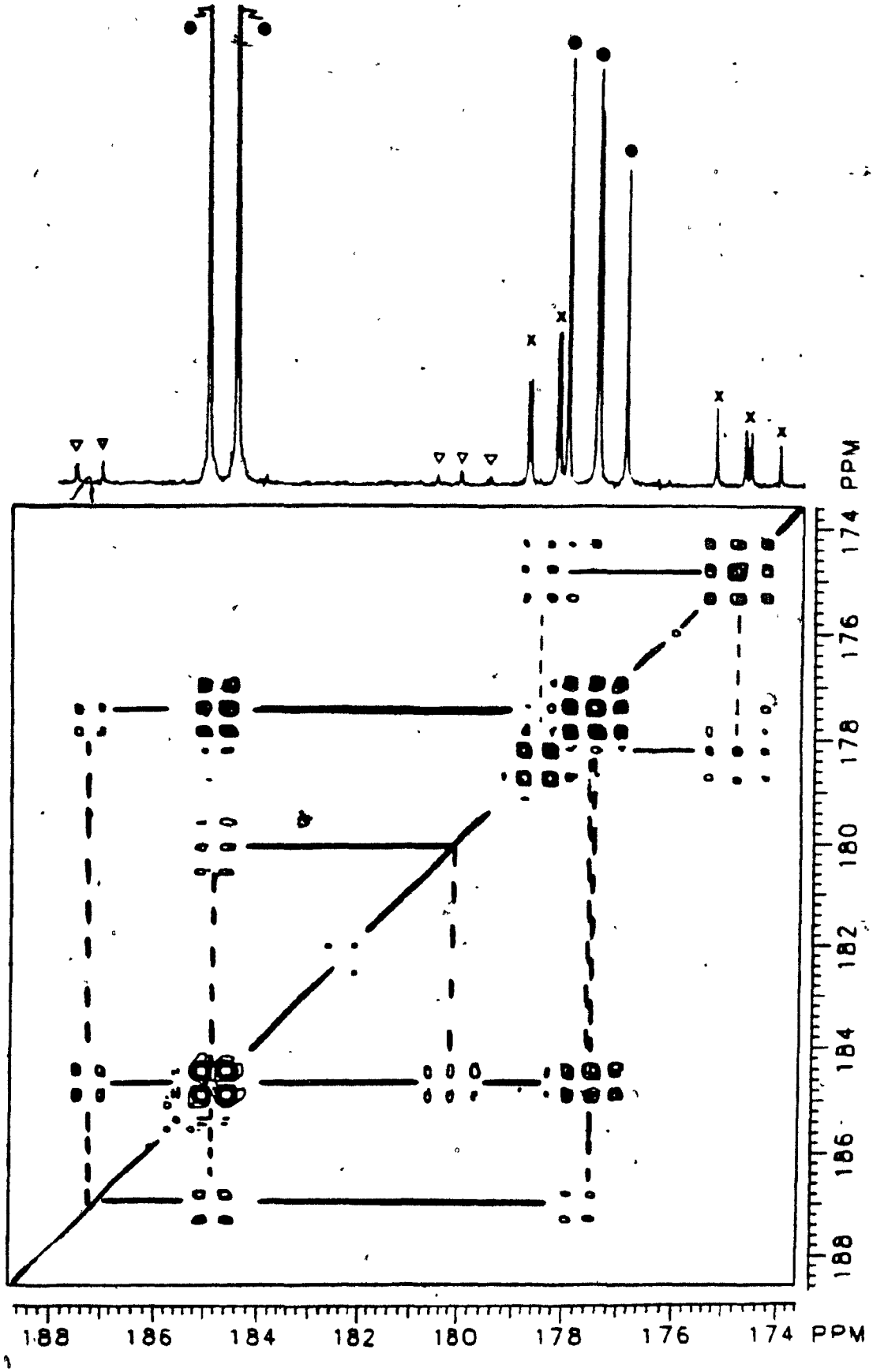
PPM
174
176
178
180
182
184
186
188
188
186
184
182
180
178
176
174
PPM

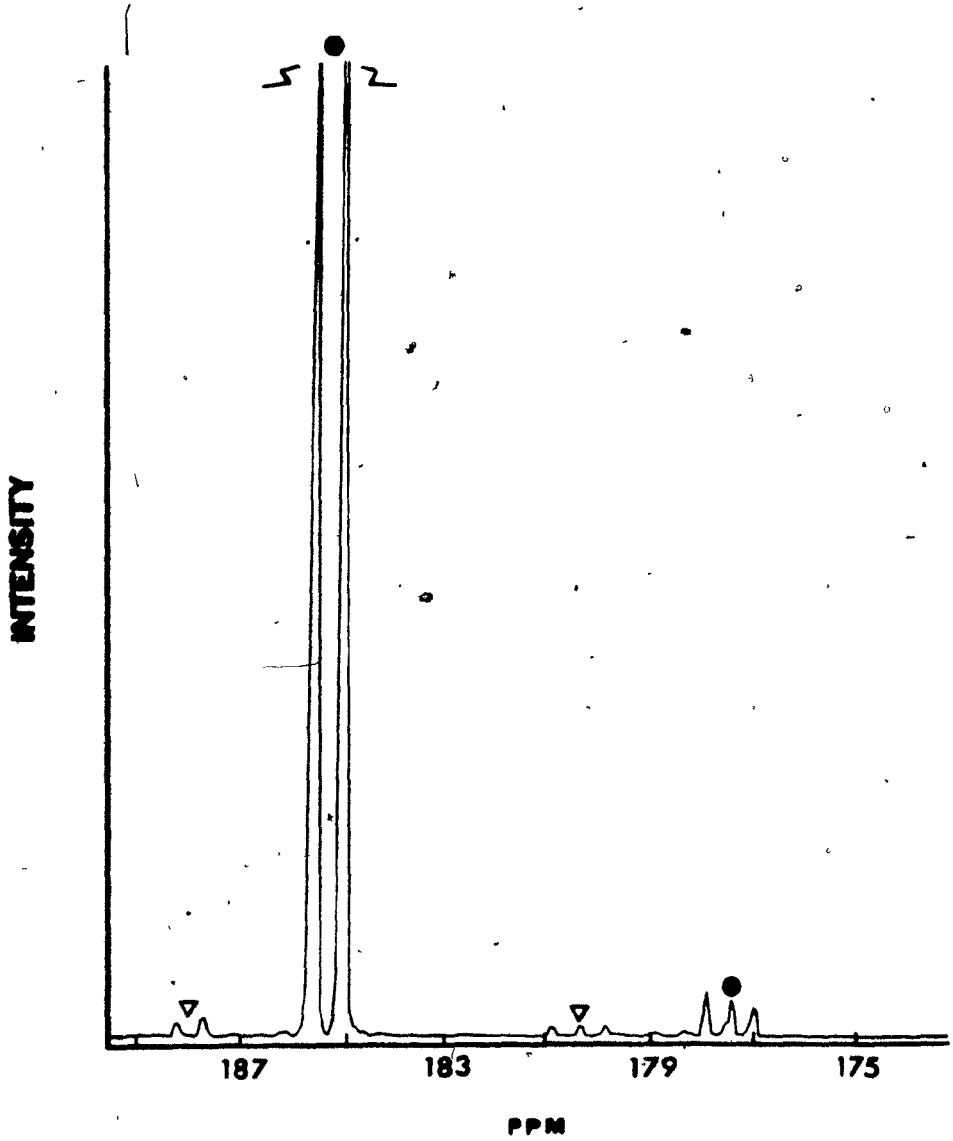

Figure 3.13. A cross section at 185 ppm in the evolution domain of Figure 3.12, displaying the correlation between the resonances of the <u>mer</u> I (●) and <u>mer</u> II (▽) isomers of $Cr(CO)_2(CSe)[(MeO)_3P]_3$.

fac to mer II interconversion was not observed at temperatures ranging up to 80°C for either the selenocarbonyl or the thiocarbonyl complex. Temperatures higher than 80°C resulted in some decomposition of these complexes.

The 2-D NMR studies of the mer I to mer II isomerization of $Cr(CO)_2(CX)[(MeO)_3P]_3$ (X = S, Se) provided information on the possible nature of the intermediates involved. The bicapped-tetrahedron mechanism would preserve the coupling pattern for each phosphorus nucleus in the two isomers (Figure 3.14). On the other hand, for the trigonal prismatic twist, the triplet of the mer I isomer would correlate with the doublet of the mer II isomer while the doublet of the mer I isomer would correlate with both the triplet and the doublet in the spectrum of the mer II isomer. The 2-D NMR spectra (Figures 3.11-3.12) illustrate both NOE and possible chemical exchange between the phosphorus nuclei of the same molecule by the distinct symmetrical off-diagonal contour on the exchange map. More importantly, however, the exchange of the mer I to mer II isomer provides convincing proof of dynamic rearrangement via a trigonal prism rather than a bicapped tetrahedron, as seen from the correlation of the off-diagonal peak of the doublet of the mer II isomer (bottom left-hand side of the contour map) to the doublet and triplet of mer I, while the triplet of the mer II is exchanging with the doublet of mer I.

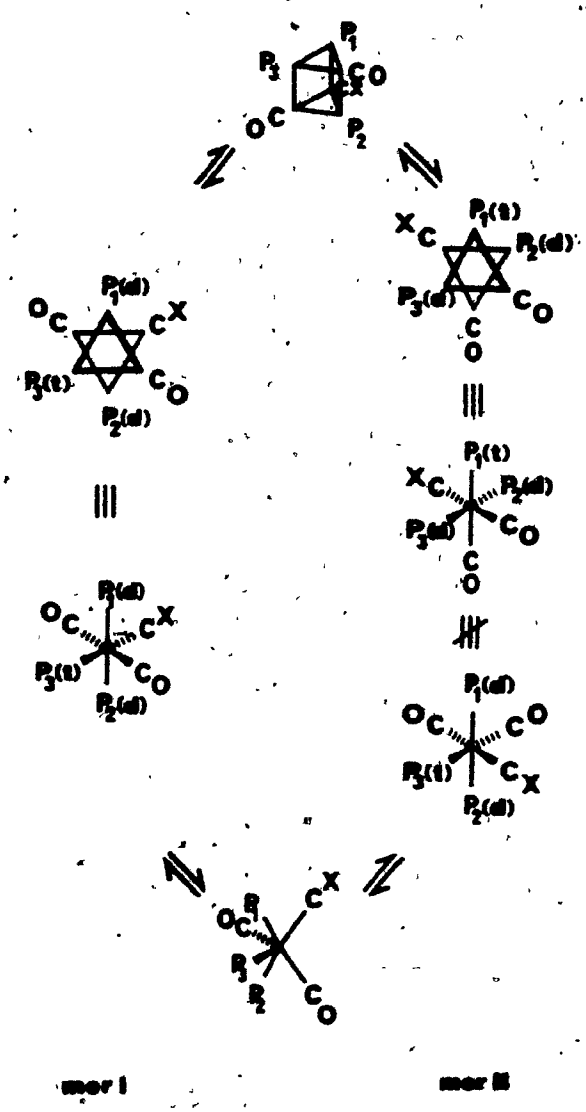

Figure 3.14. Schematic representation of possible pathways for the interconversion of the <u>mer</u> I and <u>mer</u> II isomers of $Cr(CO)_2(CX)[(MeO)_3P]_3$ (X = S, Se): top, trigonal prismatic intermediate; bottom, bicapped-tetrahedral intermediate. For the sake of clarity, the $(MeO)_3P$ ligands have been represented by P_1, P_2 and P_3.

On the basis of the observation that mer I → mer II isomerization of $Cr(CO)_2(CX)[(MeO)_3P]_3$ (X = S, Se) proceeds through a trigonal prismatic twist, it is highly probable that the mer I → fac isomerization of these complexes, as well as the fac → mer isomerization of the tricarbonyl analogue, occurs in the same manner. The failure to observe the dynamic interconversion of the fac and mer isomers may imply that the rearrangement is taking place at too slow a rate to be observed on the NMR time scale, i.e., that the phosphorus nuclei are relaxing at a faster rate than the time required for rearrangement to take place at these temperatures. This in turn indicates that the energy barrier for mer I to mer II isomerization is lower than that for mer ⟷ fac exchange. Figure 3.15 shows the schematic representation of the rearrangement of the thio- or selenocarbonyl complex through a trigonal prismatic twist. This mechanism should involve a large negative entropy for interconversion from mer I to fac due to the steric hindrance resulting from the eclipsing of two phosphites in the activated state. However, the interconversion of the mer I to mer II isomer should take place with a smaller entropy of activation; in this case, the activated state would have the phosphite ligands eclipsing CO and CX ligands, thus minimizing the steric effect. The activation parmeters obtained for the interconversion of fac and mer isomers suggest that

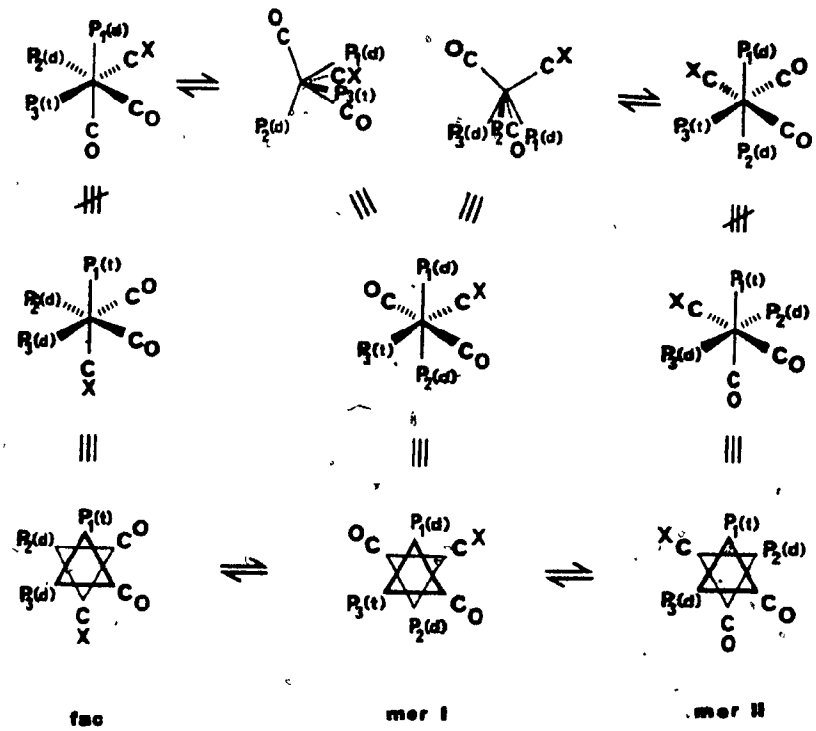

Figure 3.15. Schematic representation of the intramolecular isomerization of $Cr(CO)_2(CX)[(MeO)_3P]_3$ (X = S, Se) through trigonal prismatic (lower pathway) or bicapped-tetrahedral (upper pathway) intermediates.

in the assumed trigonal prismatic intermediate the unfavourable steric interactions between eclipsed pairs of ligands are minimized by the occurrence of some bond lengthening. Figure 3.15 illustrates that a 2-D NOE ^{31}P NMR experiment would allow the trigonal prismatic and bicapped-tetrahedron pathways to be distinguished in the case of fac → mer I isomerization as well, if this process could be detected. These two pathways would not be distinguished by 2-D ^{31}P NMR in the case of the tricarbonyl complex due to the simplicity of the spectrum of the fac isomer, with only a single resonance.

The observation of an off-diagonal correlation between the doublet and triplet of the fac isomer in the 2-D ^{31}P NMR spectrum of $Cr(CO)_2(CX)[(MeO)_3P]_3$ (X = S, Se) (Figures 3.11 and 3.12) may be due to chemical exchange between equivalent fac isomers. The energy barrier for such a rearrangement by a trigonal prismatic mechanism would be expected to be of comparable size to the barrier for mer I to mer II interconversion since the activated state would involve in this case as well the eclipsing of each phosphite by a CO or CX ligand, rather than by a second phosphite ligand. However, the possibility that the observed correlation is solely due to NOE cannot be ruled out at the present time. It is, however, possible to distinguish chemical exchange between fac isomers and NOE in the case of $(triphos)Cr(CO)_2(CX)$ (X = S, Se), since two fac configurations of these complexes are

chemically distinguishable. Initial 2-D NOE ^{31}P NMR investigation of these complexes in deuterotoluene at temperatures ranging from 60-90°C revealed no off-diagonal correlation between the **A** and **B** isomers. However, the steric constraints and electronic properties of the triphos ligand are quite different from those of the trimethylphosphite ligands in fac-$Cr(CO)_2(CX)[(MeO)_3P]_3$ so that the evidence obtained for the triphos complexes is not necessarily pertinent to the trimethylphosphite complexes.

Vancea et al. have examined the stereochemical nonrigidity of cis-$M(CO)_4(ER_3)_2$ (M = Fe, Ru, Os; E = Si, Ge, Sn, Pb; R = organic group or halogen) derivatives [21]. In these complexes, the axial and equatorial carbonyls exhibit one signal in the carbonyl region of the ^{13}C NMR spectrum at room temperature signifying that the axial and equatorial carbonyls are exchanging extremely fast on the NMR time scale, through an intramolecular rearrangement process. These complexes become stereochemically rigid at, or below, approximately -50°C. The crystal structures of cis-$Fe(CO)_4(SnPh_3)_2$ [22] and cis-$Fe(CO)_4)(SiMe_3)_2$ [23] are significantly distorted from octahedral geometry with the latter complex being particularly distorted, its structure being described as "a pseudo-bicapped tetrahedron with the trimethylsilyl groups as capping ligands" [23]. The most striking feature of this complex is the 141.2(1)° angle between

the two CO trans ligands instead of the 180° expected for a regular octahedron. Also, the Si-Fe-Si angle is 111.8(1)°. The cis-$Fe(CO)_4(SnPh_3)_2$ complex is similarly distorted with an angle between trans CO groups of 159.6(4)°, and an Sn-Fe-Sn angle of 95.95°. The above distortions provided support for the possibility that rearrangement occurs through a bicapped-tetrahedral intermediate. The authors further showed that this rearrangement involved a cis to trans to cis sequence where the carbonyls become equivalent in the trans isomer.

The crystal structures of $Cr(CO)_2(CX)[(MeO)_3P]_3$ (X = S, Se), described in Chapter 2, exhibit no marked distortions of the magnitude reported for cis-$Fe(CO)_4(SiMe_3)_2$ or cis-$Fe(CO)_4(SnPh_3)_2$. All the angles between trans ligands are approximately 174 ± 1° for both complexes. On this basis, rearrangement by a bicapped-tetrahedron mechanism would not appear to be favoured.

References

1. H.F. Fischer, E.O. Fischer and H. Werner, Angew. Chem. Internat. Edit., 11, 644 (1972).
2. H.F. Fischer, E.O. Fischer and H. Werner, J. Organometal. Chem., 73, 331 (1974).
3. B.D. Dombek and R.J. Angelici, J. Am. Chem. Soc., 98, 4110 (1975).
4. D.J. Darensbourg, Inorg. Chem., 18, 14 (1979).
5. D.J. Darensbourg and B.J. Baldwin, J. Am. Chem. Soc., 101, 6447 (1979).
6. D.J. Darensbourg, R. Kudaroski and W. Schenk, Inorg. Chem., 21, 2488 (1982).
7. D.J. Darensbourg and R.L. Gray, Inorg. Chem., 23, 2993 (1984).
8. E.L. Denham and R.J. Clark, Abstracts, 189th Meeting of the American Chemical Society, Miami, Florida, April-May, 1985, paper INOR-236.
9. A.M. Bond, S.W. Carr and R. Colton, Organometallics, 3, 541 (1984).
10. F.A. Van-Catledge, S.D. Ittle and J.P. Jesson, Organometallics, 4, 18 (1985).
11. E.L. Muetterties, J. Am. Chem. Soc., 90, 5097 (1968).
12. R. Hoffmann, J.M. Howell and A.R. Rossi, J. Am. Chem. Soc., 98, 2484 (1975).

13. A.M. English, K.R. Plowman, I.M. Baibich, J.P. Hickey, I.S. Butler, G. Jaouen and P. Le Maux, J. Organometal. Chem., 205, 177 (1981).

14. D.G. Cameron and R.N. Jones, Appl. Spectrosc., 35, 448 (1981).

15. A.M. English, K.R. Plowman and I.S. Butler, Inorg. Chem., 20, 2553 (1981).

16. P.S. Pregosin and R.W. Kunz, "^{31}P and ^{13}C NMR of Transition Metal Phosphine Complexes", Springer-Verlag, New York, 1979, p.12.

17. S.S. Woodard, R.J. Angelici and B.D. Dombek, Inorg. Chem., 17, 1634 (1978).

18. G. Bodenhausen and R.R. Ernst, J. Am. Chem. Soc., 104, 1304 (1982).

19. R. Benn, Angew. Chem., Int. Ed. Engl., 21, 626 (1982).

20. A.M. Kook, P.N. Nicklas, J.P. Selegue and S.L. Smith, Organometallics, 3, 499 (1984).

21. L. Vancea, R.K. Pomeroy and W.A.G. Graham, J. Am. Chem. Soc., 98, 1407 (1976).

22. R.K. Pomeroy, L. Vancea, H.P. Calhoun and W.A.G. Graham, Inorg. Chem., 16, 1508 (1977).

23. L. Vancea, M.J. Bennett, C.E. Jones, R.A. Smith and W.A.G. Graham, Inorg. Chem., 16, 897 (1977).

Chapter 4

Kinetic Investigations of Arene Labilization in (η-Arene)-$Cr(CO)_2(CX)$ (X = O, S, Se) Complexes

4.1 Introduction

The study of arene labilization in Group VIB metal tricarbonyl complexes has been of considerable interest for many years [1-8], and the mechanism of arene displacement reactions remains under investigation to date [9-11]. Such interest stems from the importance of these complexes in catalytic hydrogenation [5,12] as well as the potential utility of arene exchange processes in the liberation of arenes from such complexes following their derivatization by, for example, Friedel-Crafts reactions [12].

Arene and triene displacement from (η-Arene)$M(CO)_3$ and (cht)$M(CO)_3$ (M = Cr, Mo, W) by a monodentate ligand L [L = $(RO)_3P$, R_3P, RCN, $R_nCl_{3-n}P$ (n = 1,2; R = alkyl or aryl)] has been reported [2-7] to yield fac-$M(CO)_3L_3$. Kinetic investigations of arene displacement reactions of (η-Arene)$M(CO)_3$ (M = Mo, W) [2,3,5] and (η-naphthalene)$Cr(CO)_3$ [5] complexes revealed that they follow a second-order rate equation, first order with respect to both the complex and the attacking ligand. In the case of the (cht)$M(CO)_3$ (M = Cr, Mo, W) complexes, initial studies involving cht displacement by

$(MeO)_3P$ indicated that these reactions also follow a second-order rate law, first order with respect to the complex and with respect to the attacking ligand [3]. In later studies, employing RCN (R = alkyl and aryl) as entering ligand, the reaction was found to be second order in the case of Cr but third order for Mo and intermediate between second and third order for W [6].

A mechanism for arene displacement reactions of this type was first proposed by Zingales et al. [1] in their study of arene substitution by $R_nCl_{3-n}P$ (n = 1,2; R = alkyl or aryl) in $(\eta\text{-Arene})Mo(CO)_3$ complexes, and has been widely accepted. In a recent kinetic investigation of arene exchange and arene displacement reactions, Traylor et al. [10] demonstrated that this same mechanism can account for the observed kinetic behaviour of both arene displacement and arene exchange, as well as catalyzed arene exchange, reactions of $(\eta\text{-Arene})Cr(CO)_3$. The mechanism involves a slippage process whereby the ring initially undergoes a transformation from an η^6 to an η^4 bonding mode prior to attack by the incoming nucleophile.

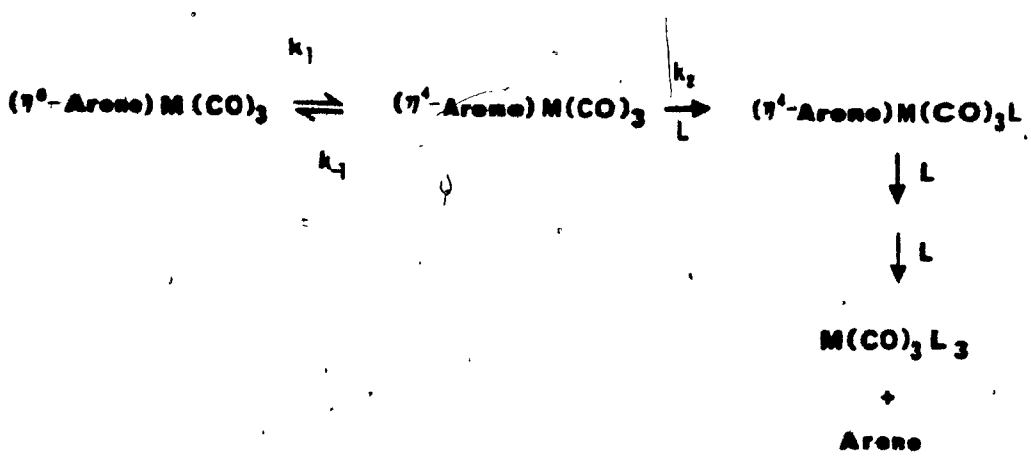

If the rate constant for the reverse process, k_{-1}, were small, then the reaction would be zero order with respect to the incoming ligand. Since this is not the case in any of the arene displacement reactions studied, where no dissociative term has been found, it is assumed that $k_{-1} >> k_2$. Thus, the arene displacement reactions exhibit a first-order dependence on the concentration of both the incoming ligand and the complex. Subsequent steps leading to total displacement of the arene are rapid, and generally do not contribute to the observed rate. The variation in the reaction order observed for cht displacement from $(cht)M(CO)_3$ (M = Mo, W) by nitriles was attributed to the weak nucleophilic strength of the nitriles resulting in comparable rates of nitrile dissociation from and coordination of a second nitrile to the proposed intermediate $(\eta^4\text{-cht})M(CO)_3(RCN)$ (M = Mo, W) [6].

The above mechanism is consistent with various considerations that have been put forward in the literature regarding the reaction pathways available to complexes of this type. Basolo [13] has stated that "Substitution reactions of 18-electron transition metal organometallic compounds may proceed by an associative mechanism provided the metal complex can delocalize a pair of electrons onto one of its ligands." Muetterties <u>et al</u>. [14] postulated for the reaction of $(bz)ML_3$ complexes with L' that "Mechanistically

a reasonable intuitive scenario would start with an η^6 to η^4 dissociation of the coordinated arene ... An associative mechanism (or an interchange mechanism of associative intimate character) for the attack of an external ligand on η^6-benzene-ML_3 would seem unlikely." Such a "ring slippage" creates a vacant orbital at the metal, providing a low-energy associative reaction pathway [14]. Muetterties et al. also stated that the resulting η^4 complex should be sensitive to steric effects induced by either a substituent on the ring or on the incoming nucleophile, and that the η^4 ring must undergo distortion from planarity to allow the incoming ligand access to the metal. They estimated that the energy required to bend the coordinated benzene ring in $(bz)Cr(CO)_3$ from planarity, as well as to distort the $Cr(CO)_3$ group to facilitate acceptance of the incoming ligand, is about 15 kcal mol^{-1} [14].

In this chapter, an investigation of the kinetics of arene displacement from $(\eta$-Arene$)Cr(CO)_2(CX)$ (X = S, Se) complexes by tertiary phosphites is reported. This represents the first kinetic study of an organometallic selenocarbonyl derivative ever undertaken. These studies will provide a quantitative measure of the influence of the chalcocarbonyl ligands on arene lability in these complexes.

4.2 Experimental

4.2.1 Sources of Materials

All (η-Arene)$Cr(CO)_2(CX)$ (X = O, S, Se) complexes and (cht)$Cr(CO)_3$ were purified by TLC prior to use, and their purity was established by the absence of any superfluous peaks in the ν(CO) region of their FT-IR spectra. Trimethyl- and triphenylphosphite, gold label purity (99+%), triethylphosphite, 99% purity, and trimethylphosphate, gold label purity (99+%), were purchased from Aldrich Chemical Co. and were used without further purification. Tri-n-butyl- and tricyclohexylphosphite were obtained from Strem Chemicals. The phosphites were handled under an atmosphere of prepurified N_2 (3 ppm O_2, 5 ppm H_2O). ^{31}P NMR spectra of the phosphites over a full spectral window (40,000 Hz) were measured periodically to verify the absence of any phosphorus-containing impurities. Fresh bottles of phosphite (100 ml) were used every third run or within four days of opening the bottle. The methylcyclohexane (99%) solvent was distilled over sodium under nitrogen and transferred under nitrogen to a nitrogen-purged flask containing a weighed amount of the complex. Dichloroethane (99%) was distilled over calcium chloride under nitrogen and transferred according to the above procedure.

4.2.2 Preparation of Samples

All procedures were performed under a nitrogen atmosphere in a stainless steel glove box which was periodically evacuated and purged with nitrogen. The nitrogen purge was maintained throughout the sample preparation procedure. Typically two samples of 1.40 mg of (η-Arene)$Cr(CO)_2CX$ (X = O, S, Se) were weighed out on a Cahn electrobalance (precision ±0.01 mg) and were transferred to two 25-ml volumetric flasks fitted with hollow Teflon plugs capped with rubber septa. The flasks were then purged with nitrogen prior to transferring the solvent. A third flask was filled with distilled solvent under nitrogen. The three flasks were then transferred to the glove box, together with at least four matched quartz cuvettes (1-cm pathlength) fitted with Viton O-rings, the bottle containing the phosphite ligand and two 1-ml (±1%) Hamilton syringes with Teflon barrels. A measured volume of the solution was syringed out and replaced by an equal volume of phosphite (providing [L] 800-3000 times in excess of [(η-Arene)$Cr(CO)_2(CX)$]). The flask was then capped and shaken vigorously. One cuvette was filled with the solution containing only (η-Arene)$Cr(CO)_2(CX)$. Another cuvette was filled with the solution containing both phosphite ligand and complex. The other two cuvettes were filled with pure solvent.

The cuvettes were transferred to a Varian Cary 210 UV-vis spectrophotometer equipped with a thermostatted multi-sample support assembly. Due to the elevated temperatures used (> 45°C), two water-cooled jackets (supplied by Varian) were placed on either side of the heating assembly to protect the spectrophotometer optics. The time to equilibrate the cuvettes to the designated kinetic run temperature was 17 min. The kinetic run temperature was determined by placing a calibrated thermocouple wire into a cuvette containing methylcyclohexane under the exact conditions of the kinetic run. No loss of solvent was observed up to 72 h at 85°C. The spectrometer was equipped with a cell programmer accessory and was interfaced to an Apple II+ computer (64K). The programs "Master Scan Storage" and "Master Kinetic Storage", both supplied by Varian, were utilized to collect and store wavelength scans (500-280 nm) and absorbances at three selected wavelengths, respectively, at programmed time intervals. Usually a run was between 10 h and 48 h in duration and the data acquisition was triggered every 10 or 15 min. The data acquired for the disappearance of the starting material were analyzed, yielding k_{obsd}, using the "Advanced Order Kinetic Program" supplied by Varian and based on a multiple-linear-regression program described in Reference 15.

Least-squares analysis for the calculation of k_1 and k_2

and the activation parameters was performed with no data smoothing or data averaging, using a "Curve Fitter" program written by P.K. Warm for Interactive Microware, Copyright (C) 1980.

4.3 Results and Discussion

The kinetics of arene displacement in (η-Arene)$Cr(CO)_2$-(CX) (X = S, Se) by trialkyl- and triarylphosphites were monitored by UV-vis spectroscopy. All reactions exhibited one isosbestic point (Figure 4.1), indicating only one process was taking place, with no side reactions. The rate of reaction under pseudo-first-order conditions (800-3000 fold excess of tertiary phosphite) was determined from the decrease in absorbance of the starting material with time. The pseudo-first-order rate constants, k_{obsd}, were determined by a multiple-linear-regression program [15].

The dependence of reaction rate on ligand concentration was investigated for the reaction of (bz)$Cr(CO)_2$(CX) (X = S, Se) with trimethylphosphite (Tables 4.1 and 4.2). Plots of k_{obsd} vs. $[(MeO)_3P]$ were linear for the range of concentrations used (Figure 4.2). Least-squares analysis was used to fit the data to the equation $k_{obsd} = k_1 + k_2[(MeO)_3P]$. The value of k_2 was obtained from the slope. For both complexes the intercept was zero within the standard deviation

Figure 4.1. Typical UV-vis spectra obtained in kinetic investigations of (η-Arene)$Cr(CO)_2(CX)$ (X= S, Se): (a) (bz)$Cr(CO)_2(CSe)$; (b) reaction of (bz)$Cr(CO)_2(CSe)$ with $(MeO)_3P$ at 53°C, showing isosbestic point; (c) $Cr(CO)_2(CSe)[(MeO)_3P]_3$.

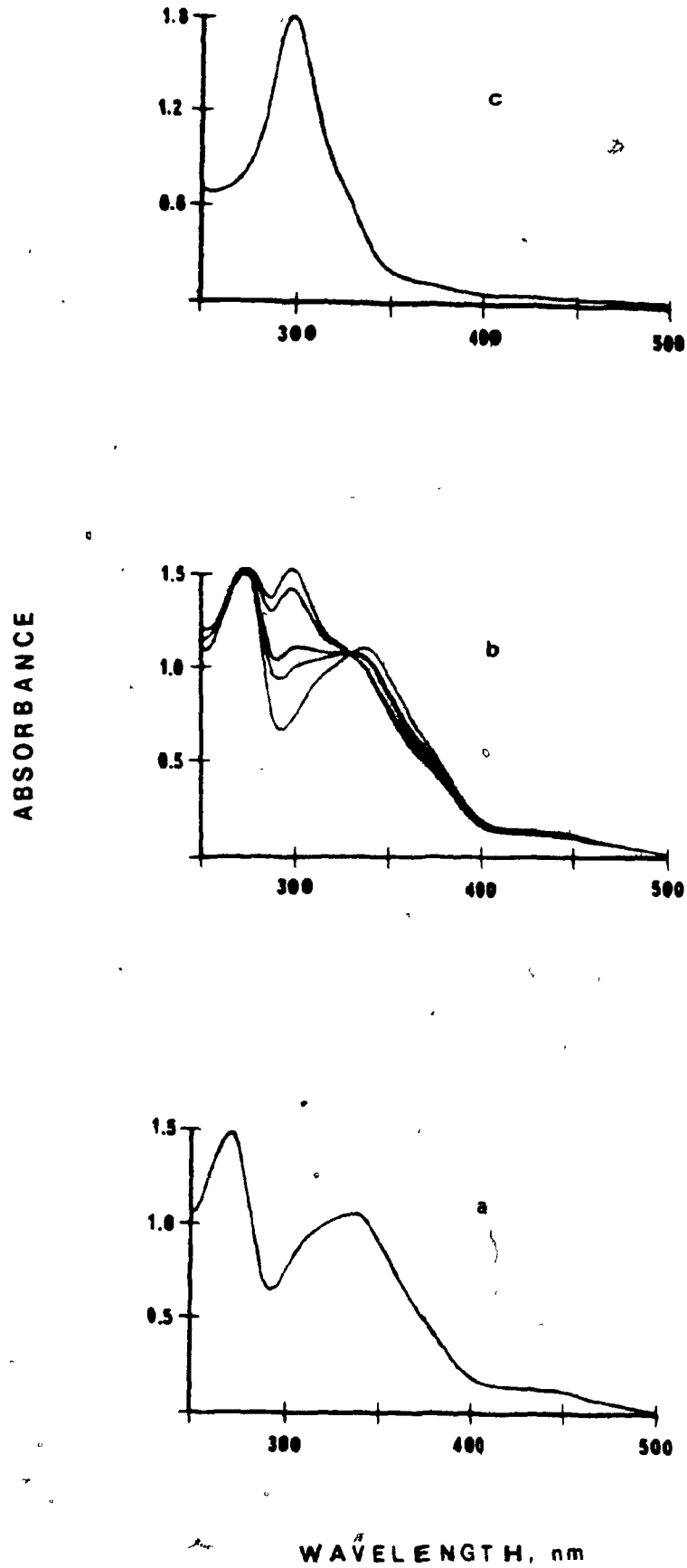
1.8
1.2
0.6
c
300
400
500
1.5
1.0
0.5
b
300
400
500
ABSORBANCE
1.5
1.0
0.5
a
300
400
500
WAVELENGTH, nm

Table 4.1. Pseudo-First-Order Rate Constants for the Reaction of $(bz)Cr(CO)_2(CS)$ with Trimethylphosphite in Methylcyclohexane at 83.3°C[a]

$[(MeO)_3P]$ X 10 M	k_{obsd} X 10^5 s^{-1}
2.37	1.52
2.37	1.43
4.07	2.24
4.07	2.17
4.07	2.24
5.10	3.24
5.10	3.20
6.10	3.35
6.10	3.38
6.10	3.43
6.78	3.96
6.78	3.74

[a]A least-squares fit of these data to the equation $k_{obsd} = k_1 + k_2[(MeO)_3P]$ yields $k_1 = (1.4 \pm 1.7) \times 10^{-6}\ s^{-1}$, $k_2 = (5.46 \pm 0.34) \times 10^{-5}\ M^{-1}s^{-1}$; $r = 0.98$.

Table 4.2. Pseudo-First-Order Rate Constants for the Reaction of $(bz)Cr(CO)_2(CSe)$ with Trimethylphosphite in Methylcyclohexane at 72.6°C[a]

$[(MeO)_3P]$ X 10 M	k_{obsd} X 10^5 s^{-1}
2.71	4.06
2.71	4.06
3.39	4.73
3.39	4.72
3.39	4.57
4.06	5.84
4.06	5.93
4.06	5.85
5.08	6.95
5.08	7.02
6.10	8.58
6.10	8.73
6.10	8.79

[a]A least-squares fit of these data to the equation $k_{obsd} = k_1 + k_2[(MeO)_3P]$ yields $k_1 = (1.2 \pm 1.8) \times 10^{-6}\ s^{-1}$, $k_2 = (1.39 \pm 0.04) \times 10^{-4}\ M^{-1}\ s^{-1}$; $r = 0.99$.

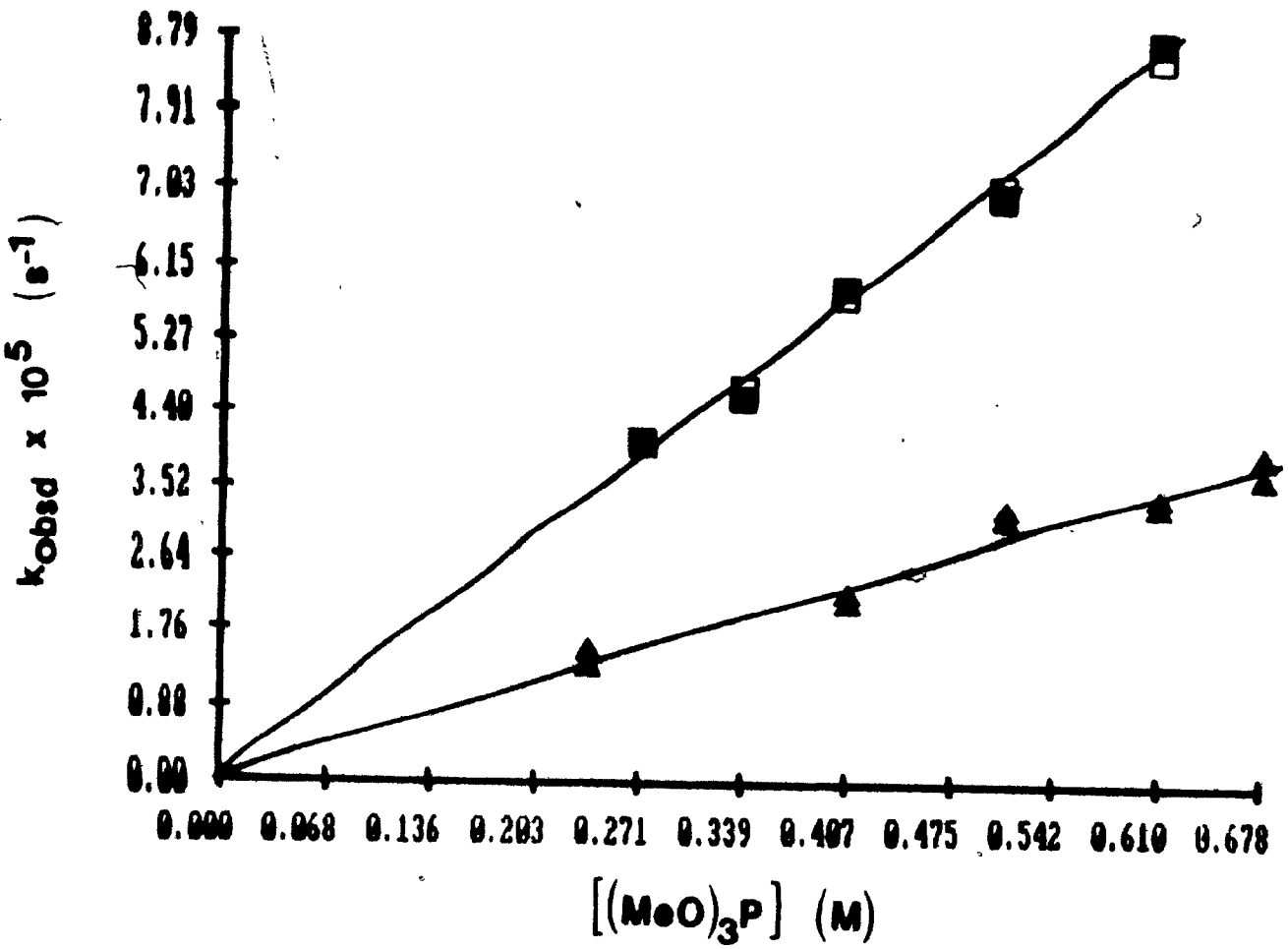

Figure 4.2. Plots of k_{obsd} vs. $[(MeO)_3P]$ for the reaction of $(bz)Cr(CO)_2(CX)$ with $(MeO)_3P$: ▲, X = S; ■, X = Se.

and hence k_1 is zero (Tables 4.1 and 4.2). Therefore, the rate of the reaction can be accurately represented by the rate expression:

$$-\frac{d[(\eta\text{-Arene})Cr(CO)_2(CX)]}{dt} = k_2[(\eta\text{-Arene})Cr(CO)_2(CX)][(MeO)_3P] \quad (4.1)$$

So, $k_2 = k_{obsd}/[(MeO)_3P]$ for the range of $(MeO)_3P$ concentrations used. It is of interest to note that all of the kinetic investigations reported to date on arene and triene displacement from chromium(0) tricarbonyl derivatives by a range of both strong and weak nucleophiles or another arene or triene did not reveal any contribution from a dissociative term.

The activation parameters were obtained by least-squares analysis of the kinetic data for the variation of k_2 with temperature (Tables 4.3 and 4.4) employing the following equation:

$$k_2 = (kt/h)e^{\Delta S^{\#}/R}\, e^{-\Delta H^{\#}/RT} \quad (4.2)$$

The enthalpy of activation was calculated from the slope of the usual ln k_2 vs. 1/T plot and is small and positive while the entropy of activation is large and negative in both the thiocarbonyl and the selenocarbonyl case (Figure 4.3). Thus the rate-determining step appears to involve a

Table 4.3. Variation with Temperature of k_2 for the Reaction of $(bz)Cr(CO)_2(CS)$ with Trimethylphosphite in Methylcyclohexane

T °C	$k_2 \times 10^5$ $M^{-1}\ s^{-1}$
83.3	5.46 ± 0.34
76.6	3.27 ± 0.09
72.4	2.42 ± 0.12
67.0	1.69 ± 0.05
59.9	0.92 ± 0.06

Table 4.4. Variation with Temperature of k_2 for the Reaction of $(bz)Cr(CO)_2(CSe)$ with Trimethylphosphite in Methylcyclohexane

T °C	$k_2 \times 10^5$ $M^{-1}\ s^{-1}$
72.6	13.9 ± 0.4
63.2	5.92 ± 0.04
57.9	4.31 ± 0.13
53.0	2.72 ± 0.07

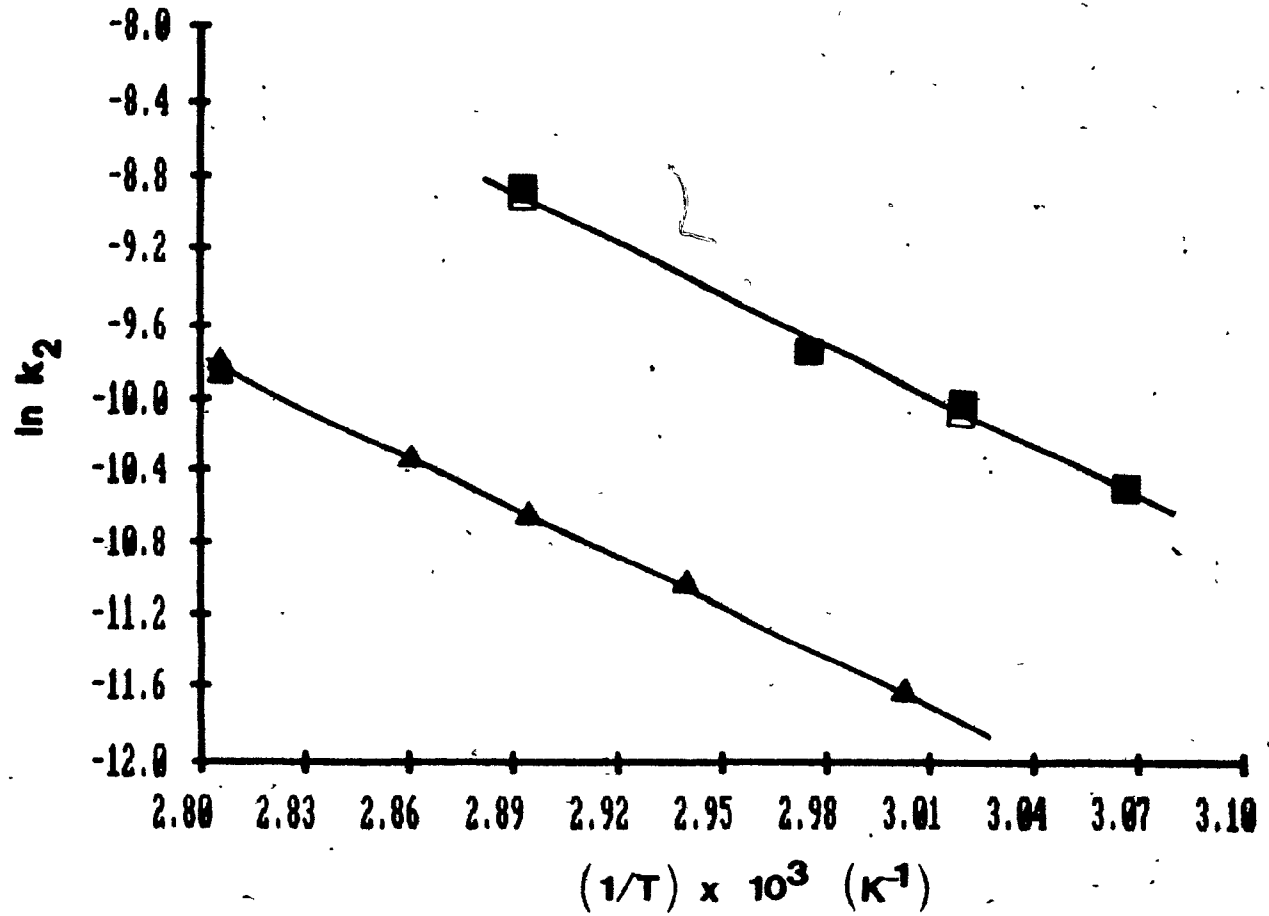

Figure 4.3. Plots of ln k_2 vs. 1/T for the reaction of $(bz)Cr(CO)_2(CX)$ with $[(MeO)_3P]$: ▲, X = S; ■, X = Se. Least-squares analysis of these data yields $\Delta H^{\#} = 17.7 \pm 0.4$ kcal mol^{-1} and $\Delta S^{\#} = -28 \pm 1$ cal mol^{-1} deg^{-1} for X = S and $\Delta H^{\#} = 17.9 \pm 1.3$ kcal mol^{-1} and $\Delta S^{\#} = -24 \pm 2$ cal mol^{-1} deg^{-1} for X = Se.

bimolecular associative process. Similar activation parameters (Table 4.5) were obtained in previous kinetic studies of the reactions of (η-Arene)$M(CO)_3$ (M = Mo, W) with a ligand L [L = $(MeO)_3P$, $R_nCl_{3-n}P$ (n = 0-2; R = alkyl or aryl)] [1,2,4] and of (cht)$M(CO)_3$ (M = Cr, Mo, W) with $(MeO)_3P$ [3]. These data were interpreted in terms of the mechanism described in Section 4.1, involving a partial displacement of the η^6-coordinated arene or triene to an η^4-bonding mode prior to attack by the ligand. This same mechanism may, therefore, be postulated to account for the kinetic data reported here for arene displacement from (η-Arene)$Cr(CO)_2$(CX) (X = S, Se).

Comparison of the activation parameters in Figure 4.3 reveals that the entropy of activation is the factor governing the difference in reactivity between (bz)$Cr(CO)_2$(CS) and (bz)$Cr(CO)_2$(CSe), while the enthalpies of activation are similar for the two complexes. That $\Delta S^{\#}$ is more negative for (bz)$Cr(CO)_2$(CS) than for (bz)$Cr(CO)_2$(CSe) may imply a closer proximity of the arene and the incoming ligand to the metal in the transition state in the thiocarbonyl complex, leading to more unfavourable steric interactions. This possibility is supported by the longer metal-arene bond in (mbz)$Cr(CO)_2$(CSe) compared to (mbz)$Cr(CO)_2$(CS), established by X-ray diffraction studies of these complexes [16]. Furthermore, the P-Cr bond lengths observed in the crystal

Table 4.5. Activation Parameters for Ring Displacement Reactions of (cht)$Cr(CO)_3$ and (η-Arene)$Cr(CO)_2$(CX) (X = O, S, Se)

Complex	Entering ligand	$\Delta H^{\#}$ kcal mol^{-1}	$\Delta S^{\#}$ cal mol^{-1} deg^{-1}
(cht)$Cr(CO)_3$[a]	$(MeO)_3P$	16.5 ± 0.7	-25 ± 2
(cht)$Cr(CO)_3$[b]	C_6H_5CN	17.7 ± 0.5	-26 ± 1
(cht)$Cr(CO)_3$[b]	CH_3CN	21.6 ± 1.0	-15 ± 3
(naphth)$Cr(CO)_3$[b]	CH_3CN	16.8	-20
(bz)$Cr(CO)_3$[c]	$C_6(CH_3)_6$	29.6 ± 1.0	-4 ± 3
(p-xyl)$Cr(CO)_3$[c]	$C_6(CH_3)_6$	29.9 ± 1.0	-12 ± 3
(mes)$Cr(CO)_3$[c]	$C_6(CH_3)_6$	25.7 ± 0.9	-18 ± 2
(η-Arene)$Cr(CO)_2$(CS)[d]	Arene*[e]	decomposition	
(bz)$Cr(CO)_2$(CS)[f]	$(MeO)_3P$	17.7 ± 0.4	-28 ± 1
(bz)$Cr(CO)_2$(CSe)[f]	$(MeO)_3P$	17.9 ± 1.3	-24 ± 2

[a]From Reference 3; methylcyclohexane solution.
[b]From Reference 6; dichloroethane solution.
[c]From Reference 8; cyclohexanone solution.
[d]Arene = C_6H_6, $C_6H_5CO_2CH_3$, $C_6H_5CH_3$.
[e]This work; Arene* = $C_6H_3(CH_3)_3$, $C_6(CH_3)_6$, C_7H_8 (neat or with THF).
[f]This work; in methylcyclohexane solution.

structure of $Cr(CO)_2(CSe)[(MeO)_3P]_3$ [especially for the P-Cr bond trans to the CSe ligand (Table 2.4)] are longer than the corresponding bond lengths in the thiocarbonyl analogue (Table 2.2). These longer P-Cr bond distances suggest a less significant steric effect due to the incoming ligand during bond formation in the activated complex in the case of the selenocarbonyl derivative.

A second factor that may be considered in accounting for the observed difference in $\Delta S^{\#}$ is the ease of distortion of the arene ring. The complexes (η-1,2,3-trimethoxybenzene)$Cr(CO)_3$ and (η-diethylaniline)$Cr(CO)_3$ have been found to exhibit a greater degree of arene lability than would be anticipated on the basis of the metal-arene bond strengths in these complexes [18]. Recently, crystal structure investigations of these complexes [19] revealed significant distortions of the arene from a planar geometry in both cases; it has been proposed [19] that these distortions allow an incoming nucleophile greater accessibilty to the metal centre, thereby effecting an enhancement in ring lability. Analysis of the crystal structure data for the complexes (mbz)$Cr(CO)_2(CX)$ (X = O, S, Se) [16] revealed minor variations in the metal-C(ring) distances. No evidence was found for arene distortions of comparable magnitude to those observed for (η-diethylaniline)$Cr(CO)_3$ or (η-1,2,3-trimethoxybenzene)$Cr(CO)_3$. However, the lack of

ring distortion in the solid-state structure does not preclude the possibility that the lower entropy of activation in the arene displacement reaction for $(bz)Cr(CO)_2(CSe)$ relative to the thiocarbonyl analogue may be due to a more facile distortion of the arene ring in the activated state.

Subsequent to establishing the rate expression for arene displacement, an examination of the effect on arene lability of substituents on the ring was undertaken. Increasing the number of methyl groups on the ring generally decreases the rate of the reaction (Table 4.6). The reaction of $(\eta$-mesitylene$)Cr(CO)_2(CS)$ with $(MeO)_3P$ was too slow to measure accurately so that only the rate for reaction with the much more nucleophilic $(\underline{n}\text{-}BuO)_3P$ (see Table 4.7) is given in Table 4.6. No attempts were made to investigate reactions of arenes with more than three electron-donating substituents because these would be too slow to monitor with any degree of accuracy. The results in Table 4.6, including the anomalously fast rate of <u>o</u>-xylene displacement, are in line with kinetic studies reported by other groups who have investigated the arene displacement reactions of $(\eta$-Arene$)M(CO)_3$ (M = Mo, W) [1,2,4]. The decrease in reaction rate upon addition of electron-donating substituents on the arene ring may be attributed to the strengthening of the metal-arene bond resulting from the increased electron density at the ring. Steric effects may also contribute to the

Table 4.6 Pseudo-First-Order Rate Constants for Arene Displacement by Trimethylphosphite from (η-Arene)$Cr(CO)_2(CS)$ Complexes at 83.3°C[a]

Complex	Arene in (η-Arene)$Cr(CO)_2(CS)$	$k_{obsd} \times 10^5$[b] s^{-1}
I	1,3,5-$C_6H_3(CH_3)_3$	0.99 ± 0.02[c]
II	p-$C_6H_4(CH_3)_2$	-- [d]
III	o-$C_6H_4(CH_3)_2$	2.06 ± 0.04
IV	$C_6H_5CH_3$	1.99 ± 0.04
V	C_6H_6	2.91 ± 0.17[e]
VI	m-$C_6H_4(CH_3)(CO_2CH_3)$	4.15 ± 0.14
VII	$C_6H_5CO_2CH_3$	7.33 ± 0.08
VIII	p-$C_6H_4(CO_2CH_3)_2$	10.2 ± 0.2
IX	p-$C_6H_4(OCH_3)_2$	20.2 ± 0.2
X	$C_6H_5N(CH_3)_2$	24.8 ± 0.2

[a]In methylcyclohexane at $[(MeO)_3P]$ = 0.508 M.
[b]Average of at least 3 runs; uncertainties are standard deviations.
[c]Rate constant for (n-BuO)$_3$P; cf. value for reaction of (bz)$Cr(CO)_2(CS)$ with (n-BuO)$_3$P in Table 4.7.
[d]Reaction too slow to yield an accurate rate constant.
[e]Value interpolated from plot in Figure 4.2; uncertainty is standard error of the least-squares-fitted line.

observed trend in that the substituents on the ring may hinder the attack of the nucleophile at the metal centre.

The presence of electron-withdrawing groups on the ring enhances ring lability (Table 4.6) in accord with the ability of these groups to decrease the electron density available at the ring for bonding to the metal. The presence of both an electron-donating and an electron-withdrawing group on the ring gives an intermediate rate for the ring displacement reaction, while the presence of a second electron-withdrawing group in the <u>para</u> position has a cooperative effect in enhancing the rate of displacement.

In order to probe further the relationship between the rate of arene displacement and metal-arene bond strength, force constant calculations for the metal-arene stretching vibrations in these complexes would be in order. These force constants can really only be acquired through detailed normal coordinate calculations [20]. Fortunately, however, the CO stretching force constants are known to reflect the electron density at the metal in complexes of this type and can be correlated with the electron-donating/withdrawing properties of the substituents on the arene [21]. Therefore, the rate constants for arene displacement for a series of (η-Arene)$Cr(CO)_2$(CS) complexes as a function of the CO stretching force constants of the complexes are plotted in Figure 4.4. The latter were calculated from the positions

($\tilde{\nu}_1$, $\tilde{\nu}_2$) of the two ν(CO) peaks in the IR spectrum according to the energy-factored force field approximation:

$$k_{CO} = (\lambda_1 + \lambda_2)/2\mu \qquad (4.3)$$

where $\lambda_i = 1/(4\pi^2c^2\tilde{\nu}_i^2)$, c is the speed of light and μ is the reduced mass of CO. A least-squares analysis of these data yields a linear relationship between the CO force constant and ln k_{obsd} (Figure 4.4) (r = 0.98, for compounds III–VIII). However, the points corresponding to the dimethylaniline and p-dimethoxybenzene complexes exhibit anomalous behaviour (r = 0.11 for compounds III–X). The same observation has been reported by Pidcock et al. in their studies of arene displacement from (η-Arene)M(CO)$_3$ (M = Mo, W) [2,4]. This may be proposed to result from distortions of the arene from a planar geometry, as observed for the diethylaniline and trimethoxybenzene chromium tricarbonyl derivatives discussed above. Thus, in the thiocarbonyl complexes studied here, a similar distortion in conjunction with the labilizing effect of the thiocarbonyl ligand can explain the anomalously fast rate of arene displacement from (η-p-dimethoxybenzene)Cr(CO)$_2$(CS) and (η-dimethylaniline)Cr(CO)$_2$(CS).

The rate of ring displacement can also be affected if the carbonyl groups are replaced by weaker π-acceptors or

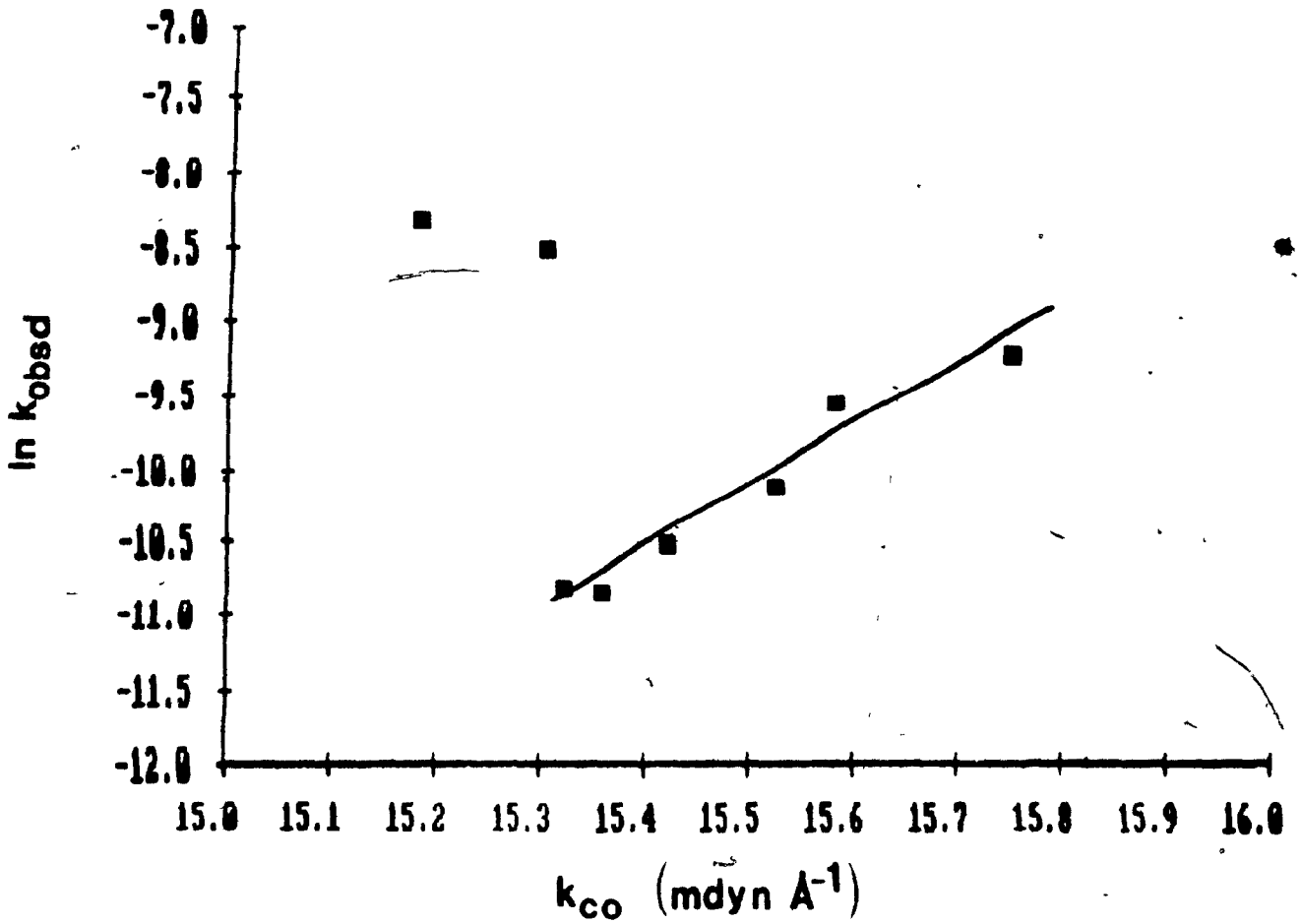

Figure 4.4. Plot of ln k_{obsd} values for the reactions of (η-Arene)$Cr(CO)_2(CS)$ complexes with $(MeO)_3P$ vs. the carbonyl stretching force constants (k_{CO}) of the arene complexes. The following k_{CO} values for the complexes given in Table 3.6 were calculated from Eq. 4.3: III, 15.32; IV, 15.36; V, 15.42; VI, 15.52; VII, 15.58; VIII, 15.75; IX, 15.30; X, 15.18 mdyn A^{-1}.

stronger σ-donors. The reactivity of (mbz)Cr(CO)$_2$(CS) was compared with that of (mbz)Cr(CO)(CS)[(PhO)$_3$P]. The monocarbonyl complex is seen to be unreactive over a period of 24 h at 87°C while (mbz)Cr(CO)$_2$(CS) reacts at 60°C in half the time. The lack of reactivity may be attributed to two factors. First, the weaker π-accepting and stronger σ-donating properties of the tertiary phosphite relative to CO increase the electron density at the metal available for π-backbonding to the arene, thus strengthening the metal-arene bond. Second, a steric effect may also contribute in that the phosphite may block the access of the attacking nucleophile to the metal. The decreased catalytic activity of (η-Arene)Cr(CO)$_2$(R$_3$P) (R = Ph, OPh) compared to (η-Arene)Cr(CO)$_3$ has been attributed to the above factors [22,23].

Table 4.7 shows the effect observed with the variation in the steric and nucleophilic character of the attacking ligand. The reaction rate increases with increasing nucleophilicity for ligands of comparable size (similar cone angles) and decreases with increasing size of the ligand. This trend has also been reported in the study of arene displacement from (η-Arene)Mo(CO)$_3$ complexes [1]. Thus, the rate of arene displacement by tertiary phosphite decreases in the order (n-BuO)$_3$P > (EtO)$_3$P > (MeO)$_3$P > (PhO)$_3$P > (C$_6$H$_{11}$O)$_3$P [no reaction was observed for (C$_6$H$_{11}$O)$_3$P].

Catalytic enhancement of ring displacement from

Table 4.7 Pseudo-First-Order Rate Constants for Arene Displacement by Tertiary Phosphites from (η-Arene)$Cr(CO)_2(CS)$ Complexes at 83.3°C[a]

Arene in (η-Arene)$Cr(CO)_2(CS)$	Phosphite	Cone angle[b] deg	$k_{obsd} \times 10^5$[c] s^{-1}
C_6H_6	(n-BuO)$_3$P	-	14.4 ± 0.3
C_6H_6	(EtO)$_3$P	109	7.16 ± 0.28
C_6H_6	(MeO)$_3$P	109	2.91 ± 0.17[d]
p-$C_6H_4(OCH_3)_2$	(MeO)$_3$P	107	20.2 ± 0.2
$C_6H_5N(CH_3)_2$	(MeO)$_3$P	107	24.8 ± 0.2
p-$C_6H_4(OCH_3)_2$	(PhO)$_3$P	128	4.82 ± 0.38
$C_6H_5N(CH_3)_2$	(PhO)$_3$P	128	5.68 ± 0.18
C_6H_6	($C_6H_{11}O$)$_3$P	135	no rxn.

[a]In methylcyclohexane at [(RO)$_3$P] = 0.508 M.
[b]From Reference 25.
[c]Average of at least 3 runs; uncertainties are standard deviations.
[d]Value interpolated from plot in Figure 4.2; uncertainty is standard error of the least-squares-fitted line.

(bz)$Cr(CO)_2(CSe)$ was seen with the addition of $(Me)_3PO$ (Table 4.8). Decomposition was observed in the absence of tertiary phosphite. The strong labilizing effect of oxygen donor bases has been noted previously [24]. Trialkylphosphine oxides have been used in various systems to catalyze CO substitution [25,26] and have been reported to enhance ring lability in (η-Arene)$Mo(CO)_3$ [2]. In the present case, the catalytic enhancement can be postulated to involve nucleophilic attack on the metal by the oxygen, forming (η^4-Arene)$Cr(CO)_2(CSe)(\leftarrow O{=}P(Me)_3)$.

The kinetic study of arene displacement in (η-Arene)$Cr(CO)_2(CSe)$ by $(MeO)_3P$ was also performed in dichloroethane (k_2 = 3.56 x 10^{-5} M^{-1} s^{-1} at 53.0°C). The reaction rate is slightly higher than that observed in methylcyclohexane (k_2 = 2.72 x 10^{-5} M^{-1} s^{-1} at 53.0°C) providing evidence that the activated complex may be polar in character and possibly solvent stabilized [1].

No kinetic data are available for arene displacement from (η-Arene)$Cr(CO)_3$ complexes due to their slow reactivity. Attempts were made in this study to measure the kinetics of arene substitution reactions of arene chromium tricarbonyls under rigorous conditions (83.3°C, $[(MeO)_3P]$: [(η-Arene)$Cr(CO)_3$] = 3000:1) and even for (η-dimethylaniline)$Cr(CO)_3$, one of the most reactive tricarbonyl complexes, after heating for 48 h there was no decrease in its

Table 4.8 Pseudo-First-Order Rate Constants for Arene Displacement from $(bz)Cr(CO)_2(CSe)$ by Trimethylphosphite in the Presence of Varying Concentrations of Trimethylphosphine Oxide at 42.6°C[a]

$[(MeO)_3P]$ M	$[(Me)_3PO]$ M	$k_{obsd} \times 10^5$ s^{-1}
0.510	–	0.61[b]
0.510	0.171	2.60
0.510	0.343	10.2
–	0.510	1.43[c]

[a]In methylcyclohexane solution.
[b]Reaction too slow to measure; value estimated as $k_2 \times [(MeO)_3P]$, with k_2 calculated using Eq. 4.2.
[c]Rate of decomposition.

UV-visible absorbance nor was there any evidence of product formation. Under the same conditions, (η-dimethylaniline)$Cr(CO)_2(CS)$ reacts completely in less than 3 h. Clearly, the effect of the thiocarbonyl ligand on the reactivity of the arene chromium carbonyl complex is quite significant. From these data it can be seen that even placing the most electron-withdrawing substituent on the arene ring in a tricarbonyl complex would not result in a labilizing effect on the metal-arene bond as great as that resulting from the substitution of one carbonyl group by a thiocarbonyl ligand. Furthermore, the effect of substitution of a selenocarbonyl ligand in place of a carbonyl ligand has even more dramatic effects on arene lability. These first kinetic results for a selenocarbonyl complex reported here have provided a quantitative measure of the increased reactivity of (η-Arene)$Cr(CO)_2(CSe)$ complexes with respect to their thiocarbonyl counterparts, the enhancement in ring lability being close to fivefold at 50°C.

Table 4.9 shows the rates recorded for various ring displacements from Group VIB metal complexes by $(MeO)_3P$. Ring lability decreases in the order (cht)$Mo(CO)_3$ > (cht)$W(CO)_3$ >> (cht)$Cr(CO)_3$ >> (bz)$W(CO)_3$ > (bz)$Cr(CO)_2(CSe)$ > (bz)$Cr(CO)_2(CS)$ > (bz)$Cr(CO)_3$. The reactivity of the cycloheptatriene derivatives has been attributed to the relative weakness of the bonds between the metal and the

Table 4.9. Rate Constants for Ring Displacement from (η-Arene)$M(CO)_2(CX)$ and $(cht)M(CO)_3$ Complexes by $(MeO)_3P$ at 50.0°C

Complex	k_2 M^{-1} s^{-1}
$(cht)Cr(CO)_3$[a]	$(11.0 \pm 0.2) \times 10^{-4}$
$(bz)Cr(CO)_3$[b]	$< 10^{-6}$
$(bz)Cr(CO)_2(CS)$[c]	$(4.11 \pm 0.26) \times 10^{-6}$
$(bz)Cr(CO)_2(CSe)$[c]	$(2.17 \pm 0.06) \times 10^{-5}$
$(cht)Mo(CO)_3$[a]	2.43 ± 0.03
$(cht)W(CO)_3$[a]	$(3.94 \pm 0.11) \times 10^{-1}$
$(bz)W(CO)_3$[d]	$(2.29 \pm 0.10) \times 10^{-5}$

[a]From Reference 3, in methylcyclohexane.
[b]Estimated value from the present study; the rate of the reaction was too slow to measure accurately under the conditions employed.
[c]From this work, in methylcyclohexane.
[d]From Reference 4, in 1,2-dichloroethane.

ring carbons adjacent to the methionine group in the cht ligand while the relative rates down the metal triad have been correlated to the ring-metal force constants and metal size [3].

A striking feature of the arene displacement reactions of (η-Arene)$Cr(CO)_2(CX)$ (X = S, Se) complexes is the involvement of an isomerization process, as evidenced by the predominant formation of the mer I isomer rather than the fac isomer which is the major product in the cht displacement from (cht)$Cr(CO)_3$. It has been shown in Chapter 3 that in the temperature range at which the reactivity of (η-Arene)$Cr(CO)_2(CX)$ with $(MeO)_3P$ has been studied the fac and mer I isomers of the products, $Cr(CO)_2(CX)[(MeO)_3P]_3$, are in equilibrium, with the mer I isomer predominating (K_{eq} = 5). Furthermore, comparison of the rates measured for the fac → mer I isomerization process with results of the kinetic studies reveals that the isomerization of fac-$Cr(CO)_2$-$(CX)[(MeO)_3P]_3$ is at least an order of magnitude faster than the rate of reaction to form $Cr(CO)_2(CX)[(MeO)_3P]_3$ at all temperatures studied. It is therefore likely that fac-$Cr(CO)_2(CX)[(MeO)_3P]_3$ is formed first in the reaction of (η-Arene)$Cr(CO)_2(CX)$ with $(MeO)_3P$, and then isomerizes to the mer I isomer. However, the possibility that isomerization also takes place in the intermediate steps of the reaction prior to the formation of the final product cannot be

ruled out. Some evidence against this latter possibility was obtained by monitoring the reaction of $(bz)Cr(CO)_2(CSe)$ with $(PhO)_3P$ by ^{31}P NMR spectroscopy. fac-$Cr(CO)_2(CSe)$-$[(PhO)_3P]_3$ was detected in a higher concentration than the mer I isomer in the initial stages of the reaction with $(PhO)_3P$ (Figure 4.5), while the final product was predominantly the mer I isomer. This observation suggests that rearrangement to the thermodynamically more stable mer I isomer occurs subsequent to the formation of the kinetically expected fac product. The initial detection of the fac isomer with the $(PhO)_3P$ ligand but not with $(MeO)_3P$ may be the result of a slower rate of isomerization in the former case due to steric effects imposed by the bulky phenoxy substituents.

The reactions of the tridentate ligands triphos-U and triphos with $(\eta$-Arene$)Cr(CO)_2(CX)$ afford fac-(L-L-L)-$Cr(CO)_2(CX)$ complexes in quantitative yield, giving added support to the hypothesis that the fac product is formed first in the reactions with the monodentate phosphite ligands. If the formation of the mer I isomer in the latter cases was the result of isomerization of an intermediate in the reaction pathway, then reaction with tridentate ligands might be expected to result either in bridging of the tridentate ligand across the metal or, if such a structure were unfavourable, in a low, rather than quantitative yield of

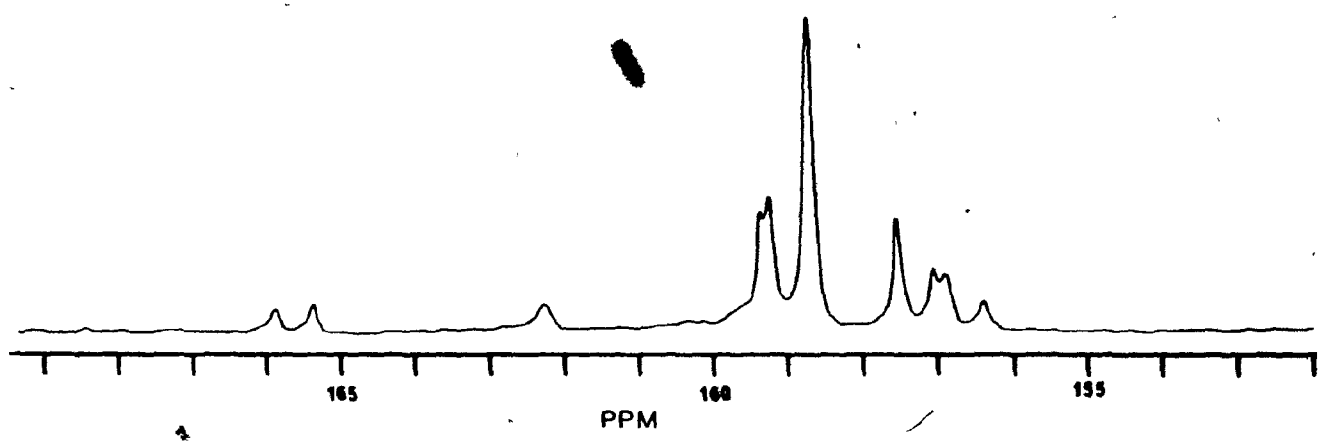

Figure 4.5. ^{31}P NMR spectrum recorded at t = 60 min of the reaction of $(bz)Cr(CO)_2(CSe)$ with $(PhO)_3P$ at 60°C, revealing the initial formation of <u>fac</u>-$Cr(CO)_2(CSe)[(PhO)_3P]_3$. Conditions: obtained on a Varian XL-300 FT spectrometer operating at 121.42 MHz; ^1H-decoupled; sweep width = 30,000 Hz; offset = 12,400 Hz; flip angle = 40°, repetition time = 0.5 s; number of scans = 400.

the fac product. However, the high effective local concentration of incoming ligand after coordination of the first phosphorus atom of the tridentate ligand to the metal would not provide much time for rearrangement of an intermediate to occur.

It is of interest to note that in earlier studies of arene displacement from (η-Arene)$M(CO)_3$, kinetic investigations of the reactions of (η-Arene)$Cr(CO)_3$ with ligands L were not undertaken because they yielded products other than the expected fac-$Cr(CO)_3L_3$. Although we were unable to obtain kinetic data for arene displacement from (η-Arene)$Cr(CO)_3$ by $(MeO)_3P$, we were able to characterize the products of these reactions as mixtures of mer- and fac-$Cr(CO)_3[(MeO)_3P]_3$ with the mer isomer predominant. Furthermore, the rate measured for fac → mer isomerization of this complex (Chapter 3) is faster by at least three orders of magnitude than the rate of arene displacement in the (η-Arene)$Cr(CO)_3$ systems (Table 4.9). Therefore, just as for the thio- and selenocarbonyl analogues, the formation of predominantly mer-$Cr(CO)_3[(MeO)_3P]_3$ in the reaction of (η-Arene)$Cr(CO)_3$ with $(MeO)_3P$ may be attributed to isomerization of the expected fac isomer at a much faster rate than its rate of formation. In the case of the reaction of (cht)$Cr(CO)_3$ with $(MeO)_3P$, the reaction rate at, for example, 50°C [3] is eight times faster (for $[(MeO)_3P]$ = 1 M)

than the rate of isomerization of $Cr(CO)_3[(MeO)_3P]_3$ at this temperature, thus accounting for the formation of the fac isomer.

4.4 Concluding Remarks

The studies of arene labilization for the thiocarbonyl complexes were initially undertaken to elucidate why such complexes lack the catalytic activity exhibited by the corresponding tricarbonyl complexes. The results described here demonstrate that the products of arene displacement reactions of the thiocarbonyl complexes exhibit a faster rate of intramolecular isomerization than the parent tricarbonyls. The rapid occurrence of rearrangement processes of the type observed in this study would not afford the necessary intermediates required for catalytic activity to take place, since it has been shown that the fac configuration is crucial in effecting hydrogenation through the mechanisms outlined in Chapter 1. In addition, the crystal structure of $Cr(CO)_2(CS)[(MeO)_3P]_3$ obtained provided evidence for a very large amount of electron density on the thiocarbonyl ligand - the C-S bond distance approximating that of a bridging CS group. Nucleophilic attack by the sulfur atom of the thiocarbonyl ligand has been reported [27] for complexes exhibiting low $\nu(CS)$ frequencies and, accordingly, long C-S bond lengths. Since hydrogenation studies take place in the presence of donor solvents, $Cr(CO)_2(CS)L_3$

species are probably formed. It is likely that the electron density on the CS ligand in such species is sufficient to cause the thiocarbonyl to act as a nucleophile leading to side reactions or autodecomposition.

Although, to date, no catalytic studies have been performed with selenocarbonyl complexes, their catalytic activity will almost certainly be the same as that of the thiocarbonyl complexes because of the similar reactivities of these chalcocarbonyl derivatives.

References

1. F. Zingales, A. Chiesa and F. Basolo, J. Am. Chem. Soc., 88, 2707 (1966).

2. A. Pidcock, J.D. Smith and B.W. Taylor, J. Chem. Soc. (A), 872 (1967).

3. A. Pidcock and B.W. Taylor, J. Chem. Soc. (A), 877 (1967).

4. A. Pidcock, J.D. Smith and B.W. Taylor, J. Chem. Soc. (A), 1604 (1969).

5. G. Yagupsky and M. Cais, Inorg. Chim. Acta, 12, L27 (1975).

6. M. Gower and L.A.P. Kane-Macguir, Inorg. Chim. Acta, 37, 79 (1979).

7. W. Strohmeier and H. Mittnacht, Z. Phys. Chem., 29, 339 (1961).

8. C.L. Zimmerman, S.L. Shaner, S.A. Roth and R.B. Willeford, J. Chem. Res.(s), 108 (1980).

9. T.G. Traylor and K. Stewart, Organometallics, 3, 325 (1984).

10. T.G. Traylor, K.J. Stewart and M.J. Goldberg, J. Am. Chem. Soc., 106, 4445 (1984).

11. C.D. Hoff and S.P. Nolan, Abstracts, 189th Meeting of the American Chemical Society, Miami, Florida, April-May, 1985, paper INOR-23.

12. M.F. Farona, in "Organometallic Reactions and Syntheses", Vol. 6, E.I. Becker and M. Tsutsui, ed., Plenum Press, New York, 1977, pp. 223-288.

13. F. Basolo, Inorg. Chim Acta, 50, 65 (1981).

14. E.L. Muetterties, J.R. Bleek, E.J. Wucherer and T.A. Albright, Chem. Rev., 82, 499 (1982).

15. G. Mieling and H. Pardue, Anal. Chem., 50, 1611 (1978).

16. J.-Y. Saillard, D. Grandjean, P. Caillet and A. Le Bauze, J. Organometal. Chem., 190, 371 (1980).

17. P.E. Baikie and O.S. Mills, J. Chem. Soc. (A), 2704 (1968).

18. P. Le Maux, J.Y. Saillard, D. Grandjean and G. Jaouen, J. Org. Chem., 45, 4524 (1980).

19. J.-Y. Saillard, D. Grandjean, P. Le Maux and G. Jaouen, Nouveau J. Chim., 5, 153 (1981).

20. A.M. English, Ph.D. thesis, McGill University, Montreal, Quebec, Canada, 1980.

21. E.W. Neuse, J. Organometal. Chem., 99, 287 (1975).

22. R. Dabard, G. Jaouen, G. Simonneaux, M. Cais, D.H. Kohn, L. Lapid and D. Tatarsky, J. Organometal. Chem., 184, 91 (1980).

23. M. Cais, M. Kaftory, D.H. Kohn and D. Tatarsky, J. Organometal. Chem., 184, 103 (1980).

24. D.J. Darensbourg, in "Advances in Organometallic Chemistry", Vol. 21, Academic Press, New York, 1982, pp. 113-149.

25. D.J. Darensbourg, N. Walker and M.Y. Darensbourg, J. Am. Chem. Soc., 102, 1213 (1980).

26. D.J. Darensbourg, M.Y. Darensbourg and N. Walker, Inorg. Chem., 20, 1918 (1981).

27. B.D. Dombek and R.J. Angelici, J. Am. Chem. Soc., 96, 7568 (1974).

PART II

Applications of FT-IR Spectroscopy and Metal Chalcocarbonyl Chemistry in Biological Systems

Chapter 5

Applications of FT-IR Spectroscopy in the Study of Biological Systems

In the 1984 May-June issue of Applied Spectroscopy, Jakobsen announced in a guest editorial the recent formation of the first National Center for Biomedical FT-IR Spectroscopy. The logo for the center is an interferogram joining

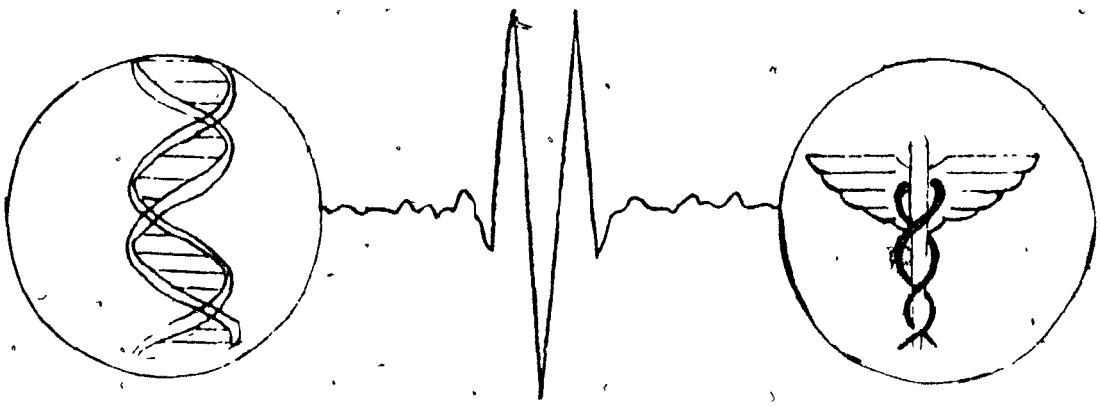

the double helix structure of DNA with a caduceus to represent the bridge of molecular spectroscopy between biology and medicine. He stated the functions of the center are "1) to advance the state-of-the-art of FT-IR; 2) to demonstrate new applications of FT-IR in both biology and medicine; 3) to collaborate with scientists outside the Center and provide them with spectroscopy information useful to their research; 4) to spread the word to the scientific community about the use of FT-IR in this research; and 5) to train

scientists in the use of FT-IR for biomedical purposes."

In the past, IR spectroscopy has been of limited usefulness in the study of complex biological systems for the following reasons:

(a) Spectra of dry protein could not provide a direct correlation to in vivo biological processes. Therefore, in order to simulate biological conditions, spectra of biological systems were generally measured in H_2O (or D_2O) solutions, resulting in a loss of large regions of the spectra because of the strong H_2O (D_2O) absorptions. The use of D_2O posed additional problems because of hydrogen-deuterium exchange which often causes conformational changes.

(b) Biological systems generally contain many different proteins, as well as numerous organic species, which can have an interfering effect in the study of the biomolecule or the biological process of interest.

(c) A large number of biologically active species exist in too low concentrations to be detected by dispersive IR spectroscopy.

The advent of FT-IR instrumentation has allowed several orders of magnitude improvement in signal-to-noise (S/N) ratio in relatively short times of data acquistion [1-13] as a result of the multiplex (Fellgett's) and throughput (Jacquinot's) advantages of the FT-IR spectrometer. Digitization of the spectra permits digital absorbance subtraction, thereby eliminating solvent and other interferences.

The following examples illustrate the types of information which have been obtained by FT-IR investigations of biological systems. This survey in part serves to indicate the rather limited extent to which FT-IR spectroscopy has been applied in biological studies. It does not include studies of the FT-IR spectra of isolated small biomolecules or model compounds, which are far more numerous.

The first applications of FT-IR spectroscopy in biological investigations were carried out by Alben and co-workers. An example of this group's work is their study of the nature of carbon monoxide binding and of the molecular binding sites in various hemocyanins [14,15]. Hemocyanins are the oxygen transport proteins in the hemolymph of many molluscs and decapod crustaceans, and reversibly bind oxygen or carbon monoxide with a stoichiometry of one ligand per two copper atoms. Relatively little was known about the ligand binding to copper in these proteins before the FT-IR studies. The IR spectra of the hemocyanin-carbon monoxide complexes of various species show great similarities. They exhibit only one narrow absorption band between 2300 and 1800 cm^{-1} due to bound carbon monoxide. Therefore, only one kind of CO environment appears to exist for each species [16]. The observed narrow half-band width, as compared to half-band widths of carbonyl peaks in solvents of different polarities, suggests that the active site of the copper is

located in a non-polar environment in the protein [14,15]. Also, the observed differences in the absorption maxima [ν(CO)] for carboxyhemocyanin in various species were attributed to differences in the amino acid groups coordinated to the copper binding the carbon monoxide [15].

Alben and his co-workers have also utilized the enhancement of the S/N ratio in FT-IR spectroscopy relative to previous IR spectroscopic methods to examine specific amino acid interactions (e.g., sulfhydryl groups [ν(SH)] of cystine residues of human carboxyhemoglobin) [17]. They showed that the absorbance of the sulfhydryl group is highly sensitive to the state of ligation, and to the tertiary and quaternary structure of the protein, thus providing a new probe of native hemoglobin structure and its conformational alterations.

More recently Alben et al. undertook a detailed FT-IR investigation of the dynamic interaction of carbon monoxide with a_3 Fe and Cu_B in cytochrome c oxidase at low temperature [18]. They found that photolyzing the Fe-CO bond results in the transfer of CO to Cu_B. This process is reversible in the absence of light above 140 K. That the a_3FeCO showed a very narrow ν(CO) peak, while the Cu_B exhibited a much broader one, indicated that the carbon monoxide in a_3FeCO is in a highly ordered environment separated from the Cu_B atom which is in less ordered, more flexible surroundings.

Mantsch and co-workers have employed FT-IR spectroscopy in the elucidation of the structure and functional properties of biomembranes. They have designed an integrated system, including hardware and software modifications [19,20], to study several aspects of the thermal behaviour of natural phosphatidylethanolamines, phosphatidylcholines and phosphatidylsulfocholines, by monitoring subtle changes in the absorption bands characteristic of specific functional groups.

FT-IR spectroscopy has recently been used to examine metal ion interactions with DNA nucleotides [21], as well as the interactions of certain drugs, such as platinum compounds with anti-tumour activity [e.g., cis-$Pt(NH_3)_2Cl_2$], with DNA [22].

The monitoring of blood protein interactions with polymers is of great importance for the assessment of the suitability of a material as an implant in the body (e.g., artificial heart valves, indwelling catheters, dialysis membranes and other artificial organs). The event which seems to determine how well the body will tolerate a given implant is protein adsorption, since adsorption of certain proteins can induce thrombosis (clotting). The coupling of FT-IR with ATR (attenuated total reflection) has provided the necessary sensitivity to detect very thin layers of adsorbed proteins on various surfaces [23-25]. Gendreau et al. have

utilized this technique for the first time to study protein adsorption from flowing, intact dog blood on a polymer-coated germanium surface [24] (Figure 5.1). They demonstrated that within the first few seconds of flow rapid adsorption of albumin and glycoproteins took place; immediately thereafter, increased amounts of fibrinogen and other proteins began to adsorb, displacing albumin until finally a clot was formed. This example represents one of the only *ex vivo* biomedical experiments involving FT-IR spectroscopy.

Clearly the use of FT-IR spectroscopy in the study of biological systems has not been widespread. As biological, biochemical and medical researchers become more aware of the enhanced sensitivity and flexibility of this nondestructive spectroscopic technique, new applications will certainly emerge. In Chapter 6, the investigation of such an application, involving the use of FT-IR spectroscopy to detect organometallic-labelled steroidal hormones in their target tissue for purposes of receptor assay, will be described. Further utility of FT-IR in the study of some selected chalcocarbonyl porphyrin derivatives will be presented in Chapter 7.

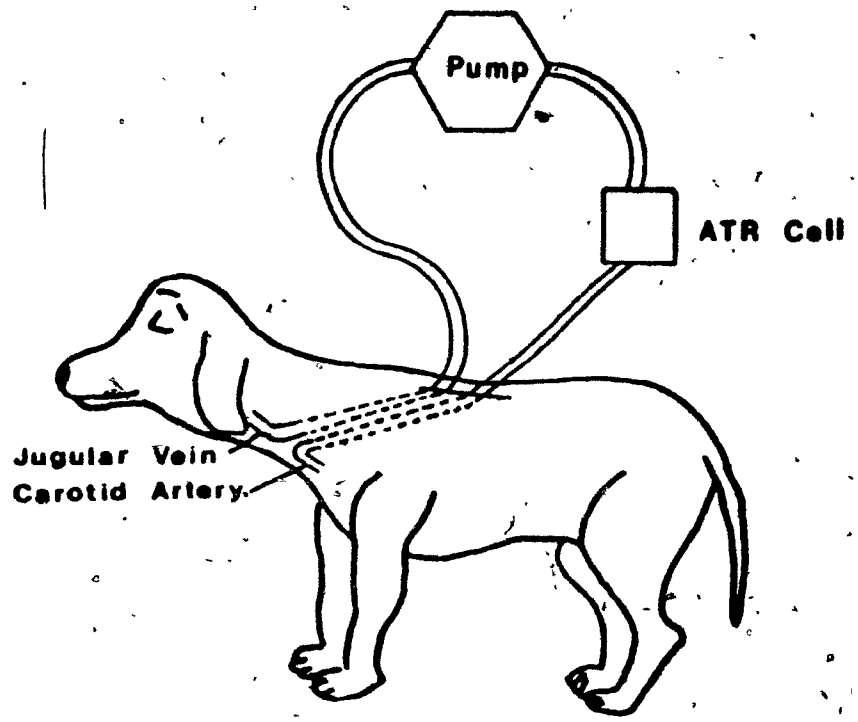

Figure 5.1. Experimental setup of Gendreau *et al.* for the study of protein adsorption from flowing, intact dog blood on a polymer-coated germanium ATR crystal. Adapted from Reference 24.

References

1. P.R. Griffiths, "Chemical Infrared Fourier Transform Spectroscopy", J. Wiley and Sons, New York, 1975.
2. J.A. Haseth in "Fourier, Hadamard and Hilbert Transforms in Chemistry", A.G. Marshall, ed., Plenum Press, New York, 1982, pp. 378-420.
3. P.R. Griffiths, Appl. Spectrosc., 31, 497 (1977).
4. C. Foskett and T. Hirschfeld, Appl. Spectrosc., 31, 239 (1977).
5. G. Mamantov, A.A. Garrisón and E.L. Wehry, Appl. Spectrosc., 36, 339 (1982).
6. P.L. Hanst in "Fourier Transform Infrared Spectroscopy", Vol. II, J.R. Ferraro and L.J. Basile, eds., Academic Press, New York, 1979.
7. D.R. Mattson, Appl. Spectrosc., 32, 335 (1978).
8. T. Hirschfeld, Appl. Spectrosc., 31, 550 (1977).
9. D.H. Anderson and T.E. Wilson, Anal. Chem., 47, 2482 (1975).
10. R. Cournoyer, J.C. Shearer and D.H. Anderson, Anal. Chem., 49, 2275 (1977).
11. H.J. Sloane and R.J. Obremski, Appl. Spectrosc., 31, 506 (1977).
12. T. Hirschfeld and C. Cody, Appl. Spectrosc., 31, 551 (1977).

13. D.L. Wall and A.W. Mantz, Appl. Spectrosc., 31, 552 (1977).

14. J.O. Alben, L. Yen and N.J. Farrier, J. Am. Chem. Soc., 92, 4475 (1970).

15. J.O. Alben and L.Y. Fage, Biochemistry, 11, 4786 (1972).

16. P.P. Moh, J.S. Rieske and O.J. Alben, Fed. Proc., 37, 1389 (1978).

17. G.H. Bare, J.O. Alben and P.A. Bromberg, Biochemistry, 14, 1578 (1975).

18. F.G. Fiamingo, R.A. Altschuld, P.P. Moh and J.O. Alben, J. Biol. Chem., 257, 1639 (1982) and references therein.

19. H.H. Mantsch, A. Martin and D.G. Cameron, Biochemistry, 20, 3138 (1981).

20. H.H. Mantsch, D.G. Cameron, P.A. Tremblay and M. Kates, Biochim. Biophys. Acta, 689, 63 (1982) and references therein.

21. T. Theophanides, in "Fourier Transform Infrared Spectroscopy", T. Theophanides, ed., D. Reidel Publishing Co., Dordrecht, Holland, 1984, pp. 83-96.

22. T. Theophanides, Appl. Spectrosc., 35, 461 (1981).

23. R.M. Gendreau and R.J. Jakobsen, Appl. Spectrosc., 32, 326 (1978).

24. R.M. Gendreau, S. Winters, R.I. Leininger, D. Fink, C.R. Hassler and R.J. Jakobsen, Appl. Spectrosc., 35, 353 (1981).

25. R.M. Gendreau, Appl. Spectrosc., 36, 47 (1982).

Chapter 6

FT-IR Spectroscopy in Biological Assay

6.1 Introduction

The determination of hormonal receptor concentrations in tissue requires highly sensitive techniques in view of the minute quantities involved (nanograms or less per gram of tissue). Radioassay has been the principal technique used in measuring such low concentrations. Though this method has proved quite powerful and is widely accepted, it has certain drawbacks: high cost of radioisotopes, health hazards, limited variety of usable isotopes, labelling difficulties, chemical and biochemical instability (including radiolysis in solution). These problems have encouraged the search for non-radioisotopic methods in biological assay.

In this chapter, the investigation of the feasibility of a new method of receptor assay will be presented. The method is based on the labelling of a steroidal hormone with a metal tricarbonyl moiety and detection of this label in the hormone-receptor complex by FT-IR spectroscopy. The receptor chosen for the investigation was the estrogen receptor. The approach to receptor assay described in this chapter represents one of the few examples reported of research on the incorporation of organometallic labels into

estrogens in order to label the estrogen receptor for diagnostic or therapeutic purposes. Recently estrogen has been labelled with boron-10 atoms (in the form of a cage carborane molecule containg ten boron atoms and two carbon atoms) by Hadd [1] (patent under review), with the hope that such a label would be taken up by cancerous cells that contain estrogen receptors. Subsequent bombardment with a low-energy neutron beam would split the ^{10}B, giving off alpha particles causing necrosis in the immediate area. Cais and co-workers [2] have investigated the determination of metal labels in steroids by atomic absorption spectrometry. Dilution of the metal-labelled steroids in phosphate buffer yielded an atomic absorption calibration curve in the 20-500 ng ml^{-1} range for Fe-labelled steriod. However, no *in vitro* or *in vivo* studies have been performed to date to assess the utility of this method for receptor assay.

The process by which specific estrogen binding to its receptor takes place has been traditionally described as follows: the estrogen enters the target cell from the blood stream and interacts with specific receptor proteins in the cytoplasm, forming a non-covalent, high-affinity complex. This complex then enters the cell nucleus and ultimately effects new protein synthesis [3] (Figure 6.1). However, recent studies utilizing monoclonal antibodies to estrophilin (estrogen receptor protein) [4] and cell enucleation [5]

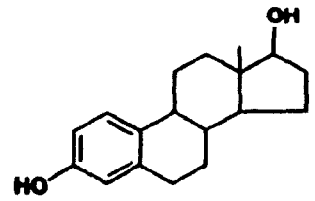

the steroidal hormone estradiol

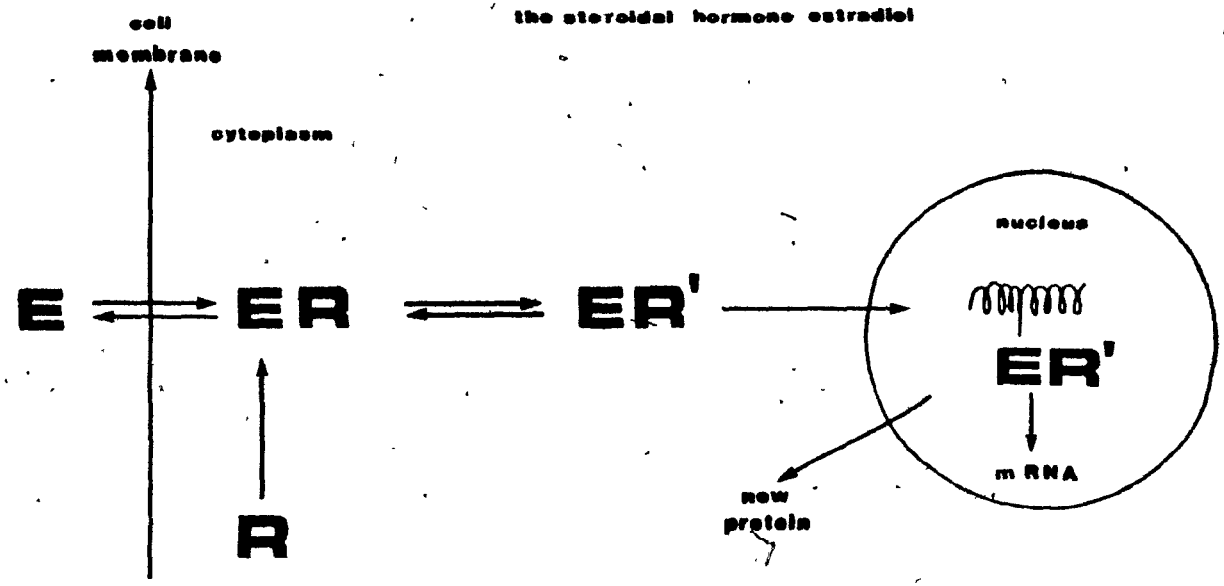

E = STEROIDAL HORMONE
R = RECEPTOR
R' = MODIFIED RECEPTOR

Figure 6.1. Traditional representation of the mode of action of a steroidal hormone in a target cell. Adapted from A.L. Lehninger, "Biochemistry", 2nd ed., Worth Publishers, New York, 1975, p. 824.

have provided evidence that the estrogen receptor resides solely in the cell nucleus. It has been postulated that the observed localization of the free receptor in the cytosolic fraction of cell homogenates occurs during homogenization [5].

The interaction of estrogens with their specific receptors has been the focus of considerable research [6] and changes in estrogen receptor levels are implicated in certain hormone-dependent cancers [7]. Estrogen receptor levels have been determined by radiochemical techniques using a variety of radiolabelled modified estrogens (e.g., ^{3}H, ^{14}C, ^{125}I) [6].

The synthesis of chromium tricarbonyl derivatives of steroids has been reported in the literature [8,9]. (est)$Cr(CO)_3$ has been prepared by heating $Cr(CO)_6$ and estradiol in the presence of donor solvents such as THF and n-Bu_2O. The A ring is the preferred site for complexation because it acts as a six-electron donor to complete an 18-electron configuration for the $Cr(CO)_3$ moiety. Since the $Cr(CO)_3$ moiety can complex on either side of the A ring, two diasteriomers with the $Cr(CO)_3$ group either trans (α) or cis (β) to the methyl group at the 13-position of the steroid are obtained. These isomers have recently been separated using thin layer chromatography [10]. The α isomer was found to be more stable as well as being the preferred pro-

duct; this situation was attributed to the greater steric hindrance encountered by the tricarbonyl moiety in the cis product due to the methyl group.

The first requirement that must be met by these derivatized hormones if the organometallic moiety is to serve as a label for receptor assay is that they must be stable in aqueous media. The second requirement is that they must retain a high specificity for their particular receptor. The presence of the hydroxyl group at the 3-position of the steroid was found to contribute to the rapid decomposition of $(est)Cr(CO)_3$ complexes in solution, yielding estradiol and chromium salts. Incorporation of a protecting group at the 3-hydroxyl group of the estradiol resulted in stabilization of the product, presumably by shielding the metal tricarbonyl moiety from attack by solvent molecules.

Enhancing the stability of the complex in solution invariably decreases receptor binding. Thus a variety of protecting groups were examined [11] in order to select the modified estradiol with the highest affinity for the estrogen receptor. The binding affinities of the modified estradiol complexes were assayed by competitive binding studies using uncomplexed, tritiated estradiol hormone. (A drawback of this procedure is the inability to measure accurately the levels of high-affinity, non-specific binding of the modified estrogen complexes.) Both the α and β complexes with a

variety of protecting groups at the 3-hydroxyl group were tested and the relative binding affinities (RBA) were calculated (Table 6.1). When the hydroxyl group is maintained away from the steroid skeleton by a spacer chain ($H-O-(CH_2)_3-$, 9) the highest affinity was observed. It appears also that the fixation site of the tripod on the A ring of the steroid strongly discriminates the α and β diasteriomers with respect to their receptor recognition properties. While the β-isomers (6, 11) show relatively modest affinities, the α-isomers (5, 7, 10) bind with significantly higher affinities. Among the complexes listed in Table 6.1, compound 10 has the highest RBA value, 28, which is very close to that of the free ligand 9 (RBA = 37), and thus may serve as an excellent choice on the basis of the recognition criteria.

In this chapter, an investigation of the utility of FT-IR spectroscopy in the detection of the modified, organometallic-labelled estrogens at physiological concentrations will be presented and the potential and limitations of the use of FT-IR in their quantitative analysis as an alternate technique to radioassay will be discussed.

Table 6.1. Relative Binding Affinities of Modified Estradiols and Their Chromium Chalcocarbonyl Derivatives[a]

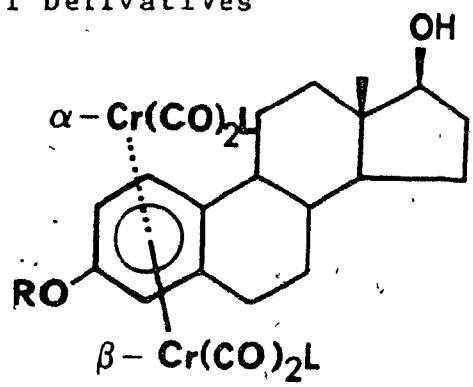

Compound	R/metal chalcocarbonyl moiety	Relative binding affinity (RBA)[b]
1	H/-	100
4	$Si(Me)_2(t\text{-}Bu)$/-	11
5	$Si(Me)_2(t\text{-}Bu)$/ α-$Cr(CO)_3$	1.05
6	$Si(Me)_2(t\text{-}Bu)$/ β-$Cr(CO)_3$	0.36
7	$Si(Me)_2(t\text{-}Bu)$/ α-$Cr(CO)_2(CS)$	1.5
9	$HO(CH_2)_3$/-	37
10	$HO(CH_2)_3$/ α-$Cr(CO)_3$	28
11	$HO(CH_2)_3$/ β-$Cr(CO)_3$	1.75

[a]Data from References 10 and 11.
[b]The relative binding affinity represents the ratio of the concentration of unlabelled estradiol to that of the compound required to inhibit half of the binding of [^{3}H]-estradiol in a competitive binding assay, with the RBA of estradiol set at 100%.

6.2 Experimental

The general procedure for organometallic labelling of the steriod has been published previously [9] and is not included here. However, the biochemical assay has not been fully published. It should be noted that the procedures described in Sections 6.2.1 and 6.2.2 were performed by A. Vessières and are only included here to provide the reader with the necessary background in the sample preparation required for the FT-IR studies.

6.2.1 Sheep Uterus Estrogen-Receptor Purification

Young sheep uteruses were obtained from the slaughterhouse and were put in ice immediately after their removal from the animal (the weight of the uterus should not exceed 10 g). All further manipulations were performed between 0 and 4°C. Surrounding fat was first removed from the uteruses, which were then washed with 0.9% NaCl solution and weighed. They were then homogenized in a "Waring Blender" in twice their volume of Tris-Saccharose (Tris pH 7.5, 50 mM; Saccharose, 0.25 M, mercaptoethanol, 1%), and centrifuged for 15 min at 800 x g. After centrifugation the supernatant was filtered through nylon gauze and centrifuged at 105,000 x g for 1 h. The supernatant from this centrifugation constitutes what is called the cytosol. The receptor concentration in the cytosol was measured for one aliquot

using the method described by Thieulant et al. [12]. The cytosol was subsequently divided into small fractions not larger than 10 ml which were kept at -70°C. Periodic measurements of the receptor concentration in these samples showed that under these conditions the level of estradiol receptor remains constant for several months. The amount of cytosol proteins was determined by the Lowry assay using BSA (bovine serum albumin) as a standard. The concentration of proteins in the above preparations was usually 10-12 mg/ml cytosol.

6.2.2 Preparation of Samples for FT-IR Studies

Varying volumes of cytosol were incubated for 4 h at 0°C with known concentrations of the organometallic-labelled estradiol derivatives to yield a final concentration of the label in the range 10^{-8} - 10^{-6} M. At the end of the incubation period, an equal volume of protamine sulfate solution (6 mg/ml) was added to precipitate the proteins. The precipitate obtained was collected by centrifugation (3300 x g, 15 min). After elimination of the supernatant, the precipitate was washed 4 times with 5 ml of phosphate buffer (0.05 M, pH 7.4), twice with 5 ml of distilled water and lyophilized. This provides a white powder which can be used without further treatment for the IR studies. The receptor concentration in these samples was established by competitive

binding assay using ^{3}H-estradiol to be in the range of 300 fmol per mg of precipitated protein.

6.2.3 Infrared Studies

All solvents used were of spectrograde purity or were distilled under nitrogen prior to use. KBr and CsI (gold label 99.999%) were obtained from Aldrich Chemical Co. Solid samples were pressed into 3- or 5-mm pellets, using a "Qwik Handi-Press Set" available from Aldrich. Samples mixed with KBr or CsI were ground in stainless steel vials using "Wig-L-Bug", also available from Aldrich.

All spectra were recorded with a Nicolet 6000 Fourier transform-infrared spectrometer equipped with a mercury cadmium telluride (MCT) detector (Infrared Associates, New Brunswick, NJ), and having a beam diameter at the focal point of 5 mm. The pellet holder was supported on an X-Y translator, so that the sample position could be adjusted to obtain maximal detector response. Ten thousand to thirty thousand scans (with a medium correlation) were accumulated and co-added using the LWA program listed in Appendix C. The mirror velocity was adjusted empirically to 0.640 cm s^{-1} for optimum detector sensitivity; the gain was increased to allow the interferogram to reach 50-75% of its height in a background scan recorded for the empty pellet holder with a source aperture of 6.3 mm. The relative gain of all the

points after the first 1024 set was increased by a factor of eight. The co-added interferograms were apodized using the Happ-Genzal function and Fourier transformed with one level of zero filling to yield a resolution of 4 cm^{-1}.

6.3 Results and Discussion

The preliminary results presented below were obtained with an organometallic-labelled estradiol derivatized at position 3 with a silyl group (compound 5, Table 6.1). The results of further studies with compound 10, having the highest RBA of any derivatized steriod complex tested, will be shown later in this section.

In the receptor assay procedure under investigation, the organometallic-labelled hormone is incubated with the cytosol containing the hormonal receptor, forming an organometallic-labelled receptor complex (OLRC), and the cytosol proteins are then precipitated by addition of protamine sulfate. The precipitate is then lyophilized, yielding a white powder. The same procedure is followed in the absence of the organometallic-labelled hormone to yield the apoproteins. Figure 6.2 shows the spectrum of the apoprotein diluted in a CsI matrix. Of particular interest here is the lack of absorption in the region between 2200 and 1800 cm^{-1}, thereby limiting any interference from the protein backbone

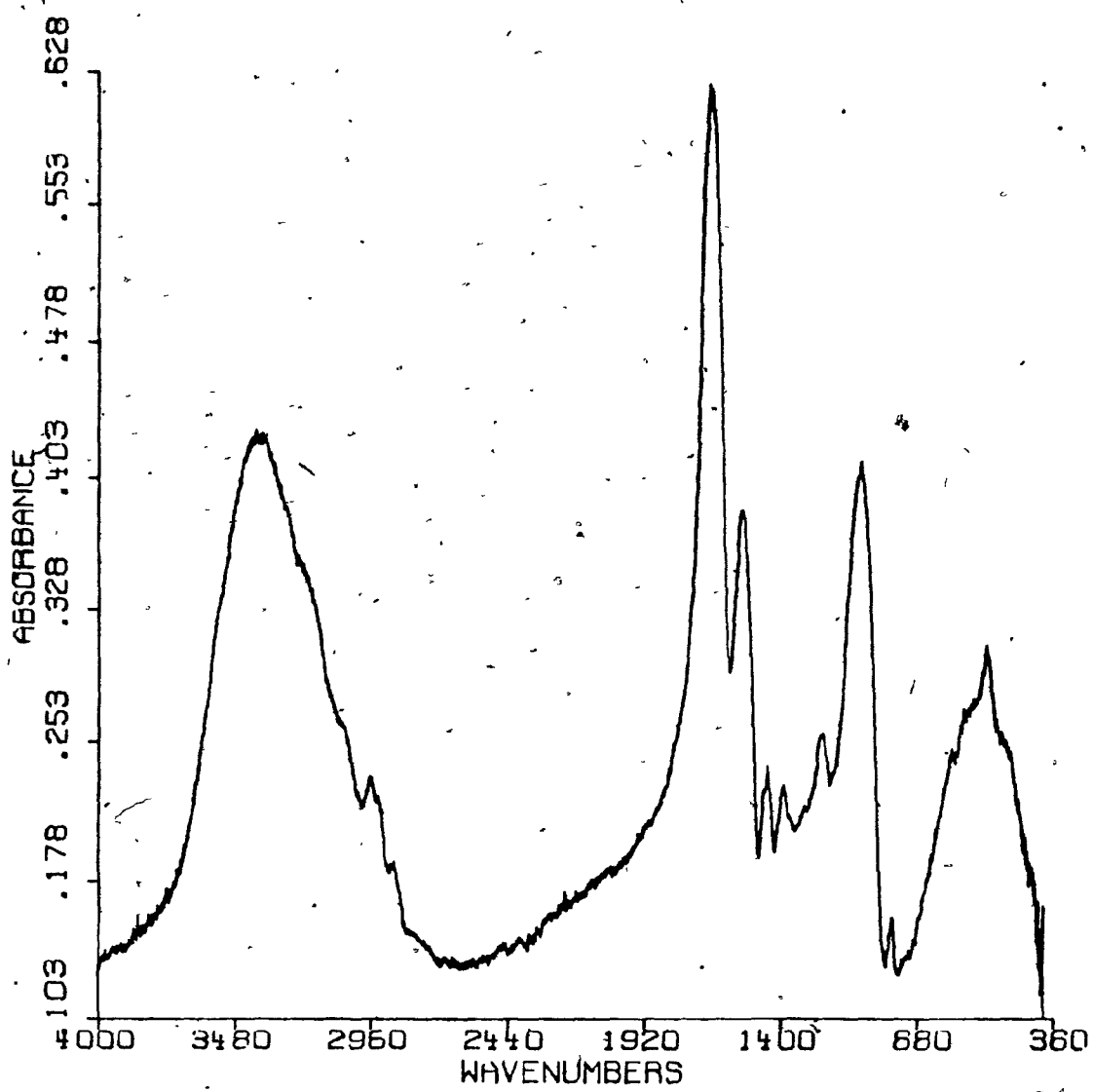

Figure 6.2. FT-IR spectrum of the proteins precipitated by protamine sulfate from the cytosol of sheep uterus (CsI pellet; 32 scans; 4 cm^{-1} resolution).

in the detection of the metal carbonyl stretching vibrations which occur in this region. Samples in which the proteins from the cytosol had been precipitated with hydroxyapatite rather than protamine sulfate were also examined. The choice of this precipitating agent proved unsuitable for the purposes of this work since the FT-IR spectra of these samples exhibited four weak peaks in the 2200-1800 cm^{-1} region, presumably due to overtones of hydroxyapatite P-O stretching modes.

The spectrum of $Cr(CO)_3$-labelled modified estradiol (compound 5) is presented in Figure 6.3. The much larger relative intensity of the metal carbonyl vibrations of the $Cr(CO)_3$ moiety at 1956(a_1) and 1876(e) cm^{-1} compared to the estradiol backbone vibrations clearly indicates the advantage of the $Cr(CO)_3$ label in the detection of low concentrations of steroids by FT-IR spectroscopy.

Since the ratio of receptor to total precipitated proteins is very small, and since mixing with CsI or KBr or dissolution would dilute the sample, thus weakening the IR intensity of the carbonyl peaks, the protein was pressed into a 3-mm diameter minipellet without addition of CsI. The choice of the 3-mm diameter, which is less than the diameter of the IR beam (5 mm), represents a compromise between allowing the maximum amount of energy to pass through the sample and minimizing the amount of protein required.

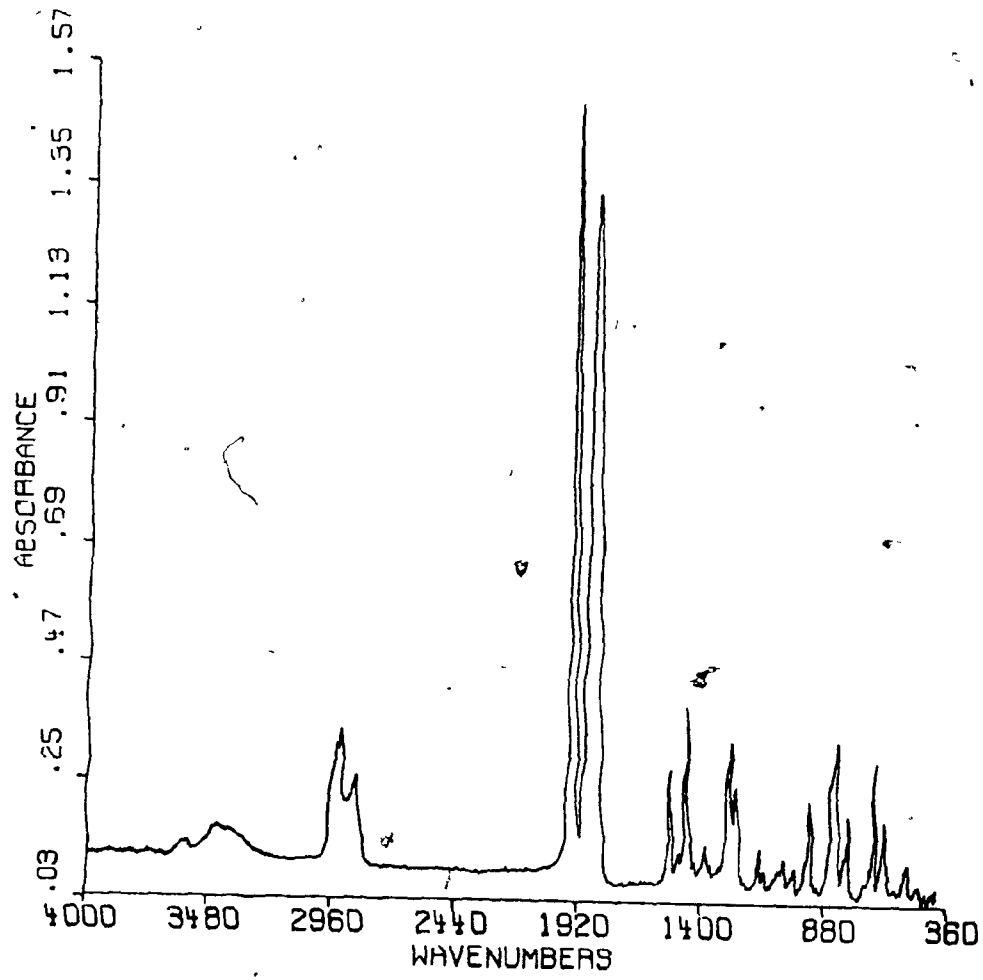

Figure 6.3. FT-IR spectrum of (RO-est)$Cr(CO)_3$ (compound 5) in CsI.

The spectrum of a pressed pellet of the precipitated proteins containing the OLRC (Figure 6.4) demonstrates the importance of the "window" in the carbonyl region since all the absorptions of the steroid skeleton are masked by the enormous absorptions due to the precipitated proteins. The carbonyl region of this spectrum is shown in Figure 6.5; two peaks at 1955(a_1) and 1881(e) cm^{-1} are observed which correspond well to the ν(CO) modes identified in the spectrum of compound 5 in a CsI matrix.

The spectrum in Figure 6.5 was obtained by co-adding 20,000 scans. Co-adding spectra results in an increase in the S/N ratio equivalent to (number of scans)$^{1/2}$. This can be a time-consuming process; however, if the number of data points collected is reduced (i.e., lower resolution), the time required to obtain a given spectrum is shortened by (lower res./higher res.)^2. Accordingly, enhancing the S/N ratio is achieved much faster at lower than at higher resolution. Since the width at half-height of the carbonyl peaks is approximately 17 and 25 cm^{-1} for the a_1 and e modes, respectively, 4 cm^{-1} resolution is quite acceptable as no further information could be gained from scanning at higher resolution [13].

In order to confirm that the peaks observed in the carbonyl region can be attributed to the carbonyl stretching vibrations of the $Cr(CO)_3$ moiety, samples of the precipita-

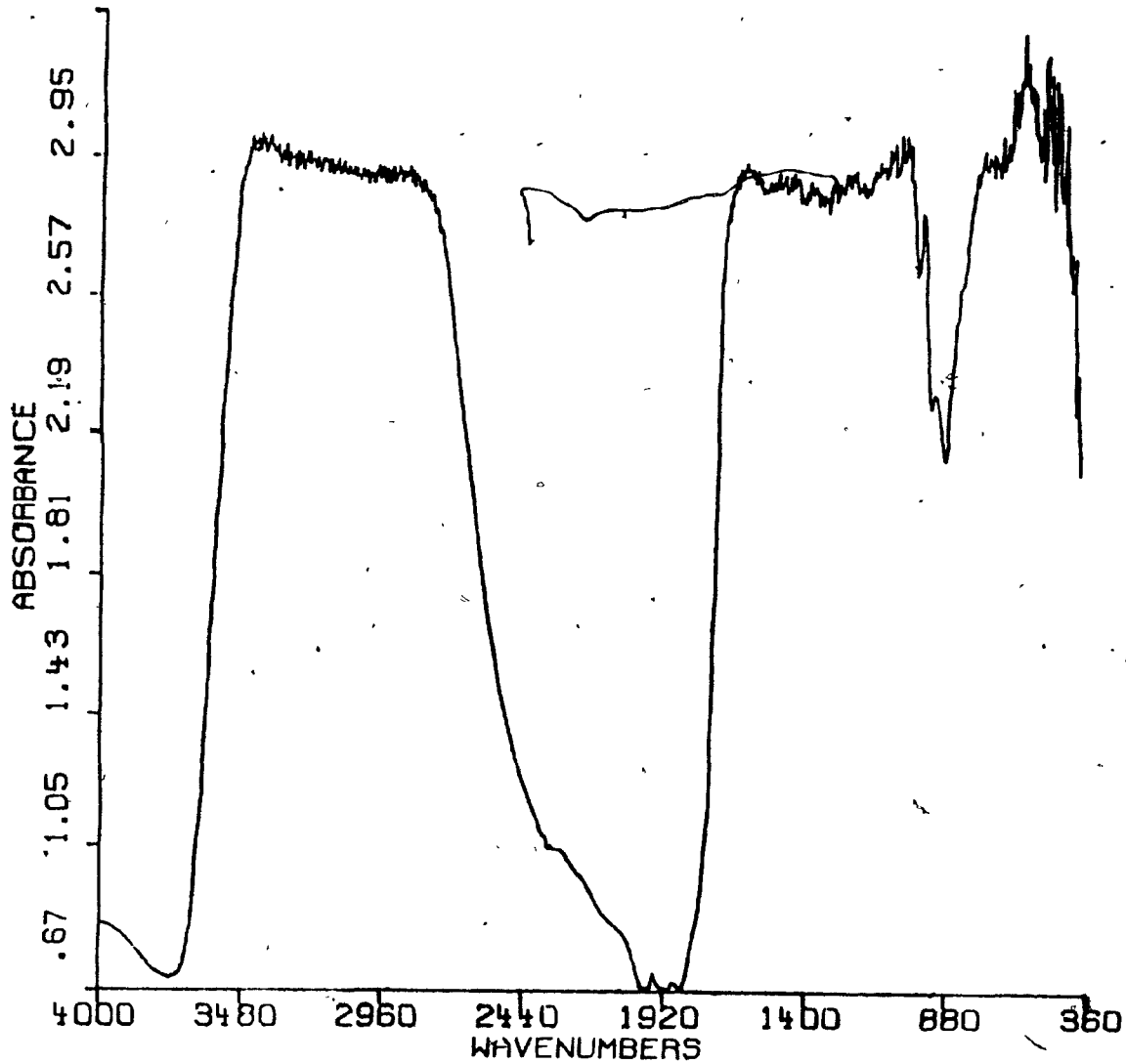

Figure 6.4. FT-IR spectrum of a pressed pellet of the proteins precipitated from the cytosol of sheep uterus after incubation with (RO-est)$Cr(CO)_3$ (compound 5) (3-mm mini-pellet; 20,000 scans; 4 cm^{-1} resolution).

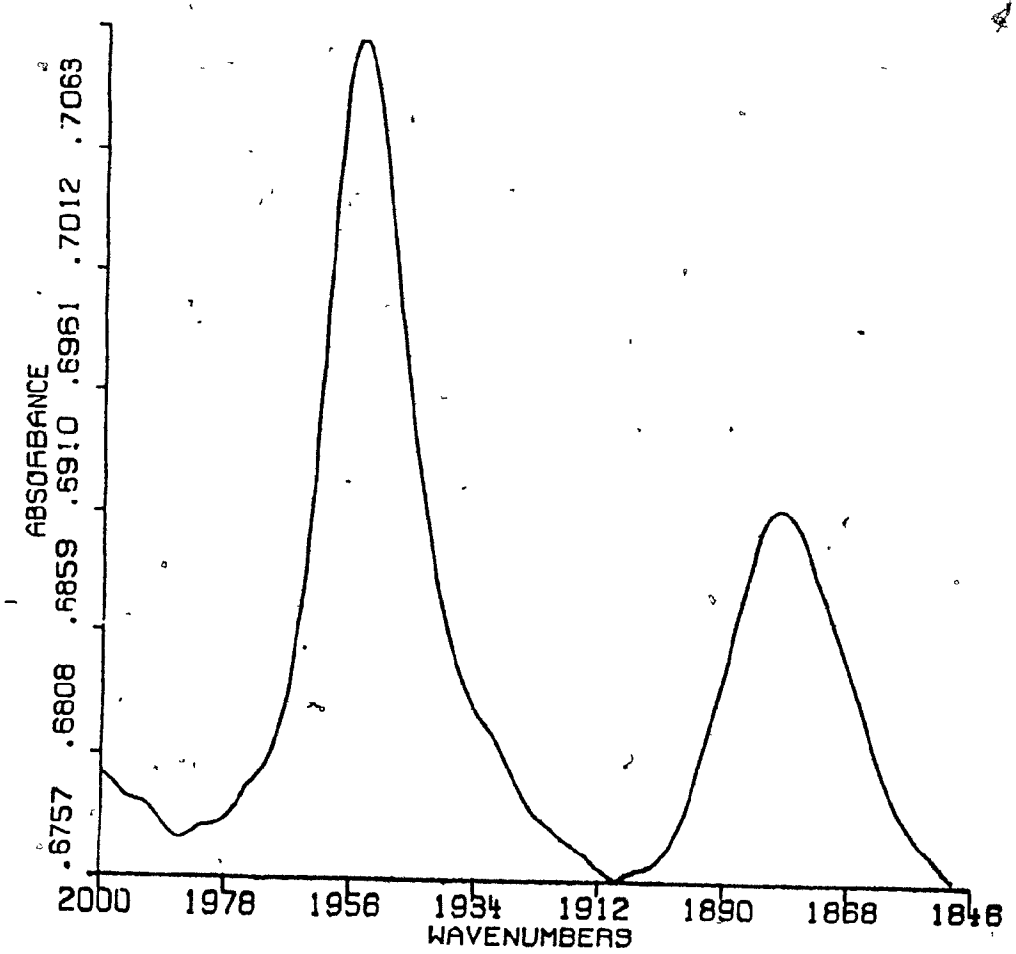

Figure 6.5. Expansion of the ν(CO) region of the FT-IR spectrum in Figure 6.4.

ted proteins obtained after incubation of the thiocarbonyl analogue of (RO-est)$Cr(CO)_3$ (compound 7) [10] in the presence of the receptor under the same conditions as described for the tricarbonyl analogue were obtained. The FT-IR spectrum of compound 7 in CsI is shown in Figure 6.6. The ν(CS) vibration is observed at 1204 cm^{-1} and the ν(CO) modes at 1954 and 1895 cm^{-1}. The carbonyl region of the FT-IR spectrum of the protein sample (Figure 6.7) shows two ν(CO) bands which are shifted as expected in going from the tricarbonyl to the thiocarbonyl analogue. This observation provides confirmation that the bands seen are indeed due to the carbonyl absorptions. The thiocarbonyl stretching vibration (1200 cm^{-1}) is buried beneath the extremely intense vibrational modes of the proteins.

In order to assess the potential of this method in quantitative determination, investigation of the intensity of the carbonyl peaks of the $Cr(CO)_3$ label as a function of pellet weight (i.e., amount of protein) was undertaken. Clearly a linear relationship is required if the FT-IR measurements are to serve as a basis for receptor assay.

Various methods of treating the data were investigated using CsI pellets of varying weights with the same concentration of (RO-est)$Cr(CO)_3$ (compound 5) so as to ascertain the best approach to the correlation of carbonyl intensity with amount of complex present (as represented by wt. of the

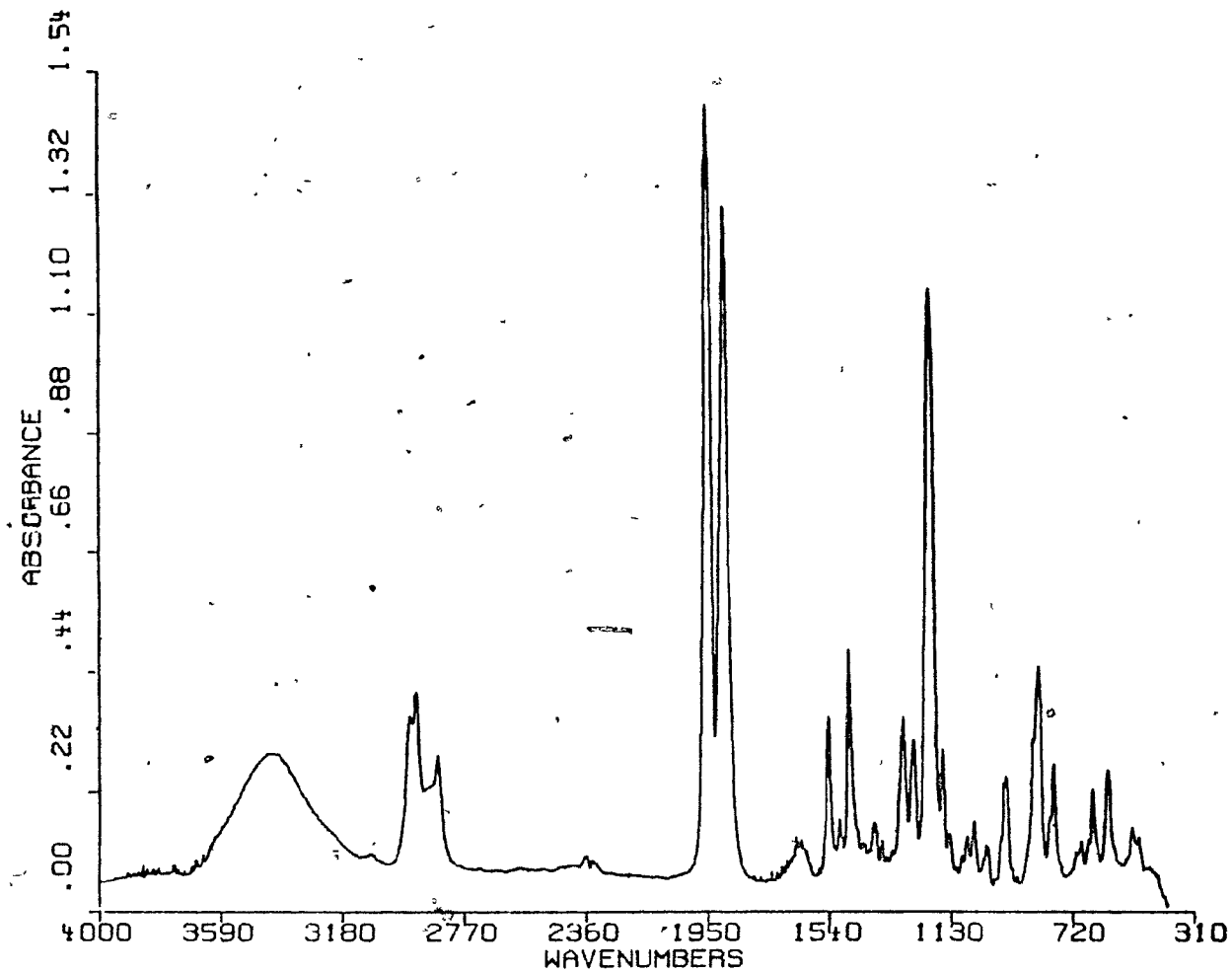

Figure 6.6. FT-IR spectrum of (RO-est)$Cr(CO)_2(CS)$ (compound 7) in CsI.

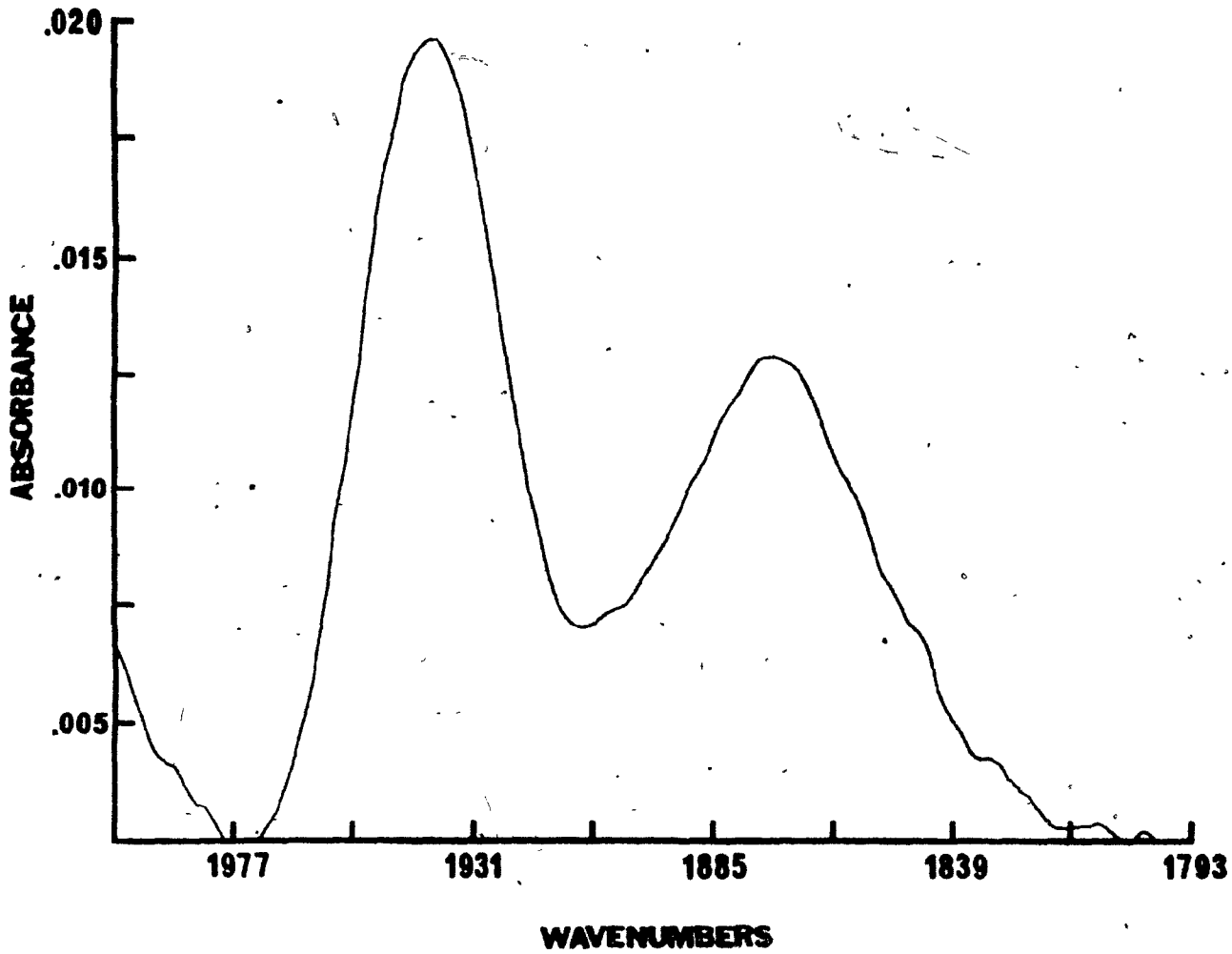

Figure 6.7. The ν(CO) region in the FT-IR spectrum of a pressed pellet of the proteins precipitated from the cytosol of sheep uterus after incubation with (RO-est)Cr(CO)$_2$(CS) (compound 7) (3-mm mini-pellet; 20,000 scans; 4 cm^{-1} resolution).

sample). Table 6.2 lists the four methods examined. These include peak height, peak area, and first derivative and second derivative techniques. In all cases, data were analyzed for the a_1 ν(CO) mode rather than the broader e mode. The results show that the integrated band area method provides the best correlation between band intensity and the concentration of the organometallic complex by virtue of having the highest correlation coefficient and the largest slope. The peak height measurements are also seen to correlate well with concentration, while the derivatives are somewhat less reliable. Differentiation enhances narrow spectral lines, and this enhancement can be used advantageously in the analysis for trace quantities of small or highly symmetrical molecules. Conversely, the broader the band the less useful this feature becomes [14]. The second derivative spectrum of the (RO-est)Cr(CO)$_3$ complex is presented in Figure 6.8. The second derivative of the a_1 mode can be clearly seen while that of the broader e mode is poorly defined.

Subsequent to these studies of compound 5 in CsI, FT-IR spectra were recorded for a series of pellets of varying weights prepared from the precipitated proteins containing the OLRC without addition of CsI. The areas under the a_1 ν(CO) mode in these spectra were plotted as a function of pellet weight (Figure 6.9). The linearity of this plot is

Table 6.2. Analysis of Peak Area, Peak Height and Derivative Methods for Quantitative Determination of (RO-est)$Cr(CO)_3$ (Compound 5) in CsI[a]

Parameter	A[b] x 10^2	B[b] x 10^2	r	Standard error x 10^2
Area[c,d]	2.56	54.10	.99992	0.92
Peak height	1.59	2.03	.9991	0.13
1st derivative, maximum	0.85	0.36	.9771	0.099
1st derivative, minimum	-0.31	-0.54	.9930	0.099
1st derivative, span	1.16	0.91	.9894	0.099
2nd derivative, span	-0.13	-0.075	.9371	0.097

[a]Results for the a_1 ν(CO) mode.
[b]Intercept, A, and slope, B, obtained from plot of parameter as a function of weight of 3-mm CsI pellet containing compound 5 at a dilution of 5.540 X 10^{-7} g/g CsI.
[c]Integration limits between 1984.0 and 1924.0 cm^{-1}.
[d]Uncorrected for background noise (i.e., an equivalent area in a non-absorbing region was not integrated and subtracted to compensate for the contribution of noise in the integration).

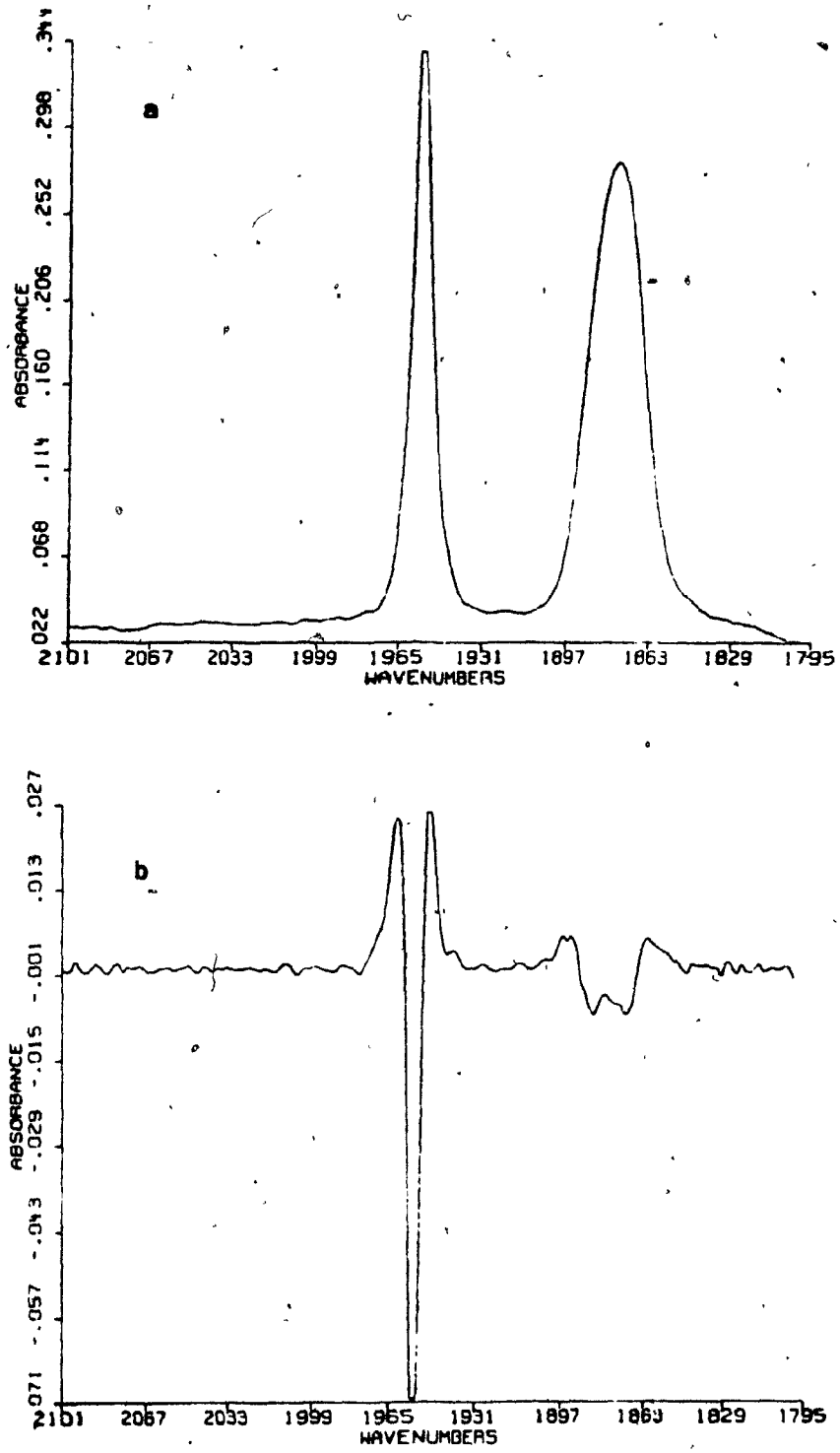

Figure 6.8. The ν(CO) region in the FT-IR spectrum of compound 5 in ethyl acetate (a) and the second derivative of this spectrum (b).

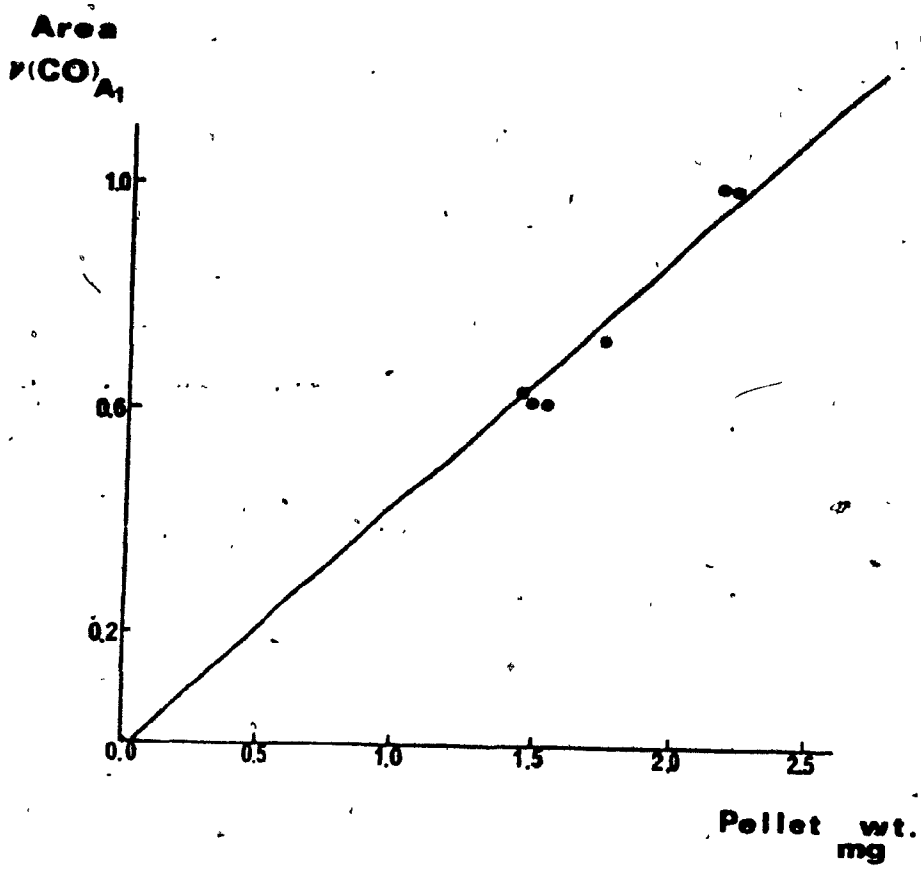

Figure 6.9. Plot of the area under the a_1 ν(CO) mode of the (RO-est)Cr(CO)$_3$ label (compound 5) in the FT-IR spectra of pressed pellets (3-mm diameter) of a protein sample vs. pellet weight.

satisfactory in the range of pellet weights from 1.4 to 2.5 mg ($r = 0.98$). Samples weighing less than 1.4 mg represent insufficient material to form a pellet. For pellet weights greater than 2.5 mg, significant deviations from linearity occurred, indicating self-absorption or a decrease in energy throughput in these thicker pellets. Therefore, although it would be advantageous to use pellets of the maximum thickness possible in order to enhance the intensity of the peaks due to the $Cr(CO)_3$ label, pellet weights under 2.5 mg must be employed for quantitative accuracy.

In order to obtain an approximate value for the amount of $Cr(CO)_3$ label in these pellets, the integrated absorptivity of the a_1 mode of (RO-est)$Cr(CO)_3$ (compound 5) in CsI was calculated from the area under the a_1 ν(CO) mode (A_{int}) as a function of pellet weight according to the following derivation:

$$A_{int} = \int A_\nu d\nu$$

$$= bc \int \varepsilon_\nu \, d\nu$$

where $\int \varepsilon_\nu d\nu$ is the integrated absorptivity = ε_{int}

b = thickness of the pellet

c = wt. of (RO-est)$Cr(CO)_3/\pi r^2 b$, for a pellet of diameter $2r$ and thickness b

This holds true if $r_{beam} > r_{pellet}$; also if $r_{pellet} = r_{beam}$, maximum throughput is achieved with minimum sample weight. The wt. of (RO-est)$Cr(CO)_3$ in the pellet, W_{com}, is given by:

$$W_{com} = C_{com} \times (\text{wt. pellet})$$

where C_{com} is the known concentration by weight of the complex in the CsI matrix and wt. pellet $\simeq$ wt. CsI in pellet. Thus

$$A_{int} = \varepsilon_{int} \times b \times (W_{com}/\pi r^2 b)$$

$$= \varepsilon_{int}/\pi r^2 \times C_{com} \times (\text{wt. pellet})$$

Plotting A_{int} vs. (wt. pellet) gives a slope $= \varepsilon_{int}/\pi r^2 \times C_{com}$.

The measurement of A_{int} (area under the a_1 ν(CO) mode integrated from 1984.0 to 1924.0 cm^{-1}) for various weights (mg) of pellets of (RO-est)$Cr(CO)_3$ in CsI having a concentration

$$C_{com} = 5.54 \times 10^{-4} \text{ g (RO-est)}Cr(CO)_3\text{/g CsI}$$

gave a slope, through least-squares analysis, of 0.541 (r = 0.9999). Thus

$$\varepsilon_{int} = \frac{0.541 \text{ mg}^{-1} \times \pi \times (0.15)^2 \text{ cm}^2}{5.54 \times 10^{-7} \text{ g (RO-est)}Cr(CO)_3\text{/mg CsI}}$$

$$= 6.88 \times 10^4 \text{ cm}^2 \text{ g}^{-1}$$

Using this value, the integrated absorbance expected for the a_1 ν(CO) mode of compound 5 (mol. wt. = 521.47) labelling all the receptor sites in a 2-mg pellet containing 300 fmol mg^{-1} of receptor protein can be estimated as:

$$A_{int} = [6.88 \times 10^4/\pi(0.15)^2] \times (300 \times 10^{-15})(521.47) \times 2$$

$$= 3.04 \times 10^{-4}$$

This estimated integrated absorbance value is significantly lower than that observed for the precipitated proteins labelled with compound 5 (Figure 6.9). This indicates a large degree of high-affinity, non-specific binding in these samples which may be attributed to the initial incubation of the receptor with a high concentration of compound 5 (10^{-6} M) and possibly insufficient washing of the precipitated proteins [11].

Further studies were carried out with compound 12 ([17α-^{3}H]compound 10). The elegant synthesis by Jaouen *et al.* [15] of this doubly labelled complex is illustrated in Figure 6.10. It should be noted that introduction of the ^{3}H label at a carbon too close to the metal resulted in autoradiolysis of the organometallic moiety. FT-IR studies of

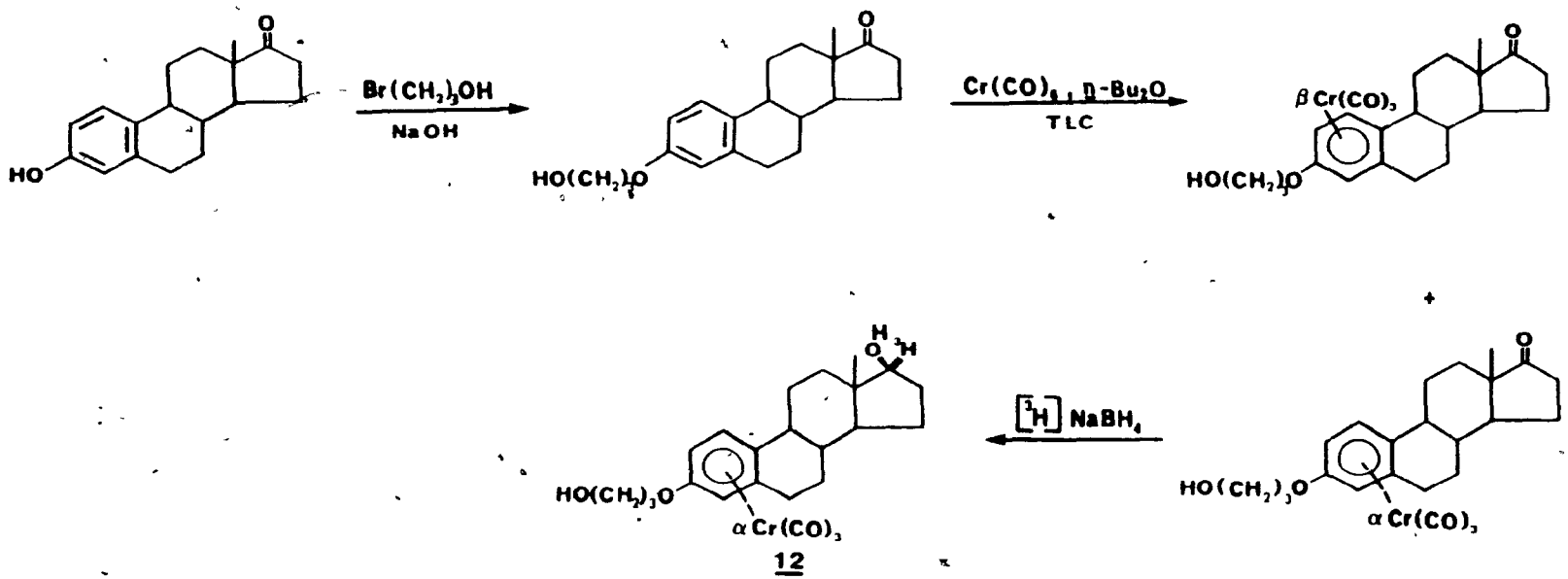

Figure 6.10. Synthesis of compound 12, a tritiated, $Cr(CO)_3$-labelled modified estradiol, as described in Reference 15.

compound 12 indicate that it is quite stable in solution.

Figure 6.11a shows the ν(CO) region of the FT-IR spectrum of a sample obtained by *in vitro* incubation of compound 12 with sheep uterine cytosol at approximately the same concentration ($\approx 10^{-8}$ M) as currently used in radiochemical assays with estradiol itself. The carbonyl intensities in this spectrum are clearly much lower than those observed with compound 5. Although the S/N ratio is high enough to discern definitively the presence of the carbonyl vibrations, the areas of these peaks cannot be measured with quantitative accuracy. The results of a competitive binding assay with free diethylstilbestrol (DES) show that compound 12 is bound specifically and reversibly to the uterine estrogen receptor [15] (Table 6.3). It should be noted that in this sample the level of non-specific binding is significantly lower than that of specific binding, indicating the high degree of specificity of compound 12 for the estrogen receptor. Therefore, the weak carbonyl peaks detected in Figure 6.11a are due in large part to the OLRC.

The reversibility of the binding between compound 12 and the receptor was demonstrated by FT-IR, as well as by radioassay. The spectrum of a sample obtained subsequent to the competitive binding experiment with excess DES was recorded. The carbonyl region of this spectrum (Figure 6.11b) reveals the absence of any peaks due to the OLRC,

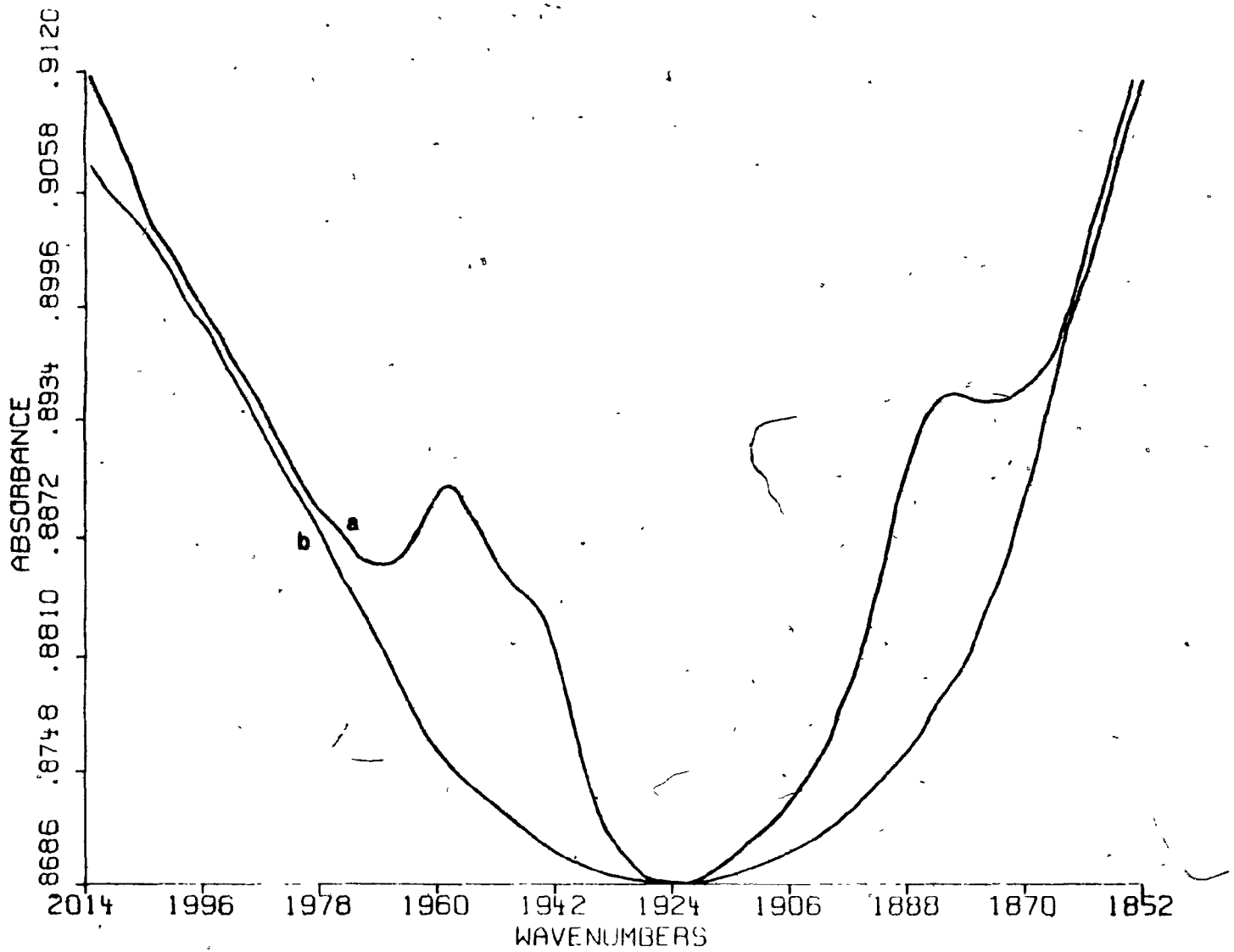

Figure 6.11. FT-IR spectrum (26,000 scans, 4 cm^{-1} resolution) in the ν(CO) region of proteins precipitated from the cytosol of sheep uterus after incubation with (a) compound 12 and (b) compound 12 and a 100-fold excess of diethylstilbestrol in a competitive binding assay.

Table 6.3. Determination of Specific and Non-specific Binding of Compound 12 and Estradiol in Sheep Uterine Cytosol by Radioassay[a]

Ligand	Radioactivity (dpm ml^{-1})			
	Added	Bound without DES	Bound with DES	Specifically bound
Compound 12	46,420	19,472	4,664	14,808 (32%)
[6,7-^{3}H]-17β-estradiol	535,466	166,333	23,080	143,253 (28%)

[a]Results from Reference 15. Portions (500 μl) of sheep uterine cytosol were incubated at 0°C for 6 h with either [6,7-^{3}H]17β-estradiol (4.7 nM; specific activity, 52 Ci $mmol^{-1}$) or compound 12 (6.3 nM; specific activity, 3.3 Ci $mmol^{-1}$). Non-specific binding was determined by using a 100-fold excess of unlabelled diethylstilbestrol (DES). Bound fractions were determined by protamine sulfate precipitation.

because of the binding of DES to the receptor, and also demonstrates the relative insensitivity of the FT-IR measurements at the present time in that the non-specific binding of compound 12 measured by the radioassay was not detected in the FT-IR spectrum.

The measurement of non-specific binding can also be accomplished by deactivating the receptor (usually by heating) and then incubating the denatured receptor with the hormone. The FT-IR spectrum of a sample prepared by thermal deactivation of the receptor protein and subsequent incubation with the organometallic-labelled hormone displayed a carbonyl intensity larger than that of the unheated sample. This situation, however, was also observed radioisotopically [11], indicating that denaturation contributes in these samples to increasing the non-specific binding.

The FT-IR spectra of the organometallic-labelled receptor complex may also be used to elicit some information on the polarity of the receptor binding site. The dependence of ν(CO) frequencies of metal carbonyl complexes on solvent polarity is well established [16]. Table 6.4 shows the shift of the carbonyl peaks of compound 10 to lower frequency as the polarity of the solvent increases. Comparison of these data with the positions of the ν(CO) modes in the protein samples suggests that the carbonyl moiety in the OLRC lies in a polar environment. However,

Table 6.4. ν(CO) Frequencies (cm^{-1}) of (RO-est)$Cr(CO)_3$ (Compound 10) in Solvents of Varying Dielectric Constant (ϵ)

Solvent	ϵ	Solubility[a]	ν(CO) A_1	ν(CO) E	ν(CO) Average
Benzene	2.3	s	1957.7	1879.3	1918.5
Carbon disulfide	2.6	ss	1959.0	1885.3	1922.2
Ethyl acetate	6.0	vs	1957.3	1877.3	1917.3
Tetrahydrofuran	7.3	vs	1955.9	1875.8	1915.8
Acetonitrile	36.2	vs	1954.0	1869.0	1911.5
CsI	-	-	1952.9	1868.4	1910.6

[a]s = soluble; ss = slightly soluble; vs = very soluble.

this does not provide definitive evidence of a polar environment at the receptor binding site since the carbonyl moiety may not be in proximity to the actual binding site. Also, the proteins were precipitated using protamine sulfate which could be a contributing factor to the polarity of the environment. Recent studies have shown that the addition of hydrophobic substituents such as aliphatic chains in the 7α-position of estradiol increases the affinity of the steroid for the receptor binding site [17]. This could be considered as evidence for hydrophobic character of the binding site. However, further studies [17] have shown that addition of aliphatic chains of varying length in the 6α-position brings about a significant decrease in the binding affinity of the steriod, thereby demonstrating the variability in the polarity of the receptor binding site.

The FT-IR measurements reported here have shown that FT-IR spectroscopy can provide qualitative information on hormone-receptor binding and has the potential to serve as a technique for quantitative determination of receptor concentration. However, the very weak intensities of the carbonyl peaks in Figure 6.11a, obtained from a sample in which there is a higher level of specific binding than of non-specific binding, indicate that receptor assay by FT-IR spectroscopy is not as yet feasible. The transformation of this technique from the qualitative to the quantitative realm will

require enhanced sensitivity of the FT-IR spectrometer in the carbonyl region of the spectrum. Possible instrumental modifications that may achieve such enhancement include the use of more sensitive detectors and larger collection mirrors after the sample. The FT-IR spectrometer can be interfaced with a variety of specialized detectors. Room temperature (triglyceride sulfate, TGS) detectors are not suited for fast-scanning spectrometers working in the mid-IR region because of their slow response time. Mercury cadmium telluride (MCT) detectors give a much faster response time and are well suited for the mid-IR region, the faster response time significantly decreasing data acquistion times. The MCT detectors are made of an alloy of HgTe and CdTe, and their spectral response is a function of both specific alloy composition and operating temperature. These detectors operate in the 5000-750 cm^{-1} (MCT A), 5000-400 cm^{-1} (MCT B) and 5000-300 cm^{-1} (MCT C) regions with a typical operating temperature range of 77-295 K. The detector used for obtaining the protein spectra in this study was the MCT B detector operating at 77K. Figure 6.12 illustrates the relative sensitivity of the different detectors commercially available over the mid-IR range. It can be seen that the InSb detector has its maximum sensitivity in the metal carbonyl region (2200-1850 cm^{-1}) and is about an order of magnitude more sensitive in this region than the MCT A

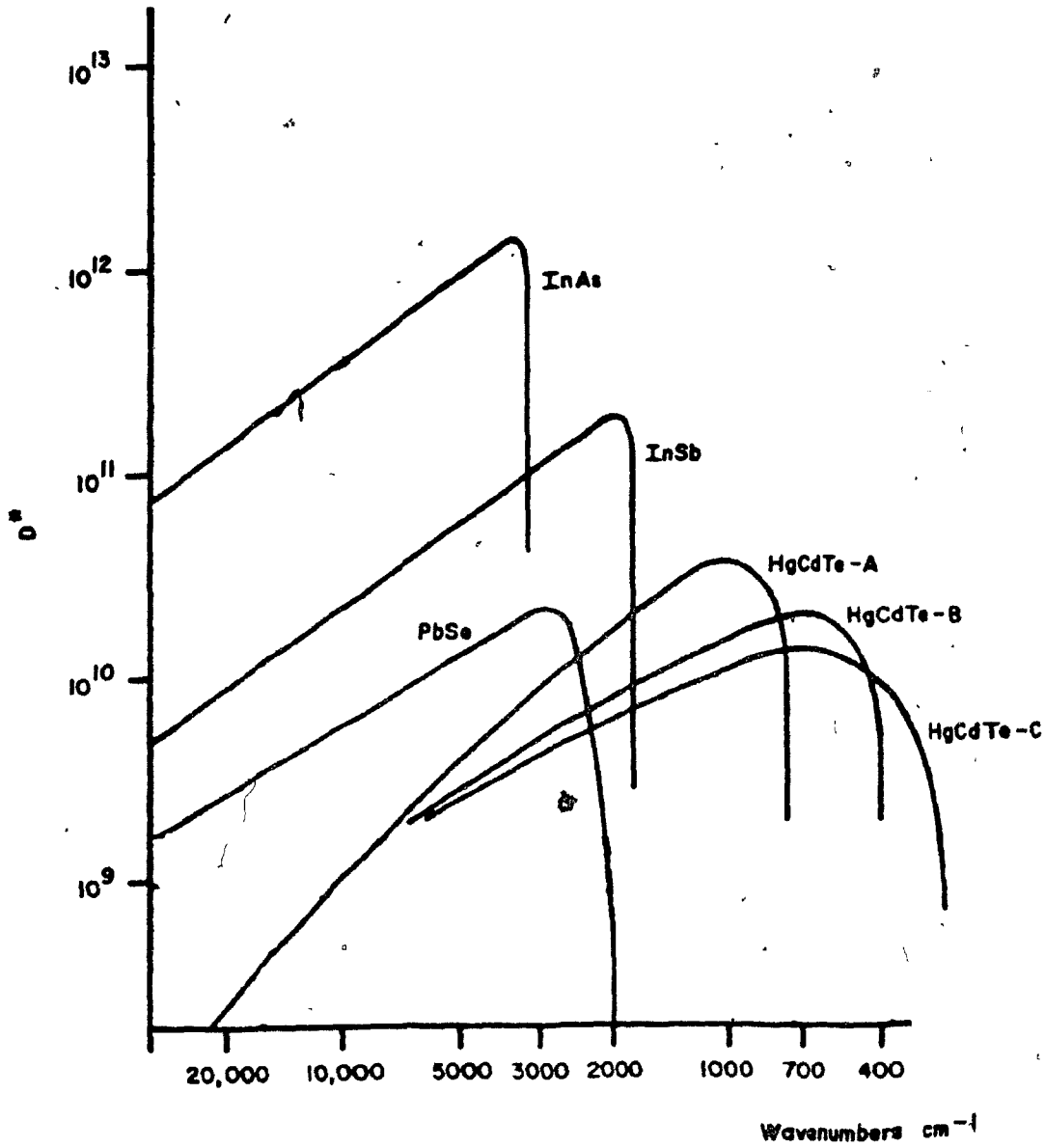

Figure 6.12. Detectors utilized in FT-IR spectrometers and their sensitivity as a function of energy. Adapted from FT-IR documentation supplied by Nicolet Instruments Corporation, Madison, Wisconsin, U.S.A.

detector and approximately forty times more sensitive than the MCT B detector used in this study. Clearly the InSb detector is the detector of choice for further research on the use of metal carbonyl labels in receptor assay. Other recommendations include directly placing the pellet onto the detector, which would reduce energy loss due to scattering. Alternatively, scattered energy could be captured and refocused by using a larger collection mirror to intercept a wider cone of diffusely scattered radiation [18].

6.4 Concluding Remarks

In the present work, it has been shown that FT-IR spectroscopy can detect very low concentrations of metal carbonyl-labelled modified estradiol in protein samples extracted from biological tissue. FT-IR spectroscopy can also in principle be used to calculate the concentration of estradiol-receptor complex in such samples providing that the extinction coefficient for the metal carbonyl peaks in the OLRC can be determined. Thus the combined efforts of judiciously labelling a hormone with an organometallic moiety and subsequent detection of the label by FT-IR spectroscopy yield a novel method for receptor assay which is both non-destructive and possesses none of the drawbacks of radioisotopic techniques. However, the development of this

technique is in its early stages. In order for it to become viable in clinical use, a minimum of two orders of magnitude increase in the sensitivity of the FT-IR measurements must be achieved. Current work in this area is also being focused on the synthesis of hormone-labelled metal carbonyl cluster complexes [11], which should yield higher integrated ν(CO) absorptivities.

References

1. Chemical and Engineering News, 62(46), 24 (1984).
2. M. Cais, S. Dani, Y. Eden, O. Gandolfi, M. Horn, E.E. Isaacs, Y. Josephy, Y. Saar, E. Slovin and L. Snarsky, Nature, 270, 534 (1977).
3. E.V. Jensen and E.R. DeSombre, Science, 182, 126 (1973).
4. R.B.J. King and G.L. Greene, Nature, 307, 745 (1984).
5. W.V. Welshons, M.E. Lieberman and J. Gorski, Nature, 307, 747 (1984).
6. J.A. Katzenellenbogen, D.F. Heiman, K.E. Carlson and J.E. Lloyd, in "Receptor-Binding Radiotracers", Vol. I, W.C. Eckelman, ed., CRC Press, Boca Raton, Florida, 1982, pp.93-126 and references therein.
7. See, for example, C.J.L.M. Meijer, J. van Marle, J.P. Persijn, W. van Niewenhuizen, J.P.A. Baak, M.E. Boon and J. Lindeman, Virchows Arch., 40, 27 (1982).
8. A. Nakamura and M. Tsutsui, Z. Naturforsch., 18, 666 (1963).
9. G. Pouskouleli, I.S. Butler and J. Hickey, J. Inorg. Nucl. Chem., 42, 1659 (1980); G. Pouskouleli, Ph.D. thesis, McGill University, Montreal, Quebec, Canada, 1981.
10. G. Jaouen, A. Vessières, S. Top, A.A. Ismail and I.S. Butler, C.R. Acad. Sci. Paris, 298, 683 (1984).

11. G. Jaouen and A. Vessières, unpublished results.

12. M.L. Thieulant, S. Samperez and P. Jouan, Endocrinolgy, 108, 1552 (1981).

13. P.R. Griffiths, "Chemical Infrared Fourier Transform Spectroscopy", J. Wiley and Sons, New York, 1975.

14. M.R. Whitbeck, Appl. Spectrosc., 35, 93 (1981).

15. G. Jaouen, A. Vessières, S. Top, A.A. Ismail and I.S. Butler, J. Am. Chem. Soc., in press (1985).

16. D.A. Brown and F.J. Hughes, J. Chem. Soc. (A), 1519 (1968).

17. J.P. Abjean, Thèse 3ième cycle, Rennes, 1983.

18. M. Friedman and J.L. Freeman, Appl. Spectrosc., 38, 700 (1984).

Chapter 7

Investigation of Chalcocarbonyl(5,10,15,20-tetraphenylporphinato)iron(II) Derivatives by FT-IR Spectroscopy

7.1 Introduction

Many metal-porphyrin derivatives have been synthesized as model compounds for the study of the binding of oxygen and other small diatomic molecules to hemoglobin and myoglobin, as well as to further the understanding of the detoxification mechanisms of porphyrin-containing cytochrome P-450 [1]. Among these porphyrin derivatives, (5,10,15,20-tetraphenylporphinato)iron(II) (FeTPP)‡ is often used because of its stability and convenient synthesis [2,3]. The structure of FeTPP is shown in Figure 7.1. Four nitrogens bind the iron in the equatorial plane through σ-donation, and two ligands can be introduced at the axial positions to complete a pseudo-octahedral structure. The bonding between the iron and the porphyrin also involves π-donation from the filled metal dπ orbitals to the vacant π* orbitals delocalized over the porphyrin ring. The extent of the π-back-bonding component of the metal-porphyrin interaction varies with the π-accepting properties of the axial ligands. FeTPP

‡Unless otherwise stated, FeTPP in the various complexes discussed in this section will represent low-spin Fe(II).

(a)

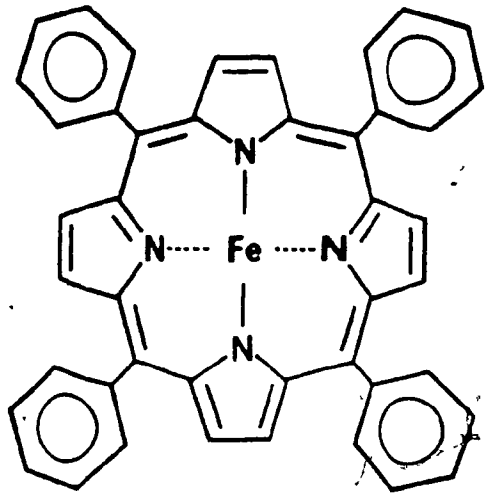

(b)

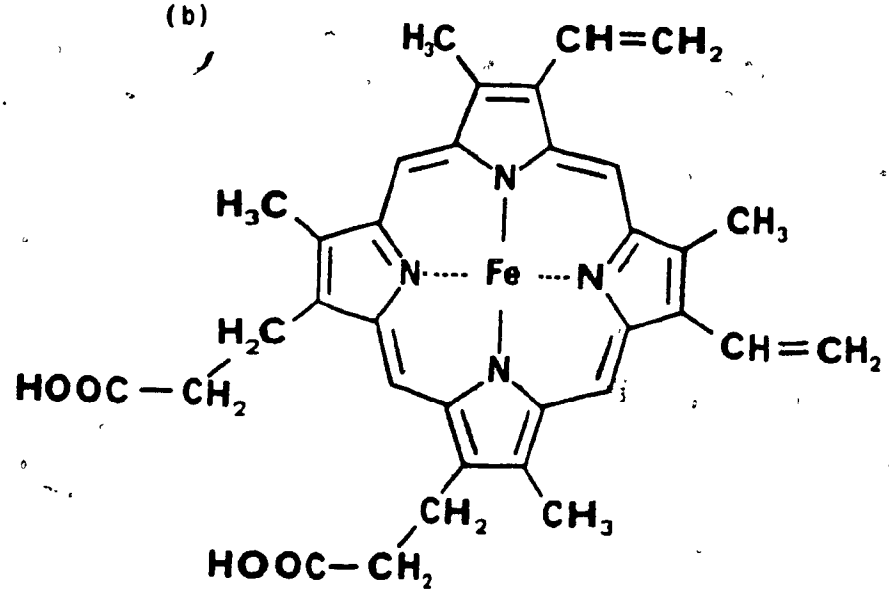

Figure 7.1. Structure of (a) iron tetraphenylporphyrin and (b) protoporphyrin IX.

differs from the naturally occurring protoporphyrin IX found in hemoglobin or myoglobin in that four phenyl groups are introduced at the meso carbons and hydrogens at the β carbons, while in hemoglobin the meso carbons are hydrogen substituted and the β positions have propionic acid, ethylenic or methyl group substituents (Figure 7.1).

Complexes of the form FeTPP(CO)L with axially bound CO trans to various ligands L (e.g., py, EtOH, Im, MeIm) are well-known synthetic models for the study of the binding of CO to hemoglobin [4]. Recently, a series of analogous complexes in which the CO ligand is replaced by a thiocarbonyl or selenocarbonyl ligand have been prepared [5-7]. In addition, the pentacoordinated species FeTPP(CX) (X = S, Se) have been obtained [6,7]. Although other metalloporphyrin complexes containing a CS ligand have been synthesized [8], FeTPP(CSe) and Fe(TPP)(CSe)L (L = py, EtOH, MeIm) represent the only examples of the incorporation of a CSe group into a metalloporphyrin system. The bonding properties of both the CS and CSe ligands have been reviewed elsewhere [9] and the stronger σ-donor and π-acceptor capabilities of CS and CSe relative to CO, giving rise to a stronger bonding to low-oxidation state metals, have been emphasized in this thesis. The CS and CSe ligands may also act as π-donors [10] and a greater flexibility in the bonding properties of these ligands relative to those of CO has been demonstrated [11].

The effect of these differences between the CS and CSe ligands, on the one hand, and CO, on the other, in the porphyrin complexes studied here is manifested by the stability of FeTPP(CX) (X = S, Se) whereas the corresponding FeTPP(CO) derivative is only stable under partial CO pressure [12]. The thio- and selenocarbonyl complexes can be heated up to 150°C under vacuum without decomposition [6]. The strength of the Fe-C(X) (X = S, Se) bond is dramatically demonstrated by the stability of the thiocarbonyl and selenocarbonyl complexes towards oxidation in aerated benzene - the half-life of FeTPP(CO)(py) is ~5 min [5] while the corresponding selenocarbonyl complex is stable for hours [7], and FeTPP(CS)(py) or FeTPP(CS) is stable to oxidation even after oxygen has been bubbled through the solution for 20 h [5]. The remarkable strength of the Fe-C(S) bond is also indicated by the two-electron oxidation of FeTPP(CS), without loss of the CS ligand, to form $Fe(III)TPP(CS)^+$ whereas FeTPP(CO) loses CO during the removal of the first electron [13].

The general synthetic route to the thiocarbonyl or selenocarbonyl FeTPP complexes involves a relatively easy procedure: Fe(III)TPPCl is stirred in benzene under argon in the presence of Fe powder to form Fe^0TPP; the subsequent addition of $PhCH_2SCCl_3$ or $PhCH_2SeCCl_3$ affords FeTPP(CS) [6] or FeTPP(CSe) [7], respectively, in very high yields (≥80%).

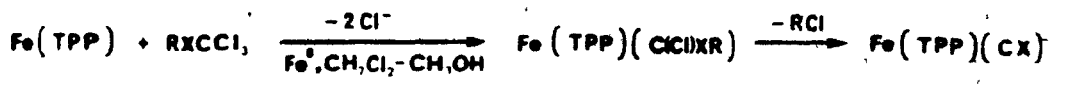

(7.1)

The above reaction is of great interest since various compounds of the formula $RSCCl_3$ exhibit fungicidal activity [e.g., Folpet (a) and Captan (b)]. Their toxicity has been postulated to stem from the generation of free radicals $RSCCl_2^{\bullet}$ (which irreversibly attach to the macromolecules of the cell) during the reduction of $RSCCl_3$ by cytochrome P-450 and subsequent formation of P-450-Fe(II)←C(Cl)SR and P-450-Fe(II)←CS [6].

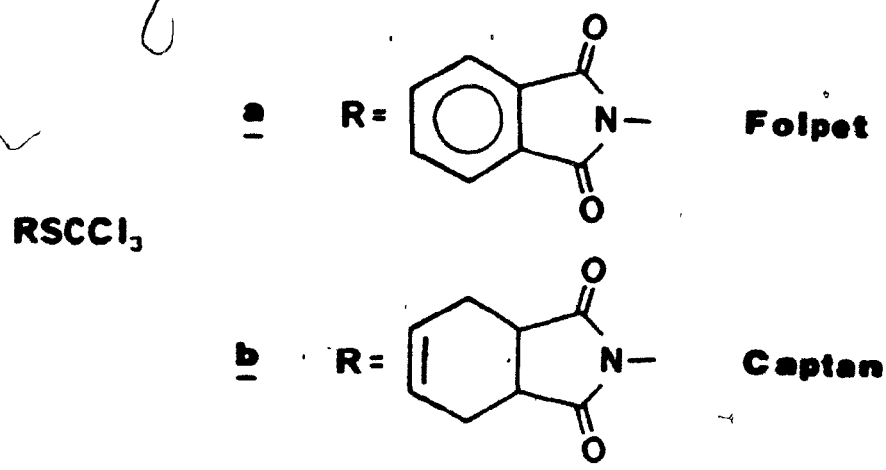

The effects on metalloporphyrins of substituents on the porphyrin ring and of axially bound ligands have been studied by a variety of spectroscopic techniques [14,15]. The use of IR spectroscopy has been fairly limited, presumably due to the complexity of the porphyrin spectra. The IR spectra of tetraphenylporphyrin and several tetraphenylpor-

phyrin metal complexes have been reported and partially assigned by Alben et al. [16,17]. The metal-nitrogen stretching vibrations of such complexes, appearing in the far-IR spectra, have also been assigned [18]. In a recent study of the IR spectra of a series of iron tetraphenylporphyrin complexes [19], bands sensitive to spin state and oxidation state were identified. In this chapter, the results of a study of the FT-IR spectra of FeTPP(CX) (X = S, Se) and FeTPP(CX)L (X = S, Se; L = py, EtOH) will be presented. This investigation was undertaken in order to examine the perturbations induced by the axially bound ligands on the metal-porphyrin interactions.

7.2 Experimental

7.2.1 Sources of Materials

Fe(III)TPPCl was purchased from Strem Chemicals. Samples of FeTPP(CX)L (X = S, Se; L = EtOH, py) were obtained from Drs. J.P. Battioni and D. Mansuy (Laboratoire de chimie de L'Ecole Normale Supérieure, Paris, France) or were synthesized utilizing the procedure given in References 6 and 7; the reagents $PhCH_2XCCl_3$ (X = S, Se) were also obtained from Drs. Battioni and Mansuy. FeTPP(CX) (X = S, Se) complexes were prepared by heating FeTPP(CX)(EtOH) at 160°C for 4 h, as described in Reference 6. FeTPP(CO)-

(py) was synthesized according to the literature procedure [4]. CsI (99.999%) was obtained from Aldrich Chemical Co.

7.2.2 Spectroscopic Measurements

The IR spectra of all FeTPP derivatives were recorded for samples pressed into CsI pellets, which were prepared in an argon-purged glove bag. FT-IR spectra were obtained on a Nicolet 6000 Fourier-transform infrared spectrometer (resolution 0.5 cm^{-1}). ^{13}C NMR spectra were measured on a Varian XL-200 spectrometer equipped with a broad-band probe. The chemical shifts reported are relative to TMS.

7.2.3 Reaction of FeTPP(CX) (X = S, Se) with CO

FeTPP(CX) (X = S, Se) (20 mg) was dissolved in deaerated spectrograde benzene (10 ml) under argon. The solution was transferred to the high-pressure apparatus described previously (Section 3.2.1) and degassed in three freeze-thaw cycles. The reaction compartment was then pressurized with CO (20 atm). After periods of 6-24 h the CO gas was removed by adsorption on charcoal in a second compartment. The FT-IR spectrum of the solution did not exhibit any peaks in the carbonyl region.

7.3 Results and Discussion

FeTPP(CO)L complexes are quite unstable with a half-life in aerated solution of the order of minutes [5]. The pentacoordinated complex, FeTPP(CO), decomposes virtually instantly on exposure to air [12]. In contrast, the compounds described here are remarkably stable; their half-life in solution is of the order of hours [FeTPP(CX)L] or days [FeTPP(CX)] (X = S, Se; L = py, EtOH) [5-7]. The pentacoordinated FeTPP(CX) (X = S, Se) species are stable in air for years in the solid state. The difference in stability between these complexes and their carbonyl analogues within the above series indicates a decreasing susceptibility of the metal toward oxidation and accordingly decreasing electron density at the metal in the order CO > CSe ≃ CS. This trend may be interpreted in terms of a greater extent of π-back-donation from the metal to the CS or CSe ligand than to CO [20].

The FT-IR spectra of these complexes were obtained to assess the effects of the differences in the bonding properties of the ligands on the metal-porphyrin interaction. The spectra of the porphyrin derivatives studied are shown in Figures 7.2-7.9, and the positions of the major peaks, together with assignments adopted from Alben *et al.* [16,-17], are listed in Table 7.1. The first row of this table

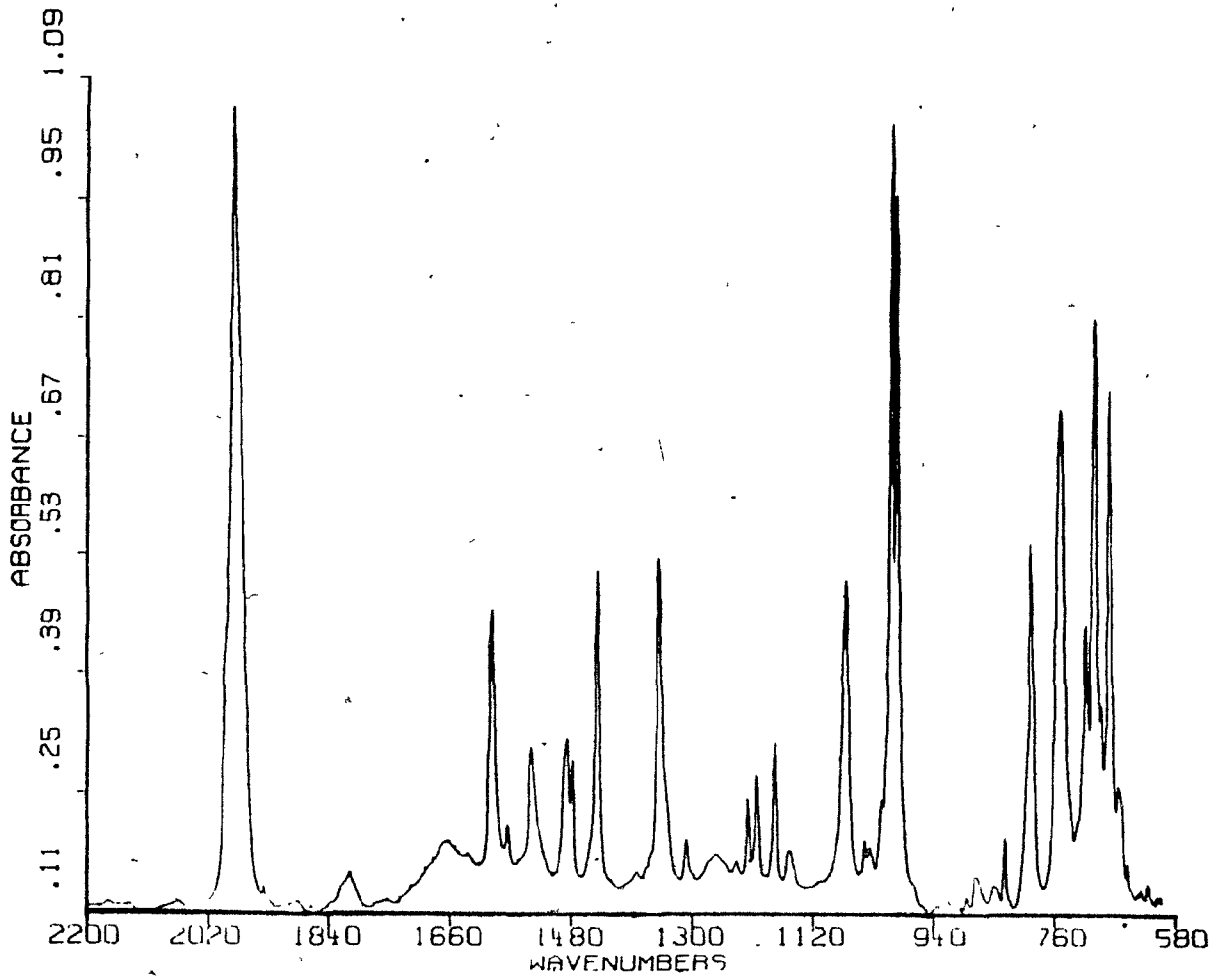

Figure 7.2. FT-IR spectrum in the 2200-600 cm^{-1} region of FeTPP(CO)(py) (CsI pellet; 200 scans; 0.5 cm^{-1} resolution).

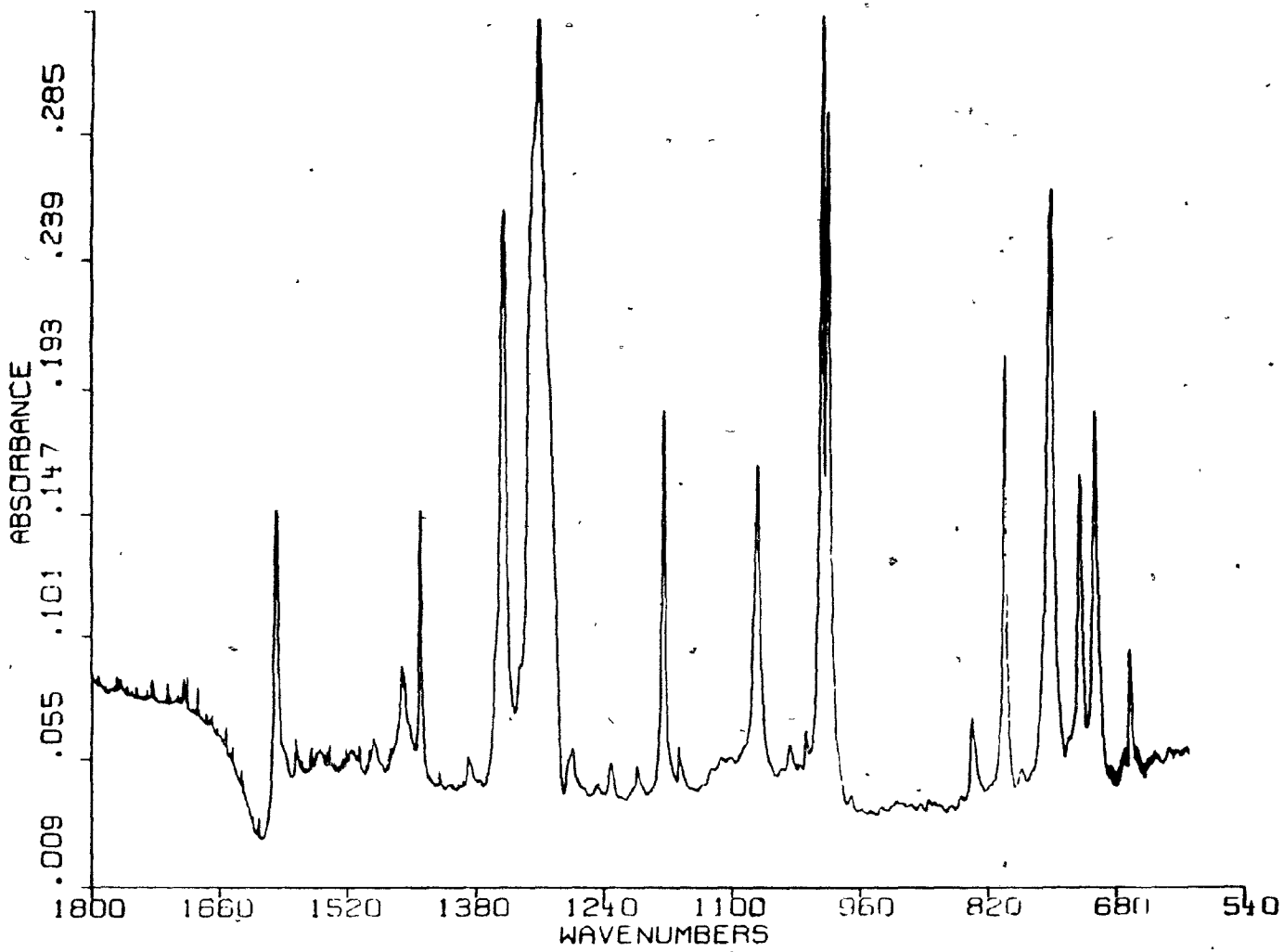

Figure 7.3. FT-IR spectrum in the 1800-600 cm^{-1} region of FeTPP(CS) (CsI pellet; 200 scans; 0.5 cm^{-1} resolution).

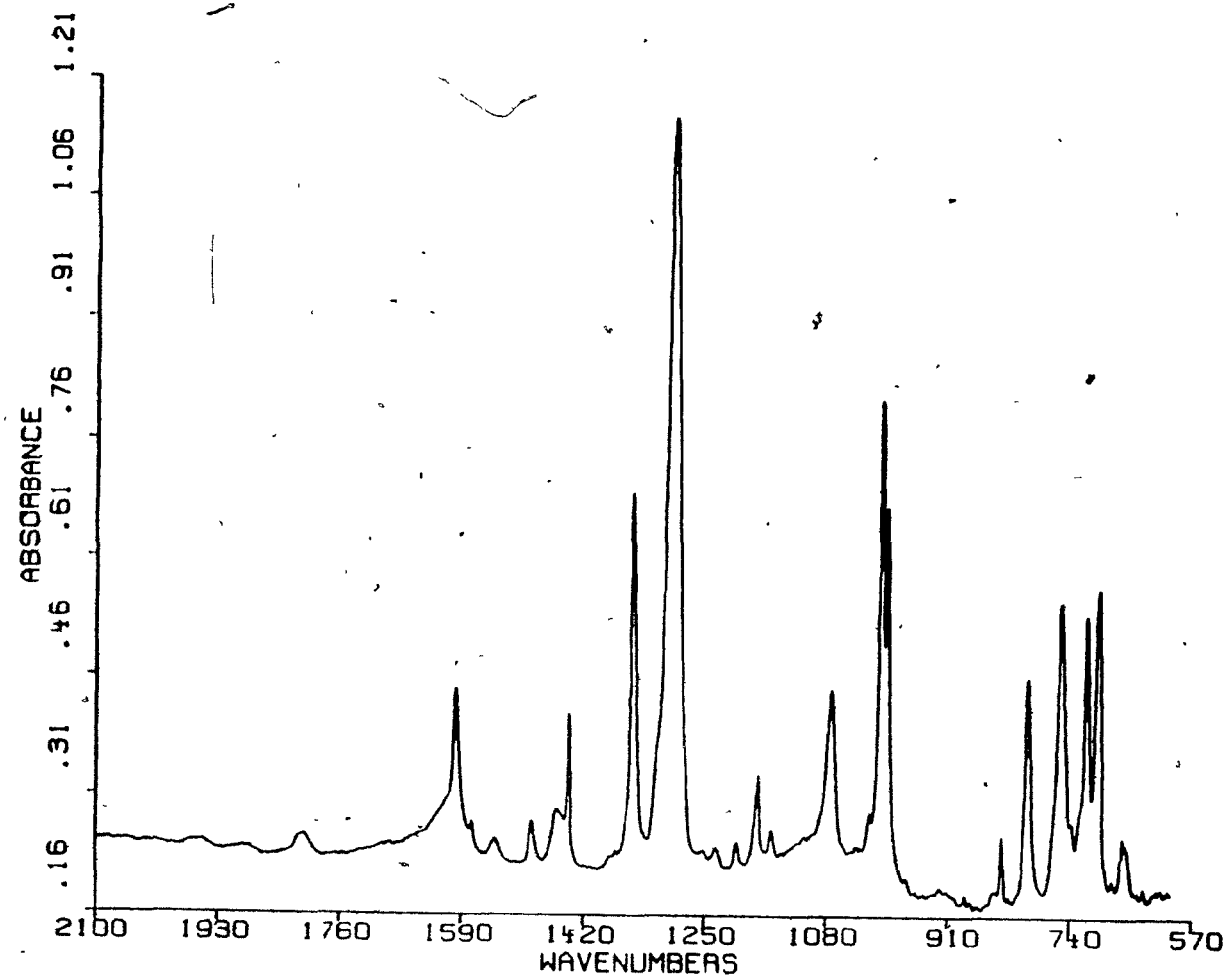

Figure 7.4. FT-IR spectrum in the 2100-600 cm^{-1} region of FeTPP(CS)(EtOH) (CsI pellet; 200 scans; 0.5 cm^{-1} resolution).

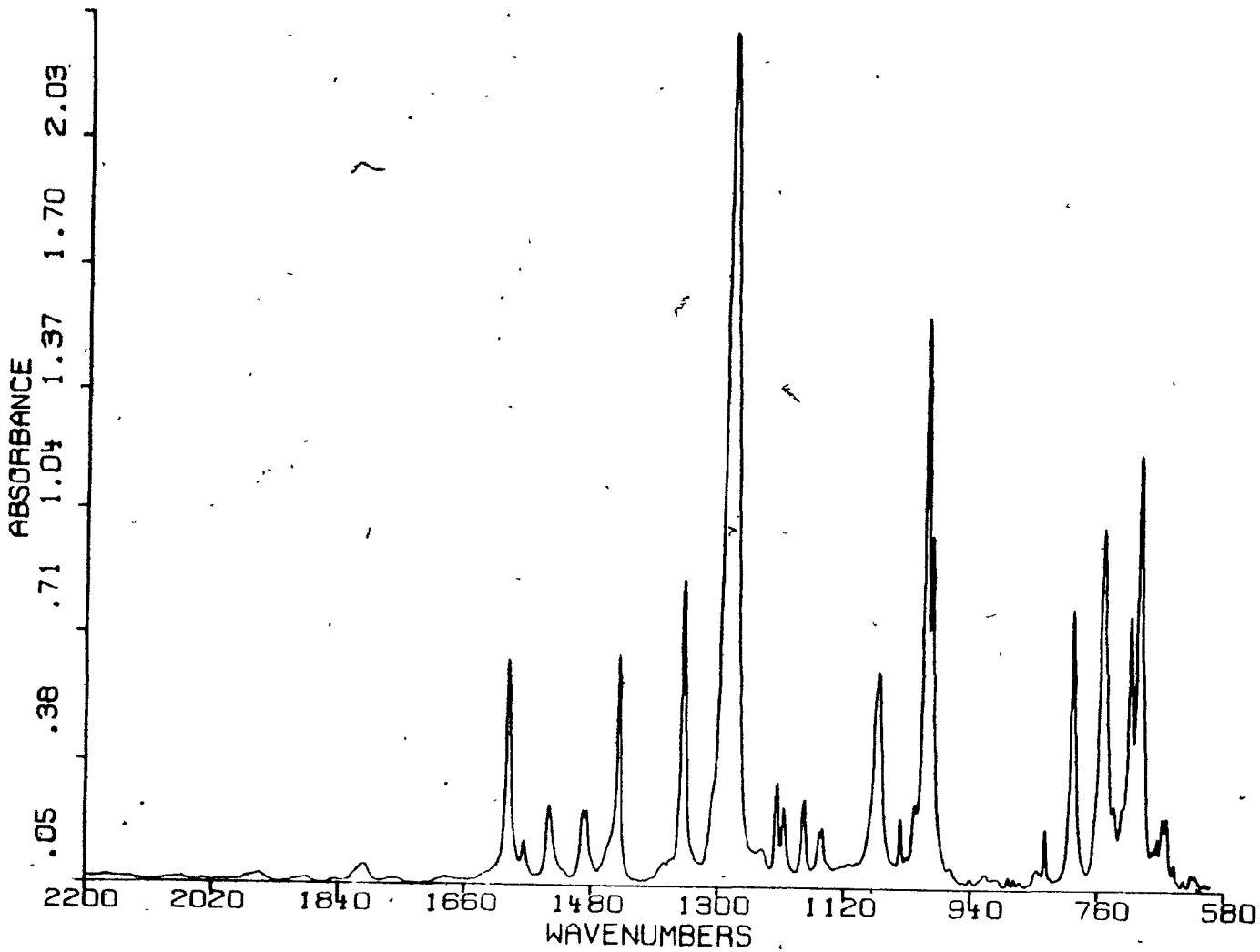

Figure 7.5. FT-IR spectrum in the 2200-600 cm^{-1} region of FeTPP(CS)(py) (CsI pellet; 200 scans; 0.5 cm^{-1} resolution).

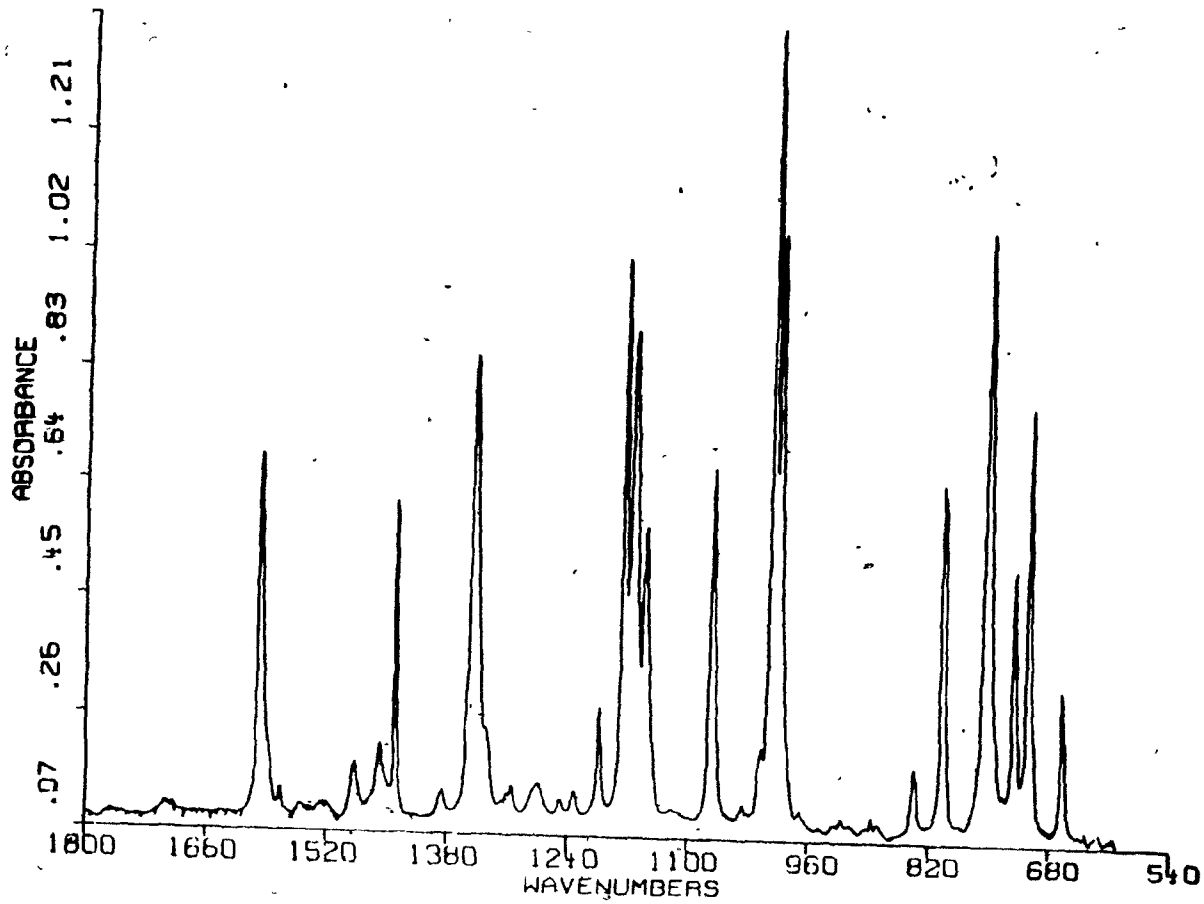

Figure 7.6. FT-IR spectrum in the 1800-600 cm^{-1} region of FeTPP(CSe) (CsI pellet; 200 scans; 0.5 cm^{-1} resolution).

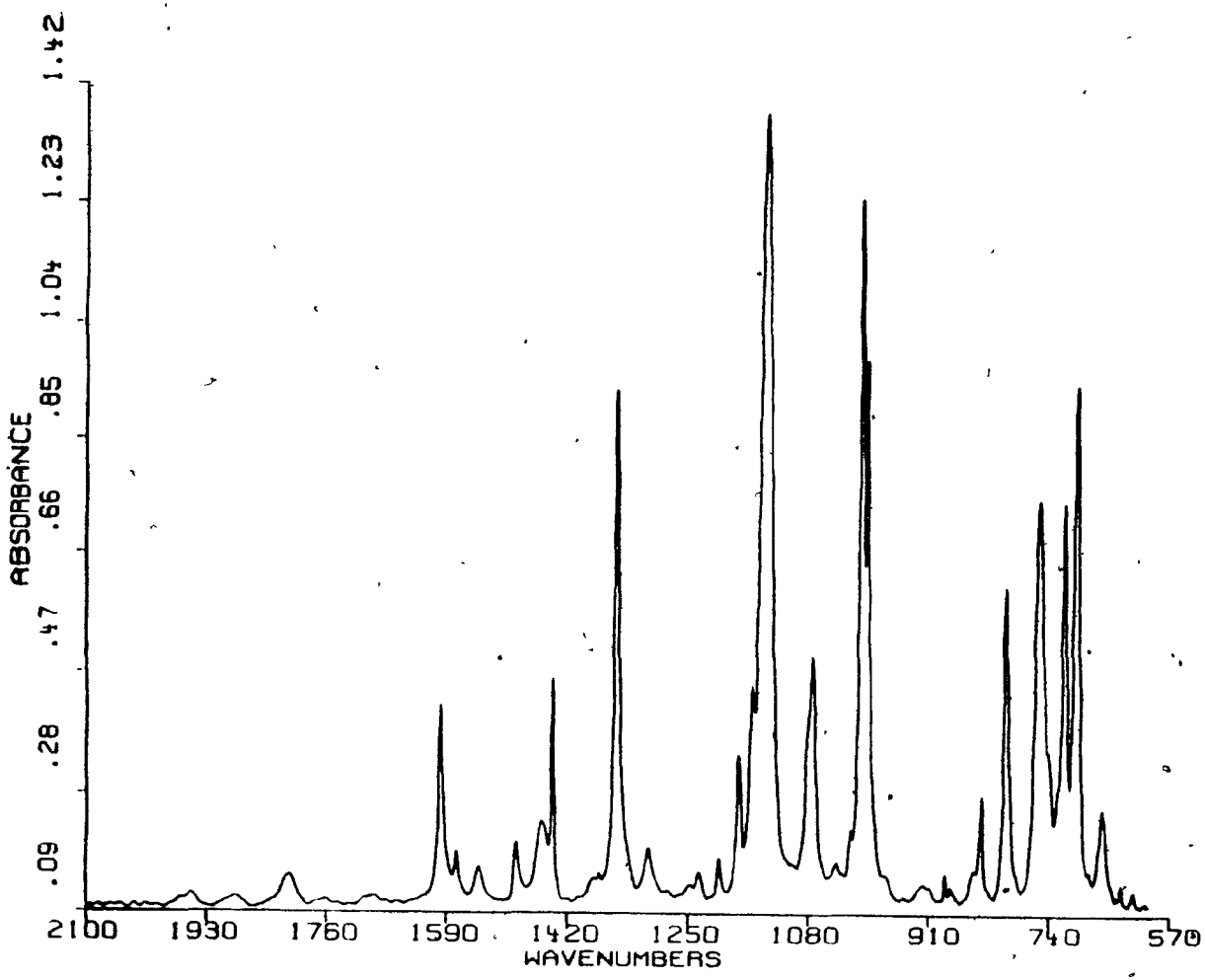

Figure 7.7. FT-IR spectrum in the 2100-600 cm^{-1} region of FeTPP(CSe)(EtOH) (CsI pellet; 200 scans; 0.5 cm^{-1} resolution).

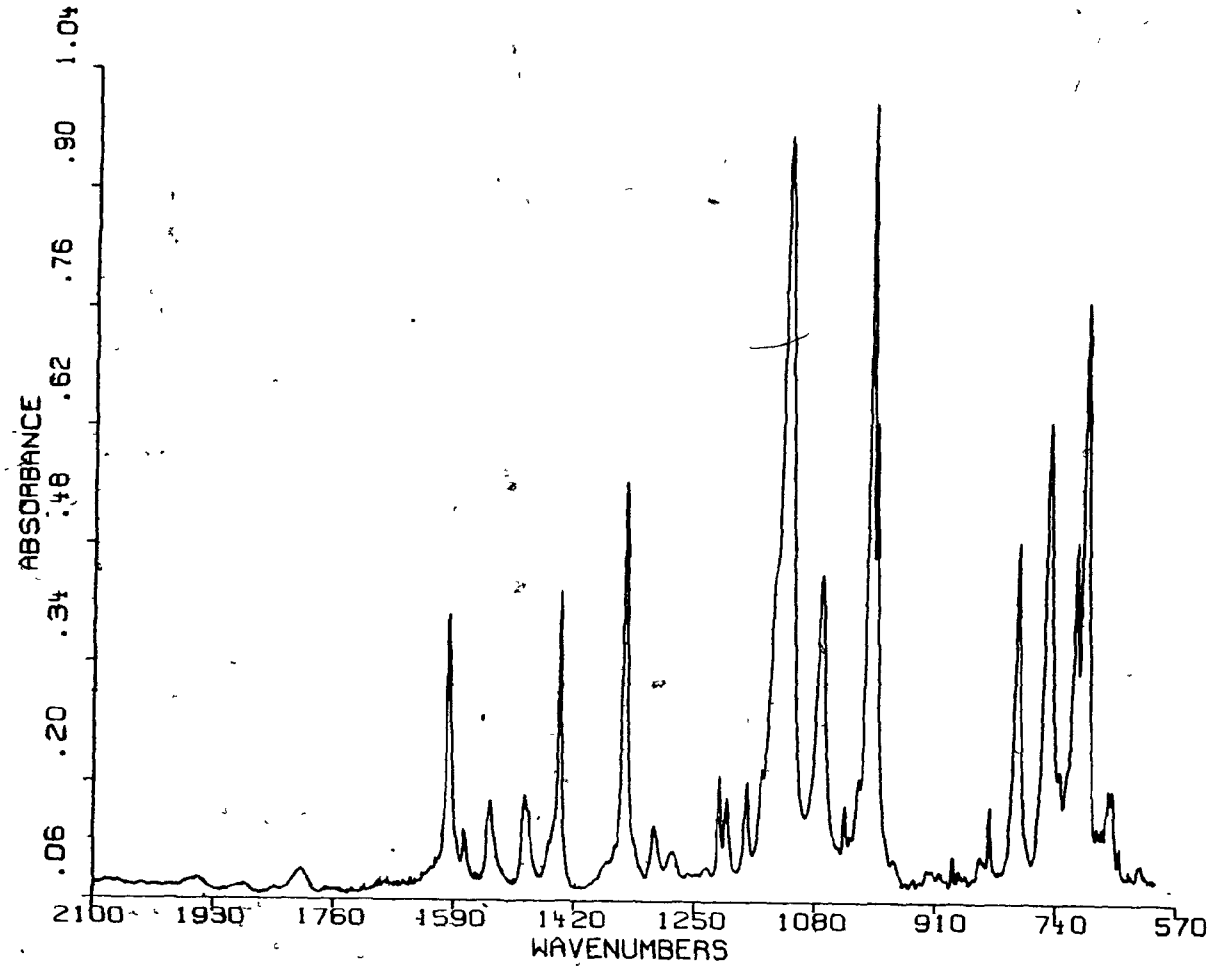

Figure 7.8. FT-IR spectrum in the 2100-600 cm^{-1} region of FeTPP(CSe)(py) (CsI pellet; 200 scans; 0.5 cm^{-1} resolution).

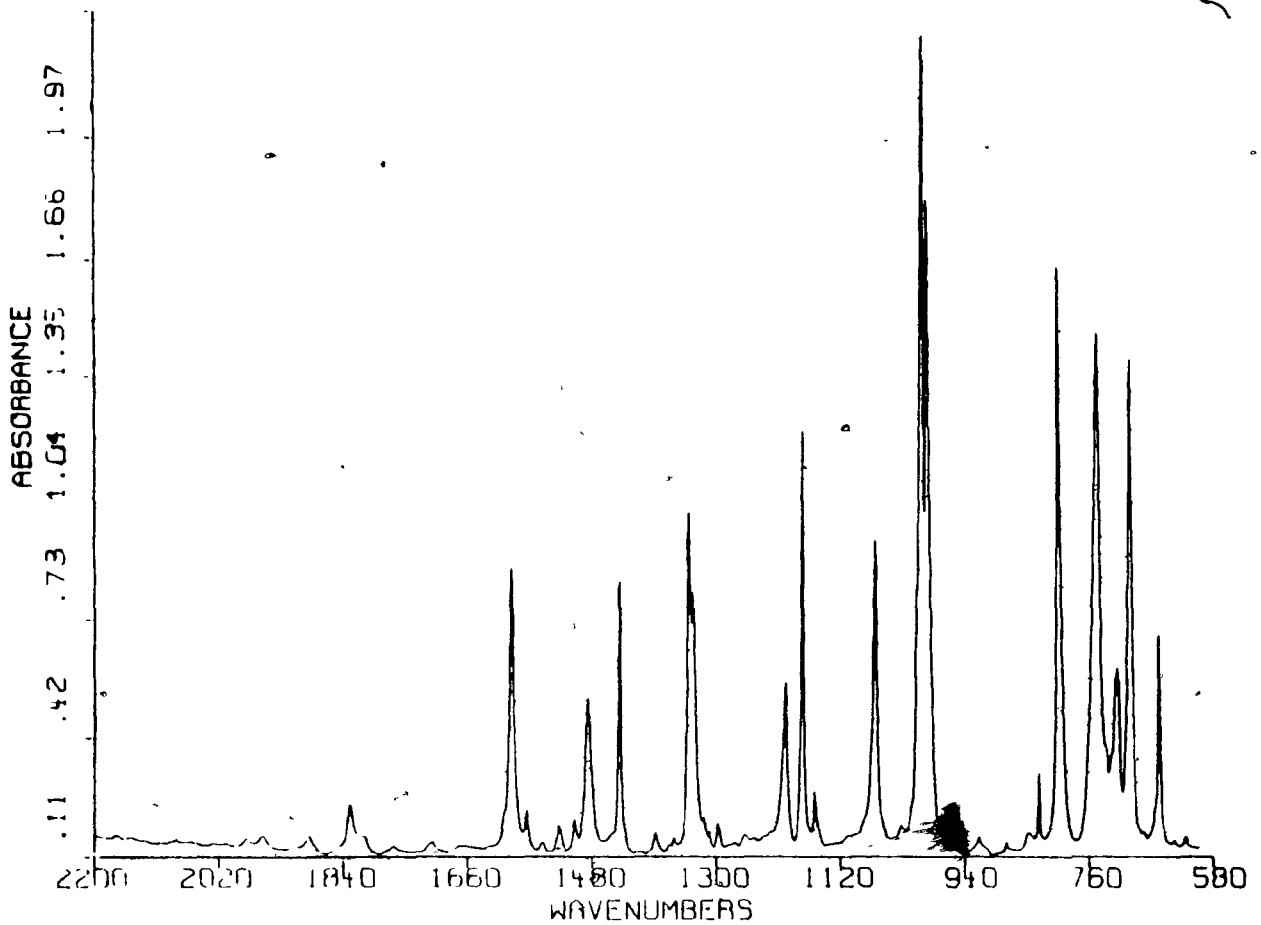

Figure 7.9. FT-IR spectrum in the 2200-600 cm^{-1} region of Fe(III)TPPCl (CsI pellet; 200 scans; 0.5 cm^{-1} resolution).

Table 7.1. Selected Frequencies (cm^{-1}) from the FT-IR Spectra of FeTPP(CX) and FeTPP(CX)(L) Derivatives and Fe(III)TPPCl

CX	CO	CS	CS	CS	CSe	CSe	CSe	-
L	py	-	EtOH	py	-	EtOH	py	Cl
Oxidation state	II	II	II	II	II	II	II	III
Spin	0	0	0	0	0	0	0	5/2
ν(CX)	1983.6	1312.4	1294.1	1282.7	1164.7	1137.9	1121.6	-
Aromatic ring vibrations[a]	1598.4	1598.6	1598.8	1598.8	1598.2	1598.8	1598.6	1596.9
	1441.1	1440.6	1440.7	1440.9	1440.6	1440.5	1440.8	1440.3
Spin state marker[b]	1349.9	1350.8	1350.4	1350.0	1350.3	1350.0	1350.0	1340.2 1334.1
Split in $TPPH_2$[a]	1176.3	1175.0	1175.7	1176.2	1175.5	1176.7	1176.9	1175.1
Unassigned	1071.2	1072.4	1072.6	1072.3	1072.3	1072.5	1072.1	1069.7
Porphyrin ring vibration[a]	1002.4	1001.2	1003.1	1003.7	1001.6	1002.9	1004.0	1002.2

Table 7.1. (Cont'd)

CX	CO	CS	CS	CS	CSe	CSe	CSe	-
L	py	-	EtOH	py	-	EtOH	py	Cl
Found at 1002 in $TPPH_2$[a]	995.3	995.3	995.7	996.4	995.5	995.7	996.5	995.5
β-pyrrole out-of-plane C-H deformation[a]	796.9	802.6	799.8	795.2	802.6	799.4	795.3	806.5
Split in $TPPH_2$[a]	752.7	753.2	753.5	752.3	752.7	752.7	752.5	750.5
Porphyrin ring deformation (split in $TPPH_2$)[a]	714.9	720.7	717.8	713.9	720.5	717.2	713.7	720.3
Unassigned	701.3	704.3	702.1	701.0	703.9	701.4	700.7	703.4

[a]See Reference 16.
[b]See Reference 19.

lists the ν(CX) vibrations, while the remaining frequencies correspond to peaks characteristic of the FeTPP moiety.

Difference spectra represent the simplest method of establishing empirically any perturbations induced by the axial ligands on the porphyrin ring vibrations. In order to illustrate the utility of difference spectra in assessing changes in metal-porphyrin bonding, the spectrum obtained by subtracting the spectrum of Fe(III)TPPCl from that of FeTPP(CSe)(EtOH) is presented in Figure 7.10. The features in this spectrum are the result of a number of factors: the different oxidation and spin states of the iron atom in the two complexes; the lower symmetry of Fe(III)TPPCl due to ring puckering [21]; and the absence of axial π-backbonding in the chloride complex.

The difference spectrum obtained by the subtraction of the spectrum of FeTPP(CS)(py) from that of FeTPP(CSe)(py) is shown in Figure 7.11. The elimination of all porphyrin vibrations in the difference spectrum indicates that the interactions of the CS and CSe ligands with the metal in these systems are similar. Specifically, the comparable extent of metal dπ → CX π* backbonding in these complexes is demonstrated by this result in that the availability of metal dπ electron density for donation to the π* orbitals of the porphyrin is a function of the amount of dπ electron density transferred to the axial ligands [20]. Therefore,

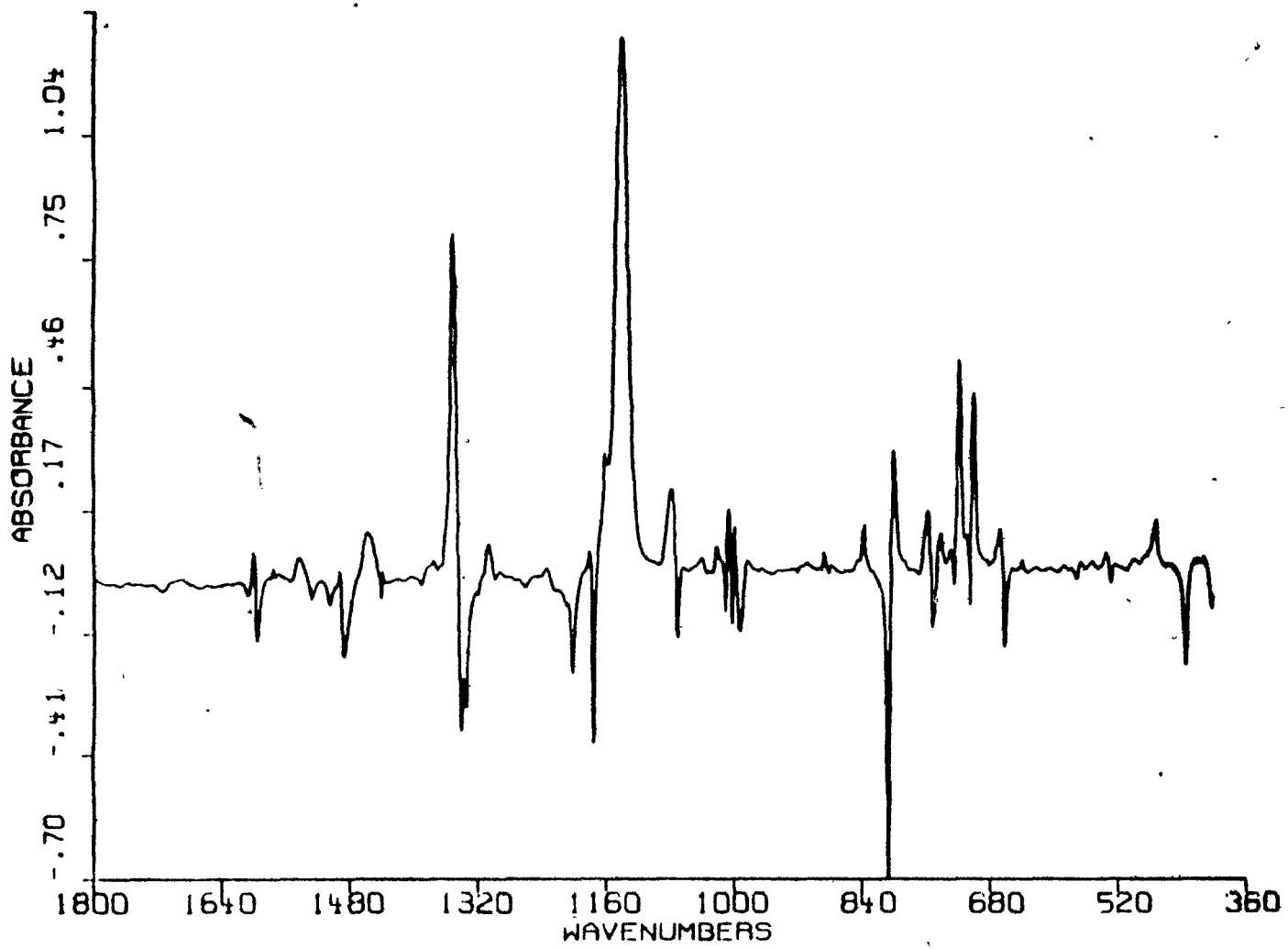

Figure 7.10. Difference spectrum obtained by the subtraction of the FT-IR spectrum of Fe(III)TPPCl from that of FeTPP(CSe)(EtOH).

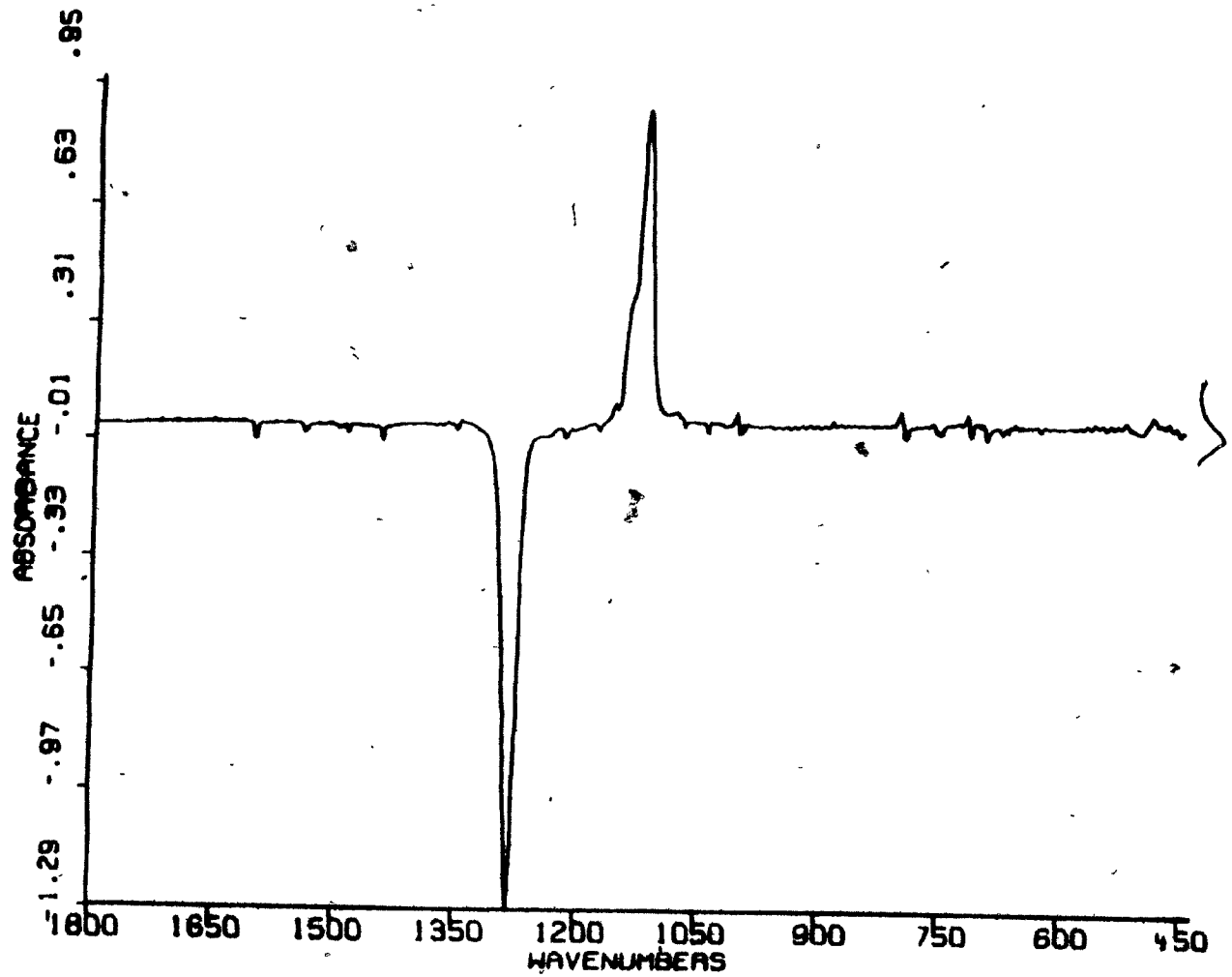

Figure 7.11. Difference spectrum obtained by the subtraction of the FT-IR spectrum of FeTPP(CS)(py) from that of FeTPP(CSe)(py).

any variation in this amount should be reflected in the frequencies of the porphyrin vibrational modes. The difference spectra obtained for the FeTPP(CX)(EtOH) (X = S, Se) pair and the pentacoordinated species, FeTPP(CX), also did not exhibit any features due to the vibrational modes of FeTPP.

Figure 7.12 displays the FeTPP(CSe)(py)-FeTPP(CO)(py) difference spectrum. The most significant features are the ν(CX) modes at 1984 (X = O) and 1122 (X = Se) cm^{-1} and a peak at 680 cm^{-1} present in the carbonyl complex only. The position of the latter peak suggests its assignment to the Fe-C-O bending mode [22]. No peaks attributable to the Fe-C-X bending modes were observed in the spectra of the thiocarbonyl and selenocarbonyl derivatives. However, these peaks may appear in the region of the spectrum below 600 cm^{-1}, which was not examined, in view of the substantial shift to lower frequencies of M-C-X bending modes with increase in mass of the terminal atom [23]. The difference spectrum in Figure 7.12 and the data in Table 7.1 reveal some small shifts (<2 cm^{-1}) in positions of porphyrin vibrational modes in the spectrum of FeTPP(CSe)(py) as compared to that of the carbonyl analogue. The small magnitudes of these shifts suggest a much greater similarity between the selenocarbonyl (or thiocarbonyl) and the carbonyl complex than do the relative stabilities described earlier in this

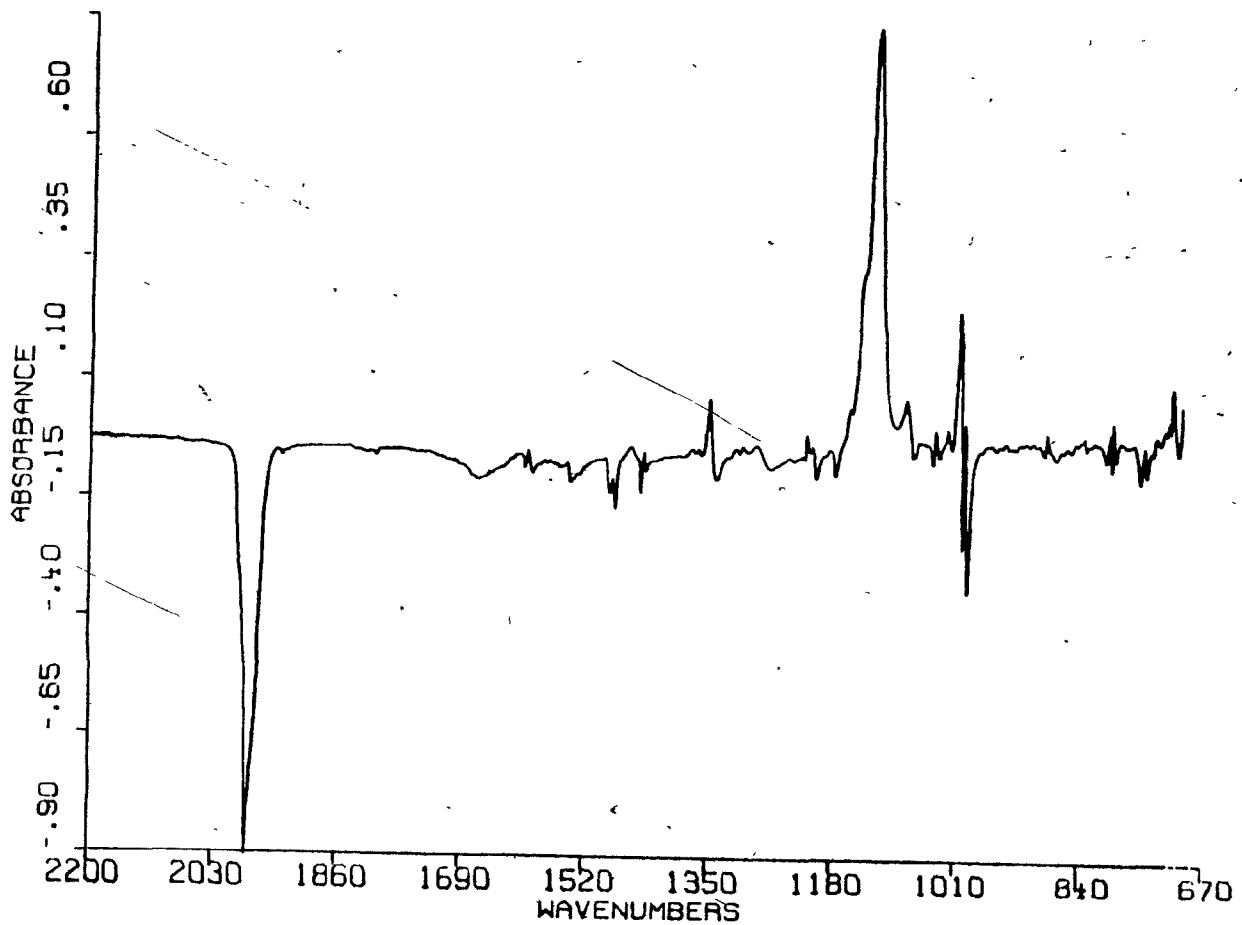

Figure 7.12 Difference spectrum obtained by the subtraction of the FT-IR spectrum of FeTPP(CO)(py) from that of FeTPP(CSe)(py).

section. It thus appears that the differences in M-C(X) bond strengths among the carbonyl, thiocarbonyl and selenocarbonyl FeTPP complexes do not induce sufficient changes in the extensively delocalized π-framework of the porphyrin to give rise to significant shifts in vibrational frequencies.

The subtraction of the spectrum of FeTPP(CSe)(EtOH) from that of the corresponding pyridine derivative (Figure 7.13) reveals several shifts in peaks due to porphyrin vibrational modes. Similar changes are observed in Figure 7.14 where the spectrum of FeTPP(CS)(EtOH) has been subtracted from that of FeTPP(CS). The positive peak in this spectrum at 1175 cm^{-1} represents a peak which appears in the spectra of both complexes but with an enhanced intensity in the spectrum of FeTPP(CS). This increased intensity may be attributed to reduced symmetry of the porphyrin ring in the pentacoordinated complex: an X-ray crystallographic study of FeOEP(CS) has revealed a 0.23-Å displacement of the iron atom out of the porphyrin plane towards the CS ligand [24]. Comparison of the data in Table 7.1 indicates that the shifts observed in the difference spectra with variation in or removal of the axial ligand L generally follow a consistent trend. The magnitude of the shift of a given peak relative to its position in the spectrum of FeTPP(CX)(py) (X = S or Se) increases in the order FeTPP(CX)(EtOH) < Fe(III)TPPCl < FeTPP(CX), while the direction of the shift

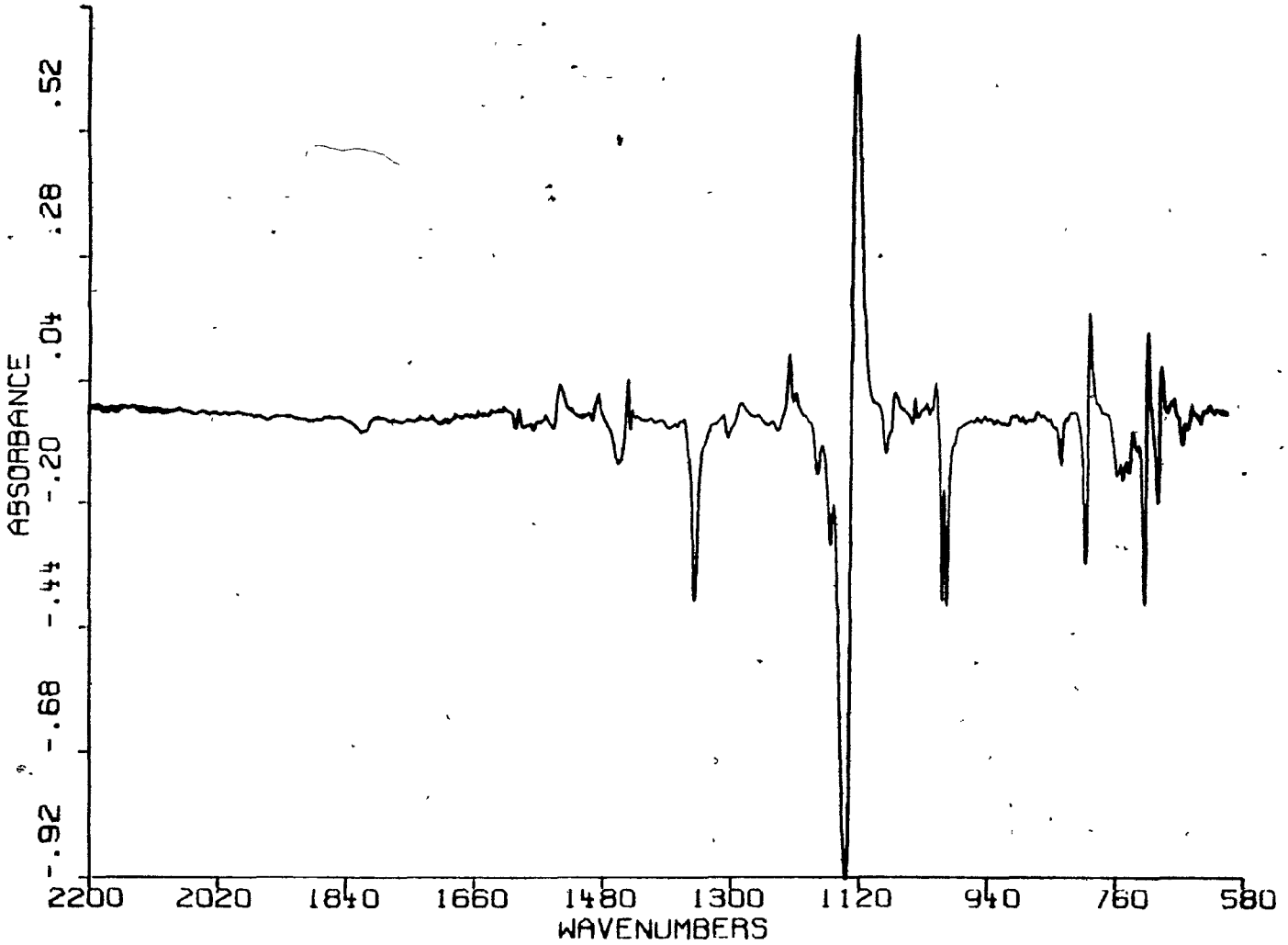

Figure 7.13. Difference spectrum obtained by the subtraction of the FT-IR spectrum of FeTPP(CSe)(EtOH) from that of FeTPP(CSe)(py).

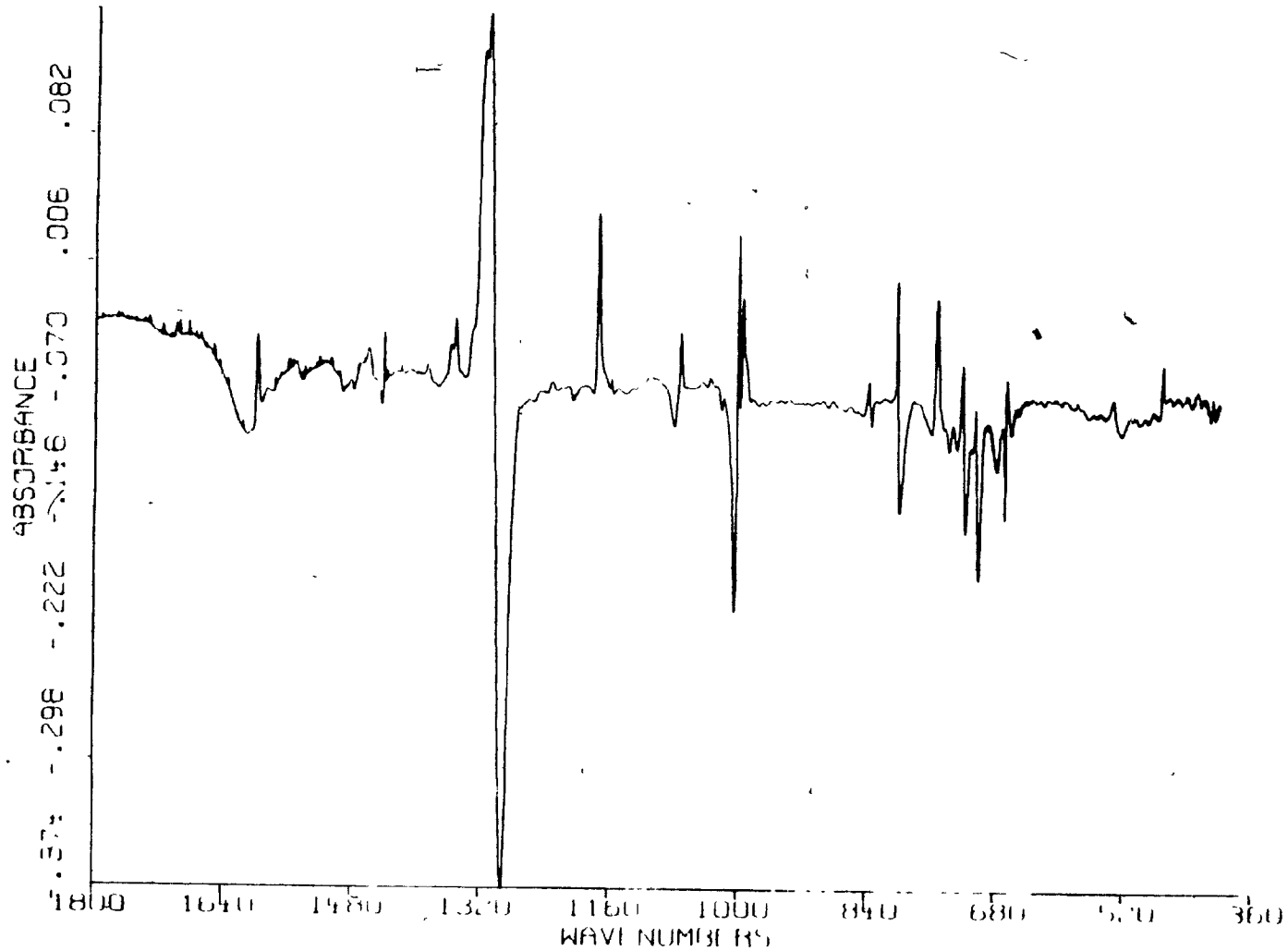

Figure 7.14. Difference spectrum obtained by the subtraction of the FT-IR spectrum of FeTPP(CS)(EtOH) from that of FeTPP(CS).

may be towards higher or lower frequencies. This order appears to parallel the extent of displacement of the iron atom out of the porphyrin plane. For instance, FeTPP(CS)-(py) exhibits planarity of the FeTPP core (data reported in Table II of Reference 25) while 0.23- and 0.38-Å displacements of the iron atom out of the porphyrin plane have been reported for FeOEP(CS) [24] and Fe(III)TPPCl [21], respectively. It is of interest to note that the 1350 cm^{-1} peak remains unshifted in the spectra of all the Fe(II) complexes. This peak has been found to be sensitive to the spin state of the metal [19], and this observation is corroborated in the present study by the appearance of this peak as a shifted doublet in the spectrum of Fe(III)TPPCl at 1340.2 and 1334.1 cm^{-1}. A second peak identified in previous work [19] as oxidation-state sensitive and slightly spin-state sensitive is observed in the 803-795 cm^{-1} range in the spectra of all the Fe(II) complexes studied here and at 807 cm^{-1} in the spectrum of Fe(III)TPPCl. Among the Fe(II) complexes, this peak shifts to higher frequency on going from FeTPP(CX)(py) to FeTPP(CX)(EtOH) and is further shifted to higher frequency in the spectrum of the penta-coordinated species. Since the shifts of peaks sensitive to oxidation state are generally interpreted in terms of changes in the amount of metal $d\pi$ electron density transferred to the porphyrin π^* orbitals [19], the above data

indicate that the extent of metal to porphyrin π-back-donation in the complexes studied here increases in the order FeTPP(CX) < FeTPP(CX)(EtOH) < FeTPP(CX)(py).

The resonance Raman spectra of FeTPP(CS) and FeTPP(CS)-(py) have been reported, as part of a resonance Raman investigation of a series of iron tetraphenylporphyrin complexes [25]. Spectra were obtained with excitation into both of the characteristic visible absorption bands of porphyrins - the Soret and α,β bands. From the data obtained for the entire series of complexes studied, two bands sensitive to the extent of metal to porphyrin π-back-donation were identified. Both these bands were observed to shift to higher frequency on going from FeTPP(CS)(py) to FeTPP(CS), indicating that less electron density is transferred from the metal to the porphyrin in the pentacoordinated complex, in agreement with the present study. This result was attributed to the displacement of the iron atom out of the porphyrin plane in FeTPP(CS), leading to less favourable overlap of the Fe dπ orbitals and the porphyrin π* orbitals than is the case in planar species such as FeTPP(CS)(py) [25].

In view of the frequency variations observed between the IR spectra of FeTPP(CX), FeTPP(CX)(py) and FeTPP(CX)(EtOH) for a given X, it is of interest to assess the extent of metal → CX π-back-donation in these various complexes.

While differences in carbonyl frequencies can be related to changes in the CO bond order (i.e., the energy-factored force field approximation is valid for ν(CO) modes) [26], the CS and CSe stretching frequencies cannot serve as direct measures of bond order due to increased mixing of M-C(X) and C-X stretching modes with increase in the mass of X [27]. This effect was noted in a study of M(II)OEP(CS)(py) (M = Fe, Ru, Os) [8], and data for FeOEP(CS) were found not to fit the relationship between ν(CS) and the C-S bond distance established for a series of thiocarbonyl derivatives [24] (see Table 2.3). However, a trend in ν(CX) values among a series of related compounds can generally be considered to reflect variations in M $\rightarrow$ CX π-backbonding. It can be seen in Table 7.1 that substitution of a pyridine ligand by an ethanol ligand results in an increase in ν(CX) (X = S, Se), indicating that when the <u>trans</u> ligand is ethanol less electron density is donated to the metal. The higher ν(CX) for the pentacoordinated complexes is indicative of a further decrease in the net electron density at the metal. The trend in ν(CX) frequencies thus suggests that the availability of metal electron density for π-back-donation to the porphyrin decreases in the order FeTPP(CX)(py) > FeTPP(CX)-(EtOH) > FeTPP(CX). This finding is consistent with the conclusions reached after examination of the porphyrin vibrational modes in both the IR and resonance Raman spectra.

An attempt was made to coordinate a CO ligand trans to CX (X = S, Se) in the pentacoordinated FeTPP(CX) complexes [Eq. 7.2], since the frequencies of the ν(CO) modes of the FeTPP(CO)(CX) complexes would provide a quantitative measure of the extent of dπ electron density transferred to the CX ligands.

$$\text{FeTPP(CX)} + \text{CO} \overset{K_t}{\rightleftharpoons} \text{FeTPP(CO)(CX)} \quad (\text{X} = \text{S, Se}) \qquad (7.2)$$

The reactions represented by Eq. 7.2 did not take place even at CO pressures of 20 atm, while the corresponding reaction of FeTPP(CO) under less than 1 atm CO pressure yields $FeTPP(CO)_2$ [12]. However, the latter complex undergoes facile CO loss. The equilibrium constants for the formation of the monocarbonyl and dicarbonyl complexes by the following reactions:

$$\text{FeTPP} + \text{CO} \overset{K_1}{\rightleftharpoons} \text{FeTPP(CO)} \qquad (7.3)$$

$$\text{FeTPP(CO)} + \text{CO} \overset{K_2}{\rightleftharpoons} \text{FeTPP(CO)}_2 \qquad (7.4)$$

have been reported [12]. K_1 [$(6.6 \pm 0.3) \times 10^4$] was found to be much greater than K_2 (140 ± 3) in direct contrast with the corresponding reaction of deuteroheme (H) with pyridine

where K_1 for the formation of H(py) is substantially smaller than K_2 for the formation of $H(py)_2$ [28]. The lower affinity of the iron atom for CO after binding of one CO ligand has been attributed to the decreased availability of Fe $d\pi$ electron density for π-back-donation to CO after formation of the first Fe-CO bond [12]. This is manifested in the substantially higher ν(CO) value for $FeTPP(CO)_2$ as compared to that of FeTPP(CO) [12]. Since it is well established that both the CS and CSe ligands are stronger π-acceptors than CO [9], the lack of CO incorporation into the FeTPP(CX) complexes (i.e., K_t [Eq. 7.2] < K_2) is not unexpected.

As part of the present study, the ^{13}C NMR spectra of FeTPP(CX) (X = S, Se) and FeTPP(CS)(py) were recorded. The positions of the resonances are listed in Table 7.2, together with the corresponding values from the literature for FeTPP(CX)(EtOH) [6,7]. Comparison of the chemical shift for the CX resonance of FeTPP(CX) with that for FeTPP(CX)-(EtOH) reveals an upfield shift in the pentacoordinated species. The CS resonance of FeTPP(CS)(EtOH) is in turn upfield from that of FeTPP(CS)(py). It has been established in studies of the ^{13}C NMR spectra of metal chalcocarbonyl complexes that an upfield shift in the position of a CX (X = O, S, Se) resonance is indicative of a decrease in the extent of metal to chalcocarbonyl π-back-donation [29,30].

Table 7.2. ^{13}C NMR Chemical Shifts of FeTPP(CX) and FeTPP(CX)(L) Complexes (X = S, Se)[a,b]

Complex	α	β	meso	$C_{1''}$	$C_{2''},C_{6''}$	$C_{3''},C_{5''}$	$C_{4''}$	CX
FeTPP(CS)[c]	146.5	133.1	122.7	141.9	134.2	127.3	128.2	308.1
FeTPP(CS)(EtOH)[d]	145.7	132.5	121.8	141.7	133.6	126.7	127.6	313.5
FeTPP(CS)(py)[e]	145.6	132.0	121.2	142.3	133.6	126.6	127.3	315.4
FeTPP(CSe)[c]	146.3	133.0	122.7	141.9	134.0	127.3	128.2	305.1
FeTPP(CSe)(EtOH)[f]	145.8	132.5	122.1	141.6	133.6	126.9	127.8	320.1

[a]Chemical shifts in ppm (±0.1 ppm) relative to TMS.
[b]Assignments adopted from Reference 15, Chapter 1, p. 43.
[c]In CD_2Cl_2 solution.
[d]Data from Reference 6; $CDCl_3$ solution.
[e]In CD_2Cl_2 solution containing 10% (v/v) pyridine-d_5.
[f]Data from Reference 7; $CDCl_3$ solution.

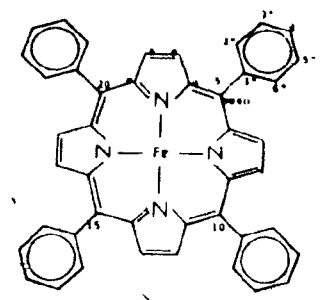

Accordingly, the trends in the CX resonances reported above are consistent with the trends observed in the ν(CX) frequencies in the IR spectra. The other peaks listed in Table 7.2 exhibit very small shifts with variation in the axial ligands. In particular, it may be noted that replacement of a CS ligand by a CSe ligand in a given complex has virtually no effect on the ^{13}C NMR spectrum of the FeTPP moiety.

References

1. P.D. Smith, B.R. James and D.H. Dolphin, Coord. Chem. Rev., 39, 31 (1981).
2. A.D. Adler, F.R. Longo, J.D. Finarelli, J. Goldmacher, J. Assour and L. Korsakoff, J. Org. Chem., 32, 476 (1979).
3. K. Rousseau and D. Dolphin, Tetrahedron Lett., 48, 4251 (1974).
4. S.-M. Peng and J.A. Ibers, J. Am. Chem. Soc., 98, 8032 (1976).
5. D. Mansuy, J.-P. Battioni and J.-C. Chottard, J. Am. Chem. Soc., 100, 4311 (1978).
6. J.-P. Battioni, J.-C. Chottard and D. Mansuy, Inorg. Chem., 21, 2056 (1982).
7. J.-P. Battioni, D. Mansuy and J.-C. Chottard, Inorg. Chem., 19, 791 (1980).
8. P.D. Smith, D. Dolphin and B.R. James, J. Organomet. Chem., 208, 239 (1981).
9. I.S. Butler, Acc. Chem. Res., 10, 359 (1977).
10. J.L. Hubbard and D.L. Lichtenberger, Inorg. Chem., 19, 3866 (1980).
11. M.A. Andrews, Inorg. Chem., 16, 496 (1977).
12. B.B. Wayland, L.F. Mehne and J. Swartz, J. Am. Chem. Soc., 100, 2379 (1978).
13. L.A. Bottomley, M.R. Deakin and J.-N. Gorce, Inorg. Chem. 23, 3563 (1984).

14. D. Dolphin, ed., "The Porphyrins", Volume III, Academic Press, New York, 1978.

15. D. Dolphin, ed., "The Porphyrins", Volume IV, Academic Press, New York, 1979.

16. J.O. Alben, S.S. Choi, A.D. Adler and W. S. Caughey, Ann. N.Y. Acad. Sci., 206, 278 (1973).

17. J.O. Alben, in "The Porphyrins", Vol. III, D. Dolphin, ed., Academic Press, New York, 1978, pp. 323-345.

18. J. Kincaid and K. Nakamoto, J. Inorg. Nucl. Chem., 37, 85 (1975).

19. H. Oshio, T. Ama, T. Watanabe, J. Kincaid and K. Nakamoto, Spectrochim. Acta, 40A, 863 (1984).

20. A. Antipas, J.W. Buchler, M. Gouterman and P.D. Smith, J. Am. Chem. Soc., 102, 198 (1980).

21. J.L. Hoard, G.H. Cohen and M.D. Glick, J. Am. Chem. Soc., 89, 1992 (1967).

22. L.H. Jones, R.S. McDowell, M. Goldblatt and B.I. Swanson, J. Chem. Phys., 57, 2050 (1972).

23. P.S. Braterman, "Metal Carbonyl Spectra", Acadamic Press, London, 1975, p. 25, Eq. 3.1.

24. R. Scheidt and D.K. Geiger, Inorg. Chem., 21, 1208 (1982).

25. G. Chottard, P. Battioni, J.-P. Battioni, M. Lange and D. Mansuy, Inorg. Chem., 20, 1718 (1981).

26. Reference 23, p. 27.

27. A.M. English, K.R. Plowman and I.S. Butler, Inorg. Chem., 20, 2553 (1981).

28. M. Rougee and D. Brault, Biochemistry, 14, 4100 (1975).

29. G.M. Bodner, Inorg. Chem., 14, 2694 (1975).

30. D. Cozak, I.M. Baibich and I.S. Butler, J. Organometal. Chem., 169, 381 (1979).

Summary and Contributions to Knowledge

1. Arene displacement from (η-Arene)$Cr(CO)_2(CX)$ (X = S, Se) complexes by ligands other than CO has been studied for the first time and has provided a route to the synthesis of chromium thiocarbonyl and selenocarbonyl derivatives containing more than one monodentate ligand (other than CO) or a tridentate ligand. The reaction of (η-Arene)$Cr(CO)_2(CX)$ (X = S, Se) complexes with excess $(RO)_3P$ (R = Me, Et, n-Bu, Ph) afforded $Cr(CO)_2(CX)[(RO)_3P]_3$ in high yield. The products were identified as mixtures of isomers consisting predominantly of the mer I isomer, in which a phosphite ligand is trans to CX, together with a small amount of the fac isomer. Very small amounts of the mer II isomer, in which a phosphite ligand is trans to CO, were detected in the ^{31}P NMR spectrum of $Cr(CO)_2(CX)$-$[(MeO)_3P]_3$. Arene displacement from (bz)$Cr(CO)_2(CX)$ by the tridentate ligands triphos-U $[(Me)C(CH_2P(Ph)_2)_3]$ and triphos $[(Ph_2PCH_2CH_2)_2PhP]$ yielded, respectively, (triphos-U)$Cr(CO)_2(CX)$ as the fac isomer and (triphos)$Cr(CO)_2(CX)$ as a mixture of two fac isomers.

2. The crystal structures of the mer I isomers of $Cr(CO)_2(CX)[(MeO)_3P]_3$ (X = S, Se) were obtained.

3. The ^{31}P NMR spectra of the complexes mentioned in 1 above were recorded. These presented the first opportunity to compare the ^{31}P resonances of tertiary phosphite and tridentate phosphine ligands cis and trans to CO, CS and CSe ligands in Group VIB metal complexes.

4. $Cr(CO)_2(CX)[(MeO)_3P]_3$ (X = O, S, Se) complexes were found to undergo intramolecular isomerization. The rate of isomerization was established to be fastest for the selenocarbonyl complex and slowest for the tricarbonyl complex.

5. Activation parameters were calculated for the fac $\longleftrightarrow$ mer isomerization of $Cr(CO)_3[(MeO)_3P]_3$ and the fac $\longleftrightarrow$ mer I isomerization of $Cr(CO)_2(CX)[(MeO)_3P]_3$ (X = S, Se).

6. In one of the few applications to date of two-dimensional NMR spectroscopy in the study of stereochemically nonrigid organometallic complexes, the interconversion of mer I and mer II isomers was observed in the 2-D NOE ^{31}P NMR spectra of $Cr(CO)_2(CX)[(MeO)_3P]_3$ (X = S, Se). Analysis of these spectra established that the observed processes involved a trigonal prismatic twist rather than a bicapped-tetrahedron mechanism.

7. Kinetic studies of arene displacement from (bz)-$Cr(CO)_2(CX)$ (X = S, Se) by $(MeO)_3P$ demonstrated that the reaction rate is first order with respect to the incoming ligand and first order in complex. These reactions were proposed to proceed by the same ring slippage mechanism postulated for arene displacement from (η-Arene)$M(CO)_3$ (M = Mo, W) complexes. The relative rates of arene displacement from (bz)$Cr(CO)_2(CX)$ by $(MeO)_3P$ and of <u>fac</u> → <u>mer</u> I isomerization of the $Cr(CO)_2(CX)[(MeO)_3P]_3$ product were found to be consistent with the possibility that the <u>fac</u> isomer is the initial product of the reaction and subsequently isomerizes to the observed <u>mer</u> I product.

8. The rate of arene displacement from (bz)$Cr(CO)_2(CSe)$ by $(MeO)_3P$ was found to be faster than that for the corresponding thiocarbonyl complex. On the basis of comparison of the activation parameters calculated for these reactions, this result was attributed to less crowding in the activated complex in the selenocarbonyl case.

9. The effects on the rate of arene displacement from (η-Arene)$Cr(CO)_2(CS)$ complexes of size and nucleophilicity of the incoming ligand and of substituents on the arene were investigated.

10. The feasibilty of a procedure for estrogen receptor assay based on the detection by FT-IR spectroscopy of $Cr(CO)_3$-labelled modified estradiol bound to estrogen receptors in target tissue was examined. The sensitivity of the FT-IR measurements proved sufficient for detection of the metal carbonyl label but not for its quantitative determination.

11. The FT-IR spectra of (5,10,15,20-tetraphenylporphinato)iron(II) (FeTPP) complexes containing axially bound chalcocarbonyl ligands were recorded. Difference spectra obtained by subtraction of spectra of pairs of complexes in the series FeTPP(CX) (X = S, Se) and FeTPP(CX)L (X = S, Se; L = py, EtOH) were examined in order to assess the perturbations of the vibrational modes of the porphyrin ring with variation in the axial ligands.

12. FeTPP(CX) (X = S, Se) was found not to bind CO at its vacant coordination site under 20 atm CO pressure, demonstrating a substantial withdrawal of Fe $d\pi$ electron density by the CX ligands.

Suggestions for Future Work

In Chapter 3 of this thesis, an example of the use of two-dimensional NMR spectroscopy in the study of stereochemical nonrigidity of organometallic complexes was described. This investigation, which represents one of the few applications to date of 2-D NMR spectroscopy in organometallic chemistry, demonstrated that 2-D NMR measurements can be employed not only to establish the occurrence of a chemical exchange process but also to elucidate rearrangement mechanisms. Accordingly, further studies by 2-D NMR spectroscopy of stereochemically nonrigid organometallic complexes are clearly worthwhile.

Further investigations of the rearrangement processes of $Cr(CO)_2(CX)L_3$ (X = O, S, Se) complexes should be undertaken. It would be of interest to assess, through the study of a variety of ligands, the effects of electronic and steric factors on the equilibrium distribution of $Cr(CO)_2(CX)L_3$ isomers and on the activation parameters for intramolecular isomerization. The synthesis of complexes of the type $Cr(CO)_2(CS)(L)_2L'$ would allow chemical exchange between <u>fac</u> isomers to be studied by 2-D NMR spectroscopy. The results of the present study suggest that interconversion between the <u>fac</u> and <u>mer</u> I or <u>mer</u> II isomers of $Cr(CO)_2(CS)[(MeO)_3P]_3$ (X = S, Se) is too slow to be observed by 2-D ^{31}P NMR spectroscopy but that the replacement of the $(MeO)_3P$

groups by ligands that minimize steric effects as well as possess electronic properties comparable to those of CX ligands may accelerate the rates of these processes. In addition, the application of 2-D ^{13}C NMR spectroscopy in these systems should be investigated since ^{13}C nuclei in most organometallic complexes relax slower than ^{31}P nuclei, thus allowing slower rearrangement processes to be observed by 2-D ^{13}C NMR. Such studies would be facilitated by ^{13}C-enrichment, which could be readily achieved by photochemical substitution of carbonyl groups by ^{13}CO in the (η-Arene)-$Cr(CO)_2(CX)$ precursors to the $Cr(CO)_2(CX)L_3$ complexes.

Scientific Publications:

1. A.A. Ismail and I.S. Butler, "Co-adding and Permanent Storage of Large Numbers of FT-IR Scans", FT-IR Spectral Lines, Vol. 5, No. 2, 14 (1983).

2. G. Jaouen, A. Vessières, S. Top, A.A. Ismail and I.S. Butler, "Voie d'application inédite des complexes des métaux carbonyle. Exemple dans la détection du récepteur de l'oestradiol", Comp. Rend. Acad. Sci. Paris, t. 298, Serie II, n° 16, 683-686 (1984).

3. A.A. Ismail, J. Sedman and I.S. Butler, "FT-IR Spectra of Coordination Compounds" in Fourier Transform Infrared Spectroscopy, ed. T. Theophanides, D. Reidel Publishing Co., Dordrecht, Holland, pp. 83-96 (1984).

4. A.A. Ismail, I.S. Butler, J.-J. Bonnet and S. Askenazy, "Crystal Structure of mer-Dicarbonyl(selenocarbonyl)-tris(trimethylphosphite)chromium(0)", Acta Cryst. C., in press (1985).

5. G. Jaouen, A. Vessières, S. Top, A.A. Ismail and I.S. Butler, "Metal Carbonyl Fragments as a New Class of Markers in Molecular Biology", J. Am. Chem. Soc., in press (1985).

6. P.H. Bird, A.A. Ismail and I.S. Butler, "Arene Activation in Chromium Chalcocarbonyl Complexes. I. Spectroscopic Properties and Crystal and Molecular Structure of mer-Dicarbonyl(thiocarbonyl)tris(trimethylphos-

phite)chromium(0)", Inorg. Chem., in press (1985).

7. A.A. Ismail, I.S. Butler and G. Jaouen, "Organometallic Linkage Isomers: Chromium Carbonyl Acyl Isocyanide and Cyanide Complexes", Inorg. Synth., accepted for publication (1985).

8. G. Jaouen, A. Vessières, S. Top, A.A. Ismail and I.S. Butler, "Metal Carbonyl Oestrogen Receptor Assay", Science, submitted for publication.

9. A.A. Ismail, F. Sauriol, J. Sedman and I. S. Butler, "Application of 2-D NOE Phosphorus-31 NMR Spectroscopy in Determining Rearrangement Mechanisms of Stereochemically Nonrigid, Octahedral Organometallic Complexes", Organometallics, accepted for publication.

10. A.A. Ismail and I.S. Butler, "Arene Activation in Chromium Chalcocarbonyl Complexes. II. Kinetics of Arene Displacement by Trialkyl- and Triarylphosphites in (η-Arene)$Cr(CO)_2(CX)$ (X = S, Se)", Inorg. Chem., submitted for publication.

Papers Presented at Scientific Conferences:

(1985)

A.A. Ismail, I.S. Butler, G. Jaouen, A. Vessières, S. Tondu and S. Top, "Detection of Physiological Levels of Hormonal Steroids Labelled with Organometallic Markers by FT-IR Spectroscopy", International Conference on Fourier and Computerized Infrared Spectroscopy, Ottawa, Ontario, June, 1985.

(1984)

A.A. Ismail and I.S. Butler, "Kinetic Study of Ring Lability in (η-Arene)$Cr(CO)_2$(CX) (X = S, Se) Complexes", Can-Am Chemical Congress (67th Canadian Chemical Conference and Exhibition), Montreal, Quebec, June, 1984.

(1983)

I.S. Butler, A.A. Ismail, G. Jaouen, A. Vessières et S. Top, "Application de la spectroscopie IRTF dans la détection des sites de réception hormonale", 51e Congrès de l'Association Canadienne-Francaise pour l'Avancement des Sciences, Trois Rivières, Québec, mai, 1983.

Papers Presented at Scientific Conferences: (Cont'd)

(1982)

A.A. Ismail, I.S. Butler and G. Jaouen, "Physicochemical Studies of Isonitrile and Nitrile Ligands in Group VIB Metal Carbonyl Complexes", 183rd National Meeting of the American Chemical Society, Las Vegas, Nevada, March-April, 1982.

A.A. Ismail, I.S. Butler and G. Jaouen, "Reactions of Selected Group VIB Metal Carbonyl Complexes with Isonitrile Ligands", 65th Canadian Chemical Conference and Exhibition, Toronto, Ontario, May-June, 1982.

I.S. Butler, A.A. Ismail, G. Jaouen and A. Vessières, "FT-IR Spectra of Organometallic-labelled Steroids", 9th Annual Conference of the Federation of Analytical Chemistry and Spectroscopy Societies, Philadelphia, Pennsylvania, September, 1982.

G. Jaouen, A. Vessières-Jaouen, S. Top, A.A. Ismail and I.S. Butler, "Hormonal Receptor Site Detection Using FT-IR Spectroscopy", 29th Annual Conference of the Spectroscopy Society of Canada, St-Jovite, Quebec, September, 1982.

Papers Presented at Scientific Conferences: (Cont'd)

(1981)

A.A. Ismail and I.S. Butler, "Organometallic-porphyrin Chemistry: FT-IR Spectra of Some Chalcocarbonyl (5,10,15,20-Tetraphenylporphinato)iron(II) Derivatives and Related Compounds", 64th Canadian Chemical Conference, Halifax, Nova Scotia, June, 1981.

A.A. Ismail and I.S. Butler, "Spectroscopic Studies on Some 5,10,15,20-Tetraphenylporphinatoiron(II) Derivatives", 28th Canadian Spectroscopy Symposium, Ottawa, Ontario, September, 1981.

APPENDICES

Appendix A

Structural Characterization of the mer I Isomer of $Cr(CO)_2(CS)[(MeO)_3P]_3$: X-Ray Data Collection, Structure Solution and Refinement

The unit cell and data collection parameters are summarized in Table A.1. Weissenberg and precession photographs showed mmm symmetry and the systematic absences: on 0kl, $k = 2n + 1$, on h0l, $l = 2n + 1$, and on hk0, $h = 2n + 1$, which uniquely define the space group Pbca (No. 61, D_{2h}^{15}). The accurate unit cell dimensions were obtained by automatic centering of 51 reflections scattered randomly in reciprocal space in the range $15^\circ < 2\theta < 25^\circ$. The following formulas were used in the data reduction

$$I = N - B(t_s/t_b), \qquad \sigma(I) = [N + B(t_s/t_b)^2]^{\frac{1}{2}},$$

$$Lp = \frac{(\sin 2\theta)(\cos^2 2\theta_m + 1)}{(\cos^2 2\theta + \cos^2 2\theta_m)}.$$

The net intensity I is derived from the total count N accumulated during the scan time t_s. The background count

B was measured for time t_b. The Lorentz-polarization correction Lp is calculated for diffraction angles $2\theta_m$ and $2\theta_s$ at the monochromator and sample crystals, respectively.

The structure was solved by conventional heavy atom techniques and refined using the block-diagonal least-squares approximation. In the last stages of the refinement all atoms were refined with anisotropic thermal parameters. A final difference Fourier map was devoid of significant features; the highest peaks were about 1% of the intensity for the last carbon atom found and were randomly located. Also, since there appeared to be no clear indication of hydrogen atom locations, these atoms were not included in the structure factor calculations.

The computer programs used for the data collection, structure solution and refinement and geometry calculations are those contained in the N.R.C. PDP-8e crystallographic package [1]. The perspective diagram was prepared by the Concordia University CDC Cyber system. The function minimized in the least-squares refinement was

$$\Sigma w(|F_o|-|F_c|)^{1/2} \qquad \text{where } w = 1/[(\sigma(F))^2 + 0.03F^2].$$

The discrepancy indices listed in Table A.1 are:

$$R_F = [\Sigma||F_o|-|F_c||/\Sigma|F_o|]$$
$$R_{wF} = [\Sigma w(|F_o|-|F_c|)^2/\Sigma|F_o|^2]^{\frac{1}{2}}$$
$$GOF = [\Sigma w(|F_o|-|F_c|)^2/(m-n)]^{\frac{1}{2}}$$

The neutral atom scattering factors and anomalous dispersion corrections were taken from standard listings [2]. The observed and calculated structure factors are listed in Table A.2. The final positional parameters are collected together in Table A.3. The final thermal parameters appear in Table A.4.

Table A.1. Crystallographic Data for X-ray Diffraction Study of $Cr(CO)_2(CS)[(MeO)_3P]_3$

Crystal Parameters

crystal system = orthorhombic

space group = Pbca

a = 15.61(1) Å

b = 15.32(2) Å

c = 18.88(1) Å

V = 4505 $Å^3$

Z = 8

calcd density = 1.466 g cm^{-3}

obsd density = 1.40(2) g cm^{-3}

temp = 295 K

formula = $C_{12}H_{27}O_{11}SP_3Cr$

mol wt = 524.0 g mol^{-1}

Measurement of Intensity Data

diffractometer = Picker Nuclear FACS-1
radiation = Mo Kα
monochromator = highly oriented graphite
detector aperture = 3 mm X 3 mm
crystal to detector distance = 25 cm
detector = scintillation counter and pulse height analyzer set for 100% of Mo Kα peak
attenuators = Ni foil used for intensities $> 10^4$ Hz
scan type = coupled θ(cryst) -2θ (detector), 2.0° min^{-1}
scan length = (2θ) = $[1.8 + (0.692 \tan\theta)]^\circ$, beginning 0.9° below the predicted peak
rotation axis [0 1 0]
reflections measured = +h, +k, +l
min and max 2θ = 3.5°, 40.0°
stds every 50 cycles = 4 3 0, 0 0 6, 0 4 3
variation = ±3% (random)
number of reflections collected = 2108
no. with $I > 3\sigma(I)$ = 1453
R_F = 5.06 %
R_{wF} = 7.30 %
GOF = 1.19

Table A.2. Observed and Calculated Structure Factors for

$Cr(CO)_2(CS)[(MeO)_3P]_3$ (mer I)

COLUMNS ARE 10FO,10FC, 10SIG

L	KFO	FC	SIG
	0,	0, L	
2	188	201	8
4	172	165	13
6	2597	2400	5
8	1504	1575	7
10	362	325	13
12	685	707	11
14	299	319	21
16	428	604	14
18	1364	1354	13
	0,	2, L	
0	1515	1458	4
1	4379	4438	10
2	442	472	5
3	1676	1398	4
4	1334	1424	5
5	1283	1220	6
6	2468	2311	6
7	1638	1706	7
8	684	648	9
9	503	543	12
10	825	815	10
11	582	606	12
12	443	420	13
14	516	512	14
16	427	436	20
17	420	403	19
	0,	4, L	
0	968	1128	6
1	414	547	8
2	1127	1097	6
3	2965	2495	5
4	2173	2001	6
5	1121	1096	7
8	583	529	10
9	510	543	11
11	344	351	16
13	694	725	13
14	253	234	26
15	327	338	22
16	414	434	21
17	559	500	17
	0,	6, L	
0	816	684	7
1	816	752	7
2	338	342	11
3	1812	1789	7
4	1095	1177	8
5	586	641	9
6	1377	1501	8
7	189	241	22
8	453	520	13
9	211	214	22
10	698	706	12
11	379	405	18
14	314	331	22
15	664	636	16
16	552	556	17
	0,	8, L	
0	510	551	11
1	851	791	9
2	716	648	9
3	1131	1140	9
4	769	875	10
5	786	778	10
6	594	599	11
7	845	845	11
8	1428	1484	10
9	411	421	16
10	1118	1134	11
11	244	273	26
12	316	307	22
13	463	461	17
14	660	707	15
15	693	705	16
	0,	10, L	
2	213	235	25
3	524	509	13
4	693	732	12
5	222	199	23
6	279	253	22
7	964	1027	11
11	817	809	13
	0,	12, L	
0	320	299	19
2	711	720	13
4	322	319	22
5	407	424	19
6	201	134	31
7	424	439	18
8	744	750	14
9	263	243	26
10	625	659	16
	0,	14, L	
0	235	271	30
3	470	505	18
4	241	320	32
5	208	169	33
	1,	0, L	
2	4165	4544	6
4	954	848	5
6	2074	1816	6
8	874	891	8
10	664	714	10
	1,	1, L	
1	118	287	14
2	1543	1454	4
3	1193	1211	4
4	1057	1194	5
5	466	502	8
6	1500	1461	6
7	221	270	15
9	538	561	10
10	420	434	12
13	284	302	19
14	636	595	13
15	257	276	26
18	230	186	30
	1,	2, L	
1	3169	3204	6
2	555	617	5
3	176	151	13
4	1232	1331	5
5	1137	1188	6
6	1340	1371	6
7	209	232	17
8	830	835	8
9	906	947	9
11	607	657	11
13	360	371	18
14	380	443	20
17	812	788	14
	1,	3, L	
1	1202	1255	5
2	508	457	6
3	912	944	6
4	1079	1011	6
5	751	696	7
6	197	161	16
7	215	178	17
8	703	696	9
9	592	598	10
11	1187	1197	10
14	296	299	20
15	425	415	17
	1,	4, L	
1	551	543	7
2	953	853	6
3	1699	1414	6
4	1035	1006	6
5	378	392	10
6	1352	1398	7
7	590	609	9
8	379	391	13
9	539	586	11
10	245	271	19
11	179	169	28
12	602	595	13
13	191	220	29
14	468	470	16
16	502	492	17
17	478	450	18

[(CH3O)3P]3 CR (CO)2 (CS)
COLUMNS ARE 10FO,10FC, 10SIG

L	KFO	FC	SIG
	1,	5, L	
1	282	315	12
2	1133	995	6
3	287	297	12
4	353	336	11
5	350	341	11
6	164	171	22
9	552	589	11
12	357	343	17
14	497	506	15
15	231	185	28
	1,	6, L	
1	1642	1530	7
2	1076	1075	7
3	329	299	12
4	852	837	8
5	925	970	8
6	217	249	17
7	791	843	10
8	379	413	14
9	284	289	19
11	742	746	12
12	483	495	15
13	917	891	12
14	741	729	14
16	404	412	21
	1,	7, L	
1	246	258	15
3	341	301	13
4	436	466	12
5	504	515	11
7	228	215	20
9	216	237	24
10	245	202	22
12	240	261	26
14	511	508	17
	1,	8, L	
1	621	637	10
2	694	713	10
4	677	739	10
5	586	563	11
6	921	923	10
7	505	508	13
8	396	378	16
9	450	466	15
10	263	271	23
12	1204	1231	12
13	388	376	19
14	557	540	17
	1,	9, L	
1	387	366	14
2	706	715	10
3	187	247	27
4	651	681	11
5	619	602	12
9	601	578	13
11	399	373	17
13	393	431	21
14	308	353	26
	1,	10, L	
2	340	358	17
4	580	601	13
5	1086	1094	11
6	718	718	13
7	1077	1070	11
9	703	718	13
11	940	985	13
12	405	399	20
13	619	612	16
	1,	11, L	
4	449	432	16
5	543	572	15
6	282	279	21
7	220	196	29
8	397	414	20
	1,	12, L	
4	332	297	21
5	1139	1168	12
6	461	466	17
7	307	319	24
8	353	348	21
9	364	375	21
10	352	371	23
	1,	13, L	
2	306	333	24
4	215	287	33
6	272	298	27
	1,	14, L	
3	254	312	32
	2,	0, L	
0	3106	3342	6
2	436	439	5
4	1798	1626	5
8	329	305	12
10	719	696	10
12	1264	1253	10
14	227	213	26
18	709	704	14
	2,	1, L	
0	1560	1585	4
1	573	600	4
2	502	408	5
3	537	474	6
4	932	797	5
5	783	782	6
6	536	496	8
7	963	1033	7
9	156	175	25
10	743	703	10
12	745	763	11
13	614	640	13
14	612	601	13
15	230	259	29
16	450	434	17
	2,	2, L	
0	2426	2349	4
1	670	671	5
2	1274	1175	5
3	236	259	11
4	1905	1739	5
5	1087	1132	6
6	1563	1560	6
7	881	965	8
8	381	382	12
9	396	391	12
10	258	264	17
11	1195	1240	10
12	578	595	13
13	242	235	24
14	217	273	28
15	548	558	15
16	415	411	19
	2,	3, L	
0	868	887	5
1	202	266	13
2	746	791	6
3	348	300	9
4	321	250	10
5	1662	1606	6
6	1155	1035	7
8	788	800	9
9	726	737	10
10	509	555	12
11	405	422	15
12	378	385	17
13	422	406	16
14	432	443	17
15	425	388	17
16	430	469	18
	2,	4, L	
0	324	309	9
1	1083	1153	6
2	269	365	11
3	1182	1060	6
4	282	287	12
5	1003	926	7
6	1446	1421	7
7	170	142	21
8	854	873	9
9	576	548	11
10	821	846	10
11	357	372	16

C(CH3O)3P]3 CR (CO)2 (CS) PAGE 3

COLUMNS ARE 10F0,10FC, 10SIG

L	KFO	FC	SIG
	2,	4, L	
12	400	428	16
13	443	460	16
14	721	709	13
15	281	282	24
16	618	598	16
17	463	435	17
	2,	5, L	
0	2246	1877	6
1	895	863	7
2	1182	1032	7
3	919	874	7
4	1374	1356	7
6	502	474	10
7	466	406	11
8	329	346	15
10	808	776	11
11	947	960	11
15	561	524	15
16	205	214	34
	2,	6, L	
1	678	709	8
2	437	430	10
3	899	840	8
4	172	117	21
5	156	126	24
7	916	940	9
10	400	401	15
11	530	537	13
13	328	320	21
14	445	472	18
15	570	561	16
	2,	7, L	
0	2143	1961	7
1	522	556	10
2	271	246	15
3	925	876	8
4	1059	1049	9
5	279	241	16
6	191	198	24
7	302	309	17
8	628	626	11
10	833	847	12
14	472	477	17
	2,	8, L	
0	538	560	11
1	176	123	22
2	498	488	11
3	380	416	14
4	798	864	10
5	172	197	25
6	330	315	15
8	702	697	12
10	442	419	15
13	358	361	22
14	549	519	15
	2,	9, L	
0	870	883	10
2	175	210	24
3	769	752	10
4	784	780	11
6	415	422	15
7	567	531	13
8	238	313	25
9	322	354	21
11	476	495	17
12	240	265	30
14	200	126	33
	2,	10, L	
0	397	399	15
1	366	346	16
2	391	401	16
3	586	612	13
4	923	959	11
5	559	545	14
7	660	646	13
9	367	344	19
11	262	242	28
	2,	11, L	
0	572	547	13
1	390	441	17
2	331	357	19
3	805	800	12
5	627	680	14
6	734	723	13
10	494	470	18
	2,	12, L	
0	1099	1098	12
2	358	380	20
3	596	588	14
4	709	737	14
5	283	264	25
7	305	344	24
8	659	646	15
	2,	13, L	
0	633	676	15
3	274	255	25
5	280	314	26
7	444	438	19
	2,	14, L	
1	704	728	15
	3,	0, L	
2	160	45	14
4	174	160	16
6	455	491	9
8	639	607	9
10	557	632	11
12	179	185	29
14	480	498	16
16	404	358	19
	3,	1, L	
1	266	253	9
2	951	987	5
3	866	739	6
4	708	691	6
5	1846	1807	6
6	491	475	9
7	170	196	20
8	866	882	8
9	888	932	9
10	832	899	10
11	364	379	15
12	908	903	11
13	662	642	12
14	227	227	27
15	502	462	15
	3,	2, L	
1	360	407	8
2	409	285	8
3	206	179	14
4	1382	1313	6
5	1723	1553	6
6	527	557	9
7	756	721	8
8	1314	1264	8
9	851	958	9
10	480	536	12
11	370	375	16
12	342	308	17
13	438	484	16
14	534	535	14
16	194	153	32
	3,	3, L	
1	1638	1480	5
2	442	460	8
4	306	338	11
5	379	396	10
6	1337	1230	7
7	892	820	8
8	557	548	10
9	240	251	19
10	1199	1219	9
11	995	1018	11
12	1177	1230	11
13	851	888	12
15	358	392	21
16	555	539	16
17	236	229	31
	3,	4, L	
1	1395	1325	6
3	909	816	7
4	1470	1375	7

C(CH3O)3P)3 CR (CO)2 (CS)
COLUMNS ARE 10FO,10FC, 10SIG

L	KFO	FC	SIG
	3,	4,	L
5	922	924	8
6	276	326	14
7	547	524	10
8	324	316	14
9	360	405	15
11	594	593	13
12	750	750	12
13	758	792	12
14	463	430	16
15	292	355	26
16	379	367	20
	3,	5,	L
2	1113	1105	7
3	630	588	8
4	699	659	8
5	175	198	21
6	377	403	12
8	363	376	14
9	1927	1920	9
10	275	268	19
12	311	326	20
13	507	560	15
15	529	564	17
	3,	6,	L
1	455	430	10
2	955	851	8
3	361	319	12
4	919	913	9
5	319	362	13
6	202	215	20
7	376	389	14
8	213	170	22
12	350	388	20
13	703	650	14
14	657	682	15
	3,	7,	L
1	502	484	10
2	577	565	10
4	332	342	14
5	1214	1160	9
8	432	439	15
9	273	238	20
10	548	585	14
11	215	201	27
13	351	323	20
14	209	138	30
15	228	244	31
	3,	8,	L
1	490	494	11
2	618	575	10
3	267	282	18
6	1075	1082	10
7	396	406	16

L	KFO	FC	SIG
9	428	463	16
10	258	303	24
12	573	544	15
	3,	9,	L
2	882	903	10
3	853	818	10
4	716	717	11
5	749	727	11
6	527	522	14
7	277	243	22
9	609	601	14
10	202	130	29
11	229	199	28
12	323	335	23
13	205	205	34
	3,	10,	L
1	390	394	16
2	447	412	15
3	464	479	15
4	347	364	18
5	533	545	14
6	805	802	12
7	700	710	14
8	769	810	13
9	291	328	24
10	391	408	19
12	230	218	30
	3,	11,	L
1	218	167	26
2	1066	1058	11
3	346	325	19
4	583	575	14
6	269	276	25
8	448	446	18
	3,	12,	L
2	951	942	12
4	410	402	19
5	497	476	17
6	664	645	14
7	681	708	15
	3,	13,	L
1	659	665	15
2	294	326	24
5	557	540	16
	3,	14,	L
1	415	435	20
3	464	472	19
4	298	300	26
	4,	0,	L
2	3494	3492	5
4	1993	1878	6
6	302	261	12
8	616	685	10
10	576	569	12

L	KFO	FC	SIG
12	300	286	20
16	549	566	17
	4,	1,	L
0	730	729	6
1	152	163	18
2	724	746	6
3	1904	1629	5
4	167	241	18
5	870	883	7
6	666	594	8
7	1464	1498	8
8	418	463	11
10	882	891	10
11	1327	1302	10
12	868	858	11
13	670	655	13
14	757	720	12
15	419	410	17
17	266	258	26
	4,	2,	L
0	872	837	6
1	2008	1921	5
2	899	520	6
3	261	229	12
4	1003	999	7
5	990	885	7
6	398	392	10
7	200	213	18
8	296	305	15
12	326	309	19
13	201	189	29
16	271	281	26
17	456	444	19
	4,	3,	L
0	2798	2471	5
1	458	530	8
2	670	701	7
3	1085	1046	6
4	1203	1171	7
6	258	279	14
7	274	351	16
8	1522	1611	9
10	1044	973	10
11	1224	1262	10
12	564	593	14
13	258	259	25
14	842	807	12
15	534	547	17
16	347	372	22
	4,	4,	L
0	346	302	11
1	1089	952	6
3	926	872	7
6	172	192	23

.F(CH3O)3PJ3 CR (CO)2 (CS)
COLUMNS ARE 10FO,10FC, 10SIG

L	KFO	FC	SIG
	4,	4, L	
7	636	650	10
13	309	296	22
14	260	234	26
15	855	876	13
16	207	232	35
	4,	5, L	
0	1187	1005	7
1	791	801	8
2	1467	1413	7
3	627	629	9
4	924	906	8
5	904	957	9
6	207	277	21
7	749	755	10
9	585	574	13
10	330	334	17
11	956	973	11
12	248	272	25
13	321	325	21
14	502	491	16
15	402	408	21
16	725	733	16
	4,	6, L	
0	1900	1800	7
1	622	570	9
5	1115	1058	9
8	307	309	17
10	325	331	18
12	347	325	19
13	211	203	30
	4,	7, L	
0	191	259	23
3	510	515	12
4	1960	1923	8
5	781	796	10
6	229	231	21
7	446	442	14
8	944	954	11
9	344	321	17
14	578	565	16
15	485	454	18
	4,	8, L	
0	299	283	17
1	264	268	18
2	318	312	15
4	779	730	11
5	552	557	12
6	577	574	13
7	306	281	18
9	204	144	27
10	521	562	15
12	234	249	30
13	219	171	31

L	KFO	FC	SIG
14	313	298	24
	4,	9, L	
0	1183	1143	9
1	859	823	10
3	857	810	11
4	357	365	18
5	1048	1055	11
6	624	573	13
7	438	436	15
8	356	355	17
	4,	10, L	
3	198	231	29
4	204	245	31
5	448	444	16
6	506	514	15
7	295	322	23
9	302	323	23
12	324	348	24
	4,	11, L	
0	1261	1258	11
1	424	462	17
2	255	260	25
4	1022	1025	12
5	328	356	20
7	345	329	20
8	250	226	27
9	206	207	32
	4,	12, L	
0	735	744	13
1	448	432	17
3	445	418	17
5	270	271	25
7	588	594	15
	4,	13, L	
0	300	278	24
1	419	376	19
3	801	794	14
4	289	318	26
5	332	318	22
7	222	209	33
	4,	14, L	
1	447	483	20
	5,	0, L	
2	881	889	7
4	2147	2101	6
8	385	332	13
10	1424	1495	9
12	1171	1163	11
14	441	390	17
16	634	622	16
	5,	1, L	
2	970	1063	6
3	1332	1234	6
4	739	738	7

L	KFO	FC	SIG
5	795	856	8
6	680	647	9
7	1099	1073	8
8	533	541	11
9	1411	1471	9
10	949	918	10
12	815	843	12
13	556	509	14
14	608	617	15
15	383	406	20
16	495	461	17
17	414	396	22
	5,	2, L	
1	1616	1442	6
2	1965	1890	6
3	1490	1423	6
4	1844	1711	7
6	530	540	10
7	176	238	22
8	953	906	9
9	484	503	12
10	563	569	12
11	447	456	14
13	394	383	19
15	402	380	20
	5,	3, L	
1	1180	1050	6
2	1508	1505	6
3	393	347	10
4	1045	971	7
5	297	275	13
6	865	885	9
8	682	687	10
9	1155	1145	10
10	983	974	10
11	257	314	23
12	214	234	28
13	573	579	14
16	479	466	19
	5,	4, L	
1	639	593	8
2	266	281	14
3	611	607	9
4	408	394	11
5	745	759	9
7	516	556	12
8	496	500	12
9	392	373	15
10	205	227	27
12	309	303	20
13	484	457	16
	5,	5, L	
1	1048	1041	8
2	223	214	17

[(CH3O)3P]3 CR (CO)2 (CS)
COLUMNS ARE 10FO,10FC, 10SIG

L	KFO	FC	SIG
	5,	5, L	
3	1314	1237	8
4	717	704	9
6	296	279	16
9	1348	1304	10
10	257	238	22
11	737	761	13
12	254	246	26
13	468	444	17
14	264	244	26
15	542	530	16
	5,	6, L	
1	364	346	13
2	683	673	9
4	573	650	11
5	566	569	11
7	399	377	14
8	363	357	16
9	813	818	11
10	817	869	12
11	460	490	16
12	874	826	12
13	428	412	17
	5,	7, L	
1	346	399	14
2	1485	1446	9
3	721	649	10
4	311	286	15
5	698	658	11
6	1549	1504	9
7	408	440	16
8	276	273	20
10	768	800	12
11	226	271	30
12	486	477	16
	5,	8, L	
1	289	305	18
2	384	335	14
3	443	455	14
4	370	359	15
5	231	220	24
6	705	694	12
9	344	357	20
10	785	793	13
11	265	270	24
12	379	376	20
13	512	496	17
14	433	411	19
	5,	9, L	
1	1284	1253	10
2	455	442	15
3	785	785	11
4	268	308	24
5	898	895	11

L	KFO	FC	SIG
7	596	562	14
8	436	430	17
13	348	313	23
	5,	10, L	
1	409	362	16
2	523	497	14
3	299	314	22
4	345	323	18
5	342	324	19
7	566	596	15
8	287	290	23
9	389	348	20
	5,	11, L	
1	432	412	16
2	898	874	12
6	561	556	16
7	201	134	30
8	271	280	26
	5,	12, L	
3	439	452	18
4	216	221	32
6	430	456	19
8	285	267	26
	5,	13, L	
1	478	460	19
3	393	404	20
5	592	549	17
	6,	0, L	
0	1697	1559	6
2	2477	2416	6
4	688	660	8
6	1004	1012	8
8	565	575	11
10	283	279	20
16	507	464	18
	6,	1, L	
0	1198	1163	6
2	277	219	12
3	884	908	8
4	881	841	8
5	605	564	9
8	1426	1497	9
9	841	806	11
10	1074	1076	10
11	710	724	12
15	606	564	15
	6,	2, L	
0	1690	1647	6
1	438	436	10
2	220	183	16
3	1475	1362	7
4	540	514	9
5	379	388	11
6	154	146	24

L	KFO	FC	SIG
8	538	489	11
9	425	432	14
10	484	457	13
12	335	335	19
14	260	196	24
15	363	352	21
	6,	3, L	
0	1385	1250	7
1	1210	1201	7
3	1126	1074	8
4	483	521	10
7	326	300	14
8	458	436	13
10	288	333	20
12	361	375	19
13	206	199	29
14	345	354	22
15	392	392	19
	6,	4, L	
1	562	490	9
2	406	355	11
3	815	837	9
5	182	219	22
7	585	571	11
11	1093	1110	11
	6,	5, L	
0	328	306	13
2	243	236	17
3	319	273	14
4	1043	1025	9
5	770	763	10
6	437	447	13
7	1229	1264	10
8	532	520	13
9	307	336	19
10	269	222	22
11	966	981	12
12	403	395	19
13	277	265	25
15	323	354	24
	6,	6, L	
0	863	825	9
4	940	918	10
8	313	338	19
9	203	175	28
10	599	601	14
11	313	330	23
12	628	653	15
	6,	7, L	
0	362	351	16
2	1226	1196	9
3	910	938	10
4	1098	1095	10
8	391	428	17

```
((CH30)3P33 CR (CO)2 (CS)
      COLUMNS ARE 10FO,10FC,   10SIG
```

L	KFO	FC	SIG
	5,	5,	L
3	1314	1237	8
4	717	704	9
6	296	279	16
9	1348	1304	10
10	257	238	22
11	737	761	13
12	254	246	26
13	468	444	17
14	264	244	26
15	542	530	16
	5,	6,	L
1	364	346	13
2	683	673	9
4	573	650	11
5	566	569	11
7	399	377	14
8	363	357	16
9	813	818	11
10	817	869	12
11	460	490	16
12	874	826	12
13	428	412	17
	5,	7,	L
1	346	399	14
2	1485	1446	9
3	721	649	10
4	311	286	15
5	698	658	11
6	1549	1504	9
7	408	440	16
8	276	273	20
10	768	800	12
11	226	271	30
12	486	477	16
	5,	8,	L
1	289	305	18
2	384	335	14
3	443	455	14
4	370	359	15
5	231	220	24
6	705	694	12
9	344	357	20
10	785	793	13
11	265	270	24
12	379	376	20
13	512	496	17
14	433	411	19
	5,	9,	L
1	1284	1253	10
2	455	442	15
3	785	785	11
4	268	308	24
5	898	895	11

L	KFO	FC	SIG
7	596	562	14
8	436	430	17
13	348	313	23
	5,	10,	L
1	409	362	16
2	523	497	14
3	299	314	22
4	345	323	18
5	342	324	19
7	566	596	15
8	287	290	23
9	389	348	20
	5,	11,	L
1	432	412	16
2	898	874	12
6	561	556	16
7	201	134	30
8	271	280	26
	5,	12,	L
3	439	452	18
4	216	221	32
6	430	456	19
8	285	267	26
	5,	13,	L
1	478	460	19
3	393	404	20
5	592	549	17
	6,	0,	L
0	1697	1559	6
2	2477	2416	6
4	688	660	8
6	1004	1012	8
8	565	575	11
10	283	279	20
16	507	464	18
	6,	1,	L
0	1198	1163	6
2	277	219	12
3	884	908	8
4	881	841	8
5	605	564	9
8	1426	1497	9
9	841	806	11
10	1074	1076	10
11	710	724	12
15	606	564	15
	6,	2,	L
0	1690	1647	6
1	438	436	10
2	220	183	16
3	1475	1362	7
4	540	514	9
5	379	388	11
6	154	146	24

L	KFO	FC	SIG
8	538	489	11
9	425	432	14
10	484	457	13
12	335	335	19
14	260	196	24
15	363	352	21
	6,	3,	L
0	1385	1250	7
1	1210	1201	7
3	1126	1074	8
4	483	521	10
7	326	300	14
8	458	436	13
10	288	333	20
12	361	375	19
13	206	199	29
14	345	354	22
15	392	392	19
	6,	4,	L
1	562	490	9
2	406	355	11
3	815	837	9
5	182	219	22
7	585	571	11
11	1093	1110	11
	6,	5,	L
0	328	306	13
2	243	236	17
3	319	273	14
4	1043	1025	9
5	770	763	10
6	437	447	13
7	1229	1264	10
8	532	520	13
9	307	336	19
10	269	222	22
11	966	981	12
12	403	395	19
13	277	265	25
15	323	354	24
	6,	6,	L
0	863	825	9
4	940	918	10
8	313	338	19
9	203	175	28
10	599	601	14
11	313	330	23
12	628	653	15
	6,	7,	L
0	362	351	16
2	1226	1196	9
3	910	938	10
4	1098	1095	10
8	391	428	17

((CH3O)3P)3 CR (CO)2 (CS)
COLUMNS ARE 10FO,10FC, 10SIG

L	KFO	FC	SIG
	6,	7, L	
10	447	467	17
12	535	509	16
14	723	728	15
	6,	8, L	
0	1580	1484	9
1	513	517	13
2	748	744	11
3	512	492	14
5	233	233	24
7	408	432	17
8	791	799	12
10	399	357	19
11	670	665	15
	6,	9, L	
0	1007	1001	11
2	360	334	17
3	985	993	11
5	473	491	15
7	787	797	13
9	261	265	24
11	531	527	17
12	245	234	29
	6,	10, L	
0	681	647	13
1	785	808	12
2	272	212	21
3	520	530	15
5	318	308	22
7	419	419	19
9	222	251	32
10	269	250	27
	6,	11, L	
2	287	279	24
4	390	358	18
5	307	338	23
6	435	414	18
7	212	195	34
8	207	180	33
	6,	12, L	
0	288	276	23
1	463	410	17
3	224	184	29
4	458	470	18
6	472	479	19
7	235	303	34
	6,	13, L	
2	239	230	30
3	576	554	17
4	293	276	27
	7,	0, L	
2	706	792	9
4	1540	1571	8
8	231	254	22
10	454	476	14
12	661	659	14
14	690	721	15
16	331	333	24
	7,	1, L	
1	617	592	9
2	1452	1476	7
3	424	443	11
4	196	252	20
5	158	115	23
6	395	370	13
7	237	247	19
8	649	661	11
9	845	893	11
10	411	419	15
12	554	537	15
15	250	280	28
16	479	489	19
	7,	2, L	
1	590	585	9
2	296	273	14
4	401	426	12
5	882	911	9
6	263	303	17
8	623	614	11
9	258	269	21
10	563	580	13
11	456	435	15
13	336	337	21
14	236	185	27
	7,	3, L	
1	512	538	10
2	1172	1202	8
3	1338	1327	8
4	205	199	21
6	236	257	19
7	602	635	12
8	1128	1176	10
9	583	579	13
10	228	248	25
11	225	219	25
13	550	554	15
	7,	4, L	
1	277	266	15
2	544	513	10
3	832	805	9
4	365	389	14
5	925	916	10
9	936	932	11
11	260	261	25
14	226	242	30
15	489	519	18
	7,	5, L	
1	639	676	10
2	945	954	9
3	333	347	15
5	956	976	10
6	908	911	10
7	797	798	11
8	862	857	11
9	647	666	13
11	192	150	31
13	683	688	14
	7,	6, L	
1	647	673	11
3	302	298	18
4	527	458	12
6	366	342	16
9	864	843	12
10	502	494	16
11	456	488	17
13	224	208	31
14	362	347	21
	7,	7, L	
1	401	375	14
2	408	388	15
4	542	544	13
5	248	217	22
6	499	501	14
7	713	756	13
8	507	479	15
10	263	257	25
12	715	743	15
	7,	8, L	
1	437	431	15
2	693	688	12
6	458	429	16
7	779	789	13
8	695	731	14
10	693	708	14
11	298	294	23
12	317	284	24
	7,	9, L	
1	661	651	13
3	501	505	15
4	636	656	14
5	345	318	19
6	503	497	15
7	240	280	28
9	494	481	16
	7,	10, L	
2	312	275	21
5	483	491	17
6	393	416	19
7	285	281	26
8	482	474	17
9	491	509	18
	7,	11, L	

[(CH3O)3P]3 CR (CO)2 (CS)
COLUMNS ARE 10FO,10FC, 10SIG

L	KFO	FC	SIG
7, 11, L			
1	280	272	25
6	256	228	28
8	627	621	16
7, 12, L			
3	267	271	27
6	563	545	17
8, 0, L			
0	478	509	11
2	295	243	15
4	1032	1103	9
6	446	507	13
8	352	334	16
10	226	187	25
14	282	309	25
8, 1, L			
0	256	284	16
1	483	511	11
3	662	643	10
5	319	322	16
8	203	172	25
9	287	303	20
11	251	297	25
12	241	245	27
14	239	239	28
8, 2, L			
0	398	439	13
1	931	916	9
2	645	704	10
3	1397	1479	9
5	365	376	15
7	258	248	20
8	227	240	25
9	394	400	16
12	429	420	17
15	511	518	18
8, 3, L			
0	1169	1164	9
1	589	582	10
2	605	575	11
3	281	303	17
4	808	863	10
5	601	601	11
7	400	391	16
8	312	320	19
11	294	317	22
13	248	213	27
8, 4, L			
0	1220	1267	9
1	650	609	11
3	813	803	10
4	1003	1031	10
6	448	472	14
7	406	400	15

L	KFO	FC	SIG
8	655	697	13
9	598	602	14
12	243	201	26
14	305	260	24
8, 5, L			
0	211	209	23
1	198	254	25
3	450	440	13
4	801	789	11
6	319	295	19
7	568	560	13
8	692	706	13
9	558	559	14
14	312	330	24
8, 6, L			
0	677	654	11
1	815	810	11
2	1112	1037	10
3	197	209	25
5	447	451	15
6	394	369	17
7	779	770	12
8	612	611	14
11	790	786	13
12	284	301	26
8, 7, L			
0	310	346	19
1	540	533	13
2	561	567	13
3	348	370	17
5	717	712	12
6	198	159	29
9	245	220	26
11	329	397	23
8, 8, L			
0	886	863	11
1	221	233	26
2	239	244	25
5	505	467	15
6	543	578	15
7	407	410	19
9	590	581	15
10	333	329	23
11	443	390	18
8, 9, L			
0	243	244	27
1	215	232	30
2	207	116	26
3	468	468	16
5	338	339	22
6	404	415	19
8	273	306	28
8, 10, L			
0	617	613	14

L	KFO	FC	SIG
4	399	398	18
5	233	209	29
6	823	841	14
7	722	693	15
8	231	209	30
8, 11, L			
3	248	272	28
4	287	317	26
7	390	417	21
8, 12, L			
0	215	158	29
1	441	432	19
9, 0, L			
2	1456	1486	9
4	260	256	19
6	834	836	11
8	317	286	19
12	212	241	30
14	536	496	17
9, 1, L			
1	519	506	12
2	253	261	20
5	303	273	17
7	564	589	13
8	487	536	15
11	480	490	16
12	189	80	31
14	393	373	21
9, 2, L			
1	673	684	10
3	1226	1215	9
5	1465	1503	10
6	882	869	11
7	666	692	12
8	228	226	25
10	187	61	29
11	262	264	25
12	252	263	27
13	502	436	17
14	341	294	22
9, 3, L			
2	613	600	11
4	443	421	14
5	607	641	12
6	763	776	12
7	186	138	28
8	338	332	19
11	372	401	20
12	848	868	13
13	414	391	20
9, 4, L			
1	769	766	11
2	1722	1745	9
3	737	751	11

[(CH3O)3P]3 CR (CO)2 (CS).
COLUMNS ARE 10FO,10FC, 10SIG

L	KFO	FC	SIG
	9,	4,	L
4	598	629	13
5	1017	1065	11
6	1138	1089	10
9	369	354	19
10	481	506	17
12	371	372	22
13	551	530	17
	9,	5,	L
1	318	290	17
2	317	348	18
3	249	208	22
4	287	288	20
6	572	611	14
7	314	294	20
10	239	259	27
12	614	621	16
13	402	394	21
	9,	6,	L
1	857	793	11
2	332	357	18
3	763	755	12
4	451	462	16
5	523	513	14
6	441	423	15
9	754	736	13
11	428	415	18
12	482	492	19
	9,	7,	L
1	422	395	17
2	725	720	13
3	197	149	28
4	463	449	16
6	224	239	29
8	457	448	18
9	597	573	15
	9,	8,	L
1	372	365	18
2	237	221	25
6	430	426	18
7	498	480	17
8	638	623	15
9	444	398	18
10	395	384	21
	9,	9,	L
1	320	339	22
3	333	351	21
4	388	397	20
6	342	329	22
7	597	565	16
8	393	389	21
	9,	10,	L
2	458	435	18
5	531	489	17

L	KFO	FC	SIG
7	226	152	30
	9,	11,	L
2	283	274	26
3	311	330	24
	10,	0,	L
2	375	405	15
4	1286	1293	10
6	324	363	20
8	732	745	13
10	534	547	15
12	443	448	19
	10,	1,	L
0	666	669	11
2	578	585	13
3	208	199	24
5	584	608	13
6	677	706	13
8	476	496	17
9	293	347	22
12	610	595	15
13	279	277	27
	10,	2,	L
0	218	248	23
1	526	540	13
3	1221	1223	10
4	397	390	16
5	323	365	20
6	335	350	19
7	783	786	12
11	713	668	14
13	206	173	34
	10,	3,	L
0	214	194	23
1	720	727	11
4	319	327	20
5	207	208	27
7	487	508	15
8	336	328	20
9	534	577	16
10	205	225	34
11	308	292	24
	10,	4,	L
0	1022	1062	11
3	560	556	13
4	1046	1010	11
5	704	722	13
6	407	418	18
8	675	684	13
9	338	305	21
10	429	415	19
12	367	392	22
	10,	5,	L
0	763	770	12
1	547	544	13

L	KFO	FC	SIG
2	214	203	26
4	318	330	20
5	706	718	13
6	282	289	23
8	240	272	28
11	399	393	20
	10,	6,	L
0	880	817	12
1	1196	1184	11
2	270	274	24
4	455	483	16
5	252	242	25
7	902	907	13
8	264	295	27
11	510	496	18
	10,	7,	L
0	592	593	15
1	772	742	13
3	376	421	19
4	413	445	19
5	217	166	28
	10,	8,	L
0	1112	1086	12
1	727	698	13
2	542	553	16
4	333	325	22
6	602	599	15
7	427	451	20
8	226	193	32
	10,	9,	L
0	436	467	18
2	501	502	16
3	433	439	18
4	225	216	30
5	481	441	17
7	472	490	19
	10,	10,	L
0	562	535	16
1	313	290	25
3	254	245	30
4	218	200	31
	10,	11,	L
0	289	263	26
	11,	0,	L
6	1024	1011	12
8	842	837	13
10	245	260	28
12	1129	1108	13
	11,	1,	L
1	528	506	13
2	186	207	30
7	1056	1057	12
8	502	497	16
11	344	363	22

F.(CH3O)3P33 CR (CO)2 (CS)

COLUMNS ARE 10FO,10FC, 10SIG

L	KFO	FC	SIG
	11,	2,	L
4	443	444	15
5	1055	1039	11
6	311	298	21
7	209	237	31
9	664	673	15
11	543	513	17
12	212	151	34
	11,	3,	L
1	274	226	21
2	330	345	19
3	193	177	29
4	257	254	25
6	541	525	15
8	284	276	23
9	595	585	14
	11,	4,	L
3	319	292	20
4	498	543	16
5	193	199	31
6	586	607	14
7	844	879	13
8	346	297	20
10	332	317	22
	11,	5,	L
2	639	637	14
3	234	241	28
4	231	189	27
5	196	227	32
6	288	284	23
7	242	268	28
8	319	299	24
10	346	347	21
	11,	6,	L
1	462	429	16
2	604	604	15
3	464	473	17
5	421	446	18
6	594	579	15
8	366	379	21
9	618	593	16
	11,	7,	L
1	732	761	13
4	399	417	19
5	215	190	30
6	236	257	29
7	255	274	28
8	315	249	23
	11,	8,	L
2	744	750	14
3	344	332	21
6	282	293	27
7	333	319	22
	11,	9,	L
1	455	426	18
2	267	269	27
4	297	283	23
	11,	10,	L
1	469	459	20
	12,	0,	L
0	552	563	14
2	430	423	16
4	219	195	29
8	328	325	22
10	617	600	16
	12,	1,	L
0	299	305	21
1	453	448	16
2	377	415	18
3	298	310	21
4	214	266	30
8	267	263	26
10	718	696	15
	12,	2,	L
0	366	386	19
1	432	446	16
2	295	256	20
4	252	252	26
5	379	375	19
6	298	258	22
7	720	710	14
8	216	163	31
	12,	3,	L
0	323	326	21
3	319	328	21
5	251	258	27
7	411	388	20
9	535	522	17
10	219	244	34
	12,	4,	L
0	377	376	19
5	409	413	19
6	421	405	18
7	303	319	24
8	460	504	19
9	429	452	20
	12,	5,	L
0	204	178	31
4	311	384	25
5	387	379	20
6	440	435	19
7	415	431	20
	12,	6,	L
1	909	929	13
6	371	356	20
7	589	590	16
8	348	361	23
	12,	7,	L
0	871	865	14
1	276	325	27
4	250	219	29
5	328	338	23
6	231	217	31
	12,	8,	L
0	722	730	15
2	346	316	22
3	299	303	24
4	243	274	30
	13,	0,	L
4	740	726	14
6	686	664	14
	13,	1,	L
1	247	295	28
3	279	306	25
4	308	336	24
5	756	728	13
6	360	363	22
8	554	519	17
9	224	204	32
	13,	2,	L
7	715	720	14
	13,	3,	L
2	360	358	20
4	329	329	23
5	286	296	25
6	445	461	20
7	426	439	20
8	331	326	23
	13,	4,	L
1	620	646	16
2	316	325	23
6	671	684	15
7	581	600	17
	13,	5,	L
1	464	489	19
3	448	451	19
5	482	483	18
	13,	6,	L
1	347	377	24
2	475	442	18
3	359	373	22
5	258	255	29
	13,	7,	L
2	749	719	15
	14,	0,	L
0	417	447	19
6	488	490	19
	14,	1,	L
0	488	457	17
3	871	900	14
4	511	502	17
5	260	316	30

((CH3O)3P)3 CR (CO)2 (CS)

COLUMNS ARE 10FO,10FC, 10SIG

L	KFO	FC	SIG	L	KFO	FC	SIG	L	KFO	FC	SIG
	14,	2, L		0	459	411	18	1	423	397	20
0	526	508	17	1	428	457	19	2	208	221	33
3	219	225	31	2	445	502	19	4	279	284	25
4	279	270	27	4	898	920	14		14,	5, L	
5	625	645	16	5	244	250	32	0	575	571	17
6	213	156	33		14,	4, L		1	490	515	19
	14,	3, L		0	341	352	24	2	290	234	24

Table A.3. Final Positional Parameters for $Cr(CO)_2(CS)[(MeO)_3P]_3$ (mer I) and Their Estimated Standard Deviations

Atom	X	Y	Z	BISO[a]
Cr	0.19911(9)	0.38303(9)	0.38742(7)	2.43(7)
P1	0.32792(15)	0.41733(16)	0.43546(12)	2.82(11)
P2	0.23895(15)	0.44281(15)	0.27786(12)	2.67(11)
P3	0.07087(15)	0.33602(16)	0.34657(13)	2.81(11)
C1	0.1663(5)	0.3483(5)	0.4733(5)	2.9(4)
S	0.13294(20)	0.32226(20)	0.54977(14)	5.17(15)
C2	0.2478(6)	0.2782(6)	0.3610(5)	3.1(4)
O2	0.2780(5)	0.2140(4)	0.3418(4)	5.6(4)
C3	0.1580(6)	0.4919(6)	0.4097(5)	3.0(4)
O3	0.1317(4)	0.5600(4)	0.4251(4)	4.8(4)
O11	0.3437(4)	0.5118(4)	0.4690(3)	3.8(3)
C11	0.3014(7)	0.5356(8)	0.5336(6)	6.0(6)
O12	0.4058(4)	0.4123(4)	0.3830(3)	3.5(3)
C12	0.4958(6)	0.4274(7)	0.4062(6)	5.2(6)
O13	0.3613(4)	0.3626(4)	0.5018(4)	4.5(3)
C13	0.3648(7)	0.2686(7)	0.4986(7)	6.0(6)
O21	0.2931(4)	0.3858(4)	0.2242(3)	4.0(3)
C21	0.2585(7)	0.3154(6)	0.1832(5)	4.9(6)
O22	0.2993(4)	0.5250(4)	0.2876(3)	3.6(3)
C22	0.3387(7)	0.5691(7)	0.2268(5)	5.1(6)
O23	0.1675(4)	0.4755(4)	0.2239(3)	3.7(3)
C23	0.1101(7)	0.5445(7)	0.2413(6)	5.1(6)
O31	-0.0097(4)	0.4015(4)	0.3464(3)	4.0(3)
C31	-0.0444(7)	0.4313(7)	0.4122(6)	5.4(6)
O32	0.0238(4)	0.2580(4)	0.3858(3)	3.9(3)
C32	0.0672(7)	0.1753(7)	0.4016(6)	5.2(6)
O33	0.0683(4)	0.3071(4)	0.2664(3)	3.6(3)
C33	-0.0101(6)	0.2719(7)	0.2333(5)	4.5(6)

[a] BISO is the arithmetic mean of the principal axes of the thermal ellipsoid.

Table A.4. Final Thermal Parameters for $Cr(CO)_2(CS)[(MeO)_3P]_3$ (mer I) and Their Estimated Standard Deviations

Atom	U11	U22	U33	U12	U13	U23
Cr	2.76(8)	3.07(9)	3.41(8)	0.04(7)	-0.08(7)	0.15(7)
P1	3.14(14)	3.88(15)	3.71(15)	-0.08(12)	-0.37(12)	0.18(12)
P2	3.30(14)	3.40(14)	3.47(13)	-0.00(12)	0.15(12)	0.04(12)
P3	3.07(14)	3.58(14)	4.02(14)	-0.09(12)	-0.05(12)	0.49(13)
C1	3.1(5)	3.0(5)	4.9(6)	-0.6(4)	-0.9(5)	-0.1(5)
S	7.88(21)	7.55(21)	4.23(17)	-0.85(17)	0.88(16)	1.01(16)
C2	3.2(5)	3.5(6)	5.1(6)	0.9(4)	-0.4(5)	0.0(5)
O2	8.1(5)	5.4(5)	7.6(5)	2.1(4)	-1.0(4)	-0.7(4)
C3	3.8(6)	3.4(6)	4.2(6)	-0.0(5)	0.3(5)	-1.4(5)
O3	6.7(5)	4.4(4)	6.9(5)	0.7(4)	0.8(4)	-1.4(4)
O11	4.1(4)	4.9(4)	5.4(4)	-0.9(3)	0.3(3)	-1.8(4)
C11	7.0(8)	8.7(9)	7.1(8)	0.7(7)	0.9(7)	-4.3(7)
O12	2.9(4)	6.0(4)	4.5(4)	0.4(3)	-0.5(3)	-0.7(3)
C12	2.8(6)	7.9(8)	9.2(9)	-1.1(6)	-0.7(6)	-1.9(7)
O13	4.7(4)	6.6(5)	5.7(4)	-1.3(4)	-1.9(4)	1.7(4)
C13	6.5(7)	5.5(8)	10.9(9)	0.3(6)	-3.3(7)	3.9(7)
O21	5.1(4)	4.9(4)	5.1(4)	0.0(3)	0.9(4)	-1.1(3)
C21	8.0(8)	5.0(7)	5.6(7)	0.0(6)	-0.1(7)	-1.7(6)
O22	4.4(4)	4.8(4)	4.6(4)	-1.3(3)	-0.2(3)	0.0(3)
C22	8.4(8)	5.6(7)	5.3(7)	-2.8(7)	2.2(6)	2.0(6)
O23	5.1(4)	4.7(4)	4.2(4)	0.0(4)	-0.5(3)	0.5(3)
C23	5.5(7)	5.7(7)	8.3(8)	2.1(6)	-1.5(6)	-0.2(7)
O31	3.8(4)	5.8(4)	5.5(4)	1.1(3)	-0.5(3)	0.2(4)
C31	5.6(7)	6.5(8)	8.2(8)	1.5(6)	2.7(7)	-1.6(7)
O32	4.4(4)	4.9(4)	5.3(4)	-1.4(3)	-0.1(3)	1.1(3)
C32	7.2(8)	4.7(7)	7.7(8)	-1.0(6)	-0.4(7)	0.6(6)
O33	4.1(4)	5.3(4)	4.4(4)	-0.6(3)	0.5(3)	-0.7(3)
C33	5.4(6)	6.4(7)	5.4(7)	-2.3(6)	-1.6(6)	-0.9(6)

[a]All the UIJ values have been multiplied by 100.

References

1. E.J. Gabe, A.C. Larson, F.L. Lee and Y. Wang, The NRC PDP-8e Crystal Structure System, NRC, Ottawa, Ontario, Canada, 1979.

2. International Tables for X-Ray Crystallography, Kynoch Press, Birmingham, England, Vol. IV, 1979, Tables 2.28-2.31.

Appendix B

Structural Characterization of the mer I Isomer of $Cr(CO)_2(CSe)[(MeO)_3P]_3$: X-Ray Data Collection, Structure Solution and Refinement

Table B.1. Crystallographic Data for X-ray Diffraction Study of $Cr(CO)_2(CSe)[(MeO)_3P]_3$

Crystal Parameters

crystal system = orthorhombic

space group = Pbca

a = 15.483(3) Å

b = 15.213(5) Å

c = 18.997(3) Å

V = 4474.6 $Å^3$

Z = 8

calcd density = 2.396 g cm^{-3}

temp = 118 K

formula = $C_{12}H_{27}O_{11}SeP_3Cr$

mol wt = 570.9 g mol^{-1}

Measurement of Intensity Data and Structure Solution

Enraf-Nonius CAD-4 diffractometer at 118 K, coupled to a VACS SDP computing system
lattice parameters by least-squares refinement of 25 medium-angle settings
range of hkl: h 0-16, k 0-18, l 0-22
$\omega/2\theta$ scan
graphite-monochromated MoKα radiation
4 standard reflections (2 2 6, 0 0 10, 4 6 0, 8 0 0): 1% variation (72.1 h exposure)
4398 unique reflections measured, 3091 with $I > 3\sigma(I)$ used
intensities corrected for Lorentz and polarization effects and for absorption
structure solved by Patterson and Fourier methods, full-matrix least-squares anisotropic refinements (254 variables) with the H atoms being included in the structure factor calculations but not refined
R_F = 0.042
R_{wF} = 0.062

Table B.2. Observed and Calculated Structure Factors for $Cr(CO)_2(CSe)[(MeO)_3P]_3$ (<u>mer</u> I)

Values of 10*Fobs and 10*Fcalc

H	K	L	Fobs	Fcalc	SigF
0	0	2	541	573	2
0	0	4	195	250	5
0	0	6	2717	3106	10
0	0	8	364	344	5
0	0	10	1327	1435	4
0	0	12	879	957	4
0	0	14	666	678	5
0	0	16	147	116	21
0	0	18	2785	2642	5
0	0	22	391	330	13
0	1	0	80	0	3
0	1	1	137	0	3
0	2	0	379	366	2
0	2	1	3118	3236	6
0	2	2	1060	1098	2
0	2	3	711	730	2
0	2	4	1087	1184	2
0	2	5	1910	2103	9
0	2	6	1884	2096	3
0	2	7	1714	1976	3
0	2	9	712	808	4
0	2	10	1557	1751	4
0	2	11	956	1219	6
0	2	13	790	768	5
0	2	14	333	407	10
0	2	15	564	597	7
0	2	16	1270	1212	5
0	2	17	397	490	12
0	2	18	501	518	9
0	2	19	806	808	8
0	2	20	1369	1120	6
0	4	0	1063	923	2
0	4	1	944	924	2
0	4	2	1078	1023	2
0	4	3	3506	3830	9
0	4	4	2131	2245	3
0	4	5	2086	2279	3
0	4	6	123	183	11
0	4	7	397	396	5
0	4	8	456	484	5
0	4	9	678	696	4
0	4	11	386	391	7
0	4	13	1733	1819	4
0	4	15	1015	1025	5
0	4	16	587	696	9
0	4	17	821	829	7
0	4	18	952	949	7
0	4	19	1054	990	7
0	4	21	608	569	10
0	4	22	855	750	9
0	6	0	126	129	12
0	6	1	1202	1115	3
0	6	2	1181	1175	3
0	6	3	2531	2597	3
0	6	4	1241	1219	3
0	6	6	1054	1147	4
0	6	7	208	197	9
0	6	8	1430	1562	4
0	6	10	1384	1411	4
0	6	12	140	129	19
0	6	13	504	560	7
0	6	14	262	360	14
0	6	15	1307	1291	5
0	6	16	227	315	18
0	6	17	485	446	9
0	6	19	409	432	13
0	6	20	1171	1086	7
0	6	21	1069	994	8
0	8	0	1753	1701	3
0	8	1	1138	1063	4
0	8	2	154	113	13
0	8	3	1366	1351	4
0	8	4	1013	1084	4
0	8	5	998	967	4
0	8	6	1371	1395	4
0	8	7	1007	1013	4
0	8	8	2716	2809	4
0	8	9	442	440	7
0	8	10	2196	2318	4
0	8	12	384	396	9
0	8	13	700	733	6
0	8	14	1006	997	6
0	8	15	879	852	6
0	8	16	244	188	16
0	8	17	455	425	10
0	8	18	555	538	9
0	8	19	507	476	11
0	8	20	441	411	12
0	10	0	737	699	5
0	10	1	379	369	7
0	10	2	661	642	5
0	10	3	1328	1405	4
0	10	4	862	850	5
0	10	5	1013	1052	5
0	10	6	598	585	6
0	10	7	716	735	6
0	10	8	881	910	5
0	10	10	671	714	6
0	10	11	699	691	6
0	10	12	354	367	11
0	10	13	776	790	7
0	10	14	541	524	9
0	10	15	1372	1379	6
0	10	16	770	764	7
0	10	17	436	436	11
0	10	18	306	291	16
0	12	0	771	698	6
0	12	1	232	259	13
0	12	2	1267	1250	5
0	12	3	656	662	6
0	12	4	604	624	7
0	12	5	1421	1505	5
0	12	7	953	1027	6
0	12	8	1270	1288	5
0	12	9	262	234	14
0	12	10	924	955	6
0	12	11	402	397	10
0	12	12	588	586	9
0	12	13	1027	1050	6
0	12	14	552	533	9
0	14	0	1208	1263	5
0	14	3	1101	1149	6
0	14	4	324	351	12
0	14	6	243	270	16
0	14	7	1122	1205	6
0	14	8	261	331	17
0	14	10	632	641	8
0	14	11	1552	1649	6
0	14	12	874	879	7
0	14	13	396	418	13
0	14	14	417	453	13
0	16	0	1268	1330	6
0	16	1	573	616	9
0	16	2	433	440	11
0	16	3	606	638	8
0	16	5	1100	1178	6
0	16	6	1229	1330	6
0	16	9	771	784	8
0	16	10	284	301	18
0	18	0	320	344	17
0	18	1	297	323	17
1	0	0	81	0	3
1	0	1	143	0	2
1	0	2	2851	2864	6
1	0	4	109	114	8
1	0	6	2489	2737	10
1	0	8	816	902	3
1	0	10	1036	1147	4
1	0	12	683	763	5
1	0	14	850	865	5
1	0	16	201	198	15
1	0	18	198	150	18
1	0	20	715	632	8
1	0	22	679	580	9
1	1	0	136	0	3
1	1	1	497	464	2
1	1	2	820	797	2
1	1	3	971	1017	2
1	1	4	1831	1971	8
1	1	5	499	503	3
1	1	6	2012	2214	10
1	1	9	948	995	3
1	1	10	684	714	4
1	1	11	170	187	12
1	1	12	869	907	4
1	1	13	350	361	8
1	1	14	1249	1303	5
1	1	19	301	432	16
1	1	22	336	309	15
1	2	1	3328	3032	6
1	2	2	959	915	2
1	2	3	446	452	3
1	2	4	1741	1817	2
1	2	5	1250	1302	2
1	2	6	1610	1720	3
1	2	[illegible]	195	293	8

Values of 10*Fobs and 10*Fcalc

H	K	L	Fobs	Fcalc	SigF
1	2	8	767	806	3
1	2	9	410	497	5
1	2	10	403	422	5
1	2	11	1033	1093	4
1	2	12	455	508	6
1	2	13	363	396	8
1	2	14	964	988	5
1	2	17	1617	1596	5
1	2	19	839	874	8
1	3	1	2112	1875	8
1	3	2	302	274	4
1	3	3	537	526	3
1	3	4	771	783	3
1	3	5	634	693	3
1	3	6	584	613	3
1	3	7	444	491	4
1	3	8	783	753	4
1	3	9	1433	1625	3
1	3	11	1731	1780	4
1	3	12	170	180	14
1	3	14	238	269	12
1	3	19	708	728	9
1	4	1	1658	1463	2
1	4	2	1100	986	2
1	4	3	2136	2093	2
1	4	4	955	978	3
1	4	5	105	74	12
1	4	6	1336	1465	3
1	4	7	142	132	11
1	4	8	360	401	5
1	4	9	1293	1378	4
1	4	10	282	333	8
1	4	11	592	611	5
1	4	12	753	742	5
1	4	13	299	341	9
1	4	14	688	682	6
1	4	15	287	391	14
1	4	16	599	608	7
1	4	19	223	626	31
1	5	1	1219	1202	3
1	5	2	978	901	3
1	5	3	701	672	3
1	5	4	747	754	3
1	5	5	675	652	4

H	K	L	Fobs	Fcalc	SigF
1	5	6	354	384	5
1	5	7	622	691	4
1	5	9	1338	1438	4
1	5	11	541	593	5
1	5	14	955	957	5
1	5	15	603	607	7
1	5	17	702	711	7
1	5	19	481	458	10
1	5	21	347	326	15
1	6	1	1392	1252	3
1	6	2	1553	1463	3
1	6	3	705	700	4
1	6	4	1563	1557	3
1	6	5	784	821	4
1	6	6	718	769	4
1	6	7	1323	1421	4
1	6	8	349	339	6
1	6	9	803	853	4
1	6	10	494	506	6
1	6	11	1223	1235	4
1	6	12	1190	1189	5
1	6	13	1161	1177	5
1	6	14	1377	1381	5
1	6	16	498	487	8
1	6	18	769	746	7
1	6	20	575	689	13
1	6	21	602	674	13
1	7	2	742	644	4
1	7	3	617	589	4
1	7	4	1267	1255	3
1	7	5	581	559	4
1	7	6	522	489	5
1	7	7	367	343	6
1	7	8	212	191	11
1	7	12	348	350	9
1	7	14	1308	1308	5
1	7	16	511	487	8
1	7	20	529	466	11
1	8	1	677	649	4
1	8	2	1452	1371	3
1	8	4	1668	1683	4
1	8	5	569	543	5
1	8	6	489	511	5
1	8	7	579	587	5

H	K	L	Fobs	Fcalc	SigF
1	8	8	689	695	5
1	8	9	637	670	5
1	8	11	222	231	13
1	8	12	995	1022	5
1	8	13	472	498	8
1	8	14	1465	1482	5
1	8	15	393	382	10
1	8	16	807	793	7
1	8	17	202	181	20
1	8	20	346	308	15
1	9	1	918	859	4
1	9	2	1496	1461	4
1	9	3	504	491	6
1	9	4	1541	1604	4
1	9	5	543	515	6
1	9	6	302	331	9
1	9	7	339	375	8
1	9	9	1098	1143	5
1	9	11	559	564	7
1	9	12	351	350	10
1	9	13	556	579	8
1	9	14	1009	1048	6
1	9	16	384	381	12
1	9	19	269	273	19
1	10	1	807	767	5
1	10	3	467	474	7
1	10	4	293	324	10
1	10	5	1362	1369	4
1	10	6	1151	1179	4
1	10	7	1893	1985	4
1	10	9	1394	1418	5
1	10	11	1578	1645	5
1	10	12	757	797	7
1	10	13	923	953	6
1	10	15	196	152	21
1	11	1	721	650	6
1	11	3	300	260	10
1	11	4	332	378	9
1	11	5	772	814	6
1	11	6	230	254	14
1	11	7	241	212	13
1	11	8	675	672	6
1	11	9	829	825	6
1	11	10	189	168	13

H	K	L	Fobs	Fcalc	SigF
1	11	11	634	634	7
1	11	13	534	565	9
1	11	17	431	402	12
1	12	1	522	496	7
1	12	2	356	332	10
1	12	3	572	564	7
1	12	4	341	343	10
1	12	5	1791	1825	5
1	12	6	631	665	7
1	12	8	477	499	8
1	12	9	1229	1260	5
1	12	10	510	503	8
1	12	11	219	233	18
1	12	12	254	260	17
1	12	13	791	787	7
1	12	14	445	450	11
1	12	15	431	424	11
1	12	16	617	608	9
1	13	1	905	909	6
1	13	2	299	266	12
1	13	3	468	478	9
1	13	4	815	828	6
1	13	5	219	289	18
1	13	6	695	755	7
1	13	7	538	582	8
1	13	8	340	351	12
1	13	11	398	422	12
1	13	12	270	288	16
1	13	13	263	265	17
1	13	14	742	750	8
1	13	15	359	348	14
1	14	2	561	568	8
1	14	3	229	228	17
1	14	4	705	739	7
1	14	6	1311	1407	5
1	14	7	502	521	9
1	14	8	410	408	11
1	14	9	1184	1234	6
1	14	10	409	412	12
1	14	11	680	701	8
1	14	12	905	961	7
1	14	13	584	605	10
1	15	2	158	209	22
1	15	3	294	302	15

Values of 10*Fobs and 10*Fcalc

H	K	L	Fobs	Fcalc	SigF
1	15	4	486	506	10
1	15	6	817	868	7
1	15	7	745	799	7
1	15	8	782	811	7
1	15	9	698	710	8
1	15	10	417	427	12
1	15	12	362	379	15
1	16	1	402	396	13
1	16	3	541	569	9
1	16	4	366	398	13
1	16	6	712	724	8
1	16	7	254	262	19
1	16	8	916	961	7
1	16	9	225	252	23
1	16	10	826	881	8
1	17	1	928	938	7
1	17	2	562	608	10
1	17	5	438	466	12
1	17	6	232	267	22
1	17	7	441	486	12
1	18	1	723	739	9
2	0	0	2756	2504	6
2	0	2	477	495	2
2	0	3	92	0	9
2	0	4	1680	1791	8
2	0	8	265	225	6
2	0	10	672	693	4
2	0	12	1463	1520	4
2	0	14	423	423	7
2	0	18	853	801	6
2	0	20	921	812	7
2	1	0	2684	2410	6
2	1	1	275	234	3
2	1	2	479	429	2
2	1	3	959	1003	2
2	1	4	788	830	2
2	1	5	1272	1308	2
2	1	6	1248	1280	3
2	1	7	1131	1243	3
2	1	8	1031	1099	3
2	1	9	232	265	7
2	1	10	1705	1764	8
2	1	11	372	411	6
2	1	12	1180	1230	4
2	1	13	1090	1143	4
2	1	14	598	598	6
2	1	15	496	490	7
2	1	16	166	153	18
2	1	18	1009	971	6
2	1	19	203	265	21
2	1	20	720	686	8
2	2	0	2447	2173	7
2	2	1	700	608	2
2	2	2	1297	1238	2
2	2	3	320	255	4
2	2	4	1884	1910	9
2	2	5	1184	1207	3
2	2	6	1517	1573	3
2	2	7	1002	1055	3
2	2	8	495	538	4
2	2	9	255	258	7
2	2	10	165	184	11
2	2	11	1436	1493	4
2	2	12	767	785	5
2	2	13	444	451	7
2	2	14	209	232	13
2	2	15	702	701	6
2	2	16	493	477	8
2	2	18	665	623	7
2	2	19	897	846	7
2	2	20	499	491	11
2	2	21	195	218	23
2	3	0	1513	1307	2
2	3	1	336	329	4
2	3	2	1109	1027	2
2	3	3	1508	1462	2
2	3	4	313	298	4
2	3	5	2660	2745	10
2	3	6	1548	1577	3
2	3	7	371	460	5
2	3	8	1193	1253	3
2	3	9	955	1064	4
2	3	10	921	999	4
2	3	11	1085	1138	4
2	3	12	417	441	7
2	3	13	1443	1520	4
2	3	14	614	635	6
2	3	15	964	974	5
2	3	16	857	845	6
2	3	19	197	200	20
2	3	21	224	245	21
2	4	0	301	247	5
2	4	1	1162	1014	3
2	4	2	180	170	7
2	4	3	1365	1275	3
2	4	4	293	298	5
2	4	5	1056	1041	3
2	4	6	1547	1526	3
2	4	8	1063	1045	3
2	4	9	696	709	4
2	4	10	840	863	4
2	4	11	612	624	5
2	4	12	627	684	5
2	4	13	510	539	6
2	4	14	786	773	5
2	4	15	372	368	9
2	4	16	996	961	5
2	4	17	507	502	8
2	4	18	604	592	8
2	4	19	812	746	7
2	4	20	405	368	12
2	5	0	3039	2685	10
2	5	1	739	617	3
2	5	2	1725	1534	3
2	5	3	2113	2022	3
2	5	4	1513	1472	3
2	5	5	1081	1114	3
2	5	6	968	971	3
2	5	7	1138	1083	3
2	5	8	878	865	4
2	5	10	1262	1285	4
2	5	11	496	487	6
2	5	12	248	234	10
2	5	13	774	766	5
2	5	15	1331	1344	5
2	5	16	614	602	7
2	5	17	372	369	11
2	5	18	514	501	9
2	5	19	167	58	23
2	5	20	464	461	11
2	5	21	418	517	16
2	6	1	798	705	3
2	6	2	516	447	4
2	6	3	1011	995	3
2	6	4	367	343	5
2	6	5	229	226	8
2	6	6	217	237	9
2	6	7	1066	1128	4
2	6	10	562	598	5
2	6	11	577	567	5
2	6	12	236	190	11
2	6	13	271	279	11
2	6	14	617	621	7
2	6	15	718	695	6
2	6	18	413	414	11
2	6	19	296	374	15
2	6	21	501	437	11
2	7	0	3954	3323	12
2	7	1	775	733	4
2	7	2	1423	1289	3
2	7	3	1507	1365	3
2	7	4	1430	1366	3
2	7	6	394	335	6
2	7	8	1729	1757	4
2	7	9	132	128	16
2	7	10	1719	1817	4
2	7	11	151	126	17
2	7	12	423	436	8
2	7	13	405	440	8
2	7	14	867	863	6
2	7	15	294	315	12
2	7	17	239	222	16
2	7	18	957	932	7
2	7	19	374	365	13
2	7	20	657	612	9
2	8	1	289	258	9
2	8	2	663	585	5
2	8	3	320	389	7
2	8	4	1005	1053	4
2	8	5	209	150	11
2	8	6	380	370	7
2	8	8	909	949	5
2	8	9	211	200	12
2	8	10	572	588	6
2	8	11	161	167	17
2	8	13	481	503	8

Values of 10*Fobs and 10*Fcalc

H	K	L	Fobs	Fcalc	SigF
2	8	14	699	706	7
2	8	17	237	224	17
2	8	20	464	429	12
2	9	2	683	613	5
2	9	3	1376	1319	4
2	9	4	1361	1278	4
2	9	5	569	536	6
2	9	7	526	554	6
2	9	8	348	364	9
2	9	9	559	555	6
2	9	10	883	861	5
2	9	11	316	314	10
2	9	12	169	192	19
2	9	13	569	563	7
2	9	15	1136	1147	6
2	9	16	587	565	8
2	9	17	227	207	18
2	9	18	536	527	10
2	9	19	345	315	15
2	10	0	466	466	7
2	10	1	644	594	6
2	10	2	540	491	6
2	10	3	891	840	5
2	10	4	1217	1200	4
2	10	5	845	861	5
2	10	7	813	840	5
2	10	9	474	510	7
2	10	11	411	410	9
2	10	13	283	274	13
2	10	14	362	369	11
2	10	15	217	217	19
2	10	16	416	418	11
2	10	17	257	284	18
2	11	0	1168	1032	5
2	11	1	1045	953	5
2	11	2	839	767	5
2	11	3	2119	1961	4
2	11	5	1891	1865	4
2	11	6	1011	1002	5
2	11	7	673	711	6
2	11	10	528	520	8
2	11	11	496	484	8
2	11	12	457	477	9
2	11	13	1106	1135	6
2	11	15	1030	1054	7
2	11	16	556	555	9
2	12	0	1941	1747	5
2	12	2	593	562	7
2	12	3	674	673	7
2	12	4	1216	1184	5
2	12	5	266	272	13
2	12	6	183	228	19
2	12	7	386	402	10
2	12	8	937	978	6
2	12	9	382	380	10
2	12	10	382	367	10
2	12	11	314	357	13
2	12	12	326	358	13
2	12	13	453	452	10
2	12	14	352	351	13
2	12	15	553	547	10
2	12	16	530	525	10
2	13	0	1585	1521	5
2	13	1	168	228	24
2	13	2	652	606	7
2	13	3	233	249	16
2	13	4	170	203	22
2	13	5	323	317	12
2	13	7	1148	1167	6
2	13	8	675	655	7
2	13	10	588	608	8
2	13	11	615	631	8
2	13	13	456	437	11
2	13	14	241	246	20
2	14	1	1218	1153	6
2	14	3	193	211	20
2	14	5	393	393	11
2	14	6	299	312	14
2	14	7	534	543	9
2	14	9	231	236	18
2	14	10	546	578	9
2	14	11	632	651	8
2	14	12	320	328	15
2	14	14	315	332	16
2	15	0	1599	1481	5
2	15	2	1162	1154	6
2	15	4	657	647	8
2	15	5	208	221	21
2	15	6	785	787	7
2	15	7	450	456	11
2	15	8	610	608	9
2	15	9	410	431	12
2	15	10	501	545	11
2	15	12	438	448	12
2	16	0	702	674	9
2	16	1	461	462	12
2	16	2	476	500	12
2	16	4	221	222	21
2	16	7	561	606	10
2	16	8	349	361	15
2	17	0	352	377	17
2	17	1	204	211	26
2	17	3	324	337	16
2	17	4	468	485	12
2	17	5	707	737	9
2	17	6	574	603	10
2	17	7	663	711	9
3	0	2	629	562	2
3	0	4	1017	1046	2
3	0	6	1114	1127	3
3	0	8	559	558	4
3	0	10	350	411	6
3	0	12	998	999	4
3	0	14	1127	1158	5
3	0	16	753	716	6
3	0	20	639	584	8
3	0	22	317	284	16
3	1	1	154	117	6
3	1	2	1594	1547	8
3	1	3	728	719	3
3	1	4	1579	1586	2
3	1	5	2021	1989	10
3	1	6	1076	1106	3
3	1	7	429	419	4
3	1	8	1147	1165	3
3	1	9	715	785	4
3	1	10	1322	1423	4
3	1	11	155	190	13
3	1	12	1575	1620	4
3	1	13	754	786	5
3	1	14	728	739	5
3	1	15	365	362	9
3	1	17	583	543	7
3	1	19	180	185	21
3	1	20	505	482	10
3	1	21	236	240	20
3	1	22	650	566	9
3	2	1	1047	952	2
3	2	2	97	81	11
3	2	3	172	161	7
3	2	4	2082	2120	9
3	2	5	1698	1686	3
3	2	7	298	291	6
3	2	8	1595	1583	3
3	2	9	1571	1698	3
3	2	10	783	797	4
3	2	11	716	729	4
3	2	13	528	556	6
3	2	14	1100	1114	5
3	2	15	243	245	12
3	2	17	302	303	12
3	2	19	515	462	9
3	2	21	505	431	10
3	2	22	216	182	22
3	3	1	2655	2416	9
3	3	2	688	578	3
3	3	3	329	361	4
3	3	5	210	198	7
3	3	6	1292	1286	3
3	3	7	1633	1685	3
3	3	8	433	428	5
3	3	9	345	383	6
3	3	10	1373	1443	4
3	3	11	1694	1743	4
3	3	12	1107	1129	4
3	3	13	1082	1119	5
3	3	14	535	521	6
3	3	16	834	823	6
3	3	17	753	741	6
3	3	18	289	247	13
3	3	19	524	503	9
3	3	20	257	229	17
3	3	21	237	207	19
3	4	1	2442	2206	10
3	4	3	573	557	3
3	4	4	1463	1423	3

Values of 10*Fobs and 10*Fcalc

H	K	L	Fobs	Fcalc	SigF	H	K	L	Fobs	Fcalc	SigF	H	K	L	Fobs	Fcalc	SigF	H	K	L	Fobs	Fcalc	SigF
3	4	5	812	775	3	3	6	11	221	225	12	3	9	6	1296	1261	4	3	12	1	836	769	6
3	4	6	253	258	7	3	6	13	893	900	5	3	9	7	578	581	6	3	12	2	1364	1295	5
3	4	7	1189	1205	3	3	6	14	1460	1496	5	3	9	8	225	251	13	3	12	4	731	703	6
3	4	8	339	361	6	3	6	16	170	172	21	3	9	9	1199	1212	5	3	12	5	418	410	9
3	4	9	1353	1368	4	3	6	17	730	695	7	3	9	10	390	405	9	3	12	6	1025	1031	5
3	4	10	195	258	11	3	6	18	421	397	11	3	9	11	389	355	9	3	12	7	1437	1447	5
3	4	11	963	988	4	3	6	19	368	376	12	3	9	12	1090	1069	5	3	12	9	409	411	10
3	4	12	841	796	5	3	6	20	269	231	17	3	9	13	245	253	14	3	12	10	496	492	9
3	4	13	1058	1082	5	3	7	1	204	192	10	3	9	14	607	599	7	3	12	11	1071	1087	6
3	4	14	622	595	6	3	7	2	1292	1214	3	3	9	15	474	477	9	3	12	12	224	213	18
3	4	15	187	202	16	3	7	4	1099	1047	4	3	9	16	419	415	10	3	12	13	369	342	12
3	4	16	409	397	9	3	7	5	1469	1392	4	3	9	18	267	244	17	3	12	14	373	401	13
3	4	17	767	732	7	3	7	6	497	473	6	3	10	1	1173	1098	4	3	12	16	326	292	15
3	4	18	327	341	12	3	7	8	432	396	6	3	10	2	746	696	5	3	13	1	1559	1446	5
3	4	19	792	751	7	3	7	10	336	356	8	3	10	3	455	420	7	3	13	2	926	895	6
3	4	21	254	225	18	3	7	11	328	336	9	3	10	4	886	837	5	3	13	4	546	500	8
3	5	1	998	915	3	3	7	12	455	484	7	3	10	5	884	875	5	3	13	5	859	843	6
3	5	2	1071	937	3	3	7	13	402	400	9	3	10	6	600	576	6	3	13	7	190	175	20
3	5	3	1023	960	3	3	7	14	691	703	6	3	10	7	597	573	6	3	13	9	445	448	10
3	5	4	420	393	5	3	7	15	275	273	13	3	10	8	1221	1248	5	3	13	11	276	273	15
3	5	5	482	450	4	3	7	16	1018	1003	6	3	10	9	1105	1115	5	3	13	12	600	625	8
3	5	6	732	720	4	3	7	17	257	272	16	3	10	10	838	819	6	3	13	13	428	433	11
3	5	7	585	643	4	3	7	20	534	467	10	3	10	11	582	586	7	3	13	14	510	505	10
3	5	8	537	529	5	3	8	1	665	605	5	3	10	13	613	605	7	3	13	15	642	643	9
3	5	9	2885	2902	4	3	8	2	196	202	12	3	10	14	464	463	9	3	14	1	368	394	13
3	5	10	587	611	5	3	8	3	264	226	9	3	10	15	263	246	15	3	14	3	833	798	7
3	5	11	141	129	16	3	8	4	709	653	5	3	10	17	581	585	9	3	14	4	987	972	6
3	5	12	649	676	5	3	8	5	154	151	15	3	10	18	414	381	12	3	14	6	361	331	12
3	5	13	685	715	6	3	8	6	2005	1958	4	3	11	1	404	418	9	3	14	7	195	193	21
3	5	15	975	964	5	3	8	7	358	341	8	3	11	2	1383	1268	4	3	14	9	758	744	7
3	5	17	489	469	9	3	8	9	728	735	5	3	11	3	883	820	5	3	14	12	204	186	23
3	5	18	472	467	9	3	8	10	159	145	17	3	11	4	579	554	7	3	14	13	213	207	22
3	5	19	486	449	9	3	8	11	188	196	15	3	11	5	228	225	14	3	15	1	438	415	11
3	5	20	210	232	22	3	8	12	1290	1293	5	3	11	6	615	600	6	3	15	2	311	261	15
3	5	21	571	499	10	3	8	13	292	272	12	3	11	7	299	308	11	3	15	3	559	571	9
3	6	1	1207	1108	3	3	8	14	287	272	12	3	11	8	799	766	6	3	15	4	605	625	9
3	6	2	610	521	4	3	8	16	324	301	12	3	11	9	221	214	16	3	15	6	737	751	8
3	6	3	324	258	6	3	8	17	215	215	19	3	11	10	303	329	12	3	15	8	735	746	8
3	6	4	1787	1693	3	3	8	19	384	363	13	3	11	12	218	250	17	3	15	10	186	206	26
3	6	5	348	359	6	3	9	1	547	444	6	3	11	13	266	231	15	3	16	2	758	754	8
3	6	6	673	690	4	3	9	2	1779	1619	4	3	11	14	323	341	13	3	16	3	279	259	18
3	6	8	122	73	17	3	9	3	1302	1221	4	3	11	15	264	249	16	3	16	4	373	385	14
3	6	9	576	611	5	3	9	4	1543	1451	4	3	11	16	223	209	20	3	16	5	231	201	20
3	6	10	137	165	17	3	9	5	712	697	5	3	11	17	245	269	20	3	16	6	213	219	23

Values of 10*Fobs and 10*Fcalc

H	K	L	Fobs	Fcalc	SigF
3	16	9	855	866	8
3	17	1	1266	1230	7
3	17	3	195	193	27
3	17	4	544	541	11
3	17	5	491	507	12
3	17	6	562	575	11
4	0	0	1574	1475	2
4	0	2	4166	4051	9
4	0	4	2249	2182	10
4	0	6	1174	1138	3
4	0	8	1811	1845	3
4	0	10	1400	1486	4
4	0	14	407	372	7
4	0	16	1571	1549	5
4	0	18	541	507	8
4	0	20	968	907	7
4	1	0	825	787	3
4	1	1	109	75	10
4	1	2	845	790	3
4	1	3	1981	1912	9
4	1	4	227	227	6
4	1	5	993	1038	3
4	1	6	741	764	3
4	1	7	1513	1552	3
4	1	8	474	484	5
4	1	10	983	990	4
4	1	11	1545	1530	4
4	1	12	1195	1233	4
4	1	13	682	685	5
4	1	14	751	736	5
4	1	15	569	595	6
4	1	16	303	306	11
4	1	17	374	352	10
4	1	20	362	299	12
4	1	21	178	148	25
4	2	0	132	123	9
4	2	1	2547	2415	9
4	2	2	1667	1634	2
4	2	3	1102	1038	3
4	2	4	1290	1241	3
4	2	5	1838	1807	3
4	2	6	145	147	10
4	2	7	220	193	7
4	2	8	1022	1046	3

H	K	L	Fobs	Fcalc	SigF
4	2	10	595	611	5
4	2	11	496	501	5
4	2	12	474	477	6
4	2	13	845	841	5
4	2	14	394	442	8
4	2	15	526	525	7
4	2	16	163	194	19
4	2	17	704	675	7
4	2	18	1031	980	6
4	2	19	410	372	10
4	2	20	585	534	9
4	2	21	229	216	20
4	3	0	2948	2643	10
4	3	1	483	431	4
4	3	2	787	742	3
4	3	3	1249	1191	3
4	3	4	1284	1241	3
4	3	5	212	179	7
4	3	6	110	89	14
4	3	7	423	501	5
4	3	8	1728	1757	3
4	3	10	1030	1024	4
4	3	11	1470	1495	4
4	3	12	693	750	5
4	3	13	140	146	18
4	3	14	1082	1059	5
4	3	15	719	700	6
4	3	16	420	411	9
4	3	17	173	167	20
4	3	18	386	377	10
4	3	19	188	194	21
4	4	0	512	444	4
4	4	1	811	726	3
4	4	3	2209	2047	3
4	4	5	1058	1032	3
4	4	6	150	114	11
4	4	7	1417	1461	3
4	4	9	307	279	7
4	4	10	268	337	9
4	4	11	610	622	5
4	4	13	1477	1517	4
4	4	14	427	436	8
4	4	15	1742	1750	5
4	4	16	403	429	9

H	K	L	Fobs	Fcalc	SigF
4	4	17	270	274	14
4	4	21	970	846	7
4	5	0	1526	1307	3
4	5	1	911	848	3
4	5	2	1642	1528	3
4	5	3	662	640	4
4	5	4	1100	1044	3
4	5	5	1074	1048	3
4	5	6	295	306	7
4	5	7	826	830	4
4	5	9	837	814	4
4	5	10	306	281	8
4	5	11	960	952	5
4	5	12	401	380	7
4	5	13	430	419	7
4	5	14	516	506	7
4	5	15	738	713	6
4	5	16	1177	1164	5
4	5	17	269	256	14
4	5	21	388	325	13
4	6	0	3157	2854	12
4	6	1	1052	951	3
4	6	2	736	833	4
4	6	3	639	578	4
4	6	4	144	129	14
4	6	5	2143	2080	3
4	6	6	471	504	5
4	6	7	536	578	5
4	6	8	372	374	7
4	6	10	1029	998	4
4	6	11	497	497	6
4	6	12	635	653	6
4	6	13	838	859	5
4	6	15	278	266	12
4	6	16	261	280	14
4	6	17	192	177	20
4	6	18	891	838	7
4	6	19	189	144	23
4	6	20	520	491	10
4	7	0	269	310	8
4	7	1	203	213	10
4	7	3	706	638	4
4	7	4	2404	2272	3
4	7	5	942	941	4

H	K	L	Fobs	Fcalc	SigF
4	7	6	474	462	6
4	7	7	671	677	5
4	7	8	1112	1086	4
4	7	9	363	342	8
4	7	11	175	168	16
4	7	12	352	352	9
4	7	13	216	237	15
4	7	14	904	918	6
4	7	15	655	646	7
4	7	17	351	331	12
4	7	18	329	293	13
4	7	19	460	421	11
4	7	20	460	413	11
4	8	0	1738	1494	4
4	8	1	264	205	9
4	8	2	1303	1207	4
4	8	3	453	445	6
4	8	4	928	876	4
4	8	5	900	884	4
4	8	6	1434	1350	4
4	8	7	305	362	9
4	8	8	1193	1186	4
4	8	10	1580	1591	4
4	8	11	313	311	10
4	8	12	764	780	6
4	8	13	298	321	12
4	8	15	444	471	9
4	8	16	1208	1209	6
4	8	17	192	196	22
4	8	18	767	748	8
4	8	19	346	303	14
4	9	0	1734	1555	4
4	9	1	1090	980	4
4	9	2	172	107	15
4	9	3	941	896	5
4	9	4	464	397	7
4	9	5	1507	1394	4
4	9	6	712	662	5
4	9	7	425	432	7
4	9	8	357	376	9
4	9	9	287	283	11
4	9	10	212	190	14
4	9	11	207	216	16
4	9	12	214	244	16

Values of 10*Fobs and 10*Fcalc

H	K	L	Fobs	Fcalc	SigF
4	9	15	410	373	10
4	9	17	330	323	14
4	10	0	689	689	6
4	10	1	532	446	7
4	10	2	215	222	14
4	10	3	485	475	7
4	10	4	322	338	10
4	10	5	1403	1328	4
4	10	6	1189	1153	5
4	10	7	779	730	6
4	10	8	457	458	8
4	10	9	624	622	7
4	10	10	399	399	9
4	10	11	696	697	7
4	10	12	923	948	6
4	10	13	699	703	7
4	10	15	269	254	15
4	10	17	456	451	11
4	10	18	510	511	11
4	11	0	1764	1614	4
4	11	1	650	620	6
4	11	2	442	415	8
4	11	3	408	418	9
4	11	4	1368	1302	5
4	11	5	449	452	8
4	11	7	419	425	9
4	11	8	258	260	14
4	11	9	242	224	15
4	11	11	370	380	11
4	11	12	413	423	10
4	11	13	253	242	16
4	12	0	1281	1187	5
4	12	1	378	351	10
4	12	2	427	425	9
4	12	3	1536	1421	5
4	12	5	536	513	8
4	12	6	262	272	14
4	12	7	1450	1430	5
4	12	8	456	447	9
4	12	9	177	192	21
4	12	10	377	385	11
4	12	11	494	511	9
4	12	12	312	345	14
4	12	13	395	404	11
4	12	14	194	201	23
4	12	15	1146	1154	7
4	13	0	497	464	10
4	13	1	497	465	9
4	13	3	1187	1157	5
4	13	4	704	700	7
4	13	5	548	532	8
4	13	12	259	251	17
4	14	0	538	464	9
4	14	1	876	832	7
4	14	2	277	236	16
4	14	3	238	273	19
4	14	4	313	295	14
4	14	5	962	937	6
4	14	6	548	546	9
4	14	8	794	789	7
4	14	9	260	246	17
4	14	10	927	933	7
4	14	12	300	305	16
4	14	13	524	515	10
4	15	0	581	552	9
4	15	1	384	378	13
4	15	2	495	505	10
4	15	3	254	244	18
4	15	4	856	850	7
4	15	5	640	658	9
4	15	6	257	296	18
4	15	11	279	301	18
4	16	0	286	252	18
4	16	1	843	822	8
4	16	2	979	944	7
4	16	3	251	232	20
4	16	5	483	481	11
4	16	8	873	876	8
4	17	0	334	318	17
4	17	1	380	371	16
4	17	2	218	228	26
4	17	3	735	733	9
4	17	4	366	373	15
5	0	2	1480	1433	3
5	0	4	1602	1532	3
5	0	6	650	669	4
5	0	8	329	291	6
5	0	10	1271	1299	4
5	0	12	2136	2150	4
5	0	16	1267	1235	5
5	0	18	302	307	13
5	0	20	629	572	8
5	1	1	345	377	4
5	1	2	1639	1552	3
5	1	3	1560	1479	3
5	1	4	1452	1507	3
5	1	5	624	617	4
5	1	6	167	175	9
5	1	8	355	397	6
5	1	9	1757	1829	3
5	1	10	824	832	4
5	1	11	235	226	10
5	1	12	333	336	8
5	1	13	664	635	6
5	1	14	1511	1506	4
5	1	15	589	592	7
5	1	16	835	812	6
5	1	17	552	508	8
5	1	18	238	217	15
5	1	20	685	598	8
5	1	21	240	204	19
5	2	1	2347	2219	10
5	2	2	2502	2376	10
5	2	3	1819	1730	3
5	2	4	2455	2403	11
5	2	5	408	433	5
5	2	6	155	190	11
5	2	7	684	761	4
5	2	8	1226	1237	4
5	2	9	1117	1111	4
5	2	10	980	995	4
5	2	11	261	251	9
5	2	12	488	487	6
5	2	13	444	429	7
5	2	14	499	499	7
5	2	15	873	869	6
5	2	17	832	815	6
5	2	18	221	225	17
5	2	19	418	403	10
5	2	20	227	227	19
5	2	21	325	293	15
5	3	1	540	488	4
5	3	2	1332	1252	3
5	3	3	1027	1009	3
5	3	4	1444	1369	3
5	3	6	1124	1158	3
5	3	7	592	599	4
5	3	8	748	744	4
5	3	9	2050	2076	4
5	3	10	1146	1146	4
5	3	11	724	779	5
5	3	12	324	362	9
5	3	13	616	630	6
5	3	14	369	391	9
5	3	15	279	286	11
5	3	16	499	480	8
5	3	17	354	334	11
5	3	19	264	283	16
5	3	20	325	306	14
5	3	21	743	650	8
5	4	1	1601	1429	3
5	4	2	215	233	8
5	4	3	1077	1013	3
5	4	4	463	401	5
5	4	5	636	634	4
5	4	7	1293	1284	4
5	4	8	422	424	6
5	4	9	187	183	12
5	4	10	220	211	11
5	4	11	690	693	5
5	4	12	469	465	7
5	4	13	596	613	6
5	4	14	190	230	16
5	4	15	195	221	17
5	4	17	723	697	7
5	4	18	332	328	12
5	4	19	535	491	9
5	4	21	205	172	23
5	5	1	1917	1770	3
5	5	2	580	526	4
5	5	3	1059	1002	3
5	5	4	1094	1044	3
5	5	6	759	702	4
5	5	7	422	387	6
5	5	8	164	211	14
5	5	9	917	934	4

Values of 10*Fobs and 10*Fcalc

H	K	L	Fobs	Fcalc	SigF	H	K	L	Fobs	Fcalc	SigF	H	K	L	Fobs	Fcalc	SigF	H	K	L	Fobs	Fcalc	SigF
5	5	10	311	310	9	5	8	3	673	650	5	5	10	15	502	482	9	5	14	10	486	451	10
5	5	11	1492	1449	4	5	8	4	378	353	7	5	10	17	518	497	10	5	14	12	356	351	14
5	5	13	645	643	6	5	8	5	389	352	7	5	11	1	1307	1191	5	5	15	2	1525	1462	6
5	5	14	521	518	7	5	8	6	1517	1438	4	5	11	2	1229	1145	5	5	15	3	329	314	15
5	5	15	355	362	10	5	8	7	230	221	12	5	11	3	530	518	7	5	15	4	845	839	7
5	5	16	681	683	7	5	8	9	547	517	6	5	11	5	293	303	12	5	15	5	347	351	14
5	5	17	901	855	6	5	8	10	705	687	6	5	11	6	594	539	7	5	15	8	386	391	13
5	5	18	349	335	12	5	8	11	201	214	16	5	11	7	588	595	7	5	15	11	278	281	19
5	5	19	824	768	7	5	8	12	1080	1114	5	5	11	8	392	378	10	5	16	1	250	216	21
5	6	1	181	174	11	5	8	13	668	698	7	5	11	9	562	582	8	5	16	3	463	462	12
5	6	2	1305	1253	3	5	8	16	876	864	7	5	11	10	294	288	13	5	16	4	605	615	10
5	6	3	324	305	7	5	8	18	336	337	14	5	11	11	533	536	9	5	16	6	949	947	7
5	6	4	1370	1307	4	5	8	19	266	260	19	5	11	12	194	187	20	5	17	1	274	247	21
5	6	5	837	762	4	5	9	1	2015	1826	4	5	11	14	192	191	22	5	17	2	374	382	16
5	6	6	640	587	5	5	9	2	330	280	9	5	11	15	290	315	16	5	17	3	442	438	14
5	6	8	514	518	6	5	9	3	848	829	5	5	11	16	426	405	12	6	0	0	1846	1655	3
5	6	9	1423	1387	4	5	9	4	259	233	11	5	12	1	749	702	7	6	0	2	2421	2359	11
5	6	10	1595	1589	4	5	9	5	1108	1037	5	5	12	3	437	404	9	6	0	4	652	598	4
5	6	11	365	334	8	5	9	6	720	662	5	5	12	4	336	317	11	6	0	6	1099	1103	3
5	6	12	1429	1398	5	5	9	7	456	454	7	5	12	5	415	401	10	6	0	8	730	709	4
5	6	13	640	627	6	5	9	8	852	808	5	5	12	6	684	652	7	6	0	10	470	471	6
5	6	14	556	551	7	5	9	9	228	188	14	5	12	7	935	933	6	6	0	12	339	340	8
5	6	15	319	334	11	5	9	10	251	231	13	5	12	8	413	425	10	6	0	16	587	573	7
5	6	17	303	256	13	5	9	11	212	197	16	5	12	9	860	844	6	6	0	18	246	206	15
5	6	19	434	413	11	5	9	12	505	480	8	5	12	11	735	723	7	6	0	20	187	195	23
5	6	20	884	816	8	5	9	13	379	355	10	5	12	14	183	196	25	6	1	0	144	116	11
5	7	1	824	762	4	5	9	14	281	274	14	5	12	15	245	253	19	6	1	1	211	288	7
5	7	2	1333	1199	4	5	9	16	194	210	22	5	13	1	302	281	14	6	1	2	471	474	4
5	7	3	918	842	4	5	9	17	552	534	9	5	13	3	1017	973	6	6	1	3	1334	1390	3
5	7	4	1261	1187	4	5	9	18	192	176	24	5	13	5	788	776	7	6	1	4	990	1023	3
5	7	5	994	942	4	5	10	1	1189	1057	5	5	13	6	289	280	15	6	1	5	149	146	11
5	7	6	2394	2391	4	5	10	2	453	402	8	5	13	7	210	201	19	6	1	6	558	551	4
5	7	7	695	679	5	5	10	3	721	667	6	5	13	8	363	345	12	6	1	7	283	269	7
5	7	8	360	383	8	5	10	4	863	821	5	5	13	9	708	692	8	6	1	8	2626	2676	3
5	7	9	283	261	10	5	10	5	605	579	6	5	13	11	271	292	16	6	1	9	1066	1013	4
5	7	10	1326	1345	4	5	10	6	150	130	20	5	13	12	179	103	24	6	1	10	2008	2012	4
5	7	12	1041	1034	5	5	10	7	1363	1316	5	5	13	14	389	400	13	6	1	11	508	489	6
5	7	13	325	336	10	5	10	8	446	431	9	5	14	1	191	178	23	6	1	12	345	349	8
5	7	14	736	764	6	5	10	9	938	892	6	5	14	2	937	894	7	6	1	13	375	391	8
5	7	15	175	175	20	5	10	10	332	348	11	5	14	3	334	327	14	6	1	14	451	444	8
5	7	16	450	432	9	5	10	11	674	664	7	5	14	4	1343	1300	6	6	1	15	1056	1049	5
5	7	17	520	497	9	5	10	12	171	131	22	5	14	6	491	485	10	6	1	16	384	367	10
5	8	1	297	275	9	5	10	13	482	513	9	5	14	7	820	809	7	6	1	17	493	474	8
5	8	2	988	875	4	5	10	14	596	574	8	5	14	9	637	655	9	6	1	18	320	302	12

H	K	L	Fobs	Fcalc	SigF
6	1	19	470	443	10
6	1	20	475	441	10
6	1	21	450	413	12
6	2	0	1756	1623	3
6	2	1	415	379	5
6	2	2	182	183	9
6	2	3	1635	1574	3
6	2	4	485	461	4
6	2	5	425	402	5
6	2	6	219	179	8
6	2	8	700	707	4
6	2	9	502	503	6
6	2	10	531	528	5
6	2	12	425	430	7
6	2	15	347	351	10
6	2	16	392	387	9
6	2	17	296	281	12
6	2	18	348	339	12
6	2	20	303	273	15
6	2	21	306	263	15
6	3	0	2040	1844	3
6	3	1	1832	1716	3
6	3	2	415	386	5
6	3	3	2196	2109	3
6	3	4	512	533	4
6	3	5	839	839	4
6	3	6	452	494	5
6	3	7	228	214	9
6	3	11	933	937	5
6	3	12	601	609	6
6	3	13	1066	1073	5
6	3	14	341	321	10
6	3	15	1081	1070	5
6	3	16	378	368	10
6	3	17	570	548	8
6	3	18	645	614	8
6	3	19	429	406	11
6	3	21	1142	1017	7
6	4	1	659	572	4
6	4	2	315	295	6
6	4	3	919	891	4
6	4	5	194	199	10
6	4	7	701	682	4
6	4	9	141	187	17
6	4	10	270	211	10
6	4	11	1479	1490	4
6	4	16	474	469	9
6	4	17	443	421	9
6	4	19	177	159	23
6	5	0	977	842	4
6	5	1	591	525	5
6	5	2	149	154	13
6	5	3	613	642	4
6	5	4	1322	1311	4
6	5	5	1881	1838	3
6	5	6	885	897	4
6	5	7	2029	2029	4
6	5	8	1161	1141	4
6	5	9	365	311	8
6	5	10	779	784	5
6	5	11	1901	1901	4
6	5	12	646	631	6
6	5	13	961	953	5
6	5	14	477	478	8
6	5	16	337	313	11
6	5	17	264	271	15
6	5	18	187	185	21
6	6	0	1067	996	4
6	6	1	1041	987	4
6	6	2	313	302	8
6	6	3	137	98	16
6	6	4	1097	1033	4
6	6	5	275	292	9
6	6	7	165	166	15
6	6	8	441	431	7
6	6	9	335	346	9
6	6	10	710	667	5
6	6	11	276	279	11
6	6	12	945	964	5
6	6	13	276	254	12
6	6	14	218	218	15
6	6	16	283	258	13
6	6	17	241	233	17
6	6	18	318	308	14
6	6	19	345	306	14
6	7	0	1630	1497	4
6	7	2	2396	2218	4
6	7	3	850	832	4
6	7	4	1179	1100	4
6	7	5	390	378	7
6	7	6	665	641	5
6	7	7	438	450	7
6	7	8	476	468	7
6	7	9	168	181	17
6	7	10	258	266	12
6	7	11	170	177	19
6	7	12	1099	1076	5
6	7	13	355	355	10
6	7	14	655	653	7
6	7	16	1459	1463	6
6	7	18	1104	1044	6
6	8	0	2263	2022	4
6	8	1	617	544	5
6	8	2	1087	1026	4
6	8	3	611	597	6
6	8	4	190	171	14
6	8	5	274	244	10
6	8	7	674	645	6
6	8	8	1104	1077	5
6	8	9	167	167	18
6	8	10	467	431	8
6	8	11	980	962	5
6	8	13	197	171	18
6	8	14	341	349	12
6	8	15	307	305	13
6	8	16	655	620	8
6	8	17	302	254	14
6	8	18	432	402	12
6	9	0	2640	2434	4
6	9	2	1194	1077	4
6	9	3	697	684	6
6	9	5	1019	941	5
6	9	6	244	238	13
6	9	7	1320	1353	5
6	9	8	587	557	7
6	9	10	487	453	8
6	9	11	1124	1133	5
6	9	12	579	571	8
6	9	13	897	900	6
6	9	15	428	402	10
6	9	16	596	580	9
6	9	17	318	302	15
6	9	18	974	935	7
6	10	0	986	939	5
6	10	1	1233	1134	5
6	10	2	235	205	14
6	10	3	907	880	5
6	10	5	439	420	8
6	10	6	294	287	11
6	10	7	523	515	8
6	10	8	453	432	9
6	10	9	395	407	10
6	10	10	429	434	9
6	10	11	207	196	18
6	10	14	537	529	9
6	10	16	518	505	10
6	10	17	667	656	9
6	11	1	268	257	13
6	11	3	663	644	7
6	11	4	458	433	9
6	11	5	1344	1354	5
6	11	6	650	641	7
6	11	7	870	848	6
6	11	8	542	512	8
6	11	9	186	168	20
6	11	10	753	743	7
6	11	11	977	968	6
6	11	12	572	549	8
6	11	13	891	876	7
6	11	14	556	552	9
6	11	15	517	511	10
6	11	16	363	342	14
6	12	0	452	457	10
6	12	1	655	598	7
6	12	2	329	300	12
6	12	3	389	394	10
6	12	4	748	712	7
6	12	5	222	225	18
6	12	6	822	811	6
6	12	7	435	425	10
6	12	8	541	542	9
6	12	10	192	185	22
6	12	13	305	336	15
6	12	14	340	322	14
6	12	15	577	586	10
6	12	0	821	741	7

Values of 10*Fobs and 10*Fcalc

H	K	L	Fobs	Fcalc	SigF
6	13	1	465	433	10
6	13	2	857	825	7
6	13	3	1685	1590	5
6	13	4	481	470	10
6	13	5	670	630	8
6	13	6	633	600	8
6	13	7	240	228	18
6	13	8	507	515	10
6	13	10	380	391	13
6	13	12	241	245	20
6	13	13	341	339	15
6	14	1	446	408	11
6	14	2	406	408	12
6	14	3	427	410	11
6	14	5	1371	1333	6
6	14	8	306	313	16
6	14	9	536	501	10
6	14	11	233	212	21
6	14	12	474	466	12
6	15	2	463	458	12
6	15	3	493	506	11
6	15	4	915	888	7
6	15	7	228	215	21
6	15	8	1239	1232	7
6	15	10	865	879	8
6	16	1	243	241	22
6	16	2	391	381	14
6	16	3	238	252	22
6	16	4	907	911	8
6	16	6	218	245	24
6	16	7	450	410	12
6	17	0	614	583	11
6	17	1	562	554	11
6	17	2	419	373	14
7	0	2	1272	1279	3
7	0	4	2462	2428	12
7	0	6	384	363	6
7	0	8	655	628	5
7	0	10	704	724	5
7	0	12	346	367	9
7	0	14	1620	1606	5
7	0	16	730	723	6
7	0	18	327	327	12
7	0	20	724	651	8

H	K	L	Fobs	Fcalc	SigF
7	1	1	390	392	5
7	1	2	2040	2094	3
7	1	3	518	509	4
7	1	4	1026	1037	3
7	1	5	146	141	13
7	1	6	1139	1074	4
7	1	7	558	562	5
7	1	8	692	674	5
7	1	9	1090	1118	4
7	1	12	1165	1154	5
7	1	13	195	199	15
7	1	14	384	395	9
7	1	15	437	459	9
7	1	16	955	939	6
7	1	17	247	240	15
7	1	20	591	549	9
7	2	2	905	844	4
7	2	3	120	138	15
7	2	4	179	142	10
7	2	5	1056	1035	4
7	2	6	809	860	4
7	2	7	490	524	5
7	2	8	602	589	5
7	2	10	552	557	6
7	2	11	915	922	5
7	2	12	470	470	7
7	2	13	488	467	7
7	2	15	178	179	18
7	2	16	677	683	7
7	2	19	344	325	13
7	3	1	170	112	11
7	3	2	1161	1154	3
7	3	3	1946	1889	3
7	3	5	449	420	5
7	3	6	613	592	5
7	3	7	1403	1354	4
7	3	8	1454	1428	4
7	3	9	1354	1301	4
7	3	10	347	362	8
7	3	11	802	792	5
7	3	12	235	238	12
7	3	13	758	739	6
7	3	14	150	107	21
7	3	15	519	501	8

H	K	L	Fobs	Fcalc	SigF
7	3	17	337	334	12
7	3	20	467	420	11
7	4	1	1049	1024	4
7	4	2	669	618	4
7	4	3	1538	1441	3
7	4	4	616	610	5
7	4	5	1398	1354	4
7	4	6	144	152	15
7	4	7	471	481	6
7	4	9	1910	1849	4
7	4	13	252	238	13
7	4	14	381	369	9
7	4	15	1125	1102	5
7	4	17	696	644	7
7	4	19	584	543	9
7	4	20	449	393	11
7	5	1	1418	1419	4
7	5	2	1442	1381	4
7	5	3	970	922	4
7	5	4	412	435	6
7	5	5	1385	1443	4
7	5	6	879	829	4
7	5	7	1603	1591	4
7	5	8	1139	1095	4
7	5	9	289	255	10
7	5	11	253	256	12
7	5	13	958	926	5
7	5	14	508	508	8
7	5	15	592	598	7
7	5	16	672	649	7
7	5	17	822	824	7
7	5	18	281	259	15
7	5	19	757	718	8
7	6	1	1284	1176	4
7	6	2	791	773	4
7	6	3	208	221	12
7	6	6	882	820	5
7	6	7	652	598	5
7	6	8	304	263	9
7	6	9	753	705	5
7	6	10	431	413	8
7	6	11	1026	1015	5
7	6	12	315	286	11
7	6	13	351	366	10

H	K	L	Fobs	Fcalc	SigF
7	6	14	168	175	21
7	6	15	276	225	14
7	6	16	313	299	13
7	6	17	437	405	10
7	6	18	390	404	12
7	6	19	449	413	11
7	7	1	703	673	5
7	7	2	1093	990	4
7	7	5	178	159	15
7	7	6	1007	994	5
7	7	7	733	724	5
7	7	8	744	691	5
7	7	10	872	836	5
7	7	11	258	236	13
7	7	12	1429	1367	5
7	7	13	393	370	10
7	7	14	180	207	21
7	7	17	260	252	17
7	7	18	362	375	14
7	8	1	656	587	6
7	8	2	418	415	7
7	8	3	202	179	14
7	8	4	685	669	6
7	8	5	169	178	17
7	8	6	1165	1141	5
7	8	7	1319	1275	5
7	8	8	1160	1165	5
7	8	10	1237	1211	5
7	8	11	449	437	9
7	8	12	850	846	6
7	8	13	212	192	18
7	8	14	717	692	7
7	8	17	529	518	10
7	9	1	1267	1210	5
7	9	2	458	429	8
7	9	3	852	800	5
7	9	4	1655	1608	4
7	9	5	508	490	7
7	9	6	1254	1233	5
7	9	7	712	705	6
7	9	8	221	215	15
7	9	9	495	486	8
7	9	10	472	464	9
7	9	11	359	383	11

Values of 10*Fobs and 10*Fcalc

H	K	L	Fobs	Fcalc	SigF
7	9	12	503	496	9
7	9	13	861	848	7
7	9	14	361	388	12
7	9	15	229	250	19
7	9	16	260	278	18
7	9	17	891	857	7
7	10	1	390	406	9
7	10	2	595	543	7
7	10	4	600	571	7
7	10	5	948	919	5
7	10	6	858	839	6
7	10	8	500	482	8
7	10	9	265	262	14
7	10	12	458	446	10
7	10	13	819	804	7
7	10	15	284	266	16
7	10	16	184	168	25
7	11	1	1090	1034	5
7	11	2	171	156	21
7	11	3	307	307	12
7	11	4	226	199	16
7	11	5	222	249	17
7	11	6	273	240	14
7	11	7	361	349	11
7	11	8	843	835	6
7	11	10	953	938	6
7	11	11	407	384	11
7	11	12	581	561	9
7	11	14	935	909	7
7	11	15	259	254	19
7	12	1	521	510	9
7	12	2	333	289	12
7	12	3	651	613	7
7	12	4	591	561	8
7	12	6	1027	997	6
7	12	7	501	503	9
7	12	8	260	224	16
7	12	9	893	895	7
7	12	10	487	484	10
7	12	11	471	473	11
7	12	12	766	771	8
7	12	13	197	207	25
7	13	1	557	511	9
7	13	2	390	343	12

H	K	L	Fobs	Fcalc	SigF
7	13	3	751	747	7
7	13	5	515	514	9
7	13	6	430	422	11
7	13	7	232	248	19
7	13	8	626	582	8
7	13	9	1346	1352	6
7	13	10	692	655	8
7	13	11	251	217	19
7	13	12	553	554	10
7	13	13	583	551	10
7	14	2	709	711	8
7	14	3	491	456	10
7	14	4	220	218	21
7	14	5	386	367	13
7	14	7	877	880	7
7	14	8	263	248	19
7	14	9	422	425	13
7	14	10	199	241	26
7	14	11	411	426	13
7	15	2	1103	1056	7
7	15	4	649	626	9
7	15	6	278	259	18
7	15	9	462	478	13
7	16	1	335	318	17
7	16	2	495	517	12
7	16	4	386	373	15
7	16	5	233	190	28
7	16	6	535	549	11
8	0	0	732	654	4
8	0	2	1514	1384	3
8	0	4	1440	1508	4
8	0	6	150	157	14
8	0	8	1425	1410	4
8	0	10	1152	1111	4
8	0	14	778	746	6
8	0	16	786	786	6
8	0	18	430	389	10
8	0	20	471	415	11
8	1	1	606	610	4
8	1	2	131	108	15
8	1	3	771	762	4
8	1	5	510	477	5
8	1	6	151	169	14
8	1	7	236	193	10

H	K	L	Fobs	Fcalc	SigF
8	1	8	301	316	8
8	1	9	391	367	7
8	1	10	166	163	16
8	1	11	469	478	7
8	1	12	337	360	9
8	1	14	218	217	15
8	1	15	198	159	18
8	1	18	178	151	22
8	1	19	322	305	14
8	2	0	1369	1307	4
8	2	1	1477	1477	4
8	2	2	1357	1308	4
8	2	3	2220	2326	3
8	2	4	224	252	10
8	2	5	1251	1222	4
8	2	6	190	179	12
8	2	7	153	115	15
8	2	8	948	950	4
8	2	9	409	428	7
8	2	10	404	383	7
8	2	11	678	707	6
8	2	12	971	979	5
8	2	13	791	768	6
8	2	14	222	213	15
8	2	15	1143	1113	6
8	2	16	991	961	6
8	2	17	242	226	16
8	2	18	527	508	9
8	2	19	642	592	8
8	2	20	396	356	13
8	3	0	1329	1292	4
8	3	1	759	700	4
8	3	2	770	693	4
8	3	3	337	386	7
8	3	4	1068	1057	4
8	3	5	705	737	5
8	3	7	558	561	6
8	3	8	476	465	6
8	3	9	330	331	9
8	3	11	447	433	7
8	3	13	285	263	13
8	3	16	262	249	15
8	3	17	321	293	13
8	3	18	456	422	10

H	K	L	Fobs	Fcalc	SigF
8	3	19	186	188	24
8	4	0	1544	1594	4
8	4	1	1248	1155	4
8	4	3	152	124	15
8	4	4	1306	1280	4
8	4	5	1005	981	4
8	4	6	497	510	6
8	4	7	1098	1099	4
8	4	8	935	916	5
8	4	9	691	687	5
8	4	10	167	173	17
8	4	11	932	931	5
8	4	12	350	340	10
8	4	13	1038	1033	5
8	4	14	436	404	9
8	4	17	1118	1074	6
8	4	18	447	421	10
8	4	19	186	202	24
8	5	0	418	414	7
8	5	1	328	329	8
8	5	2	206	212	12
8	5	3	428	469	7
8	5	4	915	871	4
8	5	6	369	346	8
8	5	7	625	648	6
8	5	8	944	950	5
8	5	9	767	776	5
8	5	10	204	179	15
8	5	11	198	198	16
8	5	14	442	432	9
8	5	18	220	302	20
8	5	19	285	252	16
8	6	0	319	237	9
8	6	1	790	788	5
8	6	2	2045	1950	4
8	6	3	553	497	6
8	6	4	290	294	9
8	6	5	1210	1126	4
8	6	6	892	907	5
8	6	7	1356	1319	4
8	6	8	1455	1458	4
8	6	10	475	472	[illegible]
8	6	11	1494	1459	5
8	6	12	703	719	[illegible]

Values of 10*Fobs and 10*Fcalc

H	K	L	Fobs	Fcalc	SigF
8	6	13	262	239	14
8	6	14	184	134	20
8	6	15	302	287	14
8	6	16	1584	1544	6
8	6	17	300	296	15
8	6	18	521	482	10
8	7	0	652	648	8
8	7	1	731	684	5
8	7	2	614	556	6
8	7	3	325	298	9
8	7	5	948	908	5
8	7	6	188	187	16
8	7	8	254	230	12
8	7	9	385	370	9
8	7	11	689	683	7
8	7	13	199	214	19
8	7	15	579	553	8
8	7	16	431	410	11
8	8	0	2047	1907	4
8	8	1	370	347	9
8	8	2	397	413	8
8	8	5	554	547	7
8	8	6	1416	1398	5
8	8	7	765	755	6
8	8	8	802	824	6
8	8	9	672	674	7
8	8	10	321	328	11
8	8	11	675	660	7
8	8	12	1297	1281	5
8	8	15	379	362	12
8	8	16	428	431	11
8	8	17	267	253	18
8	9	0	219	188	15
8	9	1	263	235	13
8	9	2	172	173	19
8	9	3	626	592	7
8	9	4	283	247	12
8	9	5	438	438	8
8	9	6	594	596	7
8	9	8	417	395	9
8	9	9	271	281	14
8	9	10	305	314	13
8	9	11	44[illegible]	418	10
8	9	12	174	160	20
8	9	13	231	226	18
8	9	15	515	492	10
8	10	0	480	479	9
8	10	1	171	169	21
8	10	2	780	716	6
8	10	3	922	908	6
8	10	4	535	556	8
8	10	5	899	886	6
8	10	6	923	897	6
8	10	7	1534	1522	5
8	10	8	989	972	6
8	10	10	862	843	6
8	10	11	1802	1767	5
8	10	13	1032	1014	7
8	10	14	260	240	17
8	11	0	256	257	16
8	11	1	191	158	20
8	11	3	385	348	10
8	11	4	459	463	9
8	11	5	418	433	10
8	11	7	654	640	8
8	11	8	711	699	7
8	11	10	414	429	11
8	11	11	552	554	9
8	11	12	509	514	10
8	11	13	341	322	14
8	11	14	616	579	9
8	12	0	277	213	15
8	12	1	1094	1037	6
8	12	2	292	274	14
8	12	3	379	323	11
8	12	4	197	209	21
8	12	5	1244	1234	6
8	12	6	489	491	10
8	12	8	419	408	11
8	12	9	466	453	11
8	12	10	528	519	10
8	12	12	733	721	8
8	12	13	948	937	7
8	13	0	407	406	12
8	13	3	494	514	10
8	13	5	326	334	14
8	13	6	352	345	10
8	13	7	450	471	11
8	13	8	439	461	12
8	13	9	328	327	15
8	13	10	493	487	11
8	13	11	545	534	10
8	13	12	396	402	14
8	14	1	213	204	23
8	14	2	738	744	8
8	14	3	681	663	9
8	14	4	251	246	19
8	14	5	183	189	26
8	14	6	252	262	19
8	14	7	659	640	9
8	14	8	1119	1118	7
8	14	9	195	146	27
8	14	10	959	975	8
8	15	0	290	243	18
8	15	1	314	274	17
8	15	4	209	193	25
8	15	5	288	277	18
8	16	0	1036	1055	8
8	16	1	219	197	26
8	16	2	347	311	16
8	16	3	410	423	15
9	0	2	2189	2121	4
9	0	4	1031	940	4
9	0	6	645	608	5
9	0	8	614	594	6
9	0	10	601	564	6
9	0	12	173	154	18
9	0	14	1329	1279	5
9	0	16	1007	955	6
9	1	1	952	925	4
9	1	2	835	817	4
9	1	3	222	185	10
9	1	4	547	536	5
9	1	5	159	142	15
9	1	6	514	509	6
9	1	7	900	906	5
9	1	8	821	819	5
9	1	9	609	563	6
9	1	10	196	199	15
9	1	11	682	665	6
9	1	12	430	421	8
9	1	14	212	220	17
9	1	15	565	524	8
9	1	16	349	358	12
9	1	17	594	568	8
9	1	18	487	479	10
9	1	19	264	246	18
9	2	1	187	162	12
9	2	2	484	506	6
9	2	3	1640	1663	4
9	2	4	786	824	5
9	2	5	1693	1720	4
9	2	6	1590	1575	4
9	2	7	1341	1432	4
9	2	8	328	311	9
9	2	9	439	459	7
9	2	10	320	313	10
9	2	11	770	784	6
9	2	12	744	727	6
9	2	13	785	760	6
9	2	14	193	152	18
9	2	15	400	403	10
9	2	16	455	449	10
9	3	1	627	587	5
9	3	2	826	770	5
9	3	3	190	209	13
9	3	4	357	318	7
9	3	5	943	899	4
9	3	6	1106	1059	4
9	3	7	642	630	5
9	3	8	210	206	13
9	3	9	492	492	7
9	3	10	215	206	14
9	3	12	1378	1362	5
9	3	13	616	627	7
9	3	15	369	360	11
9	3	16	450	406	10
9	3	17	624	593	8
9	3	18	388	378	12
9	3	19	421	404	12
9	4	1	1710	1632	4
9	4	2	2170	2099	4
9	4	3	1226	1203	4
9	4	4	710	717	5
9	4	5	1438	1487	4
9	4	6	1424	1443	4

Values of 10*Fobs and 10*Fcalc

H	K	L	Fobs	Fcalc	SigF	H	K	L	Fobs	Fcalc	SigF	H	K	L	Fobs	Fcalc	SigF	H	K	L	Fobs	Fcalc	SigF
9	4	7	170	179	16	9	7	14	397	396	11	9	11	11	418	414	12	10	1	16	1149	1113	6
9	4	9	1208	1193	5	9	7	15	387	404	12	9	11	12	328	332	15	10	1	17	431	427	11
9	4	10	700	674	6	9	7	16	341	340	13	9	11	14	243	268	21	10	1	18	700	643	8
9	4	12	544	527	8	9	8	1	590	572	7	9	12	3	690	657	8	10	2	0	189	205	14
9	4	13	733	701	7	9	8	2	285	305	12	9	12	4	233	222	18	10	2	1	617	593	5
9	4	14	340	310	11	9	8	3	180	118	18	9	12	5	335	324	13	10	2	3	1341	1344	4
9	4	15	994	965	6	9	8	4	847	829	6	9	12	6	750	742	8	10	2	4	436	420	7
9	4	16	591	576	8	9	8	5	244	232	14	9	12	7	915	914	7	10	2	5	423	459	7
9	4	17	806	758	7	9	8	6	1084	1070	5	9	12	8	553	527	10	10	2	6	474	425	7
9	4	19	534	487	10	9	8	7	634	613	7	9	12	9	1332	1330	6	10	2	7	1084	1048	5
9	5	1	243	254	11	9	8	8	994	949	6	9	12	10	537	526	10	10	2	9	179	198	17
9	5	2	652	643	5	9	8	9	598	582	7	9	12	12	984	987	7	10	2	11	972	943	5
9	5	3	481	471	7	9	8	10	842	822	6	9	13	1	584	551	9	10	2	15	920	872	6
9	5	5	206	167	13	9	8	12	880	851	6	9	13	2	246	219	19	10	2	16	419	398	11
9	5	6	921	902	5	9	8	13	456	437	10	9	13	3	369	356	13	10	2	17	261	234	17
9	5	8	258	243	12	9	8	14	392	371	12	9	13	6	193	201	24	10	3	1	1146	1122	4
9	5	9	294	283	11	9	9	2	306	291	12	9	13	10	318	330	17	10	3	2	341	334	8
9	5	10	178	182	18	9	9	3	667	667	7	9	14	2	936	944	7	10	3	3	1002	994	5
9	5	12	1099	1093	5	9	9	6	171	200	21	9	14	4	437	447	12	10	3	4	308	307	9
9	5	13	708	698	7	9	9	7	1032	1057	6	9	14	5	680	688	9	10	3	5	1177	1182	4
9	5	16	252	230	17	9	9	8	401	390	10	9	14	6	246	250	20	10	3	7	1161	1141	5
9	6	1	1525	1434	4	9	9	10	383	383	11	9	14	7	348	334	15	10	3	9	556	553	7
9	6	2	868	820	5	9	9	15	424	431	12	9	14	9	744	734	9	10	3	11	1087	1098	5
9	6	3	759	760	5	9	9	16	502	495	11	9	15	4	763	761	9	10	3	12	257	255	14
9	6	5	699	696	6	9	10	1	543	519	8	9	15	5	335	344	16	10	3	13	759	726	7
9	6	6	1007	998	5	9	10	2	1000	940	6	9	15	6	612	615	10	10	3	14	306	315	13
9	6	7	379	366	9	9	10	3	434	410	10	10	0	2	545	509	6	10	3	15	522	526	9
9	6	8	153	145	20	9	10	4	439	429	9	10	0	4	1516	1518	4	10	3	16	190	179	22
9	6	9	515	492	7	9	10	5	1016	963	6	10	0	6	353	385	11	10	3	17	392	383	12
9	6	10	225	188	15	9	10	6	302	272	13	10	0	8	970	982	5	10	4	0	1238	1166	4
9	6	11	955	936	6	9	10	7	641	625	7	10	0	10	724	676	6	10	4	3	576	546	6
9	6	12	1193	1175	5	9	10	8	398	420	11	10	0	12	807	796	6	10	4	4	1234	1221	4
9	6	13	645	622	7	9	10	10	517	497	9	10	0	14	1058	1003	6	10	4	5	1025	1029	5
9	6	15	173	143	23	9	10	11	455	426	10	10	0	16	336	307	13	10	4	6	505	444	7
9	6	16	277	271	16	9	10	12	272	293	17	10	0	18	348	338	14	10	4	7	234	236	13
9	6	17	651	600	8	9	10	13	972	959	7	10	1	0	169	163	15	10	4	8	885	896	5
9	7	1	666	657	6	9	10	14	483	485	11	10	1	2	1502	1448	4	10	4	9	591	570	7
9	7	2	1531	1465	4	9	11	1	893	887	6	10	1	5	391	385	7	10	4	10	533	523	7
9	7	4	1289	1251	5	9	11	2	452	455	10	10	1	6	1458	1477	4	10	4	12	583	585	8
9	7	8	941	950	5	9	11	3	772	746	7	10	1	7	581	606	6	10	4	13	573	542	8
9	7	9	1151	1169	5	9	11	4	221	239	18	10	1	8	1367	1372	4	10	4	14	601	583	8
9	7	10	517	526	8	9	11	6	476	472	9	10	1	9	355	354	9	10	4	15	213	218	19
9	7	12	501	491	9	9	11	7	653	649	8	10	1	10	662	646	6	10	4	18	434	388	13
9	7	13	460	477	9	9	11	9	983	965	6	10	1	12	1211	1305	5	10	5	0	373	370	9

Values of 10*Fobs and 10*Fcalc

H	K	L	Fobs	Fcalc	SigF	H	K	L	Fobs	Fcalc	SigF	H	K	L	Fobs	Fcalc	SigF	H	K	L	Fobs	Fcalc	SigF
10	5	1	1105	1091	5	10	8	4	438	406	9	10	11	12	343	324	15	11	1	11	485	486	8
10	5	2	453	445	7	10	8	5	219	191	16	10	11	13	406	416	13	11	1	12	503	518	9
10	5	3	947	955	5	10	8	6	937	976	6	10	12	0	1159	1124	6	11	1	13	359	350	12
10	5	4	615	620	6	10	8	7	589	586	8	10	12	1	615	577	9	11	1	14	595	590	8
10	5	5	1772	1822	4	10	8	8	350	314	11	10	12	2	262	247	18	11	1	15	274	257	16
10	5	6	761	736	6	10	8	11	353	330	12	10	12	3	549	543	9	11	1	16	441	414	11
10	5	7	547	559	7	10	8	12	620	605	8	10	12	4	482	472	10	11	1	17	263	249	18
10	5	8	689	685	6	10	9	0	1370	1322	5	10	12	6	298	300	16	11	2	1	212	236	14
10	5	10	244	256	14	10	9	1	187	159	20	10	12	8	256	239	19	11	2	2	189	176	15
10	5	11	977	965	6	10	9	2	1336	1310	5	10	12	9	341	342	15	11	2	3	439	491	8
10	5	12	217	202	17	10	9	3	859	845	6	10	12	11	249	210	20	11	2	5	1356	1404	5
10	5	13	1142	1127	6	10	9	4	575	544	8	10	13	0	411	406	13	11	2	7	190	163	16
10	5	15	610	598	8	10	9	5	222	293	17	10	13	1	411	411	13	11	2	8	251	249	12
10	5	16	423	410	11	10	9	6	565	559	8	10	13	2	1037	1033	7	11	2	9	588	590	7
10	6	0	1179	1031	5	10	9	7	1037	1014	6	10	13	3	700	684	8	11	2	10	264	255	12
10	6	1	1752	1649	4	10	9	8	1013	995	6	10	13	5	1015	1032	7	11	2	11	436	420	9
10	6	2	458	427	8	10	9	9	330	339	13	10	13	6	654	656	9	11	2	12	432	444	10
10	6	3	174	183	18	10	9	10	722	724	7	10	13	8	523	543	11	11	2	13	1774	1757	5
10	6	4	673	668	6	10	9	11	598	610	9	10	13	9	312	305	17	11	2	14	266	268	16
10	6	5	398	387	9	10	9	12	448	433	11	10	14	0	988	965	8	11	2	15	219	191	19
10	6	6	200	234	16	10	9	13	306	283	15	10	14	1	218	140	24	11	2	17	794	748	8
10	6	7	1298	1279	5	10	9	14	570	554	10	10	14	3	825	804	8	11	3	1	350	372	9
10	6	8	343	349	10	10	9	15	335	323	15	10	14	5	393	378	14	11	3	2	620	608	6
10	6	11	740	737	7	10	10	0	702	676	7	10	14	6	291	280	18	11	3	3	464	470	7
10	6	14	636	620	8	10	10	1	599	551	8	10	15	0	683	681	10	11	3	4	725	707	6
10	6	17	475	460	11	10	10	2	453	463	10	10	15	1	504	520	12	11	3	5	244	261	13
10	7	0	192	171	17	10	10	3	377	394	11	10	15	2	247	223	23	11	3	6	618	593	6
10	7	1	877	833	6	10	10	4	251	252	16	11	0	2	763	722	5	11	3	7	521	538	7
10	7	2	1043	989	5	10	10	7	369	357	12	11	0	4	516	528	7	11	3	8	231	224	14
10	7	3	401	374	9	10	10	8	563	575	9	11	0	6	1988	1948	4	11	3	9	1578	1550	5
10	7	4	705	677	6	10	10	9	280	286	16	11	0	8	1291	1303	5	11	3	10	171	137	20
10	7	6	374	331	10	10	10	10	297	301	15	11	0	10	501	494	8	11	3	11	559	542	8
10	7	8	849	835	6	10	10	11	531	526	10	11	0	12	1866	1869	5	11	3	12	523	519	8
10	7	10	573	543	8	10	10	13	222	228	21	11	0	14	743	718	7	11	3	13	343	331	12
10	7	11	393	409	11	10	11	0	242	239	18	11	0	18	403	432	13	11	3	14	168	174	24
10	7	12	617	618	8	10	11	1	655	648	8	11	1	1	979	924	5	11	3	15	403	381	11
10	7	13	230	243	18	10	11	2	379	396	12	11	1	2	664	714	6	11	3	17	458	437	11
10	7	14	188	119	22	10	11	3	267	265	16	11	1	4	778	755	5	11	4	1	850	819	5
10	7	15	523	499	10	10	11	4	200	222	21	11	1	5	330	319	10	11	4	3	694	674	6
10	7	16	566	534	10	10	11	5	472	460	10	11	1	6	400	363	8	11	4	4	627	674	6
10	8	0	1785	1735	5	10	11	6	522	517	9	11	1	7	1566	1550	4	11	4	6	873	857	5
10	8	1	1011	950	5	10	11	7	574	582	9	11	1	8	732	732	6	11	4	7	1732	1748	5
10	8	2	845	827	6	10	11	9	294	260	16	11	1	9	323	321	11	11	4	8	364	332	10
10	8	3	318	329	11	10	11	11	582	557	9	11	1	10	230	246	15	11	4	9	177	194	20

Values of 10*Fobs and 10*Fcalc

H	K	L	Fobs	Fcalc	SigF	H	K	L	Fobs	Fcalc	SigF	H	K	L	Fobs	Fcalc	SigF	H	K	L	Fobs	Fcalc	SigF
11	4	10	570	558	8	11	7	13	195	184	22	11	13	3	453	459	12	12	2	16	317	314	15
11	4	11	568	541	8	11	7	14	719	714	8	11	13	5	690	717	9	12	3	0	323	300	11
11	4	12	1001	986	6	11	8	2	1466	1419	5	11	13	6	445	423	12	12	3	2	388	421	9
11	4	14	337	343	13	11	8	3	397	393	10	11	14	1	851	805	8	12	3	3	555	558	7
11	4	15	479	481	10	11	8	4	482	476	9	11	14	3	421	420	14	12	3	4	170	148	19
11	4	16	363	338	13	11	8	7	592	594	8	12	0	0	276	258	12	12	3	5	321	307	11
11	4	17	606	570	9	11	8	8	429	429	10	12	0	2	1477	1450	5	12	3	6	170	164	20
11	5	1	634	598	6	11	8	9	367	352	12	12	0	4	260	228	12	12	3	7	643	684	7
11	5	2	957	930	5	11	8	10	700	689	8	12	0	6	334	324	10	12	3	9	825	847	6
11	5	3	180	174	17	11	8	11	203	212	21	12	0	8	306	322	12	12	3	10	265	275	15
11	5	4	578	557	7	11	8	12	449	431	11	12	0	10	190	154	19	12	3	11	681	684	7
11	5	5	296	335	12	11	8	13	216	244	21	12	0	12	615	610	8	12	3	12	292	315	15
11	5	6	578	593	7	11	8	14	514	513	10	12	0	14	599	573	8	12	3	14	349	337	13
11	5	7	253	239	14	11	8	15	397	379	13	12	0	16	1043	990	7	12	3	15	566	567	9
11	5	8	411	397	9	11	9	1	889	910	6	12	1	0	446	432	8	12	4	0	618	620	7
11	5	9	560	527	8	11	9	5	181	189	22	12	1	1	484	487	7	12	4	2	224	226	15
11	5	10	356	349	11	11	9	6	650	640	8	12	1	2	523	555	7	12	4	3	851	817	6
11	5	11	579	575	8	11	9	7	561	552	9	12	1	3	565	565	7	12	4	4	187	160	18
11	5	12	573	561	8	11	9	8	599	586	8	12	1	4	408	400	9	12	4	5	257	265	13
11	5	13	196	178	21	11	9	11	279	271	16	12	1	6	246	233	14	12	4	6	525	539	8
11	5	16	452	441	11	11	9	12	556	569	10	12	1	7	223	203	15	12	4	7	997	1031	6
11	6	1	342	356	10	11	9	14	187	148	26	12	1	8	469	435	8	12	4	8	704	721	7
11	6	2	1022	1030	5	11	10	1	465	455	10	12	1	10	1044	1025	6	12	4	9	672	669	7
11	6	3	866	837	6	11	10	3	722	714	7	12	1	11	614	589	8	12	4	10	522	511	9
11	6	4	630	647	7	11	10	4	695	713	8	12	1	12	380	358	11	12	4	11	362	382	12
11	6	5	564	568	7	11	10	5	332	315	13	12	1	13	273	271	15	12	4	12	503	492	9
11	6	6	371	347	10	11	10	6	322	301	13	12	1	14	429	403	11	12	4	13	173	175	24
11	6	7	160	155	22	11	10	7	299	307	15	12	1	15	742	727	8	12	4	14	293	303	15
11	6	8	674	674	7	11	10	9	677	686	8	12	1	16	488	469	10	12	4	15	822	780	8
11	6	9	1182	1157	5	11	10	10	416	398	12	12	1	17	217	202	22	12	5	1	251	247	14
11	6	12	340	343	13	11	11	1	1266	1236	6	12	2	0	1244	1176	5	12	5	4	532	528	8
11	6	13	249	234	17	11	11	2	653	646	8	12	2	1	920	909	5	12	5	5	620	608	7
11	6	15	224	179	20	11	11	3	658	679	8	12	2	2	767	749	6	12	5	6	515	528	8
11	6	16	574	555	10	11	11	5	445	450	11	12	2	3	701	707	6	12	5	7	628	619	7
11	7	1	1289	1264	5	11	11	7	380	404	13	12	2	4	447	434	8	12	5	8	291	321	14
11	7	2	414	426	9	11	11	8	393	388	13	12	2	5	1287	1299	5	12	5	10	365	355	12
11	7	4	1224	1236	5	11	11	9	607	608	9	12	2	6	580	585	7	12	5	11	203	183	20
11	7	5	330	333	11	11	12	1	916	890	7	12	2	7	1244	1264	5	12	5	12	231	217	18
11	7	6	799	817	6	11	12	2	1374	1344	6	12	2	8	761	733	6	12	5	13	332	326	14
11	7	7	494	502	9	11	12	4	533	533	10	12	2	10	456	449	9	12	6	0	1158	1120	5
11	7	8	431	441	10	11	12	6	409	406	12	12	2	11	1497	1496	5	12	6	1	1641	1616	5
11	7	10	624	644	8	11	12	7	331	334	15	12	2	12	368	351	12	12	6	2	548	538	8
11	7	11	181	160	22	11	12	8	366	372	14	12	2	13	947	923	7	12	6	3	302	307	13
11	7	12	836	820	7	11	12	10	388	399	14	12	2	14	344	339	13	12	6	4	308	285	12

Values of 10*Fobs and 10*Fcalc

H	K	L	Fobs	Fcalc	SigF
12	6	5	699	669	7
12	6	6	925	908	6
12	6	7	591	609	8
12	6	8	970	980	6
12	6	10	868	866	7
12	6	11	176	127	23
12	6	12	510	509	10
12	6	13	754	746	8
12	6	14	644	629	9
12	6	15	399	372	13
12	7	0	1167	1174	6
12	7	1	356	354	12
12	7	4	542	528	8
12	7	5	233	279	17
12	7	6	334	333	12
12	7	7	323	311	13
12	7	8	612	603	8
12	7	11	291	280	15
12	7	14	265	251	19
12	8	0	321	305	13
12	8	1	216	249	19
12	8	2	1122	1103	6
12	8	3	515	508	9
12	8	4	252	271	16
12	8	8	1269	1291	6
12	8	10	1032	1054	7
12	8	11	373	371	13
12	9	0	941	949	7
12	9	1	414	412	11
12	9	2	222	216	19
12	9	3	230	237	19
12	9	5	405	407	11
12	9	6	357	342	13
12	9	8	261	289	18
12	9	9	356	331	13
12	9	11	294	283	16
12	9	12	291	259	18
12	10	0	449	442	11
12	10	1	842	804	7
12	10	2	304	313	15
12	10	3	1632	1676	6
12	10	5	817	866	7
12	10	7	273	268	17
12	10	10	307	300	16

H	K	L	Fobs	Fcalc	SigF
12	10	11	310	301	17
12	11	0	840	801	8
12	11	2	371	342	14
12	11	3	255	245	19
12	11	4	489	491	11
12	11	5	430	424	12
12	11	7	261	275	19
12	11	9	226	184	22
12	12	0	1339	1317	6
12	12	2	211	197	24
12	12	3	413	406	13
12	12	4	732	710	9
12	12	5	469	476	12
12	12	7	636	633	9
12	12	8	307	299	18
12	13	0	418	416	14
12	13	1	465	465	13
12	13	2	493	515	12
12	13	3	721	699	9
12	13	4	614	595	10
13	0	2	446	487	9
13	0	4	1671	1681	5
13	0	6	1426	1436	5
13	0	12	1015	1012	6
13	0	14	928	932	7
13	1	1	745	724	6
13	1	3	468	461	9
13	1	5	1161	1130	5
13	1	6	872	858	6
13	1	8	961	965	6
13	1	9	163	132	22
13	1	10	460	464	10
13	1	11	283	259	14
13	1	12	627	614	8
13	1	13	847	837	7
13	1	15	277	256	18
13	2	1	518	482	8
13	2	2	219	222	16
13	2	4	488	493	8
13	2	6	238	215	15
13	2	7	754	757	7
13	2	9	465	459	9
13	2	12	208	219	21
13	2	13	322	302	14

H	K	L	Fobs	Fcalc	SigF
13	2	14	657	636	9
13	3	1	540	523	8
13	3	2	753	727	6
13	3	3	290	275	13
13	3	4	553	532	8
13	3	5	536	532	8
13	3	6	440	444	9
13	3	7	906	939	6
13	3	8	583	574	8
13	3	9	681	680	7
13	3	10	232	212	17
13	3	11	387	409	12
13	3	12	315	328	14
13	3	13	534	522	9
13	3	14	428	417	12
13	3	15	257	187	19
13	4	1	1561	1561	5
13	4	2	494	462	8
13	4	3	366	378	11
13	4	4	228	236	17
13	4	6	1007	1028	6
13	4	7	1371	1393	5
13	4	9	704	696	7
13	4	10	326	332	13
13	4	11	810	799	7
13	4	12	367	381	13
13	4	13	581	554	9
13	4	15	457	459	12
13	5	1	417	410	10
13	5	2	331	332	12
13	5	3	973	970	6
13	5	5	616	612	8
13	5	6	296	272	13
13	5	7	201	235	20
13	5	8	467	475	10
13	5	9	897	885	7
13	5	10	519	505	9
13	5	11	462	477	10
13	5	12	451	433	11
13	5	14	205	193	23
13	6	1	246	232	16
13	6	2	556	554	8
13	6	3	715	716	7
13	6	4	631	619	8

H	K	L	Fobs	Fcalc	SigF
13	6	5	204	205	19
13	6	6	406	409	11
13	6	7	452	492	10
13	6	8	591	618	8
13	6	9	860	842	7
13	6	10	271	262	16
13	6	11	202	205	22
13	6	12	214	203	22
13	6	14	510	476	11
13	7	2	1464	1456	5
13	7	4	585	593	8
13	7	5	411	396	11
13	7	9	641	625	8
13	7	10	378	400	13
13	7	11	412	416	12
13	8	1	603	593	8
13	8	2	756	750	7
13	8	3	247	218	18
13	8	4	949	943	7
13	8	5	203	207	21
13	8	6	717	705	8
13	8	7	202	235	22
13	8	8	205	230	22
13	8	9	522	483	10
13	8	11	249	254	19
13	8	12	508	505	11
13	9	1	342	325	14
13	9	2	273	274	17
13	9	3	781	756	8
13	9	4	195	198	23
13	9	5	327	362	14
13	9	6	199	207	23
13	9	7	339	355	15
13	9	8	268	255	18
13	9	9	843	847	8
13	9	10	208	221	24
13	9	11	479	504	12
13	10	1	235	209	20
13	10	4	630	676	9
13	10	5	363	365	14
13	10	6	290	292	17
13	10	8	313	282	17
13	10	9	1020	1066	
13	11	1	339	316	16

Values of 10*Fobs and 10*Fcalc

H	K	L	Fobs	Fcalc	SigF
13	11	2	741	734	9
13	11	3	588	591	10
13	11	4	425	433	13
13	11	6	354	359	15
13	11	7	542	554	11
13	12	1	805	824	9
13	12	2	666	661	10
13	12	3	239	262	23
13	12	4	822	818	8
14	0	0	824	855	6
14	0	2	278	265	14
14	0	4	480	477	9
14	0	6	712	727	7
14	0	8	338	335	12
14	0	12	575	575	9
14	0	14	272	281	18
14	1	0	1425	1383	5
14	1	2	653	631	7
14	1	3	1006	1042	6
14	1	4	731	723	7
14	1	5	686	709	7
14	1	6	512	522	9
14	1	7	318	331	13
14	1	8	683	700	7
14	1	9	298	285	14
14	1	10	747	733	7
14	1	11	192	193	22
14	1	12	461	450	11
14	1	13	369	380	14
14	1	14	274	298	18
14	2	0	1040	994	6
14	2	2	487	502	9
14	2	3	216	228	18
14	2	4	484	477	9
14	2	5	935	935	6
14	2	6	286	317	15
14	2	9	458	466	10
14	2	10	364	382	12
14	2	12	269	272	17
14	2	13	522	514	10
14	2	14	473	430	11
14	3	0	346	328	12
14	3	1	403	392	10
14	3	2	587	570	8
14	3	3	782	795	7
14	3	4	1364	1380	5
14	3	5	1255	1259	6
14	3	6	204	202	20
14	3	7	1200	1199	6
14	3	8	576	590	8
14	3	9	345	317	13
14	3	10	434	426	11
14	3	11	668	677	8
14	3	12	290	280	16
14	3	13	491	488	11
14	3	14	440	428	12
14	4	0	472	462	10
14	4	1	652	661	8
14	4	2	358	358	12
14	4	3	460	492	10
14	4	4	412	417	11
14	4	5	204	227	20
14	4	6	299	292	14
14	4	8	429	444	11
14	4	11	319	337	15
14	4	13	271	257	18
14	5	0	1263	1237	6
14	5	1	970	962	6
14	5	3	1716	1701	5
14	5	4	430	417	11
14	5	5	406	374	11
14	5	6	591	615	8
14	5	7	257	257	17
14	5	12	307	307	16
14	5	13	694	690	9
14	6	0	1212	1197	6
14	6	1	586	576	8
14	6	3	230	195	19
14	6	4	288	261	15
14	6	8	259	279	18
14	6	10	611	603	9
14	6	12	219	199	23
14	7	2	446	461	11
14	7	4	673	668	8
14	7	5	301	296	15
14	7	8	1001	1023	7
14	7	9	254	269	19
14	7	10	746	733	8
14	7	11	375	376	14
14	8	0	292	243	16
14	8	3	477	473	11
14	8	4	420	426	12
14	8	5	365	392	14
14	8	6	213	206	22
14	8	7	398	414	13
14	8	8	224	217	22
14	8	9	188	180	27
14	8	10	449	466	12
14	9	0	1122	1106	7
14	9	1	620	598	9
14	9	2	782	795	8
14	9	3	767	769	8
14	9	4	184	135	26
14	9	5	304	316	16
14	9	7	196	221	26
14	9	8	658	670	9
14	9	9	274	259	19
14	10	0	398	375	14
14	10	2	365	363	15
14	10	3	309	309	17
14	10	4	247	257	21
14	10	5	835	840	8
14	10	6	458	478	12
14	10	7	305	311	18
14	11	0	1039	1024	7
14	11	3	682	680	9
14	11	4	386	397	15
14	11	5	460	475	13
15	0	2	455	476	10
15	0	4	584	580	9
15	0	8	292	296	15
15	0	12	250	248	19
15	1	1	950	952	6
15	1	2	528	527	9
15	1	3	303	316	14
15	1	4	739	749	7
15	1	5	912	921	7
15	1	6	1143	1160	6
15	1	8	222	225	19
15	1	9	573	585	9
15	1	10	284	280	16
15	1	11	379	379	13
15	1	12	224	215	22
15	2	1	303	310	14
15	2	3	276	301	16
15	2	6	411	409	11
15	2	7	423	402	11
15	2	9	386	410	13
15	2	11	525	538	10
15	2	12	564	544	10
15	3	1	1025	1031	6
15	3	2	1056	1069	6
15	3	3	606	621	9
15	3	4	488	478	10
15	3	5	410	453	12
15	3	6	218	220	20
15	3	7	426	427	11
15	3	9	398	414	12
15	3	11	856	834	8
15	4	1	377	341	12
15	4	2	254	265	17
15	4	3	264	260	17
15	4	5	474	506	10
15	4	9	387	406	13
15	5	1	280	280	16
15	5	2	654	640	8
15	5	3	503	529	10
15	5	4	579	565	9
15	5	5	658	670	8
15	5	6	799	804	7
15	5	7	254	246	18
15	5	8	286	290	16
15	5	9	830	846	8
15	5	10	550	544	10
15	5	11	487	478	11
15	6	1	225	227	20
15	6	2	479	479	11
15	6	4	281	231	16
15	6	5	305	315	16
15	6	6	719	723	8
15	6	8	383	349	13
15	7	2	889	926	7
15	7	3	832	849	8
15	7	4	1258	1276	6
15	7	6	421	439	12
15	7	7	278	305	18

Values of 10AFobs and 10AFcalc

H	K	L	Fobs	Fcalc	SigF
15	7	9	755	757	9
15	8	3	286	269	17
15	8	4	257	231	19
15	8	7	274	309	19
15	8	8	489	505	12
15	9	2	272	240	19
15	9	3	313	315	17
15	9	5	227	230	23
15	10	3	339	350	17
16	0	0	1787	1786	6
16	0	6	373	413	13
16	0	8	315	324	15
16	0	10	642	646	9
16	1	0	874	848	7
16	1	2	223	238	20
16	1	3	1309	1318	6
16	1	4	939	968	7
16	1	5	295	316	16
16	1	6	376	397	13
16	1	10	221	202	22
16	2	0	798	785	8
16	2	1	509	537	10
16	2	2	548	546	10
16	2	3	673	679	8
16	2	5	824	840	7
16	2	7	481	467	11
16	2	8	262	241	18
16	2	9	312	284	16
16	2	10	605	597	10
16	3	0	327	299	15
16	3	1	756	770	8
16	3	2	723	719	8
16	3	3	253	291	18
16	3	4	549	561	10
16	3	5	459	449	11
16	3	6	410	411	12
16	3	7	437	455	12
16	4	0	548	555	10
16	4	3	404	423	12
16	4	4	498	486	10
16	4	5	1157	1156	7
16	4	7	241	256	20
16	5	0	434	442	12
16	5	1	235	259	21
16	5	2	580	601	10
16	5	3	916	936	7
16	5	4	332	328	15
16	5	5	498	508	11
16	5	7	358	379	15
16	5	8	288	280	18
16	5	9	268	300	20
16	6	0	581	540	10
16	6	2	216	234	23
16	6	3	776	793	8
16	6	4	298	275	17
16	6	8	447	457	12
16	7	1	266	265	20
16	7	2	268	245	19
16	7	4	497	505	11
16	7	5	509	544	11
16	7	6	559	559	11
16	8	0	1010	1009	8
16	8	2	389	357	14
16	8	4	283	287	19
16	8	5	286	276	19
17	0	2	389	382	13
17	0	4	1224	1233	7
17	0	6	983	1016	7
17	0	8	913	920	8
17	1	2	414	414	13
17	1	4	726	724	9
17	1	5	746	758	8
17	1	8	231	247	22
17	2	1	743	729	8
17	2	3	344	349	15
17	2	5	206	182	24
17	2	6	611	647	10
17	2	8	362	366	15
17	3	2	376	393	14
17	3	4	467	462	12
17	3	5	220	185	23
17	4	1	956	966	8
17	4	2	251	237	21
17	4	6	594	576	10
17	5	1	792	787	8
17	5	3	198	76	25
17	5	5	222	238	23
17	6	4	700	744	9
18	0	0	558	572	11
18	0	4	265	318	21
18	1	0	784	778	9
18	1	1	332	340	17
18	1	3	800	835	9
18	2	0	321	326	17
18	2	1	389	389	15
18	2	2	379	391	15
18	2	3	198	250	27
18	3	0	478	459	13
18	3	2	522	541	12

Table B.3. Final Positional Parameters for $Cr(CO)_2(CSe)[(MeO)_3P]_3$ (Compound I) and Their Estimated Standard Deviations

Atom	x	y	z	B(A2)
CR	0.19914(5)	0.38146(5)	0.38628(4)	0.74(1)
P1	0.32976(8)	0.41673(9)	0.43460(7)	0.90(2)
P2	0.24156(8)	0.44238(8)	0.27659(7)	0.89(2)
P3	0.06939(8)	0.33459(9)	0.34383(7)	0.88(2)
C1	0.1646(3)	0.3461(3)	0.4713(3)	1.2(1)
SE	0.12779(4)	0.31681(4)	0.55521(3)	1.61(1)
C2	0.2489(3)	0.2733(4)	0.3587(3)	1.2(1)
O2	0.2804(3)	0.2085(3)	0.3405(2)	2.16(9)
C3	0.1546(3)	0.4943(4)	0.4080(3)	1.2(1)
O3	0.1271(3)	0.5609(3)	0.4242(2)	2.01(8)
O11	0.3453(2)	0.5121(2)	0.4688(2)	1.27(7)
C11	0.2989(4)	0.5360(4)	0.5327(3)	2.0(1)
O12	0.4090(2)	0.4127(2)	0.3809(2)	1.25(7)
C12	0.4976(3)	0.4240(4)	0.4051(3)	1.6(1)
O13	0.3628(2)	0.3607(2)	0.5014(2)	1.40(7)
C13	0.3661(4)	0.2660(4)	0.4977(3)	2.0(1)
O21	0.2994(2)	0.3850(2)	0.2240(2)	1.32(7)
C21	0.2640(4)	0.3129(4)	0.1844(3)	1.7(1)
O22	0.3010(2)	0.5266(2)	0.2872(2)	1.27(7)

Table of Positional Parameters and Their Estimated Standard Deviations (cont.)

Atom	x	y	z	B(A2)
C22	0.3337(4)	0.5708(4)	0.2266(3)	1.9(1)
O23	0.1705(2)	0.4780(2)	0.2203(2)	1.22(7)
C23	0.1113(4)	0.5433(4)	0.2388(3)	1.9(1)
O31	-0.0114(2)	0.4014(2)	0.3434(2)	1.35(7)
C31	-0.0469(4)	0.4317(4)	0.4086(3)	1.7(1)
O32	0.0211(2)	0.2542(2)	0.3829(2)	1.26(7)
C32	0.0650(4)	0.1732(4)	0.3997(3)	1.5(1)
O33	0.0691(2)	0.3051(2)	0.2630(2)	1.25(7)
C33	-0.0079(4)	0.2688(4)	0.2306(3)	1.7(1)
H11A	0.3146	0.5942	0.5458	*****
H11B	0.2385	0.5335	0.5245	*****
H11C	0.3141	0.4965	0.5691	*****
H12A	0.5367	0.4197	0.3675	*****
H12B	0.5038	0.4800	0.4276	*****
H12C	0.5110	0.3794	0.4395	*****
H13A	0.3874	0.2425	0.5410	*****
H13B	0.3103	0.2422	0.4888	*****
H13C	0.4041	0.2475	0.4606	*****
H21A	0.3077	0.2867	0.1568	*****

Table of Positional Parameters and Their Estimated Standard Deviations (cont.)

Atom	x	y	z	B(A2)
H21B	0.2415	0.2698	0.2166	*****
H21C	0.2184	0.3331	0.1554	*****
H22A	0.3729	0.6204	0.2425	*****
H22B	0.3764	0.5319	0.2020	*****
H22C	0.2956	0.5918	0.1958	*****
H23A	0.0730	0.5539	0.1996	*****
H23B	[illegible]765	0.5252	0.2779	*****
H23C	0.1406	0.5954	0.2499	*****
H31A	-0.0941	0.4703	0.4008	*****
H31B	-0.0672	0.3824	0.4361	*****
H31C	-0.0040	0.4616	0.4358	*****
H32A	0.0261	0.1337	0.4229	*****
H32B	0.0862	0.1459	0.3583	*****
H32C	0.1122	0.1846	0.4308	*****
H33A	0.0033	0.2540	0.1823	*****
H33B	-0.0257	0.2161	0.2543	*****
H33C	-0.0541	0.3099	0.2320	*****

Starred atoms were refined isotropically.
Anisotropically refined atoms are given in the form of the isotropic equivalent thermal parameter defined as:
(4/3) A [a2AB(1,1) + b2AB(2,2) + c2AB(3,3) + ab(cos gamma)AB(1,2) + ac(cos beta)AB(1,3) + bc(cos alpha)AB(2,3)]

Table B.4. Final Thermal Parameters for $Cr(CO)_2(CSe)[(MeO)_3P]_3$ (<u>mer</u> I) and Their Estimated Standard Deviations

Table of General Temperature Factor Expressions - B's

Name	B(1,1)	B(2,2)	B(3,3)	B(1,2)	B(1,3)	B(2,3)	Beqv
CR	0.49(3)	0.33(3)	1.40(3)	-0.00(2)	-0.04(3)	0.05(3)	0.74(1)
P1	0.61(5)	0.56(5)	1.53(5)	-0.04(4)	-0.06(4)	-0.01(4)	0.90(3)
P2	0.71(5)	0.46(5)	1.51(5)	-0.04(4)	0.01(4)	0.02(4)	0.89(2)
P3	0.54(4)	0.53(5)	1.57(5)	0.00(4)	-0.00(4)	0.07(4)	0.88(2)
C1	0.7(2)	0.6(2)	2.2(2)	0.2(2)	-0.4(2)	-0.5(2)	1.2(1)
SE	1.91(2)	1.40(2)	1.53(2)	-0.18(2)	0.28(2)	0.22(2)	1.61(1)
C2	0.9(2)	1.1(2)	1.8(2)	-0.2(2)	-0.1(2)	0.2(2)	1.2(1)
O2	2.4(2)	1.3(2)	2.9(2)	0.5(1)	-0.2(2)	-0.3(1)	2.16(9)
C3	0.9(2)	1.2(2)	1.7(2)	-0.3(2)	0.0(2)	0.0(2)	1.2(1)
O3	2.1(2)	0.7(1)	3.2(2)	0.5(1)	0.5(2)	-0.3(1)	2.01(8)
O11	1.0(1)	0.8(1)	2.0(1)	-0.3(1)	0.2(1)	-0.5(1)	1.27(7)
C11	1.6(2)	1.9(2)	3.6(3)	-0.1(2)	0.1(2)	-1.1(2)	2.0(1)
O12	0.6(1)	1.4(1)	1.7(1)	0.1(1)	-0.1(1)	-0.3(1)	1.25(7)
C12	0.5(2)	1.5(2)	2.8(3)	-0.1(2)	-0.1(2)	-0.2(2)	1.6(1)
O13	1.2(1)	1.0(1)	2.0(2)	-0.3(1)	-0.5(1)	0.3(1)	1.40(7)
C13	1.6(2)	1.3(2)	3.1(3)	0.0(2)	-0.8(2)	0.8(2)	2.0(1)
O21	1.1(1)	1.0(1)	1.9(1)	-0.0(1)	0.3(1)	-0.3(1)	1.32(7)
C21	2.2(2)	1.2(2)	1.7(2)	0.1(2)	0.1(2)	-0.4(2)	1.7(1)
O22	1.2(1)	0.8(1)	1.8(1)	-0.4(1)	0.1(1)	-0.0(1)	1.27(7)

Table of General Temperature Factor Expressions - B's (Continued)

Name	B(1,1)	B(2,2)	B(3,3)	B(1,2)	B(1,3)	B(2,3)	Beqv
C22	2.0(2)	1.3(2)	2.5(2)	-0.7(2)	0.5(2)	0.3(2)	1.9(1)
O23	1.0(1)	0.8(1)	1.9(1)	0.1(1)	-0.2(1)	0.1(1)	1.22(7)
C23	1.6(2)	1.2(2)	2.8(3)	0.6(2)	-0.6(2)	0.1(2)	1.9(1)
O31	0.7(1)	1.2(1)	2.1(2)	0.4(1)	-0.0(1)	0.1(1)	1.35(7)
C31	0.8(2)	1.6(2)	2.6(2)	0.3(2)	0.4(2)	-0.3(2)	1.7(1)
O32	1.0(1)	0.8(1)	2.1(2)	-0.2(1)	0.1(1)	0.2(1)	1.26(7)
C32	1.8(2)	0.8(2)	2.0(2)	-0.2(2)	0.1(2)	0.3(2)	1.5(1)
O33	0.8(1)	1.2(1)	1.7(2)	-0.2(1)	-0.1(1)	-0.0(1)	1.25(7)
C33	1.1(2)	1.6(2)	2.4(2)	-0.4(2)	-0.5(2)	-0.1(2)	1.7(1)

The form of the anisotropic thermal parameter is:
exp[-0.25(h2a2B(1,1) + k2b2B(2,2) + l2c2B(3,3) + 2hkabB(1,2) + 2hlacB(1,3) + 2klbcB(2,3))] where a,b, and c are reciprocal lattice constants.

Table of Refined Temperature Factor Expressions - Beta's

Name	B(1,1)	B(2,2)	B(3,3)	B(1,2)	B(1,3)	B(2,3)
CR	0.00051(3)	0.00036(3)	0.00097(2)	-0.00000(5)	-0.00007(1)	0.00008(5)
P1	0.00064(5)	0.00061(5)	0.00106(4)	-0.00008(9)	-0.00011(7)	-0.00002(7)
P2	0.00074(5)	0.00050(5)	0.00104(3)	-0.00008(9)	0.00001(7)	0.00003(7)
P3	0.00056(5)	0.00058(5)	0.00108(4)	0.00001(9)	-0.00000(7)	0.00012(7)
C1	0.0007(2)	0.0007(2)	0.0015(2)	0.0003(4)	-0.0006(3)	-0.0008(3)
SE	0.00200(2)	0.00151(2)	0.00106(1)	-0.00038(4)	0.00048(3)	0.00039(3)
C2	0.0009(2)	0.0011(2)	0.0012(1)	-0.0004(4)	-0.0002(3)	0.0003(3)
O2	0.0025(2)	0.0013(2)	0.0020(1)	0.0012(3)	-0.0003(3)	-0.0005(3)
C3	0.0009(2)	0.0012(2)	0.0012(2)	-0.0007(4)	0.0000(3)	0.0000(3)
O3	0.0022(2)	0.0008(2)	0.0022(1)	0.0010(3)	0.0008(3)	-0.0005(2)
O11	0.0010(1)	0.0008(1)	0.0014(1)	-0.0007(3)	0.0003(2)	-0.0008(2)
C11	0.0017(2)	0.0020(3)	0.0018(2)	-0.0002(4)	0.0001(4)	-0.0019(4)
O12	0.0006(1)	0.0016(2)	0.0012(1)	0.0003(3)	-0.0002(2)	-0.0004(2)
C12	0.0005(2)	0.0016(2)	0.0019(2)	-0.0003(4)	-0.0001(3)	-0.0003(4)
O13	0.0012(2)	0.0011(2)	0.0014(1)	-0.0005(3)	-0.0008(2)	0.0005(2)
C13	0.0016(2)	0.0014(3)	0.0021(2)	0.0000(4)	-0.0014(4)	0.0014(4)
O21	0.0011(1)	0.0011(2)	0.0013(1)	-0.0000(3)	0.0005(2)	-0.0005(2)
C21	0.0023(3)	0.0012(2)	0.0012(1)	0.0002(4)	0.0003(3)	-0.0008(3)
O22	0.0012(2)	0.0009(2)	0.0013(1)	-0.0009(3)	0.0001(2)	-0.0001(2)

Table of Refined Temperature Factor Expressions - Beta's (Continued)

Name	B(1,1)	B(2,2)	B(3,3)	B(1,2)	B(1,3)	B(2,3)
C22	0.0021(2)	0.0014(2)	0.0017(2)	-0.0014(4)	0.0009(4)	0.0006(3)
O23	0.0011(1)	0.0008(1)	0.0013(1)	0.0002(3)	-0.0004(2)	0.0001(2)
C23	0.0017(2)	0.0013(2)	0.0019(2)	0.0012(4)	-0.0010(4)	0.0002(4)
O31	0.0007(1)	0.0013(2)	0.0015(1)	0.0009(3)	-0.0001(2)	0.0001(2)
C31	0.0009(2)	0.0017(3)	0.0018(2)	0.0006(4)	0.0006(3)	-0.0005(4)
O32	0.0010(1	0.0008(1)	0.0014(1)	-0.0004(3)	0.0002(2)	0.0004(2)
C32	0.0019(2)	0.0009(2)	0.0014(2)	-0.0005(4)	0.0001(3)	0.0005(3)
O33	0.0009(1)	0.0013(2)	0.0012(1)	-0.0005(3)	-0.0002(2)	-0.0001(2)
C33	0.0011(2)	0.0018(2)	0.0017(2)	-0.0009(4)	-0.0009(3)	-0.0001(3)

The form of the anisotropic thermal parameter is:
exp[-(B(1,1)Ah2 + B(2,2)Ak2 + B(3,3)Al2 + B(1,2)Ahk + B(1,3)Ahl + B(2,3)Akl]

Table of General Temperature Factor Expressions - U's

Name	U(1,1)	U(2,2)	U(3,3)	U(1,2)	U(1,3)	U(2,3)
CR	0.0062(4)	0.0042(4)	0.0177(4)	-0.0000(3)	-0.0005(3)	0.0006(3)
P1	0.0078(6)	0.0071(6)	0.0194(7)	-0.0005(5)	-0.0008(5)	-0.0001(5)
P2	0.0090(6)	0.0058(6)	0.0191(6)	-0.0005(5)	0.0001(6)	0.0002(5)
P3	0.0069(6)	0.0067(6)	0.0198(7)	0.0000(5)	-0.0000(5)	0.0009(5)
C1	0.009(2)	0.008(2)	0.028(3)	0.002(2)	-0.005(2)	-0.006(2)
SE	0.0242(3)	0.0177(3)	0.0193(3)	-0.0023(2)	0.0036(2)	0.0028(2)
C2	0.011(2)	0.013(3)	0.023(3)	-0.003(2)	-0.002(2)	0.002(2)
O2	0.030(2)	0.015(2)	0.037(2)	0.007(2)	-0.002(2)	-0.004(2)
C3	0.011(2)	0.015(3)	0.022(3)	-0.004(2)	0.000(2)	0.000(2)
O3	0.026(2)	0.009(2)	0.041(2)	0.006(2)	0.006(2)	-0.004(2)
O11	0.013(2)	0.010(2)	0.026(2)	-0.004(2)	0.002(2)	-0.006(2)
C11	0.031(3)	0.024(3)	0.033(3)	-0.001(3)	0.001(3)	-0.014(3)
O12	0.007(2)	0.018(2)	0.022(2)	0.002(2)	-0.003(2)	-0.003(2)
C12	0.006(2)	0.019(3)	0.025(3)	-0.002(2)	-0.001(2)	-0.002(3)
O13	0.015(2)	0.013(2)	0.025(2)	-0.003(2)	-0.006(2)	0.004(2)
C13	0.020(3)	0.017(3)	0.039(3)	0.000(3)	-0.010(3)	0.010(3)
O21	0.014(2)	0.013(2)	0.024(2)	-0.000(2)	0.004(2)	-0.004(2)
C21	0.038(3)	0.015(3)	0.021(3)	0.001(3)	0.002(2)	-0.006(2)
O22	0.015(2)	0.010(2)	0.023(2)	-0.005(2)	0.001(2)	-0.000(2)

Table of General Temperature Factor Expressions - U's (Continued)

Name	U(1,1)	U(2,2)	U(3,3)	U(1,2)	U(1,3)	U(2,3)
C22	0.025(3)	0.016(3)	0.031(3)	-0.008(2)	0.006(3)	0.004(3)
O23	0.013(2)	0.010(2)	0.023(2)	0.001(2)	-0.003(2)	0.001(2)
C23	0.020(3)	0.015(3)	0.035(3)	0.007(2)	-0.007(3)	0.001(3)
O31	0.009(2)	0.015(2)	0.027(2)	0.005(2)	-0.001(2)	0.001(2)
C31	0.011(3)	0.020(3)	0.033(3)	0.004(2)	0.005(2)	-0.004(3)
O32	0.012(2)	0.010(2)	0.026(2)	-0.003(2)	0.001(2)	0.003(2)
C32	0.023(3)	0.010(3)	0.025(3)	-0.003(2)	0.001(2)	0.004(2)
O33	0.010(2)	0.015(2)	0.022(2)	-0.003(2)	-0.002(2)	-0.001(2)
C33	0.013(3)	0.021(3)	0.030(3)	-0.005(2)	-0.007(2)	-0.001(2)

The form of the anisotropic thermal parameter is:
exp[-2PI2(h2a2U(1,1) + k2b2U(2,2) + l2c2U(3,3) + 2hkabU(1,2) + 2hlacU(1,3) + 2klbcU(2,3))] where a,b, and c are reciprocal lattice constants.

Appendix C

Co-adding and Permanent Storage of Large Number of FT-IR Scans

The following is a listing of a program (named LWA) written as a macro compatible with the Nicolet FT-IR software. The program was created in order to overcome the problem of insufficient data collection due to correlation drifting inherent in the collection of large numbers of FT-IR scans. It enables any convenient number of scans to be collected at a time and stored in specified destination files prior to co-addition and subsequent transfer to the permanent storage disk.

```
OMD
THIS MACRO COLLECTS, CO-ADDS AND STORES INTERFEROGRAMS FOR MULTIPLE SAMPLES
QIT = 3
OMD
ENTER NUMBER OF SAMPLES
QIT
SRT = 30
OMD
ENTER NUMBER OF FILES TO BE CO-ADDED
SRT
NSD = 1000
OMD
ENTER NUMBER OF SCANS PER FILE
NSD
EXT = 000
OMD
SPECIFY A FILE NAME, DO NOT ADD AN EXT (USE 6 CHARACTERS OR LESS)
```

```
IFN
FOR III = 1 TIL QIT
PAU INSERT SAMPLE, PURGE IF DESIRED,THEN PRESS RETURN
DFN = 5
FOR LLL = 1 TIL SRT
DFN = DFN + 1
CLD
NXT LLL

OFN = DFN
FOR KKK = 2 TIL SRT
OFN = OFN - 1
CAD
NXT KKK
AFP
EXT = EXT + 1
NXT III
END
```